Dairy Effluent Steroidal Hormones Characteristics and Treatment by Anaerobic Digestion (Covered Anaerobic Pond) and Biochar

A thesis

submitted in fulfilment

of the requirements for the degree of

Doctor of Philosophy in Engineering

at

The University of Waikato

by

Asaf Rachmani

THE UNIVERSITY OF
WAIKATO
Te Whare Wānanga o Waikato

2024

Abstract

Endocrine disrupting compounds such as estrogenic steroid hormones (ESHs) are problematic when present in waterways in terms of both the health of the ecosystem and downstream water treatment. Dairy farms are some of the largest contributors to ESHs in the environment. This study focused on a farm located in the Waikato region, New Zealand, which housed 550, primarily grass-fed dairy cows. The farm included a rotary milking shed, feed pad, sump, covered anaerobic pond and storage pond, with effluent and sludge being applied to land. In this study concentrations of the conjugated and unconjugated ESHs, 17α-estradiol (17α-E2), 17β-estradiol (17β-E2) and estrone (E1), in both dissolved and solid phases of dairy shed effluent, and covered anaerobic pond sludge and effluent, were measured from grab samples over a period of nine months. These were used to investigate seasonal variation and performance of the covered anaerobic pond in removing the ESHs and their conversion from one form into another. Previously published methods of ESH analysis were validated and adapted for ESH analysis in dissolved and solid phases, and a new enzymatic method for conjugate ESH analysis was tested and used. In addition, the effect of dosing the effluent with biochar was examined on ESH removal. A covered anaerobic pond model was developed to examine the efficacy of a dairy farm-based covered anaerobic pond treatment system to settle, transform, absorb and remove ESHs. The model was calibrated utilising ESH measurements and used to examine the effect of biochar addition and operational parameters on ESH removal.

Overall ESH concentrations in the covered anaerobic pond influent, sludge and effluent were 4,171 ng/L, 93,601 ng/L and 4,346 ng/L respectively. ESH concentrations peaked in dairy shed effluent during April and July, which correlated with the late pregnancy and calving periods on the farm. The mean organic carbon normalised adsorption coefficient (K_{oc}) for ESHs in the samples from the pond treatment system ranged between 3.06 mL/g to 3.78 mL/g, comparable with published values in soil and wastewater sludge. Up to 99% of the total mass of ESHs in the sludge and between 70-80 % in influent and effluent were retained in the solids phase. The predominant ESH in the influent samples was 17α-E2 (2,869 ng/L), but E1 predominated in the sludge (85,414 ng/L) and in the effluent (3,140 ng/L). The dissolved and solid phases of dairy shed effluent contained the highest relative

proportions of conjugated ESHs with means of 25.1 % and 3.38 % respectively and corresponding mean concentrations of 113 ng/L and 137 ng/L. In contrast, sludge and effluent samples (dissolved and solid phases) from the covered anaerobic pond contained smaller relative proportions of conjugated ESHs, 0.90 % and 1.21 %, and 7.17 % and 0.43 % respectively and corresponding mean concentrations of 6.65 ng/L and 967 ng/L, and 52.5 ng/L and 19.7 ng/L respectively. These results demonstrate the importance of considering the solid fraction within effluent treatment systems when analysing ESHs, otherwise estrogenic load can be greatly underestimated. The conjugated ESHs were present in both the dissolved and solid phases of all samples collected, indicating that conjugated ESHs are persistent and can pass through anaerobic treatment systems contributing to estrogenic load once applied to pasture, and potentially leach into groundwater or migrate to nearby surface waters. Overall anaerobic treatment of dairy waste decreased the contribution of 17α-E2 and 17β-E2 while increasing that of E1, however, 17β-E2 was the main contributor to total estrogenicity.

The calibration of the model developed provided a good fit with experimental data with an R^2 of 0.98-0.99. Addition of biochar into dairy shed effluent and the model covered anaerobic pond system resulted in an 89 % reduction of free ESHs but had a minimal impact on conjugated ESH. Addition of biochar increased the solid phase ESH concentration by 19 % settling out into the sludge and reducing overall estrogenic load in the effluent. Operational factors such as higher influent flow rates and sludge accumulation negatively impacted the covered anaerobic pond ESH removal performance. Sludge accumulation and short-circuiting caused by infrequent removal and shallow depth of the covered anaerobic pond system resulted in mixing of fresh influent with the upper layer of pond sludge, leading to decreased removal efficiency. To enhance the covered anaerobic pond system's performance, increasing the retention time and reducing sludge carry over by increasing pond volume and depth, resulted in ESH removal increasing to 67.9 % (no biochar) and 73.0 % (with biochar), and estrogenicity reduction improving to 70.4 % (no biochar) and 73.5 % (with biochar).

Acknowledgments

Firstly, I would like to thank my chief supervisor, Dr Mark Lay for his friendship and support, ability to see things as they were, pushing when it really mattered and his relaxed and positive outlook, where nothing was a big deal. I would also like to acknowledge Professor Merilyn Manley-Harris for her wisdom, valuable knowledge and experience, her ability to keep us focussed on the end goal, her availability and prompt feedback, along with her grammar and technical reviewing proficiency. Thank you Mark and Merilyn for your assistance in putting this thesis together.

I would like to thank my external supervisor, Dr Grant Northcott (From Northcott Research Consultants Limited) for arranging access to the Plant and Food Research Laboratory, ensuring I had all the equipment and consumables I needed for the experiments and analysis work, sharing his knowledge and expertise, spending long hours at the lab with me, and providing vigorous supervision and maintaining high standards. Thank you to Bridget Wise for the much-appreciated help in the laboratory, and your company and friendship. Thank you, Dwayne Jensen, and Tania Trower of Plant and Food Research for allowing me access to expensive instruments and for happily sharing their expertise. Thanks to the staff at Plant and Food Research for their hospitality and the entertaining table tennis matches.

I would also like to thank Dr Alzbeta Bouskova, Dr Graeme Glasgow and Dr Rupert Craigs for their assistance in the initial phase of this research and for their advice provided along the way. I would also like to acknowledge a past staff member of Waikato University, Cheryl Ward, for her amazing attitude and willingness to help with formatting and referencing. Thank you to Associate Professor Jim Jones for the friendly approach and for providing the material (Biochar) used in this research.

Finally, I would like to acknowledge the constant support of my wife, Rachel Rachmani, who tolerated many hours of researching and working on this thesis. Without Rachel's forbearance and understanding, this venture could never be accomplished. To my kids, Noa, Aviv and Alon, this Thesis is dedicated to you. Thank for your patience. I hope that this work will be a role model to you, showing that with the right mindset, focus,

dedication, and hard work everything is possible. I wish you all the best with your future plans, I love and cherish you and always will.

Table of Contents

List of Figures

List of Tables

Abbreviations

^{13}C6-E1	DL-Estrone-13,14,15,16,17,18-13C6
^{13}C6-E2	DL-Estradiol-13,14,15,16,17,18-13C6
17α-EE	17α-ethinyl estradiol
17α-E2	17α-estradiol
17α-E2-3-S	17α-estradiol-3-sulphate
17β-E2	17β-estradiol
17β-E2-d4	17β-estradiol-2,4,16,16-d4
βE2-3,17-diS	β-Estradiol-3,17-disulphate
βE2-3-G	17β-estradiol-3-glucuronide
βE2-17-G	Estradiol-17β-glucuronide
Σ	Summation of parameters
ACN	Acetonitrile
AEE/s	Assessment of environmental effects
AP/s	Alkyphenol/s
ASE	Accelerated solvent extraction
BET	Brunauer-Emmett-Teller
BPA	Bisphenol-A
BGS™	β-Glucuronidase / Sulfatase Mix
CAFO	Concentrated animal feeding operations
CAP	Covered anaerobic pond
C_e	ESH equilibrium concentration
DOC	Dissolved Organic Carbon
DSE	Dairy shed effluent
E1	Estrone
E1-3-S	Estrone-3-sulphate
E1-d4	Estrone-2,4,16,16-*d*4
E2	Estradiol
E3	Estriol
EC	European Commission
EDC/s	Endocrine disrupting chemical/s
EDS	Electron dispersive spectroscopy

EEQ/s	Estrogen equivalent/s
ELISA	Enzyme-linked immunosorbent assay
ER	Estrogen receptor
ESH/s	Estrogenic steroid hormone/s
ETI	Estuarine trophic index
ETS	Effluent treatment system
GAC	Granular activated carbon
GC	Gas chromatography
GC-MS	Gas Chromatography Mass Spectrometry
GPC	Gel permeation chromatography
HLB	Hydrophilic-Lipophilic-Balanced
HTT	Heat Treatment Temperature
IBI	International Biochar Initiative
ICP-MS	Inductively Coupled Plasma Mass Spectrometry
IPA	Isopropyl alcohol (2-propanol)
K_d	Distribution coefficients
K_{oc}	Mean organic carbon normalised adsorption coefficient
LC	Liquid chromatography
LC-MS-MS	Liquid chromatography-tandem mass spectrometry
log K_{oc}	Base 10 Logarithm of the Organic carbon partition coefficients
log K_{ow}	Base 10 Logarithm of the Octanol-water partition coefficient
MDL/s	Method detection limit/s
MS	Mass spectrometry
MSD	Mass selective detector
MSTFA	*N*-Methyl-*N*-(trimethylsilyl)-trifluoroacetamide
NZ	New Zealand
OC	Organic carbon
OECD	The Organisation for Economic Cooperation and Development
OM	Organic matter
PAC	Powdered activated carbon

PBB/s	Polybrominated biphenyl/s
PCB/s	Polychlorinated biphenyl/s
PCT/s	Polychlorinated terphenyl/s
PNEC/s	Predicted no effect concentration/s
POC	Particulate organic carbon
POM	Particulate organic matter
POP/s	Persistent organic pollutant/s
PTFE	Polytetrafluoroethylene
QA	Quality assurance
q_t	ESH absorbed at time
R^2	Coefficient of determination
REACH	Registration, evaluation, authorisation, and restriction of chemicals
RPF	Relative potency factor
SEM	Scanning electron microscope
SI	Supplementary information
SIG/s	Special interest group/s
SIM	Selected ion monitoring
SPE	Solid-phase extraction
SOE	State of environment
SPEED	Strategic Programs on Environmental Endocrine Disruptors
SSE	Sum of Square Errors
SULT/s	Sulfotransferase
TEA	Triethylamine
TEF	Toxic equivalency factor
TFA	Trifluoroacetic acid
TMSI	Trimethylsilylimidazole
TOC	Total Organic Carbon
TS	Total solids
UGT	Uridine 5'-diphospho-glucuronosyltransferase (UDP- glucuronosyltransferase)
US EPA	United States Environmental Protection Agency
VTS	Volatile total solids

WHO	World Health Organisation
YES	Yeast estrogen screen

Chapter 1:
Introduction

This chapter provides background information for the research topic and the justification and scope of the research. It includes information regarding the endocrine system, the production and role of hormones and excretion mechanism. This chapter also provides information about endocrine system disrupting chemicals and the link to estrogenic steroid hormones, as well as the general impact of steroid hormones as exogenous pollutants on humans and ecosystem when these are released into the environment. Also included are the analytical methods to determine estrogenic steroid hormones, the related regulations and guidelines, and the scope and justification of the research including the knowledge gaps.

1.1 Background

The hypothesis that there are chemicals within the environment that may exhibit endocrine disrupting effects was raised in the early 1900's (Allen *et al*., 1924; Dodds *et al*., 1938). The concern was raised due to reports of increased incidences of endocrine related diseases in humans, as well as physiological effects observed in wildlife. Despite early evidence, environmental issues associated with endocrine disrupting chemicals (EDCs) only became a popular topic for research in the last 10-30 years (Birkett, 2003). The popularity is due to the link between EDCs and the significant potential risk to interfere with normal biological functions leading to health effects associated with the reproductive system and other endocrine related diseases (Adeel *et al*., 2017; Kabir *et al*., 2015; Mills & Chichester, 2005; Moore *et al*., 2016; Tetreault *et al*., 2011; Toppari & Skakkebæk, 2000; U.S. Environmental Protection Agency, 1997; World Health Organization, 2012a; Ziegler et al., 2015).

According to the United States Environmental Protection Agency (US EPA), "endocrine disruptors, are chemicals that interfere with the synthesis, secretion, transport, binding, action, or elimination of natural hormones in the body that are responsible for maintenance, reproduction, development, and/or behaviour" (U.S. Environmental Protection Agency, 1997).

EDCs include a wide range of substances that have been shown to exhibit endocrine disrupter activity. These include both natural and man-made chemicals, including alkylphenols (APs), phthalates, bisphenol-A (BPA), pesticides, estrogenic steroid hormones (ESHs) and inorganic substances such as cadmium and mercury (Figure 1-1) (Birkett, 2003a; Khetan, 2014). These compounds have different chemical structures but all of them have the capacity to disrupt normal hormonal actions when released into the environment (Birkett, 2003b; Khetan, 2014).

Due to the high incidence and increased trends of many endocrine related disorders in humans, the observed endocrine related effects in wildlife populations and the identification of chemicals with endocrine disrupting properties linked to disease outcomes in research studies, the World Health Organisation (WHO) has published a list of evidence for endocrine disruption in human and wildlife; the list comprises many hundreds of studies. Some examples of areas in which EDC in the form of ESHs were found to be or suspected to be related to human and wildlife health are reproduced below (World Health Organization, 2012).

- Female reproductive health.
- Male reproductive health.
- Female and male sex ratio imbalances in humans and wildlife.
- Thyroid-related disorders.
- Hormone-related cancers such as breast, endometrial, ovarian and prostate cancers.
- Neurodevelopmental disorders in children and wildlife.
- Metabolic disorders such as obesity and diabetes.
- Bone disorders.
- Immune function and diseases in humans and wildlife.

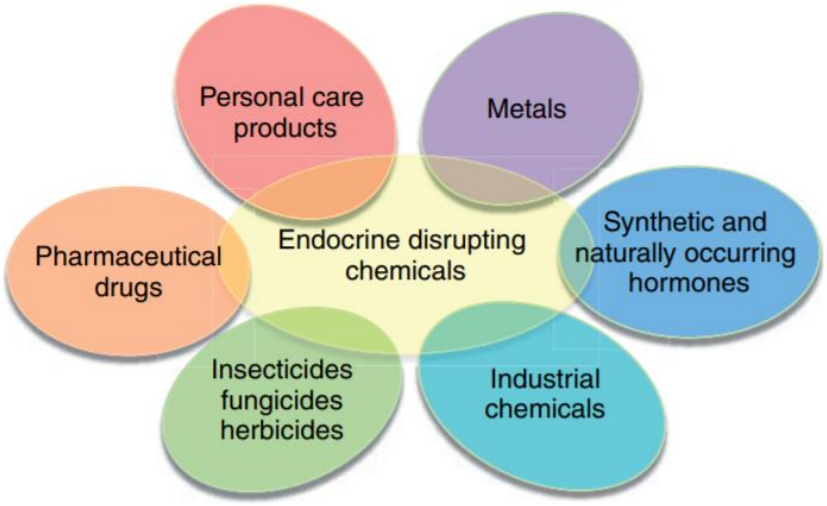

Figure 1-1: Groups of potential endocrine disrupters (Khetan, 2014)

Global and New Zealand (NZ) studies have found that dairy cows and dairy shed effluent (DSE) are the largest source of naturally occurring endogenous steroid hormones entering the environment (Lange *et al*., 2002; Hanselman *et al*., 2003; Kolodziej *et al*., 2004) and they exceed any other agricultural activity or municipal and industrial sources (Sarmah *et al*., 2006; Gadd *et al*., 2010a; Gadd *et al*., 2010b). Therefore, this research was designed to focus on DSE and DSE treatments.

1.2 The endocrine system

The endocrine system is found in all vertebrates and many invertebrates and is comprised of the brain and hypothalamic neuroendocrine systems, glands (such as the pituitary, thyroid and mammary), hormones and receptors that respond to the hormones, the cardiovascular system, adipose tissue, and pancreas, the ovary and uterus in females and testes and prostate in males, all of which can be susceptible to EDCs when these enter the body via the digestive system or by other routes (Birkett, 2003a; Khetan, 2014).

The similarities of the anatomy of human and dairy cow bodies are presented in Figure 1-2.

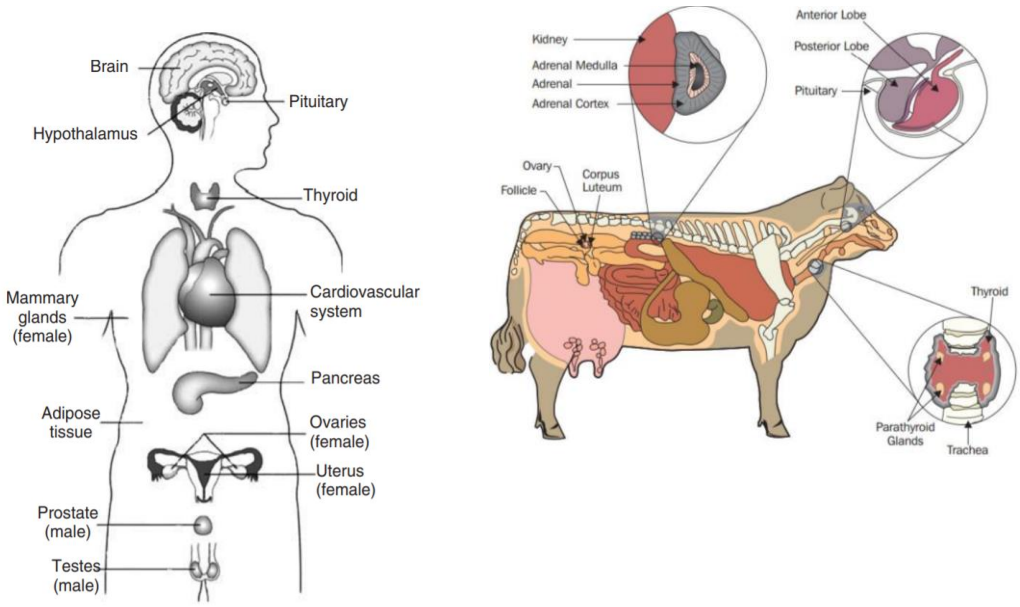

Figure 1-2: Endocrine systems in human (Khetan, 2014) and dairy cow (Hormones Endocrine System).

Hormones play an important communication role within the endocrine system. They act as natural chemical signals produced from particular groups of cells to influence bodily functions (Rattan and Sharma, 2017). Hormones provide communication from one tissue/cell to others within an organism and are involved in the dynamic control of biochemical and physiological functions. For example, hormones control and regulate blood sugar levels, body growth and energy production, neuroendocrine and immunological system and the function of reproductive organs (Rattan and Sharma, 2017).

1.2.1 Estrogenic steroid hormones

ESHs are a group of natural hormones that play a critical role in many physiological processes in both females and males. ESHs include three main hormones: estradiol (E2) (most abundant and most potent), estrone (E1) and estriol (E3) (Khetan, 2014). The roles of ESHs include normal growth, development, reproduction, behaviour, metabolism, bone homeostasis, and regulation of the nervous and cardiovascular systems (Kazeto *et al*., 2004). In males, ESHs regulate the sexual behaviour, maintenance of the skeleton and the cardiovascular system, and the functioning of testes and the prostate (Khetan, 2014). Only ~20% of the ESHs are produced by the testes in men, with the remainder from local production that converts testosterone to ESHs by adipose tissue, brain, skin and bone by reactions catalysed by the enzyme aromatase (Cooke *et al*., 2017). In woman, ESHs help

develop and maintain both the reproductive system and female characteristics. These are largely produced by the ovaries and the placenta (the latter during pregnancy only). E2 is the most common type of ESH in females during their reproductive years, while E3 and E1 levels increase during pregnancy and the post reproduction period respectively (Khetan, 2014).

1.2.2 Biological function and excretion of estrogenic steroid hormones

When ESHs produced in the body enter the blood, they are either free or bound to a protein. The free ESHs penetrate the cell surface of target tissues due to their lipid-soluble characteristics and then bind to a protein known as an estrogen receptor (ER) (alpha or beta). The interaction between the hormone and its receptor triggers a cascade of biochemical reactions in the target cell that eventually modify the cell's activity (Khetan, 2014) (Figure 1-3).

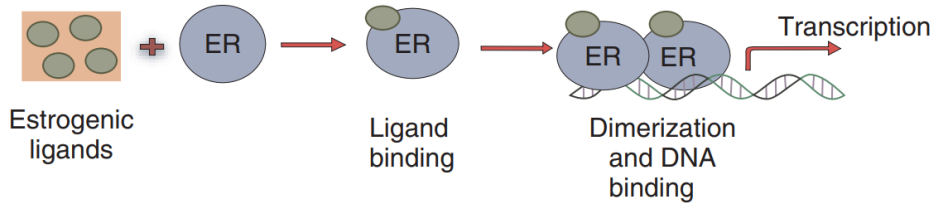

Figure 1-3: Activated ESH receptor signalling and initiation of responsive genes (Khetan, 2014).

Inactivation of the ESHs occurs when ESHs do not reach the target cells or when protein synthesis is completed. The non-functional ESHs will typically pass via the liver and kidneys, be modified to a weaker form and/or be conjugated by the addition of sulphate or glucuronide groups before excretion; conjugation increases water solubility thus facilitating removal in the urine or other aqueous secretions (Norris and Carr, 2005) (Information regarding the chemical structure and properties of the free and conjugated ESHs are presented in Chapters 2 and 3). ESHs are excreted primarily through the urine and faeces but smaller amounts can be found in saliva, sweat, and breast milk. Daily excretion rates of ESHs depend on the type, sex and reproductive state of the animal/human. Previous studies in NZ identified dairy cows as the main source of potent biologically active ESHs entering the NZ environment, and DSE in NZ has been demonstrated to contain higher concentrations of ESHs compared to effluents from

piggeries, goat farms, or municipal wastewater (Sarmah *et al*., 2006; Gadd *et al*., 2010a; Gadd *et al*., 2010b).

1.3 Endocrine disruption and estrogenic steroid hormones

ESHs are among the most potent endocrine disrupting chemicals in nature (Khetan, 2014). When the ESHs (free and/or conjugated) excreted from the body (human and/or an animal) are not treated appropriately and are released into the environment, they can create health effects by impacting the endocrine system of wildlife and human. These effects include interferences with receptor signalling or activation of other signalling pathways and/or artificial binding that mimics or blocks the natural estrogens. All these effects can create abnormal responses that prevent correct functioning of the body (Birkett, 2003; Khetan, 2014). Further examples of the endocrine disrupting impacts of ESHs will be presented in subsequent chapters within this thesis.

1.4 Regulation and guidelines related to estrogenic steroid hormones

To date, EDCs are unregulated globally. This is likely due to the existing gaps associated with the linkage between exposure to EDCs and endocrine diseases in humans and limited validated test methods for the identification of endocrine disrupting effects (World Health Organization, 2012). However, the United States, Japan and the European Union have recognised the potential risk that these emerging contaminants are presenting to the environment and the impact on human and wildlife. As part of this recognition, several strategies have been put in place which include the development of monitoring methods and assessment of the risks of EDCs (European Commission, 2016; U.S. Environmental Protection Agency, 2017b).

The European Commission (EC) established the registration, evaluation, authorisation, and restriction of chemicals (REACH). REACH aims to improve the protection of human health and the environment through earlier identification of potentially problematic chemical substances. In REACH, EDCs are of similar regulatory concern as substances of very high concern (European Commission, 2016). The EC is currently working on a proposal for science-based criteria for EDCs, to assess the risks posed by EDCs, using a combination of computer methods and automated laboratory tests (Anderson et al., 2012) as well as on a “Better Regulation Guidline”. Previously the EC produced a roadmap of

defining criteria for identifying EDCs in the context of the implementation of plant protection products and biocidal products for regulation. An advisory group was established with the aim of supporting the establishment of criteria for identification of EDCs and produced a priority list of EDCs substances for further evaluation. Among the prioritised list of EDCs, evidence supported the inclusion of 17β-E2 and E1 as affecting reproduction and development of fish (Johnson and Harvey, 2002).

The Japanese Ministry of Environment regards endocrine disrupting effects on human health and wildlife as an important issue and has published strategic programmes on environmental endocrine disruptors (SPEED) (Ministry of the Environment, 2010). The purpose of SPEED was to promote further studies and monitoring of EDCs, as well as observation of wildlife. In July 2010, "Further Actions to Endocrine Disrupting Effects of Chemical Substances" was published (EXTEND2010). The programme aimed to accelerate the establishment and implementation of assessment methodologies toward the goal of properly assessing the environmental risk of endocrine disrupting effects of chemical substances and to take management measures as necessary.

In 1996, legislation in the United States approved the decision to establish a screening programme that would provide the necessary information to make regulatory decisions about endocrine effects of chemicals (U.S. Environmental Protection Agency, 2017a). Since then, advisory committees, screening methods and programmes and work plans have been formed and lists have been published of chemicals and substances that may cause endocrine disruption (U.S. Environmental Protection Agency, 2017b).

In NZ, there are many potential guidelines in which EDCs might be included to ensure they are monitored and mitigated. Some examples include the Australian and NZ guidelines for fresh and marine water quality and NZ Municipal Wastewater Monitoring Guidelines. While ESHs may not be explicitly mentioned in some of the guidelines, they are often classified under the broader category of persistent organic pollutants (POPs). For instance, the NZ Municipal Wastewater Monitoring Guidelines have a section on endocrine disruptors in the effluent monitoring section, and the Landfill Guidelines include organic contaminants such as Polybrominated biphenyls (PCBs), Polychlorinated terphenyls (PCTs), and Polychlorinated biphenyls (PBBs) that are considered EDCs. The

management of ESHs in NZ is also achieved through resource consent applications, which involve the assessment of environmental effects (AEEs), technical reports, and resource consent monitoring. The management of ESHs through consent application is being increasingly applied during reconsenting of wastewater treatment plant discharges. The applicant is often asked and/or required to assess the risk of emerging organic contaminants in the discharged treated effluent which includes natural and synthetic steroid hormones, the industrial phenolic xenoestrogens, BPA and phthalate esters. Additionally, the state of the environment (SOE) monitoring reports produced by regional councils might provide valuable information on the health of ecosystems and the presence of ESHs in different regions. NZ also has various tools and programmes which might aid in the monitoring and management of ESHs, including the Envirolink programme, which provides a range of tools such as the Estuarine Trophic Index (ETI) Tool, Urban water quality tool, and eco sediment guideline value tool, among others. Council special interest groups (SIGs) and other data gathering initiatives might also provide additional information on the presence and effects of ESHs in the environment.

1.5 Determination of estrogenic steroid hormones

Methods available to determine steroid hormones include gas chromatography (GC) or liquid chromatography (LC) (Gunatilake *et al.*, 2013; Hanselman *et al.*, 2006) coupled with mass spectrometry (MS), usually with prior isolation of the ESH from the matrix. For a mixture of estrogens in a matrix, total estrogenic activity can be tested using *in vitro* assays such as the E-screen (Gadd *et al.*, 2010b; Tremblay *et al.*, 2018), binding assay (Sarmah *et al.*, 2006), enzyme-linked immunosorbent assay (ELISA) and a yeast estrogen screen (YES) (Zhao *et al.*, 2009).

The most cost-effective method is to initially undertake activity screening of samples which might contain a large number of compounds (Beresford *et al.*, 2000). The screening can be done relatively quickly, normally by an *in vitro* assay (Beresford *et al.*, 2000; Voulvoulis & Scrimshaw, 2003). The assay analysis will confirm the existence of estrogenic chemicals and if the test was found to be positive, chemical analysis can be undertaken to identify the present of individual EDCs (Voulvoulis & Scrimshaw, 2003).

Another approach is using the activity assay methods to guide chemical analysis methods. The assay results provide a measure of total estrogenic activity, which can be compared with the sum of the estrogenic equivalent activity calculated from the measured concentrations of individual EDCs and their corresponding bioassay specific estradiol equivalent factors (EEQ). This approach has been used in a number of previous studies (Gadd *et al.*, 2010b; Sarmah *et al.*, 2006; Tremblay *et al.*, 2018).

Chemical analysis of EDCs has some challenges, especially when the sampling involves a complex matrix such as dairy effluent that may contain many compounds that can interfere with the analysis (Gunatilake *et al.*, 2013; Hanselman *et al.*, 2006; Zhao *et al.*, 2009). The chemical analysis for testing steroid hormones in dairy effluent and solids uses either GC-MS or LC-MS instruments (Gadd *et al.*, 2010b; Hafner *et al.*, 2017; Hanselman *et al.*, 2006; Liu *et al.*, 2012b; Sarmah *et al.*, 2006; Tremblay *et al.*, 2018; Zhang *et al.*, 2014b). Both LC-MS and GC-MS methods are multi-residue techniques that are suited to determining several components at the same time. Many of the current studies analysing steroid hormones use GC-MS to measure free parent estrogens, such as 17α-E2, 17β-E2, and E1, following chemical derivatisation (Gadd *et al.*, 2010b; Hanselman *et al.*, 2006; Sarmah *et al.*, 2006; Tremblay *et al.*, 2018), while the more polar and labile conjugated estrogens are analysed using LC-MS-MS for higher sensitivity and specificity (Gadd *et al.*, 2010b; Zhang *et al.*, 2014b).

To ensure reliable analysis, preservation, filtration, and purification/clean up steps of raw sample extracts are required before derivatisation and/or instrumental analysis (Gunatilake *et al.*, 2013; Hanselman *et al.*, 2006; Sarmah *et al.*, 2006; Socas-Rodríguez *et al.*, 2017). The method used in this research was GC-MS for both free and conjugated ESHs. Details regarding the preparation steps and the chemical analytical methods and quality assurance used in this research are presented in Chapters 2 and 3.

1.6 Research Scope and Justification

1.6.1 Agricultural and environmental aspects

During recent years, the approach to disposal of effluent, both domestically and internationally has involved applying animal waste or sludge bio-solids back onto the land (U.S. Environmental Protection Agency, 2001; Dairy NZ, 2014; Adeel *et al*., 2017). The rationale driving this approach was the realisation that the beneficial nutrients contained in dairy shed effluent promoted superior growth of grass (Manono *et al*., 2016; Fan *et al*., 2017), as well as reduced rates of nutrient leaching into ground water compared to inorganic fertilisers (Fan *et al*., 2017). However, these effluents contain significant quantities of steroidal hormones, which are naturally excreted by cows (Sarmah *et al*., 2006; Gadd *et al*., 2010; Sim *et al*., 2011) and which, even in small concentrations as low as parts per trillion, have an impact on human, animal and aquatic life in terms of reproductive health, sex ratio imbalances and hormone-related cancers and disorders (Gomes and Lester, 2003; World Health Organization, 2012; Adeel *et al*., 2017). Steroidal hormones in effluent discharged onto land may accumulate and percolate through the soil into the ground water or run off in surface water and enter waterways (Steiner *et al*., 2010; Mina *et al*., 2017; Tremblay *et al*., 2018). It is clear that monitoring and reduction of ESH in effluent is necessary.

Domestically, the dairy industry and regional authorities have encouraged dairy farmers to manage the dairy shed and feed pad effluent using a farm dairy effluent system. The farm dairy effluent system includes many different configurations. Farmers can select the effluent system according to their financial requirements, the farm's future intentions, and operational and soil conditions, as long as they adhere to the regional council restrictions. These restrictions are specific to every regional authority and normally include maximum effluent application depth and rate, and maximum nutrient loading, along with other measures such as sufficient effluent storage during wet conditions, properly sealed pond/s and no irrigation near water courses. However, little is known about the performance of any of the dairy farm effluent systems, particularly covered anaerobic ponds (CAPs), in removing emerging contaminants such as ESHs. The absence of advanced dairy treatment systems such as enhanced aerobic biological processes makes the dairy effluent the

highest contributor of steroidal hormone contamination to the NZ environment, and thus a risk both to humans and other organisms.

1.6.2 Research aspects

Currently there is an overall gap in research knowledge associated with as the environmental impact of ESHs in dairy shed effluent. Science and regulatory organisations worldwide are required to collect more information regarding the testing methods, occurrence, fate and removal of EDCs in animal and human waste (Ministry of the Environment, 2010; World Health Organization, 2012). The research described in this thesis contributes to an increased understanding of ESH in dairy effluent and their fate and could be used to inform regulations and practices regarding the management of these chemicals as follows:

1. Testing method: Chemical methods to analyse the free and conjugated ESHs in both dissolved and solid phases of DSE were developed and verified.
2. Occurrence: A longitudinal study was conducted to identify the levels of ESHs present in treated effluent and sludge, and their DSE source.
3. Fate: A longitudinal study was conducted to understand how ESHs are transported and degraded in a DSE treatment system, a covered anaerobic pond.
4. Removal: A longitudinal study and experimental work were conducted to identify a cost effective and farm friendly method for removing ESHs from DSE, as well as preventing it reaching the environment.

1.6.3 Research scope

This research focussed upon steroid hormones conjugated and unconjugated and their metabolites in dairy shed effluent. These have already been demonstrated to be a problem in the NZ ecosystem (Gadd *et al.*, 2010b; Tremblay *et al.*, 2018). The research characterised and quantified the ESHs released from a 550 dairy cow farm milking shed and feed pad, and within the sludge and effluent of the CAP. Following characterisation and quantification, adsorption of the ESHs in both solution and real sample by powdered biochar was investigated. Ultimately the data gathered from the analysis work and kinetic and adsorption trials was used to feed a model that was designed to simulate the performance of an effluent treatment system comprised of covered anaerobic and storage ponds with and without upgraded treatment by powdered biochar. The model was used to assess the treatment performance and potential environmental implication and provide recommendations for future work (Chapter 7).

This research aims to provide answers to the following overall questions. Sub questions and objectives derived from these research questions are mentioned in each individual research chapter (Chapters 2 – 6).

1. What are the quantities and forms of ESHs present in dairy farm effluent?
2. What is the fate of ESHs in CAP dairy farm effluent treatment systems?
3. Is it possible to improve the performance of an on-farm dairy effluent treatment system in removing ESH loads by using biochar made from waste residue from the timber industry?
4. What is the efficacy of a dairy farm-based CAP treatment system to transform and remove ESHs?

1.7 Thesis Structure

This thesis is divided into six further chapters. Chapters 2 to 6 are research chapters, and the final chapter presents general conclusions and recommendations. The research chapters are presented in this thesis in a way that one piece of research provides the basis for the following research work. Each research chapter includes its own associated introduction (literature review), materials and methods, results and discussion, and conclusion sections and are formatted in a way that can be easily transferred into a manuscript for publication.

A brief description of the content included in each chapter will be presented below.

Chapter 2: Ignoring the solid phase significantly underestimates free ESHs in dairy shed effluent and effluent treatment systems – This chapter presents the results of a longitudinal study investigating the fate and transformation of the free ESHs of a CAP / anaerobic digestion dairy effluent treatment system by conducting a chemical analysis of the free ESHs in the CAP influent, effluent, and sludge in both dissolved and solid phases. The literature review includes information concerning dairy farming as a principal source of ESHs into the environment, the ability of ESHs to reach water sources, the physicochemical properties of the most abundant free ESHs and the characteristics of CAP as animal wastewater treatment system. This research required the development and refinement of an analytical method to analyse the free ESHs in the dissolved and solid phases of dairy effluent and sludge.

Chapter 3: The importance and fate of the conjugated ESHs in dairy shed effluent and an effluent treatment system – This chapter presents the results of a longitudinal study investigating the fate and transformation of the conjugated ESHs of a CAP / anaerobic digestion dairy effluent treatment system by conducting a chemical analysis of the conjugated ESHs in the CAP influent, effluent and sludge in both dissolved and solid phases. The literature review includes information regarding the different types of conjugated ESHs associated with dairy cows, the physicochemical properties, and characteristics of the conjugated ESHs and the removal and transformation of conjugated ESHs during wastewater treatment processes. The literature review also discusses the different methods to analyse the conjugated ESHs. This research included the validation

work of a new commercial enzymatic deconjugation product and required the development and refinement of an analytical method to deconjugate the conjugated ESHs in the dissolved and solid phases of dairy effluent and sludge so that the conjugated ESHs could be analysed (as free) using the analytical method developed and presented in Chapter 2.

Chapter 4: Sorption of ESHs on NZ grown *Pinus radiata* powdered biochar – This chapter presents the results of the characterisation of the biochar used to adsorb the ESHs, and clean water adsorption and kinetic studies. The literature review presents information regarding adsorption as a mechanism to remove ESHs, kinetic and isotherm adsorption, characterisations of different adsorbents and the pyrolysis system and production of the powdered biochar. This research included the preparation and analysis of a selected biochar to be used to adsorb ESHs, determination of powdered biochar to solution ratio, kinetic and isotherm experiments and calculation of adsorption and distribution coefficients. The analytical method developed in Chapter 2 was used in this paper to analyse the ESHs adsorbed onto the powdered biochar.

Chapter 5: Sorption of ESHs by dairy shed effluent dosed with powdered biochar – This chapter presents a preliminary investigation into the adsorption of ESHs by dairy shed effluent dosed with powdered biochar. The literature review includes information regarding the inorganic and organic materials found in dairy shed effluent, adsorption interference mechanisms, common adsorption pre-treatment methods, anaerobic digestion system and the benefits and usages of biochar. Similar to Chapter 4, this paper includes kinetic and isotherm experiments, calculation of adsorption and distribution coefficients and the use of the analytical method developed in Chapters 2 and 3.

Chapter 6: Modelling the efficacy of a dairy farm based CAP treatment system to transform and remove ESHs – This chapter presents modelling of ESH removal capabilities of a dairy farm effluent management system which includes a dairy shed and feed pad, effluent sump, a CAP and a storage pond designed to recover the treated effluent and sludge to fertilise the farm pasture, as well as an estimated performance of an improved effluent treatment system based on the treatment method and the research results presented in Chapter 4 and 5. The literature review includes details regarding the

NZ dairy farming waste loads and dairy farm operation protocols and treatment systems. It provides the results reported by previous studies assessing the treatment capabilities of different treatment systems to remove ESHs and the different removal mechanisms of ESHs. This research included additional estrogenic steroid hormone analysis work and the development and testing of a model.

Chapter 7: Conclusions and Recommendations – This chapter provides conclusions with respect to the overall objective of the research as well as presenting recommendations for future research.

Chapter 2:
Ignoring the solid phase significantly underestimates free estrogenic steroid hormones in dairy shed effluent and effluent treatment systems

Previous studies investigating the fate and concentration of estrogenic steroid hormones (ESHs) in dairy shed effluent (DSE) treatment systems have focussed solely on the dissolved phase and ignored the solid phase. By doing so, these studies have ignored a substantive source of, and sink for, ESHs within dairy shed effluent treatment systems. The main objective of this study is to provide new insights and perspectives on the distribution and fate of ESHs beyond that of previous studies by measuring the concentration of free ESHs in both dissolved and solid phases during treatment in a covered anaerobic pond (CAP).

2.1 Introduction

The endocrine disrupting impacts of ESHs within aquatic ecosystems and human health are well recognised and documented (Sumpter, 1995; Barber *et al*., 2011; Bergman, 2013). Municipal wastewater effluent and animal wastes are the two largest sources of ESHs to the environment (Hanselman *et al*., 2003; Hutchins *et al*., 2007). Dairy cows are the largest source of agricultural sourced endogenous steroid hormones entering the environment (Lange *et al*., 2002; Hanselman *et al*., 2003; Kolodziej *et al*., 2004), excreting larger quantities of ESHs than swine or chicken (Zhang *et al*., 2014). Dairy cows are estimated to contribute around 79% of total ESHs released by farmed animals in the European Union and 90% in the United States (Lange *et al*., 2002; Kolodziej *et al*., 2004).

Previous studies in New Zealand (NZ) identified dairy farm effluents as the principal source of potent biologically active ESHs entering the NZ environment, and DSE in NZ has been demonstrated to contain higher concentrations of ESHs compared to effluents from piggeries,

goat farms, or municipal wastewater (Sarmah *et al*., 2006; Gadd *et al*., 2010a; Gadd *et al*., 2010b).

ESHs, which have been deposited or discharged onto land via direct faecal and urinary deposits, irrigation using treated effluent, or land application of pond sludge or dewatered manure, can leach through soil into groundwater (Arnon *et al*., 2008; Steiner *et al*., 2010) or migrate with surface runoff into adjacent waterways (Kjaer *et al*., 2007; Mansell *et al*., 2011). Consequently, intensive dairy farming has been demonstrated to be a significant source of ESHs in streams and groundwater in freshwater catchments in NZ (Tremblay *et al*., 2018), and other countries (Matthiessen *et al*., 2006; Arnon *et al*., 2008; Alvarez *et al*., 2013).

In 2017, more than 17,550 square kilometres of land were used for dairy farming in NZ (Ballingall and Pambudi, 2017), supporting 6.4 million dairy cows in 2018 (StatsNZ, 2019) and generating approximately 380,000 m^3 of captured dairy effluent per day (Heubeck. *et al*., 2014). Dairy farming operations are increasingly challenged to treat and manage the high volumes of dairy cow waste captured from milking, feeding, and sheltering systems.

The naturally occurring endogenous steroids 17α-estradiol (17α-E2), 17β-estradiol (17β-E2), and estrone (E1) are the most abundant ESHs in dairy farm waste (Sarmah *et al*., 2006; Hutchins *et al*., 2007; Zheng *et al*., 2008; Gadd *et al*., 2010b). The physicochemical properties of E1, 17α-E2, and 17β-E2 (Figure 2-1) are such that they distribute between the dissolved and solid phases due to hydrophobic partitioning to particulate organic matter (POM) (Scrimshaw and Lester, 2003; Sarmah *et al*., 2008).

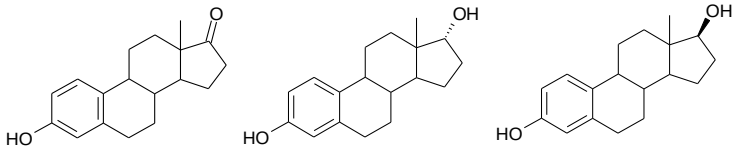

Estrogenic steroid hormone	Estrone	17α-estradiol	17β-estradiol
Formula	$C_{18}H_{22}O_2$	$C_{18}H_{24}O_2$	$C_{18}H_{24}O_2$
Molecular weight (g/mol)	270.37	272.39	272.39
Aqueous solubility (mg/L at 25°C)[A]	0.8	3.90	3.90
Log Kow[B]	3.43	3.94[C]	3.94
EEQ[D]	0.02	0.01	1.00

[A] (Kennedy and Jin, 2006), [B] (Ying et al., 2002), [C] Assumed to be similar to 17β-estradiol, [D] Estrogen equivalents from ER Calux (Kolkman *et al*., 2013).

Figure 2-1: Physicochemical properties of the most common estrogenic steroid hormones in dairy farm effluent.

Chapter 2: Ignoring the solid phase significantly underestimates free estrogenic steroid hormones in dairy shed effluent and effluent treatment systems

Treated dairy farm effluent and sludge have a relatively high solids content (0.3 % to 6 %) enriched with organic matter (OM) (40 % to 60 %), (Fyfe *et al*., 2016). This OM, derived from plant residues, proteins, fats, carbohydrates, lignin, celluloses, humic material, and microorganisms (Page *et al*., 2014; Fyfe *et al*., 2016) provides a diverse organic substrate for hydrophobic sorption and retention of ESHs (Lee *et al*., 2003; Bonin and Simpson, 2007).

Previous studies have investigated the concentration and fate of ESHs in dairy shed effluent (DSE), treated pond effluent, manures, and animal waste (Raman *et al*., 2004; Hutchins *et al*., 2007; Gadd *et al*., 2010b). Most studies reporting the fate of ESHs during DSE treatment have investigated multiple pond or lagoon systems (Kolodziej *et al*., 2004; Raman *et al*., 2004; Sarmah *et al*., 2006; Hutchins *et al*., 2007; Zheng *et al*., 2008) or advanced pond treatment systems (Gadd *et al*., 2010b). In comparison, little is known about the fate of ESHs in DSE during treatment in anaerobic ponds or lagoons, and particularly in CAPs that are being increasingly used to recover methane for on-site energy co-production. Similarly, relatively few studies have analysed ESHs in both the liquid and solid phases of DSE and dairy farm effluent treatment systems (Zhang *et al*., 2014; Noguera-Oviedo and Aga, 2016). The growing practice of recycling pond sludges and treated effluent recovered from DSE to land in NZ as a source of soil nutrients means a previously unquantified and significant source of ESHs entering the environment is likely to have escaped attention.

This chapter describes how to address this knowledge gap by:

- measuring the concentration of free ESHs in the dissolved and solids phases of influent, sludge, and effluent of a CAP treatment system.
- calculating the distribution of free ESHs between solids and dissolved phases of CAP influent, sludge, and effluent.

2.2 Materials and Methods

2.2.1 The study farm

Samples of influent, sludge and effluent were obtained from a CAP effluent treatment system (ETS) in a 200-hectare dairy farm supporting a herd of 550 dairy cows in the Waikato Region of NZ. Photographs of the dairy shed, feed pad and effluent collection sump, CAP and sludge port, CAP outlet chamber, and storage pond are presented in Figure 2-2.

(a) Dairy Shed with milking yard in the foreground

(b) Feed pad displaying feeding trough running through the centre and combined faecal and urine waste

(c) Sump – collection point of Influent sample to the CAP

(d) CAP and collection port for obtaining sludge samples (arrow)

(e) CAP outlet chamber – collection point of effluent samples

(f) CAP effluent storage pond

Figure 2-2: Photographs of the farm effluent treatment systems and sampling points

During and after milking the dairy shed is washed with bore water, the milking yard with recycled green water from the treated effluent storage pond (approximately 4 m^3/day) and both are collected in a flood wash tank. The contents of the flood wash tank are used to wash cow manure and urine from a feeding pad (1,400 m^2) throughout the year. Approximately 39 m^3/day of combined milking shed and feeding pad wash water (described hereafter as DSE) is collected daily in a mechanically mixed sump (50 m^3) and pumped once or twice a day into the CAP treatment system (1,500 m^3, 3.75 m deep, approximately 35 days retention time) designed to capture methane for energy production. The treated effluent from the CAP discharges into a 5,000 m^3 lined storage pond from whence it is spray irrigated onto farm pasture. The sludge retained within the CAP accumulates for 10 to 16 months before it is spread onto farm pastures as a nutrient source.

2.2.2 Sample collection and preservation

Grab samples of DSE, sludge and effluent were collected from March to November 2018 from the influent sump (A), CAP sludge port (B) and outlet of the CAP (C) (Figure 2-3) after morning milking and washing of the dairy shed and feed pad. The influent within the sump was mixed by a mechanical stirrer for five minutes before collecting a sample with a stainless-steel bucket. Sludge was sampled from the CAP at the de-sludge pipe located halfway along the side of the pond and 300 mm above the pond floor. The CAP effluent was collected with a stainless-steel bucket from the outlet weir.

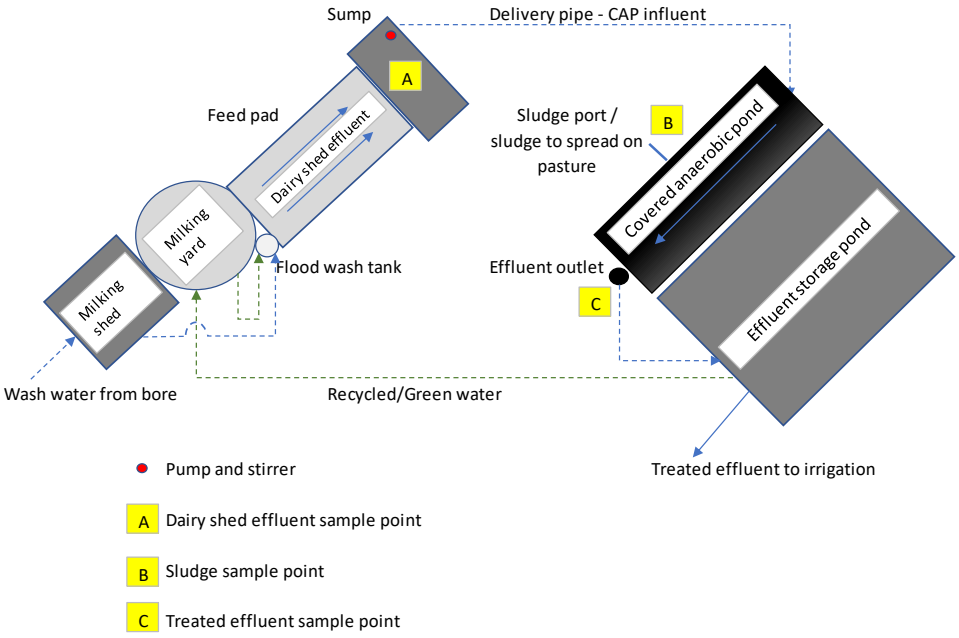

Figure 2-3: A plan view of the study farm CAP effluent treatment system and sampling points

Each sample was mixed, pH and temperature were measured, and the sample transferred into pre-cleaned 2-L glass Schott bottles and 1-L polyethylene bottles and transported on ice to the laboratory. The 1-L samples were analysed for physical and chemical parameters. The 2-L samples were preserved within 4 hours of collection by adjusting the pH to 2.5 with concentrated sulphuric acid. The acidified samples (~1.5 L) were transferred into 250 mL polyethylene centrifuge tubes and centrifuged in a Sorvall RC 5C Plus centrifuge (10 °C, 30 min,10,000 rpm). The supernatant was decanted and filtered through a glass microfiber filter (topped with a 5 mm layer of Hyflo Supercell C22 filter aid) and collected in a glass Schott bottle (1 L) and subsequently stored at 4 °C before extraction of ESHs (within 20 hours of collection). The pellets of solids were transferred into glass jars, capped, frozen (-20 ^{o}C), lyophilized (Labconco FreeZone 12 plus freeze dryer) and stored at -20 ^{o}C.

2.2.3 Chemicals and materials

All solvents (HPLC grade), glass microfiber filters (GE Healthcare GF/F, 47 mm diameter), Hyflo Supercell C22 filter aid (VWR Chemicals) were supplied by ThermoFisher Scientific, NZ. Deionized water was supplied by a Milli-Q Millipore Integral 5 system. DL-Estrone-13,14,15,16,17,18-13C6 (^{13}C6-E1) and DL-Estradiol-13,14,15,16,17,18-13C6 (^{13}C6-E2) with an isotopic purity>99 %, were supplied by Cambridge Isotope Laboratories, 17β-estradiol-

2,4,16,16-d4 (17β-E2-d4) and Estrone-2,4,16,16-d4 (E1-d4) (isotopic purity>98 %) were supplied by CDN Isotopes, and 17α-E2, 17β-E2 and E1 (purity>99 %) were supplied by Sigma Aldrich NZ. General purpose Ottawa sand (20-30 mesh), 19 mm diameter cellulose and GF/F filters (Dionex), and Hydromatrix (Dionex) used for accelerated solvent extraction (ASE), together with di-potassium hydrogen orthophosphate and monopotassium phosphate (both Ajax FineChem, >99 %) were obtained from ThermoFisher NZ Ltd. Waters Oasis HLB solid-phase extraction (SPE) cartridges (6 mL/500 mg and 12 mL/1 g) were obtained from Alphatech Systems Ltd NZ. Biotage Isolute Florosil (6 mL/1 g and 15 mL/2 g) cartridges and bulk aminopropyl (NH2) sorbent were obtained from ThermoFisher NZ Ltd. Granular anhydrous sodium sulphate was obtained from Merck NZ. *N*-Methyl-*N*-(trimethylsilyl)-trifluoroacetamide (MSTFA) (UCT SMSTFA-0, Selectra-Sil) was supplied by PM Separations Australia. Triethylamine (purity>99 %), ammonium iodide (purity >99 %) and 2-mercaptoethanol (purity>98 %) were obtained from Sigma Aldrich NZ.

2.2.4 Sample preparation and SPE

The method used to extract and analyse free ESHs in the solid and dissolved phases of the samples is summarised in Figure 2-4.

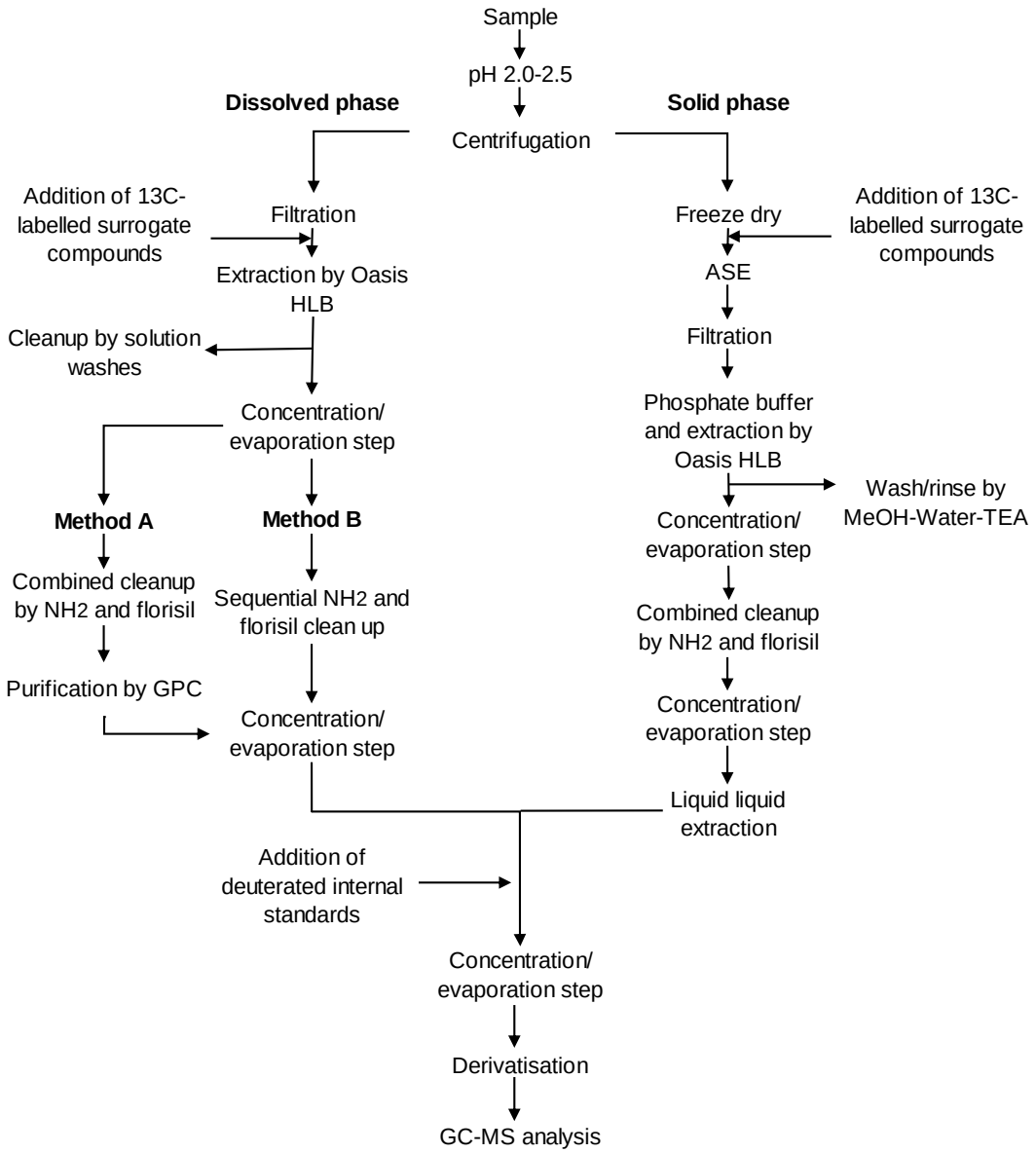

Figure 2-4: Schematic diagram of the procedure for isolation and analysis of free steroid hormones in dissolved and solids phases

2.2.5 Dissolved phase extraction and clean-up

Two methods (A and B) were applied to extract ESHs from the dissolved phase.

2.2.5.1 Dissolved phase extraction and clean up (March and April Samples – Method A)

All glassware and hardware used in the preparation of samples was rinsed twice sequentially with methanol, acetone, and dichloromethane (DCM), and dried before use. The filtered supernatant (dissolved phase, 1 L) was spiked with a surrogate recovery standard of ^{13}C6-E1

and ^{13}C6-E2 at an equivalent concentration of 100 ng/L. ESHs in the liquid effluent samples were extracted by SPE using the method of Gadd *et al*. (2010b). The effluent samples were passed through previously conditioned Oasis HLB SPE (500 mg, 6 mL) cartridges via Teflon transfer lines at a flowrate of 5–10 mL/min together with Milli-Q water rinses (3 x 10 mL) of the sample bottle, polytetrafluoroethylene (PTFE) transfer lines and Oasis Hydrophilic-Lipophilic- Balanced (HLB) cartridge. The Oasis HLB SPE cartridges were dried under vacuum to remove the bulk of residual water. The SPE cartridges were sequentially rinsed with solutions of MeOH/Acetic Acid/ Milli-Q water (8 mL, 30:2:68 *v/v*), MeOH/Acetic Acid/ Milli-Q water (8 mL, 60:2:38 *v/v*), MeOH/Ammonium Hydroxide/Milli-Q water (8 mL, 30:2:68 *v/v*) and MeOH/Ammonium Hydroxide/Milli-Q water (5 mL, 75:2:68 *v/v*) to remove highly polar co-extracted interferences and dried under full vacuum. Clean-up columns were prepared according to Burkhardt *et al*. (2005) by adding bulk aminopropyl adsorbent (NH_2, 0.5 g) onto the bed of a Florosil SPE cartridge (1 g, 6 mL), topping it with a polypropylene SPE frit to which a ~3cm layer of anhydrous granular sodium sulphate (dried overnight at 450 °C) was added. The combined clean-up column was washed with acetone (15 mL) and dried under vacuum before use. The clean-up columns were connected to the outlet of the Oasis HLB SPE cartridges using a Teflon connector and mounted in a SPE vacuum extraction manifold. ESHs were eluted from the Oasis SPE cartridges and through the Florosil-NH_2-sodium sulphate clean-up columns with a binary mixture of DCM/methanol (30 mL, 95:5 *v/v*). The purified column eluent was collected in 40 mL amber glass EPA vials, evaporated to dryness under a stream of oxygen-free nitrogen gas (30 °C) and redissolved in DCM/methanol (95:5 *v/v*). Gel permeation chromatography (GPC) clean-up was performed using a Shimadzu 10A HPLC fitted with a large volume injector and fraction collector. The sample extracts (1.5 mL) were injected onto a Phenogel pre-column (21 mm x 50 mm, 100 A^o) and GPC column (21 mm x 300 mm, 100 A^o) connected in series and eluted with a binary solvent mixture of DCM/methanol (95:5, *v/v*) at a flow rate of 2.5 mL.min^{-1} at room temperature. The fraction of GPC eluent corresponding to the target ESHs was collected in 22 mL glass vials. The GPC purified extracts were evaporated under a stream of oxygen-free nitrogen gas (30 °C), redissolved in acetone (1 mL) using DCM/MeOH (95:5, *v/v*) and stored at 4 $^{\circ}$C in a refrigerator prior to derivatisation.

2.2.5.2 Dissolved phase extraction and clean up (May to November Samples – Method B)

ESHs in the liquid effluent samples were extracted by passing the samples through conditioned Oasis HLB SPE (500 mg, 6 mL) cartridges. After drying under vacuum the SPE columns were rinsed with a solution of methanol/water containing triethylamine (12.5 mL, 60:40 *v/v* methanol/milli-Q water with 0.005M TEA) (Labadie and Budzinski, 2005). The cartridges were dried under vacuum and the ESHs eluted with methanol (20 mL), evaporated by rotary evaporation (Büchi Rotavapor R-200), and redissolved in ethyl acetate and methanol (4 mL, 4:1 *v/v*) (Labadie and Budzinski, 2005). The ethyl acetate/methanol extracts were purified by elution through aminopropyl (NH_2, 0.5 g) cartridges (Labadie and Budzinski, 2005), dried under nitrogen gas (30 °C) and redissolved in hexane and dichloromethane (5 mL, 3:1 *v/v*). This extract was purified by eluting through Florosil (1 g, 6 mL) (Zhang *et al*., 2014) cartridges with acetone and hexane (12 mL, 3:1 *v/v*) (Zhang et al., 2014). The eluent was dried under nitrogen gas at 30 °C, re-dissolved in acetone (2 mL) and stored at 4 $^{\circ}$C in a refrigerator prior to derivatisation.

2.2.6 Solid phase extraction and clean-up

Lyophilised solids (1.0 g) were combined with hydromatrix (7 g) and homogenised in an IKA A11 blender. The homogenised mixtures were packed into 33 mL stainless steel ASE cells containing cellulose and glass microfiber filters in the base and the void volume filled with pre-cleaned Ottawa sand. A cellulose filter was inserted in the top and the cell sealed with the stainless-steel screw cap. Each cell was sequentially extracted using a 50/50 mix of Isopropyl propanol (IPA)/water, followed by an 80/20 mix of IPA/water, both at a temperature of 120 °C and pressure of 1850 psi. The sequential extracts were collected in separate 60 mL ASE glass vials, cooled to room temperature and filtered through a 47 mm glass microfiber filter topped with a layer of Hyflo Supercell C22 and combined in a solvent cleaned 1-L glass Schott bottle. Each of the ASE sample vials was rinsed with phosphate buffer (4 x 25 mL, pH 7, 0.4 M) that was added to the solvent extract and adjusted to a final volume of 650 mL with phosphate buffer. The phosphate buffer sample solutions were extracted by SPE using preconditioned Oasis HLB cartridges (1 g). The HLB SPE columns were rinsed using a methanol/water mix (25 mL, 60:40 *v/v*).) containing 0.005 M TEA to remove polar co-extracted matrix components (Labadie and Budzinski, 2005). The HLB SPE columns were connected in series to a Florosil cartridge (2 g, 15 mL) topped with aminopropyl (0.5 g) (Burkhardt *et al*., 2005) and ~3 cm

layer of anhydrous granular sodium sulphate (dried overnight at 450 °C). The connected cartridges were mounted in a SPE vacuum extraction manifold and the ESHs simultaneously eluted and purified by passing through DCM/methanol (30 mL, 95:5 *v/v*). The collected eluent was dried under nitrogen gas (30 °C), redissolved in acetonitrile (€) (5 mL), and partitioned against hexane (3 x 10 mL) to remove extraneous co-extracted material (Chen *et al*., 2012; Zhang *et al*., 2014). The purified ACN extract was dried under nitrogen gas (30 °C), redissolved in acetone (2 mL), and stored at 4 ˚C prior to derivatisation.

2.2.7 Quality assurance

All samples including quality assurance (QA) blank and spike samples were spiked with a surrogate standard mixture (^{13}C6-E1 and ^{13}C6-E2), and the QA spiked recovery samples with a mixture of target ESHs. Each batch of dissolved phase samples (n = 8) included as QA samples: a milli-Q water (1 L) blank sample; and a milli-Q water (1 L) sample spiked with a mixture of target ESHs at a final spiked concentration of 100 ng/L each. All samples were spiked prior to extraction with surrogate recovery standards (^{13}C6-E1 and ^{13}C6-E2) at an equivalent final spiked concentration of 100 ng/L.

Each batch of solid samples (n=4) included a QA blank and QA spike recovery blank sample (both prepared with hydromatrix and Ottawa sand), and a duplicate solid sample for the validation of results. Each sample was spiked with surrogate standards (^{13}C6-E1 and ^{13}C6-E2) at an equivalent final spiked concentration of 100 ng/g and the QA spike recovery blank sample with a mixture of target ESHs at an equivalent final spiked concentration of 500 ng/mL before extraction.

For determining overall recovery of the extraction method, a comparative standard was prepared by dispensing corresponding aliquots of the surrogate standard (^{13}C6-E1 and ^{13}C6-E2) and target compound (17α-E2, 17β-E2, E1) spike mixes into a reacti-vial for the calculation of their recovery.

Calibration solutions were freshly prepared with each batch of samples for derivatisation and analysis. Eight calibration standards were prepared at concentrations of 5, 10, 25, 50, 100, 250, 500, and 1,000 ng/mL. An internal standard solution containing 17β-E2-d4 and E1-d4 was

added to sample extracts, comparative standards, and calibrations standards prior to derivatisation to give a final concentration of 250 ng/mL.

2.2.8 Derivatisation and Gas Chromatography Mass Spectrometry analysis

The sample and QA extracts, comparative recovery standards, and calibration standards were dried to approximately 0.5 mL under nitrogen (30°C), internal standard solution added (equivalent to 250 ng each of 17β-E2-d4 and E1-d4) and evaporated to dryness under nitrogen. All samples were derivatised using an activated MSTFA/TMSI mix (30 µL for dissolved phase sample extracts and 100 µL for solid phase sample extracts) and incubated at 65 °C for 40 minutes as described by Budzinski *et al*. (2006). During derivatisation the samples were vortexed twice to ensure the reaction mixtures were fully mixed. The derivatised sample extracts were adjusted to a final volume of 0.5 mL or 1 mL with *iso*-octane, vortexed and transferred into Gas Chromatography-Mass Spectrometry (GC-MS) vials.

The derivatised sample extracts and calibration solutions were analysed using an Agilent 6890 gas chromatograph with an Agilent 5975 mass selective detector (MSD) and ATAS Multipurpose auto-sampler. Aliquots of samples and calibration standards (1 µL) were injected into an Agilent split/splitless inlet held at 280 °C. The inlet was operated in pressure pulsed injection mode (30 psi for 1.1 mins) with a splitless time of 1 minute and split flow of 50 mL/min The oven temperature was programmed at 90 °C (1.5 min. hold); 20 °C/min.→130 °C; 4 °C/min→232 °C; 50 °C/min→320 °C (7 min. hold) for a total run time of 37.7 min. The injected samples were separated on an Agilent J&WDB-5MS capillary column (30 m x 0.25 mm x 0.25 µm) using helium as carrier gas at a constant flow of 1mL/min. The MSD was operated at 70 eV with a solvent delay of 6.5 minutes and ion source and quadrupole temperatures of 230 °C and 150 °C, respectively. Mass spectral data was acquired in synchronous scan/single ion monitoring mode using compound specific mass/charge ions (Table 2-1).

Table 2-1: ESH retention times, mass ions for identification and method detection limits

Compound	Retention time (min)	Internal Standard	T/Q1/Q2[A]	MDL[B]	
				Dissolved[C]	Solids[D]
17α-E2	9.982	E1-d4	**416**/285/417	1 ng/L	2 ng/g
E1-d4	10.134	NA[E]	**417**/402/418	NA	NA
^{13}C6-E1	10.154	E1-d4	**420**/404/421	1 ng/L	2 ng/g
E1	10.154	E1-d4	**414**/399/415	1 ng/L	2 ng/g
E2-d4	10.294	NA	**420**/287/421	NA	NA
^{13}C6-E2	10.308	E2-d4	**422**/288/423	1 ng/L	2 ng/g
17β-E2	11.308	E2-d4	**416**/285/417	1 ng/L	2 ng/g

A T is the target quantitation mass ion (in bold), Q1 and Q2 are the corresponding qualifier mass ions used for compound identification and quantification quality acceptance. **B** MDL = method detection limit. **C** dissolved phase of sample. **D** solid phase of sample, ng/gram dry weight solids. **E** NA = not applicable

Selected ion monitoring (SIM) data was used to identify and quantitate isotopically labelled and native ESHs. Residues of ESHs were quantitated by internal standard quantitation using Agilent Chemstation Data Analysis software. The quantified results were transferred into Excel spreadsheets to calculate the final concentrations of ESHs in the DSE and quality assurance samples, the recovery of surrogate standards, and recovery of target analytes from QA spike samples.

Method detection limits (MDLs) for both native and carbon-13 labelled ESHs were determined by adopting a minimum signal to noise ratio of 3:1 for the response of the compounds in chromatograms of the extracts of dissolved and solid phases of the ETS samples. The equivalent concentration of ESH corresponding to a peak with a minimum signal to noise ratio of 3 determined from the low concentration calibration standards, met the quality assurance acceptance threshold (± 20%) of the relative abundance ratios of qualifier mass ions. The MDLs for target ESHs (17α-E2, 17β-E2 and E1) and surrogate standards (^{13}C6-E1 and ^{13}C6-E2) in the dissolved and solid phase samples were 1 ng/L and 2 ng/g respectively (Table 2-1).

2.2.9 Other parameters

Temperature and pH were analysed on site using a Eutech pH 150 meter. Total solids (TS) (APHA 2540B) and volatile total solids (VTS) (APHA 2540E) were analysed by an external certified laboratory (Hills Laboratory). POM was determined by loss after ignition (Matthiessen *et al*., 2005) assuming the VTS was OM (Metcalf and Eddy, 2014). Particulate

organic carbon (POC) was calculated assuming OM contains 54 % organic carbon (OC) (Jimenez and Garcia, 1992; Nelson and Sommers, 1996).

2.2.10 Statistical analysis

Statistical differences between sample groups were identified using the student t-test (two-tailed and 95% confidence interval) in Excel.

2.2.11 Partitioning of ESHs between the dissolved and solids phases

Distribution coefficient (K_d) was calculated using Equation (1-1).

$$\mathrm{Kd} = \frac{C\ solids}{C\ dissolved} \tag{1-1}$$

Where K_d = distribution coefficient (mL/g), C_{solids} = concentration of ESHs in solid phase (µg/g), $C_{dissolved}$ = concentration of ESHs in dissolved phase (µg/mL).

Organic carbon partition coefficients (K_{oc}) were calculated using Equation (1-2).

$$\mathrm{Koc} = \frac{100}{\%OC} \times Kd \tag{1-2}$$

Where Kd = distribution coefficient (mL/g), K_{oc} = organic carbon normalised adsorption coefficient (mL/g) and %OC = organic carbon content (%).

2.3 Results and discussion

2.3.1 Physical and chemical parameters

The physical and chemical parameters of DSE samples are summarised in Table 2-2 (full data in the appendices, Table A-1). The pH of the CAP sludge and effluent (6.9) was within the recommended pH range for anaerobic digestion systems (Metcalf and Eddy, 2014). The anaerobic pond/sludge temperature (20 °C) was typical for the Waikato region. The TS concentrations in the CAP influent, sludge and effluent are comparable to those measured in conventional 2-stage dairy effluent pond treatment systems (Longhurst *et al*., 2000; Fyfe *et al*., 2016) and demonstrate 50% of the total solids (TS) from the influent was metabolised or settled as sludge. The 70% removal of volatile total solids (VTS) within the CAP is comparable to that of conventional 2-stage dairy effluent pond treatment systems (Fyfe *et al*., 2016). The reduced VTS/TS ratio in effluent (~37%) compared to influent (60%) within the CAP is consistent with the conversion of OM to methane and carbon dioxide.

Table 2-2: Physical and chemical parameters of CAP influent, sludge and effluent

Parameter	Units	Influent	Sludge	Effluent
pH		7.6 (0.5, n=5) [A]	6.9 (0.1, n=5)	6.9 (0.3, n=5)
Temp	°C	15.9 (3.4, n=5)	19.7 (7.1, n=5)	16.2 (3.8, n=5)
TS	mg/L	6950 (1554, n=4)	82020 (8458, n=2)	3450 (778, n=2)
VTS	mg/L	4175 (1072, n=4)	38380 (0, n=1)	1270 (85, n=2)
POM[B]	%	79 (4, n=6)	59 (6, n=6)	55 (17, n=5)
POC[C]	%	42 (2, n=6)	32 (3, n=6)	30 (9, n=5)

[A] values are expressed as (mean (SDev, n)). [B] particulate organic matter. [C] particulate organic carbon.

2.3.2 Quality assurance outcomes

No residues of the target free ESHs or carbon-13 labelled surrogate standards were detected in the QA blanks. The recovery of the surrogate standards ^{13}C6-E1 and ^{13}C6-E2 from solid and dissolved phase samples was within acceptable limits (59-122 %) (Table 2-3). There were no significant statistical differences (P range = 0.27 to 0.82) in the recovery of ^{13}C6-E1 and ^{13}C6-E2 between the three different samples of the dissolved and solid phases. The applied methods were therefore robust and performed consistently across a range of complex sample matrices.

Table 2-3: Recovery of target free ESHs (17α-E2, 17β-E2 and E1) and surrogate standards (^{13}C6-E1 and ^{13}C6-E2) from dissolved and solid phase samples

Recovery from dissolved samples					
	17α-E2 [A]	**17β-E2 [A]**	**E1 [A]**	**^{13}C6-E2 [A]**	**^{13}C6-E1 [A]**
Influent				59 (15.8, n=5) [B]	81 (36.5, n=6)
Sludge				76 (21.1, n=5)	74 (9.7, n=6)
Effluent				64 (14.9, n=5)	91 (32.5, n=6)
Spiked Blank	92 (5.2, n=2)	79 (14.1.9, n=2)	74 (9.0, n=2)	76 (0.0, n=1)	81 (11.2, n=2)
Mean	92	79	74	69	82
Recovery from solid samples					
	17α-E2 [C]	**17β-E2 [C]**	**E1 [C]**	**^{13}C6-E2 [D]**	**^{13}C6-E1 [D]**
Influent				79 (16.9, n=6)	122 (26.0, n=4)
Sludge				92 (5.3, n=6)	108 (33.8, n=6)
Effluent				88 (1.7, n=6)	99 (35.4, n=4)
Spiked Blank	92 (10.9, n=5)	80 (8.3, n=5)	126 (55.5, n=5)	88 (4.5, n=5)	138 (61.5, n=4)
Mean	92	80	126	83	119

[A] spiked at 100 ng/L concentration. [B] values are expressed as (mean (%) (SDev, n)). [C] spiked at 400 ng/g concentration. [D] spiked at 100 ng/g concentration.

The mean recovery of ^{13}C6-E2 and ^{13}C6-E1 from dissolved phase samples (69 and 82 % respectively) were comparable to those previously reported for E2-d4 and E1-d4 in DSE (91 % for E2-d4 and 92 % for E1-d4) in DSE (Sarmah *et al*., 2006; Gadd *et al*., 2010b), and 17β-E2 and for E1 (125 % for 17β-E2 and 101 % for E1) in flushed dairy manure wastewater (Hanselman *et al*., 2006). The recovery of target ESHs from spiked Milli-Q water (Table 2-3) were similarly comparable to those reported by Gadd *et al*. (2010b) (70 to 96 %).

The recovery of target ESHs from solid phase samples was comparable to that of E1 and 17β-E2 (84±4.6 % for E1 and 67±2.4 % for 17β-E2) from cow, swine, and chicken faeces (Zhang *et al*., 2014), 17β-E2 from fresh swine manure (Combalbert *et al*., 2010), and E1 and 17β-E2 from activated sludge (75 % and 88 % respectively) (Chen *et al*., 2012). In conclusion, the QA data demonstrated that the analysis methods performed as well as those from previous studies measuring ESHs in complex animal wastes and treatment pond effluents. However, the precision and reproducibility of the measurements are uncertain due to the detected recovery range and its associated standard deviation. To attain a more reasonable level of certainty, a substantial augmentation in the number of measurements per sample is imperative. Regrettably,

such augmentation was precluded by the protracted time commitment necessitated for the analytical procedures.

2.3.3 Concentration of individual free ESHs in the dissolved and solid phases

A statistical summary of the concentration of individual and total free ESHs (ΣESH) in the dissolved and solid phases of samples is presented in Table 2-4 (full data and statistical summary can be found in the appendices, Table A-2 and Table A-3).

2.3.4 Concentration of individual free ESHs in the dissolved phase

The mean concentration for individual free ΣESH measured in the dissolved phase decreased in the order influent (1,230 ng/L) > effluent (949 ng/L) > sludge (786 ng/L).

Table 2-4: Mean (March -November 2018) mass (ng) of individual free ESHs measured in the dissolved and solid phases of 1 litre of raw influent, sludge and effluent of the CAP ETS.

	17α-E2	**17β-E2**	**E1**	**ΣESHs**
Influent (n=6)				
Dissolved	973 (21.7-2869)[A]	103 (7.04-242)	153 (5.19-415)	1230 (41-3526
Solids	1896 (166-4789)[B]	269 (115-241)	776 (320-2057)	2942 (630-5983)
Total	2869 (188-5854)	372 (122-657)	930 (325-2125)	4171 (671-7262)
Sludge (n=6)				
Dissolved	30.1 (21.4-38.9)	46.3 (33.5-64.9)	710 (561-881)	786 (621-975)
Solids	2566 (2028-3109)	5545 (3805-6947)	84705 (61528-116124)	92816 (67784-125887)
Total	2596 (2062-3133)	5591 (3851-7012)	85414 (62409-116895)	93601 (68759-126758)
Effluent (n=6)				
Dissolved	267 (4-782)	72.1 (3.11-143)	610 (43.7-1098)	949 (75.3-1606)
Solids	623 (9.04-1907)	245 (12.9-503)	2530 (90.7-4074)	3398 (113-5584)
Total	889 (12.5-2689)	317 (16.0-645)	3140 (160-5085)	4346 (189-7190)

[A] mass in ng in 1 litre is equivalent to ng/L concentration (mean (range min to max)). [B] mass in ng in 1 litre volume of sample calculated using the corresponding measured TS concentrations for influent, sludge and effluent samples.

The relative concentrations of individual ESHs in the dissolved phase of DSE entering the CAP (17α-E2 > E1 > 17β-E2) was consistent with previous analyses of DSE (Hanselman *et al*., 2006; Zheng *et al*., 2008; Gadd *et al*., 2010b; Noguera-Oviedo and Aga, 2016) (Table 2-5). In contrast, E1 was the predominant ESH in the dissolved phase of sludge and effluent samples with mean concentrations of 710 ng/L and 610 ng/L respectively.

Table 2-5: Reported concentration of free ESHs (ng/L) in the dissolved phase of different dairy cow effluent streams, treatment pond systems, and treated pond effluent

Sample description	17α-E2	17β-E2	E1	ΣESHs	Number [A]	Reference
Dairy shed effluent or treatment pond influent						
Dairy shed effluent	973 (21.7 – 2869) [B]	103 (7.04-242)	153 (5.19-415)	1230 (40.8-3526)	6	This study
Dairy shed effluent	2190 (2098-2283) [C]	194 (156-230) [C]	281 (262-298) [C]	2665	6	(Zheng *et al*., 2008)
Dairy shed effluent	1115 (110-11000)	26 (3-85)	87 (10-480)	1229 (199-11544)	19	(Gadd *et al*., 2010a)
Dairy shed manure waste	4525 (3527-5169) [C]	976 (951-1024) [C]	1528 (1293-1683) [C]	7029 (5771-7876) [C]	3	(Noguera-Oviedo and Aga, 2016)
Flushed dairy manure waste	2282 (1750-3270	643 (351-957)	879 (370-2356)	3804 (2742-5103)	5	(Hanselman *et al*., 2006)
Treatment pond or storage lagoon						
CAP	30.1 (21.4-38.9)	46.3 (33.5-64.9)	710 (561-881)	786 (621-975)	6	This study
Dairy CAFO lagoon	224 (177-283)	148 (110-168)	70.5 (56.6-79.7)	443 (362-531)	3	(Hutchins *et al*., 2007)
Dairy waste lagoon	NM [D]	N.D [E] – 9.5–[C]	75 - 650–[C]	75 - 660 [C]	2	(Kolodziej *et al*., 2004)
Dairy holding pond	3350 [C]	1624 [C]	8274 [C]	13248 [C]	3	(Raman *et al*., 2004)
Dairy waste lagoon	85 (79-90) [C]	89 (76-101) [C]	260(236-283) [C]	433 (391-474) [C]	6	(Zheng *et al*., 2008)
Treated effluent						
CAP	267 (3.50-782)	72.1 (3.11-142)	610 (43.7-1098)	949 (75.3-1606)	6	This study
Advanced pond system	760	310	580	1650	1	(Gadd *et al*., 2010a)
Dairy oxidation ponds	781 (N.D-1600)	76 (2-170)	228 (14-450)	1084 (16-1952)	8	(Gadd *et al*., 2010a)
Dairy oxidation ponds	305 (N.D-1028)	114 (N.D-331)	998 (N.D-3123)	1417 (N.D-4416)	7	(Sarmah *et al*., 2006)
Anaerobic digester	935 (569-1324) [C]	114 (78-137) [C]	2774 (1936-3548) [C]	3823 (2583-4999) [C]	3	(Noguera-Oviedo and Aga, 2016)

[A] number of samples analysed. [B] mean concentration (minimum to maximum concentration in brackets). [C] values estimated from published graphs.

[D] Not measured. [E] Not detected

The concentration of ESHs in the dissolved phase of DSE samples measured in this study are comparable to those previously reported in DSE in NZ by Gadd et al. (2010b), but considerably lower than those reported for flushed dairy manure wastewater (Hanselman *et al*., 2006; Noguera-Oviedo and Aga, 2016) and dairy shed manure waste (Hanselman *et al*., 2006; Noguera-Oviedo and Aga, 2016) in the United States of America (USA) (Table 2-5). The comparability of results between this study and that of Gadd *et al*. (2010b) can be attributed to the concurrence of months during which sampling took place. Furthermore, practices to wash and retain dairy cow waste from NZ milking sheds have not significantly changed over the twelve years between the two studies. The higher concentrations of ESHs measured in dairy shed manure and flushed dairy manure waste in the USA may be attributable to a month of intensive sampling in the US study, versus the 8-month period in the current study and Gadd *et al*. (2010b). This would be especially relevant if the intensive month of sampling corresponded with peak excretions of estrogenic hormones from the dairy herd associated with late pregnancy and calving. Another explanation is the use of blade scraping to collect dairy wastes in US milking parlours which reduces water use and produces DSE, which is more concentrated in ESHs.

To the best of our knowledge, our data provides the first measurements of free ESHs in sludge from a CAP system designed to treat DSE. The mean concentration of 786 ng/L for ΣESH that we measured in the dissolved phase of the CAP sludge is comparable to that previously reported in the dissolved phase effluents of single oxidation pond, two pond (anaerobic and facultative), and advanced pond systems treating DSE in NZ (Sarmah *et al*., 2006; Gadd *et al*., 2010a), in liquid wastes within dairy concentrated animal feeding operations (CAFO) system and waste lagoons (Kolodziej *et al*., 2004; Hutchins *et al*., 2007; Zheng *et al*., 2008) in the USA, and less than a dairy holding pond (Raman *et al*., 2004) and effluent of a dairy manure mixed-waste anaerobic digester (Noguera-Oviedo and Aga, 2016) in the USA (Table 2-5). For comparison, the mean concentration of ΣESH in the dissolved phase of sludge from an anaerobic lagoon treating swine waste was an order of magnitude greater at 7008 ng/L (Yost *et al*., 2013).

The reason for the disparity in the concentration of free ESHs in the dissolved phase of sludge from the CAP and holding ponds or lagoons treating dairy waste effluent is uncertain, but the

paucity of relevant studies, geographically disperse sites, different climatic conditions and variance of operational conditions are plausible reasons. Likewise, the similarity in concentration of ESHs in the dissolved phase of effluent from these different dairy waste treatment systems is perplexing but could result from common features of the ETS. The standardisation of on-farm milking practices produces similar quantities of waste, ESHs and water per cow entering DSE treatment systems. DSE treatment systems are predominantly designed to reduce and stabilise OM and not degrade ESHs that are fortuitously co-metabolised by bacteria. These treatment systems are typically passive, with no mechanical mixing, aeration, or temperature control, which limits the degradation of OM, and thereby ESHs. Furthermore, the contribution of conjugated forms of ESHs was not factored in this study. The contribution of the conjugated ESHs may vary depending on the treatment system and can influence the total load of free ESHs (Chapter 3). Consequently, the concentration of ESHs within on-farm DSE treatment systems between different countries is broadly similar.

The concentration of ESHs in the dissolved phase of the CAP effluent exceeded that in sludge on four of the six sampling events (appendices, Table A-2). The CAP accumulates solids for up to 16 months, during which POM concentrates and provides a substrate for the sorption of ESHs. These settled solids congeal at the pond base where the desludging pipe sampling point was located. The sampling point for CAP effluent at the outlet weir preferentially samples the "overlying" water layer of the pond which is relatively depleted in TS, (20 to 30 times less, appendices, Table A-1) This reduced concentration of TS in the CAP effluent increases the apparent concentration of ESHs in the dissolved phase, compared to that in the CAP sludge.

2.3.5 Concentration of individual free ESHs in the solids phase

A summary of the concentration (ng/g) of individual free ESHs measured monthly in the solids phase of samples from the CAP ETS is presented in Table 2-6.

Table 2-6: Concentration (ng/g) of individual free ESHs in the solid phase of raw influent, sludge, and effluent of the CAP ETS

Influent										
Compound	**Mar**	**Apr**	**Jul**	**Aug**	**Oct**	**Nov**	**Mean**	**Range[A]**	**Median**	**SDev [B]**
17α-E2	309	413	689	174	28.1	23.9	273	23.9-689	242	255
17β-E2	61.0	50.1	63.4	16.7	16.6	24.4	38.7	16.6-63.4	37.3	22.0
E1	71.3	59.3	108	89.0	46.0	296	112	46.0-296	80.2	92.9
ΣESHs	441	522	861	280	90.7	344	423	90.7-861	393	260
Sludge										
17α-E2	25.3	24.7	37.9	32.2	34.3	33.3	31.3	24.7-37.9	32.7	5.23
17β-E2	51.0	46.4	75.5	70.2	84.7	77.8	67.6	46.4-84.7	72.9	15.4
E1	750	1036	873	813	1416	1309	1033	750-1416	954	274
ΣESHs	826	1107	986	916	1535	1420	1132	826- 1535	1046	285
Effluent										
17a-E2	2.62	29.0	553	304	126	69.2	180	2.62-553	97.4	212
17b-E2	3.74	27.9	121	146	96.8	30.8	71.0	3.74-146	63.8	58.0
E1	26.3	428	944	690	1181	1131	733	26.3-1181	817	447
ΣESHs	32.6	485	1618	1139	1403	1231	985	32.6- 1618	1185	603

A minimum to maximum. **B** Standard deviation.

The concentration of individual ESHs in the solids of the influent decreased in the order 17α-E2 (273 ng/g), >E1 (112 ng/g), > 17β-E2 (38.7 ng/g). As expected, the mean concentration of ΣESHs in the solids phase of CAP sludge (1,132 ng/g) was considerably higher than in the DSE/influent. However, the consistently higher concentration of ΣESHs measured in the solids phase of the CAP effluent collected from July to November (1139 to 1618 ng/g) compared to the DSE/influent (90.7 to 861 ng/g) was unexpected.

TS and POC in the CAP effluent were significantly lower than the DSE/influent entering the CAP (Table 2-2). The observed reduction in VTS and the ratio of VTS/TS between the CAP effluent and DSE/influent samples indicates biologically labile OM is being consumed by the microbial biomass in the CAP. The residual POC will be more refractory and have an increased sorption affinity for free ESHs due to its aromatic nature which could explain the higher concentration of ΣESHs in the solids phase of the CAP effluent.

ESHs in DSE/influent will be deconjugated into their respective free forms (Noguera-Oviedo and Aga, 2016) by the microbial biomass within the CAP to be adsorbed by POC in the CAP The maintenance of anaerobic conditions in the CAP will inhibit the oxidative degradation of accumulating POM and ESHs which will also increase the concentration of free ESHs in the solids of the CAP and released effluent. In comparison to the influent, the mean concentration of individual ESHs in the solids phase of the CAP sludge and effluent samples was clearly dominated by E1 due to the conversion of 17α-E2 to E1 (Noguera-Oviedo and Aga, 2016).

The mean concentration of individual free ESHs in the solid phase of the CAP ETS measured in this study are comparable with those reported in previous studies of DSE, dairy cow manures and manure dry stacks, pond sludges and effluents (Table 2-5 and Table 2-7).

Table 2-7: Reported mean concentrations of ESHs in the solid phase (ng/g) of DSE, dairy cow manure and dairy effluent treatment systems

Sample description	17α-E2	17β-E2	E1	ΣESHs	Reference
Dairy shed effluent or dairy cow manure					
Dairy shed effluent (n=6)	273 (24- 689)[A]	38.7 (17- 63)	112 (46- 296)	423 (91- 861)	This study
Dairy manure	120-190	46-50	28-72	194- 312	(Vethaak *et al*., 2005)
Dairy cow manure (n=4)	N.M[B]	21.8-101	0-9.7	110	(Zhang *et al*., 2014)
Fresh dairy cow manure (n=6)	1416	153	535	2,104	(Noguera-Oviedo and Aga, 2016)
Dairy cow manure (n=6)	420	160	61	641	(Noguera-Oviedo and Aga, 2016)
CAFO dairy cow manure (n=1)	6.2	16.6	16.1	38.9	(Andaluri *et al*., 2012)
Dairy manure press cake	32	N.D[C]	98	130	(Raman *et al*., 2001)
Dairy dry stack semisolid (n=30)	508	136	287	931	(Raman *et al*., 2004)
Dairy dry stack (n=15)	220	67	220	507	(Raman et al., 2004)
Piled manure (n=6)	172	37	697	906	(Noguera-Oviedo and Aga, 2016)
Slotted dams (n=6)	8-43	N.D- 18	68-107	76-154	(Noguera-Oviedo and Aga, 2016)
Treatment pond or storage lagoon					
CAP sludge (n=6)	31.3	67.6	1033	1132	This study
Dairy holding pond (n=48)	280	115	815	1210	(Raman *et al*., 2004)
Treatment pond effluent					
CAP effluent (n=6)	180	71	733	985	This study
Anaerobic digester (n=6)	160	47	470	677	(Noguera-Oviedo and Aga, 2016)

[A] mean (min-max). [B] NM = not measured. [C] N.D = not detected.

2.3.6 Total concentration of free ESHs

A summary of ESHs measured in the dissolved and solid phases and whole samples of the CAP ETS was presented in Table 2-4. The concentration of total ΣESHs in the influent of the CAP reached maxima in April (7156 ng/L) and July (7262 ng/L), correlating with late pregnancy and early calving in the farm herd which produce peak concentrations of ESHs in the faeces and urine of cows (Hoffmann *et al*., 1997). The concentration of free ΣESHs summed over the whole sample of the CAP ETS were considerably greater than the dissolved phase alone (Table 2-4) with mean total concentrations of 4,171 ng/L, 93,601 ng/L, and 4330 ng/L in the influent, CAP sludge and effluent samples respectively.

The mean concentration of total free ΣESHs measured in the CAP effluent in this study (4330 ng/L) is comparable to the maximum concentrations of 4,004 ng/L and 4,416 ng/L previously reported in the dissolved phase of effluent from two-pond DSE treatment systems in NZ (Sarmah *et al*., 2006). This suggests the concentration of total free ΣESHs in the whole effluent of the two-pond DSE treatment systems would have been considerably greater, that is if the solid phase had been taken into consideration.

The data in Table A-2 (appendices) clearly demonstrates that the solid phase contributes a significant proportion of ESHs within each sample with a mean proportion and range (min to max) of 78 % (51-96 %), 99 % (98.6-99.4 %) and 74 % (57-98 %), respectively for the CAP influent, sludge and effluent. These results confirm analysis solely of ESHs in the dissolved phase of animal wastes and ETS significantly underestimates the quantity of ESHs that are released into the environment by effluent discharge to waterways and/or application of treated effluent and pond sludges to pasture.

2.3.7 Relative percentages of individual ESHs in CAP ETS

The profile of free individual ESHs in the dissolved and solid phases of CAP influent was dominated by 17α-E2 followed by E1, then 17β-E2 (Figure 2-5). This profile changed significantly within the CAP where E1 comprised over 90 % of the ESHs in both phases of the CAP sludge. E1 continued to dominate the profile of ESHs in the CAP effluent, followed by 17α-E2, and 17β-E2.

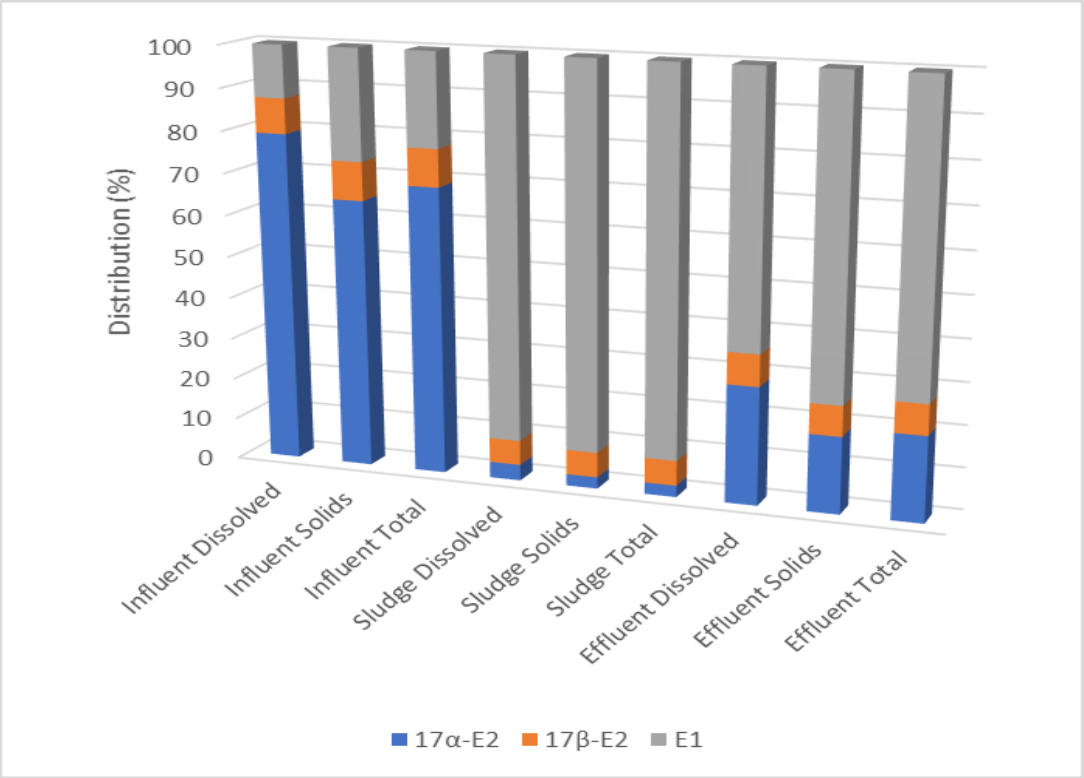

Figure 2-5: Mean relative distribution of 17α-E2( ), 17β-E2 ( ), and E1( ) in the solid and dissolved phases of the influent, sludge and effluent of the CAP effluent treatment system.

The mean percentages of E1 and 17α-E2 in the dissolved phase of the CAP effluent measured in this study are comparable to those previously measured in dairy effluent from oxidation ponds (Sarmah *et al*., 2006) and anaerobically digested manure (Noguera-Oviedo and Aga, 2016), and approximately 3 times higher than the percentage of E1, and 2.5 times lower than the percentage of 17α-E2, measured in the dissolved phase of effluents from a two pond and advanced pond system treating DSE (Gadd *et al*., 2010a) (Table 2-8). This study confirms previous observations that 17α-E2 is transformed to E1 during anaerobic treatment of DSE (Sarmah *et al*., 2006; Noguera-Oviedo and Aga, 2016).

Table 2-8: Relative percentage (%) of individual ESHs in the dissolved phase of different dairy cow effluent streams, treatment pond systems, and treated pond effluent.

Sample description	17α-E2	17β-E2	E1	Reference
Dairy shed effluent or treatment pond influent				
Dairy shed effluent	79.1	8.37	12.5	This study
Dairy shed effluent	82.1	7.3	10.5	(Zheng *et al*., 2008)
Dairy shed effluent	90.7	2.2	7.1	(Gadd *et al*., 2010a)
Dairy shed manure waste	64.4	13.9	21.7	(Noguera-Oviedo and Aga, 2016)
Flushed dairy manure waste	60.0	16.9	23.1	(Hanselman *et al*., 2006)
Treatment pond or storage lagoon				
CAP	3.82	5.89	90.3	This study
Dairy CAFO lagoon	50.6	33.4	16.0	(Hutchins *et al*., 2007)
Dairy holding pond	25.3	12.3	62.4	(Raman *et al*., 2004)
Dairy waste lagoon	19.6	20.5	59.9	(Zheng *et al*., 2008)
Treatment pond effluent				
CAP	28.1	7.59	64.3	This study
Advanced pond system	67.8	8.9	23.3	(Gadd *et al*., 2010a)
Dairy oxidation 2-ponds	72.0	7.0	21.0	(Gadd *et al*., 2010a)
Dairy oxidation ponds	21.6	8.0	70.4	(Sarmah *et al*., 2006)
Anaerobic digester	24.5	3.0	72.5	(Noguera-Oviedo and Aga, 2016)

2.3.8 Partitioning of ESHs between the dissolved and solid phases

The percentages of free ΣESHs associated with the solids phase of the CAP influent, sludge, and effluent varied from 51-96 %, 98.6-99.4 %, and 57-97 % respectively (Figure 2-6, Figure 2-7 and Figure 2-8). These results are comparable to the 98 % of ESHs in the solid phase of dairy manure (Noguera-Oviedo and Aga, 2016) and 68 % in the solid phase of swine manure (Combalbert *et al*., 2012).

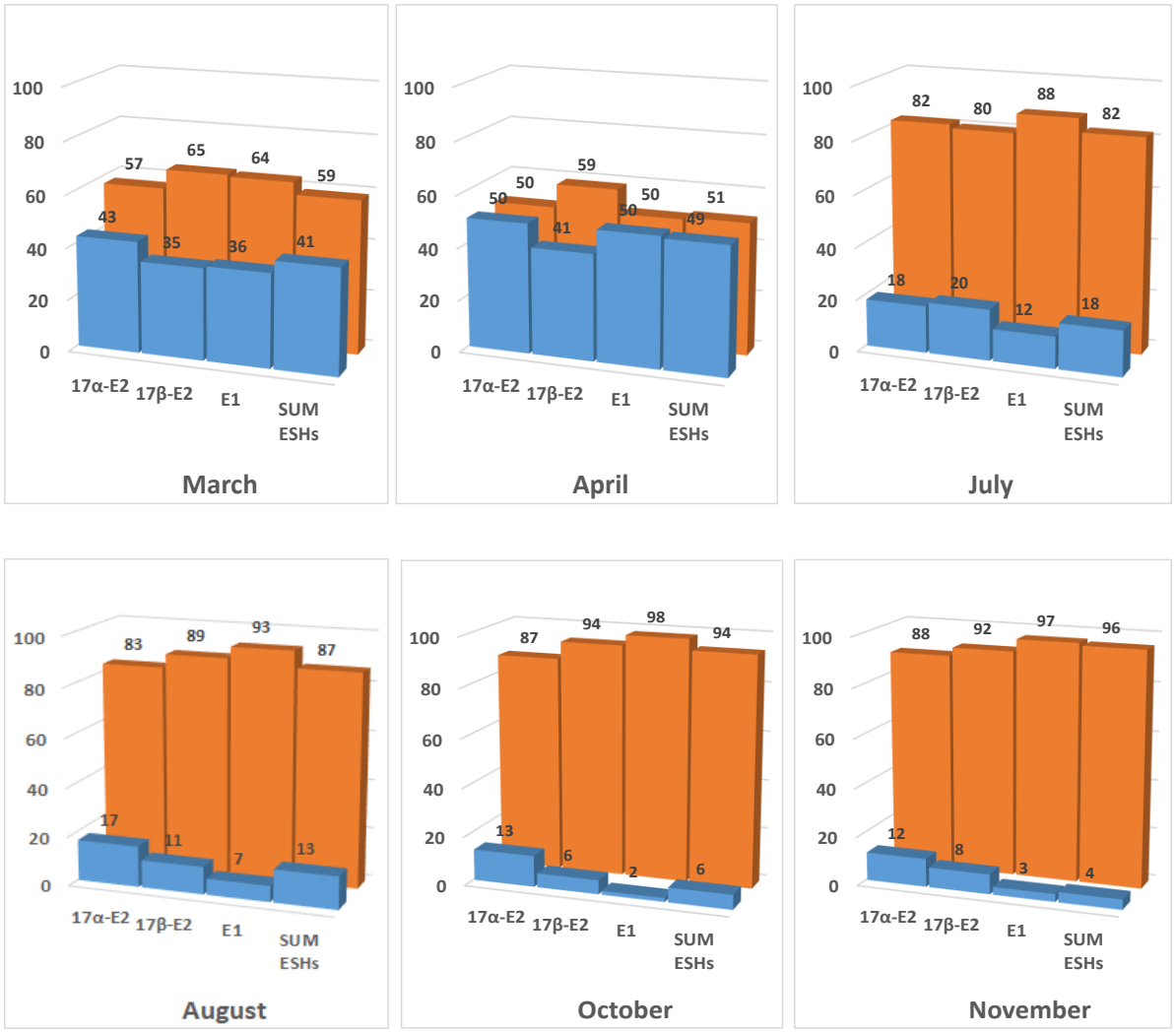

Figure 2-6: Relative distribution of ESHs between the dissolved ( ) and solid ( ) phases of CAP Influent (DSE) at each sampling event

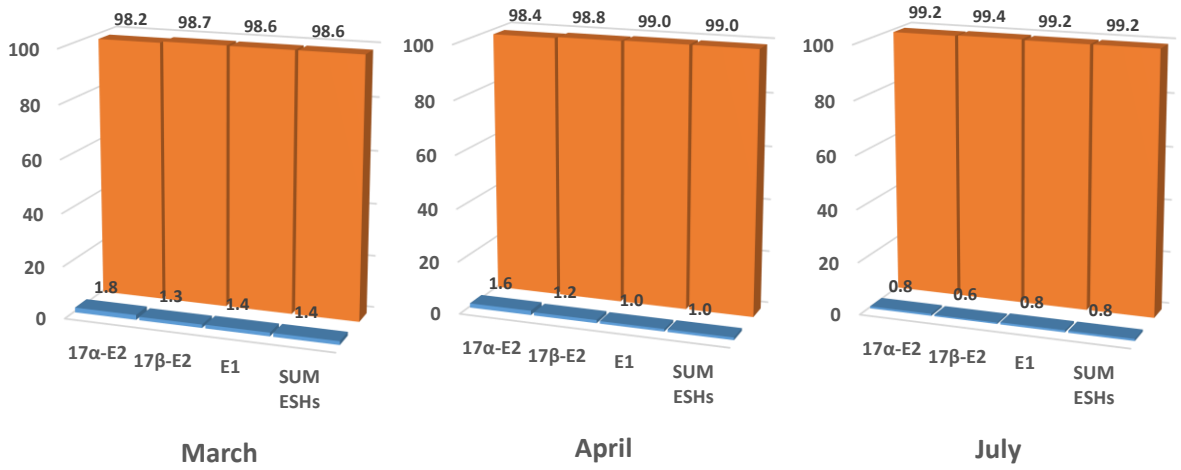

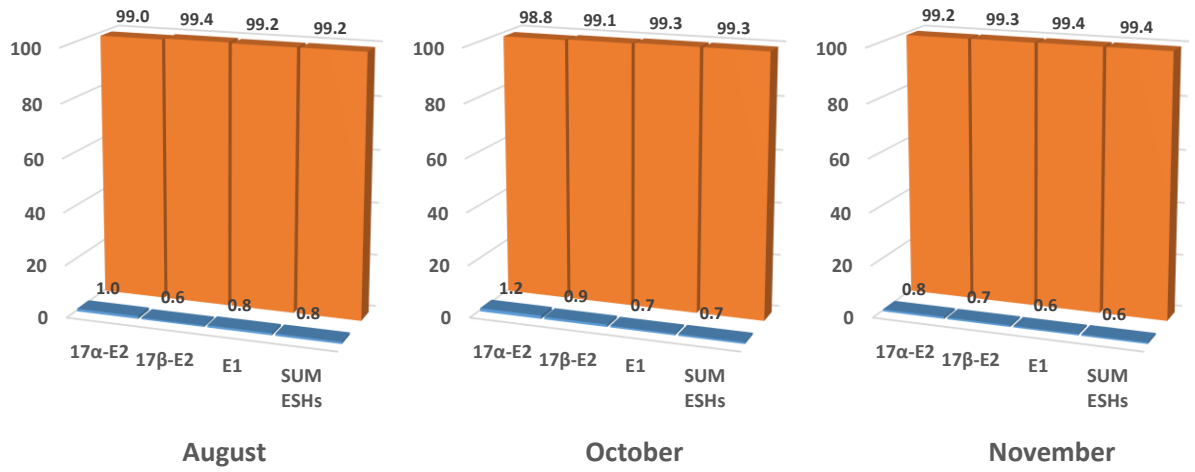

Figure 2-7: Relative distribution of ESHs between the dissolved ( ) and solid ( ) phases of CAP sludge at each sampling event

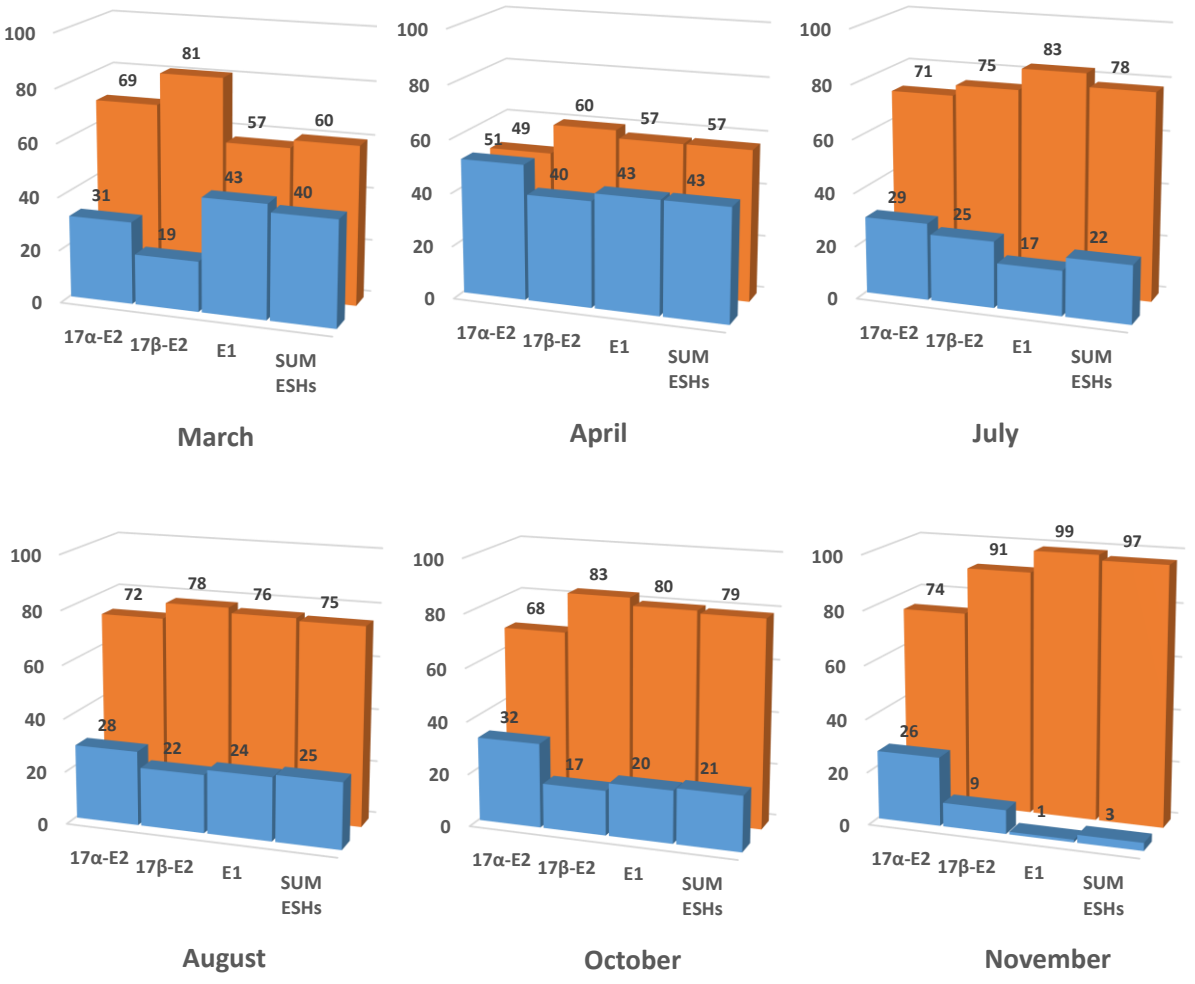

Figure 2-8: Relative distribution of ESHs between the dissolved ( ) and solid ( ) phases of CAP effluent at each sampling event

Although the influent had the highest OC content (42 %) followed by CAP sludge (32 %) and CAP effluent (30 %), the sludge exhibited the highest ratio of free ESH associated with solids to free ESH associated with the dissolved phase. This distribution of free ESHs is attributed to the greater TS content of the CAP sludge and extended contact and equilibrium time between the CAP sludge and ESHs (Casey *et al*., 2003; Mansell *et al*., 2004; Sarmah *et al*., 2008), and the chemical properties of residual OC in the CAP sludge.

The distribution coefficients (K_d) and organic carbon partition coefficients (log K_{oc}) for the ESHs in samples of the CAP ETS were calculated according to the Organisation for Economic Co-operation and Development (OECD) guideline 106 (Table 2-9 and Table 2-10). The calculated mean log K_{oc} for the three ESHs varied from 3.06 to 3.80 demonstrating that sorption of ESHs results from hydrophobic partitioning to organic carbon within the solids phase of the samples (Grathwohl, 1990; Lai *et al*., 2000). The calculated log K_{oc} for 17α-E2, 17β-E2 and E1 in the samples in this study are slightly higher than the range of 2.70-3.46 reported in soil (Lai *et al*., 2000; Sarmah *et al*., 2008) and 2.97-3.69 in municipal wastewater (Langford and Lester, 2003).

Table 2-9: Partition distribution coefficients (Kd) of ESHs in the raw influent, sludge and effluent of the CAP effluent treatment system (mL/g)

Influent										
Compound	**Mar**	**Apr**	**Jul**	**Aug**	**Oct**	**Nov**	**Mean**	**Range[A]**	**Median**	**SDev[B]**
17α-E2	192	144	647	718	981	1102	631	144-1102	683	396
17β-E2	262	207	587	1132	2357	1622	1028	207-2357	860	847
E1	253	143	1023	2035	8803	4335	2775	143-8803	1529	3359
Sludge										
17α-E2	650	732	1568	1191	973	1560	1112	650-1568	1082	398
17β-E2	923	1001	2199	2098	1306	1807	1556	923-2199	1557	555
E1	852	1240	1502	1450	1836	2083	1494	852-2083	1476	434
Effluent										
17α-E2	749	274	707	730	603	818	647	274-818	718	195
17β-E2	1203	427	854	1024	1403	2728	1273	427-2728	1113	786
E1	382	390	1384	912	1168	25862	5016	382-25862	1024	10220

[A] minimum to maximum. [B] Standard deviation

Table 2-10: log Koc values for ESHs in the influent, sludge and effluent of the CAP effluent treatment system (mL/g)

Parameter	Mar	Apr	Jul	Aug	Oct	Nov	Mean	Range[B]	Median	SDev [C]
INFLUENT										
17α-E2	2.63	2.52	3.20	3.26	3.37	3.41	3.06	2.63-3.63	3.23	0.39
17β-E2	2.77	2.58	3.16	3.56	3.75	3.57	3.23	2.77-3.75	3.31	0.44
E1	2.75	2.51	3.40	3.71	4.42	4.00	3.45	2.51-4.42	3.55	0.71
SLUDGE										
17α-E2	3.32	3.45	3.70	3.57	3.47	3.64	3.52	3.32-3.64	3.52	0.14
17β-E2	3.47	3.59	3.85	3.81	3.60	3.71	3.67	3.47-3.85	3.65	0.14
E1	3.43	3.68	3.68	3.65	3.75	3.77	3.66	3.43-3.77	3.68	0.12
EFFLUENT										
17α-E2	N.A[A]	3.17	3.33	3.33	3.26	3.57	3.33	3.17-3.57	3.24	0.15
17β-E2	N.A	3.37	3.42	3.47	3.63	4.09	3.60	3.37-4.09	3.47	0.31
E1	N.A	3.33	3.63	3.42	3.55	5.07	3.80	3.33-5.07	3.55	0.72

[A] N.A = not available due to absence of % organic carbon. [B] minimum to maximum. [C] Standard deviation.

A T. Test (two tailed, 95 % confidence interval of difference) was used to determine the statistical differences between the log K_{oc} values derived for each of the measured ESHs in the influent, sludge, and effluent of the CAP effluent treatment system samples. The results demonstrate no significant statistical differences (P range = 0.07 to 0.71) in log K_{oc} values for the ESHs between the solids phase of the influent, sludge or effluent (Table 2-11).

Table 2-11: t. Test P values for log Koc values of ESHs between the three sample types

Description	17α-E2	17β-E2	E1
Influent vs sludge	0.07	0.07	0.20
Influent vs effluent	0.10	0.11	0.53
Sludge vs effluent	0.70	0.71	0.19

2.3.9 Estrogenic potency in the CAP ETS

The estrogen equivalents (EEQs) of the analysed CAP ETS samples were predicted by multiplying the measured concentration of each steroid (by GC-MS) by its relative potency factor (RPF) obtained by the ER-CALUX bioassay (Kolkman *et al*., 2013). The EEQs for each compound measured in a sample were summed to obtain the total predicted EEQ for each sample. This approach, based on the toxic equivalency factor (TEF) approach, has been shown to be appropriate for mixtures where each component acts

through the same pathway and the dose-response curves are parallel for individual compounds (Kolkman *et al.*, 2013).

A statistical summary of the calculated EEQs of ESHs measured in the dissolved and solid phases of samples from the CAP ETS are presented in Table 2-12 (full data set is provided in appendices, Table A-4). The calculated estrogenicity of samples from the CAP ETS demonstrates the estrogenic potency of the samples is dominated by the contribution of 17β-E2, with mean contributions of 88.6 %, 76.3 % and 81.5 % of the total estrogenicity respectively for influent, CAP sludge, and CAP effluent.

Table 2-12: Mean Estrogenic equivalents of ESHs measured in the dissolved and solid phases of 1 litre of raw influent, sludge and effluent of the CAP effluent treatment system.

	17α-E2	**17β-E2**	**E1**	**ΣESHs**
		Influent (n=6)		
Dissolved	9.7 (0.22 -28.7)[A]	103 (7.04-242)	3.07 (0.10- 8.3)	116 (7.43-279)
Solids	19.0 (1.66-47.9)[B]	269 (115-441)	15.5 (6.40-41.1)	304 (123-504)
Total	28.7 (1.88-59)	372 (122-657)	18.6 (6.50-42.5)	420 (131-710)
		Sludge (n=6)		
Dissolved	0.30 (0.21-0.39)	46.3 (33.5-64.9)	14.2 (11.20 -17.6)	60.7 (45.0-80.7)
Solids	25.7 (20.3-31.1)	5545 (3805-6947)	1694(1231 - 2323)	7264 (5434-9298)
Total	26.1 (20.6-31.3)	5591 (3851-7012)	1708 (1248-2338)	7325(5506-9379)
		Effluent (n=6)		
Dissolved	2.67 (0.04-7.82)	72.1 (3.11-142)	12.1 (0.87-21.7)	86.9 (4.52-163)
Solids	6.2 (0.09 -19.1)	245 (12.9-503)	50.6 (1.81-81.5)	302 (14.8-561)
Total	8.90 (0.13-26.9)	317 (16.0-645)	62.8 (3.19-102)	389 (19.3-722)

[A] EEQ in 1 litre of sample (mean (range min to max)). [B] EEQ in 1 litre volume of sample calculated using the corresponding measured TS concentrations for influent, sludge and effluent samples.

The observed reduction in the concentration of 17α-E2 and increase in the concentration of E1 as DSE passes through the CAP is matched by similar changes to their contributions to total estrogenicity. The mean contribution of 17α-E2 to total estrogenicity was 6.83 % in influent, 0.36 % in CAP sludge, and 2.29 % in CAP effluent, while that of E1 was 4.42 % in influent, 23.3 % in CAP sludge, and 16.1 % in the CAP effluent. These results clearly demonstrate that any potential endocrine disrupting impact associated with the re-cycling and re-use of effluent or sludge from the CAP ETS will principally arise from the presence of residues of 17β-E2.

2.4 Conclusions

- A significant proportion of the total load of free ESHs in dairy shed effluent, and sludge and effluent of the CAP ETS are associated with the solids phase.
- Ignoring the contribution of free ESHs associated with the solid phase of DSE, pond sludges and effluent of dairy effluent treatment systems significantly underestimates the total mass of free ESHs that might be applied to pasture.
- The log K_{oc} calculated from the partitioning of 17α-E2, 17β-E2 and E1 between the dissolved and particulate phases of the ETS samples are similar to those for soils and wastewater and confirms hydrophobic partitioning to particulate organic matter is the primary sorption mechanism.
- 17α-E2 is transformed to the more persistent E1 in the CAP which concurrently decrease the estrogenicity of the CAP sludge and effluent.
- Regardless of the conversion of 17α-E2 to E1, the EEQs calculated for the samples clearly demonstrate the greater proportion of estrogenic activity at all sampling points is attributable to 17β-E2.
- This study was restricted to the free form of ESHs in the ETS. Further work is required to determine the contribution of conjugated forms of ESHs to the total load of free ESHs in dairy ETS effluents (Chapter 3).
- Further ESHs analysis work and modelling of the performance of the CAP, taking into account physical design features will improve understanding of the transformation of ESHs, and identify factors that can increase their removal and environmental implication (Chapter 6).

Chapter 3:
The importance and fate of the conjugated estrogenic steroid hormones in dairy shed effluent and an effluent treatment system

In the previous chapter (Chapter 2), further work was identified to be required to determine the contribution of conjugated forms of estrogenic steroid hormones (ESHs) to the total load of free ESHs. The main objective of this part of the study was to measure the concentration of the conjugated ESHs in the dissolved and solids phases of influent, sludge, and effluent of a covered anaerobic pond (CAP) treatment system and to provide a better understanding regarding the overall concentration of ESHs in the dairy shed effluent (DSE) and the performance of the CAP effluent treatment system.

3.1 Introduction

ESHs are a class of endocrine disrupting compounds that can, upon their release into the environment through the discharge of municipal and agricultural wastewater and sludge, interfere with the endocrine system and the function of natural hormones in organisms exposed to them (Barber *et al*., 2011; Bergman, 2013). Previous studies in New Zealand (NZ) and globally have demonstrated that dairy cows are responsible for far greater amounts of ESHs entering the environment than other agricultural and municipal sources (Lange *et al*., 2002; Hanselman *et al*., 2003; Sarmah *et al*., 2006; Gadd *et al*., 2010; Sim *et al*., 2011). Endogenous ESHs are naturally excreted by animals with conjugated forms of ESHs primarily excreted via urine because conjugation increases aqueous solubility and free ESHs via faeces (Hoffmann *et al*., 1997; Lange *et al*., 2002; Zhang *et al*., 2014). The relative proportion of ESHs excreted as free or conjugated ESHs is dependent upon the type, age, and reproductive status of animals (Lange *et al*., 2002).

Conjugated ESHs incorporate glucuronide or sulphate groups on the hydroxyl groups of endogenous free ESHs (17α-estradiol (17α-E2), 17β-estradiol (17β-E2), estrone (E1), estriol (E3)) at a single or multi carbon positions 3, 16 or 17 (Table 3-1). The conjugation of ESHs mainly occurs in the liver of animals through glucuronidation and sulfation reactions using glucuronosyltransferase (UGT) and various sulfotransferase enzymes (SULTs) (James, 2011). Consequently, conjugated ESHs excreted by dairy cows are present in different structural forms of which 17α-estradiol-3-sulphate (17α-E2-3-S) (Hutchins *et al*., 2007) and estrone-3-sulphate (E1-3-S) (Gadd *et al*., 2010) are the principal contributors.

The water solubility of conjugated ESHs is as much as 78 times greater than their corresponding free form (Casey *et al*., 2019), facilitating their depuration from the body by the kidneys and release in the urine. These highly water-soluble compounds (aqueous solubility range from 2-999 g/L) have a low octanol-water partition coefficient (log K_{ow}) between 0.29-2.90 (Lai et al., 2000) and organic carbon partition (log K_{oc}) of 2.21 (E1-3-S) and 2.46 (17α-E2-3-S) (Chen and Hu, 2010) comparing to the free ESHs log K_{ow} range between 3.43 – 3.94 (Ying *et al*., 2002). Consequently, conjugated ESHs preferentially partition into aqueous solutions and bind to solid material to a much lesser extent than their corresponding free forms (Scherr *et al*., 2009; Shrestha *et al*., 2012; Bai *et al*., 2013; Goeppert *et al*., 2015). Therefore, conjugated ESHs are significantly more mobile than their corresponding free forms and can contaminate surface and groundwater when agricultural waste and effluent is applied to land (Yost *et al*., 2014; Ma *et al*., 2016; Casey *et al*., 2020).

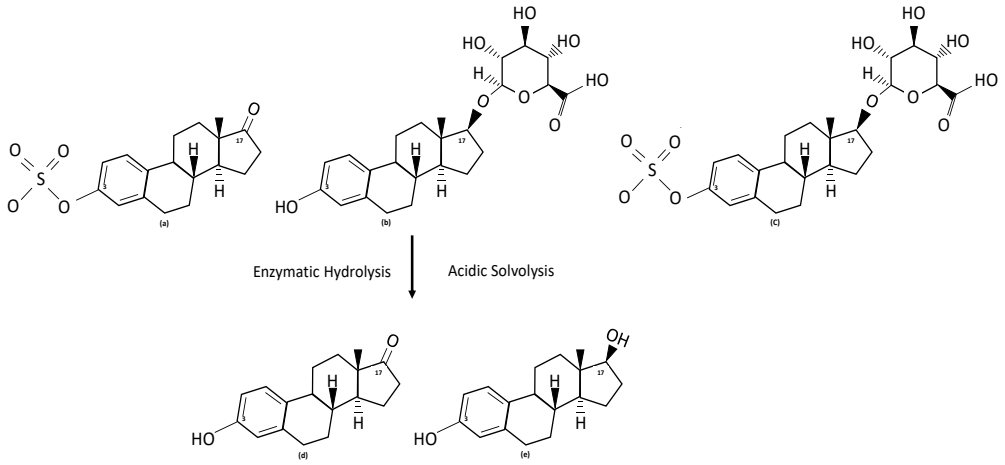

Figure 3-1: Three examples for glucuronide, sulphate and both glucuronide and sulphate groups attached to the ESHs, E1 and 17β-E2. (a) sulphate group attached to E1 at position 3. (b) glucuronide group attached to 17β-E2 at position 17. (c) glucuronide and sulphate group attached to 17β-E2 at positions 17 and 3 respectively. (d) and (e) parent ESHs, E1 and 17β-E2 produced through enzymatic hydrolysis and solvolysis processes

Conjugated ESHs do not interact with the estrogen receptors within humans and animals and therefore are not biologically active (Norris and Carr, 2005). Upon their entry into wastewater treatment systems or release into the environment, conjugated ESHs are de-conjugated by arylsulfatase and β-glucuronidase enzymes derived from bacteria yielding their respective biologically potent free forms (Zheng *et al*., 2012; Noguera-Oviedo and Aga, 2016; Ben *et al*., 2017).

The removal and transformation of conjugated ESHs during wastewater treatment is reported to increase with solids retention times and temperature (Gomes *et al*., 2009b; Kumar *et al*., 2015; Ben *et al*., 2017). Numerous studies demonstrate glucuronide conjugates of ESHs are more susceptible to deconjugation than the corresponding sulphate conjugates in dairy cow excreta and treatment lagoons (Hutchins *et al*., 2007; Gadd *et al*., 2010; Zhang *et al*., 2014), soils (Goeppert *et al*., 2015; Ma and Yates, 2017), river water (Kumar *et al*., 2012) and raw sewage (Ben *et al*., 2017).

Analysis of conjugated ESHs is more challenging than the free forms due to their higher polarity and hydrophilic nature. They are typically analysed by either Gas chromatography-mass spectrometry (GC-MS) or liquid chromatography-tandem

mass spectrometry (LC-MS-MS). GC-MS is commonly used for indirect analysis of conjugated ESHs in drugs, urine, and animal waste. This is preceded by enzymatic (commonly using commercial preparations of *Helix pomatia* β-glucuronidase enzyme) and/or chemical solvolysis reactions that respectively cleave the glucuronide and sulphate groups to produce free ESHs. These free ESHs are subsequently derivatised for gas chromatographic separation and analysis (Meng and Sjövall, 1997; Labadie and Budzinski, 2005b; Combalbert *et al*., 2010).

When using GC-MS to analyse conjugated ESHs, the deconjugation process is challenging due to the inherent instability, and consequent variability of commercial β-glucuronidase enzyme preparations, inefficiencies in the deconjugation of the sulphate conjugates, and the complexity and laborious nature of multi-step procedures (Gomes *et al*., 2009a). In comparison, LC-MS-MS provides the advantage of being able to analyse conjugated ESHs directly thereby alleviating the issues concerning deconjugation and derivatisation procedures and allowing simultaneous and direct analysis of both free and conjugated ESHs (Reddy *et al*., 2005; Gadd *et al*., 2010; Zhang *et al*., 2014). However, in contrast to GC-MS instruments, the relatively high cost of sensitive LC-MS-MS instruments means they remain inaccessible to many laboratories, including the laboratory used in this research. Furthermore, the analysis of ESHs by LC-MS-MS is affected by co-extracted residues from complex sample matrices that impact the ionisation of ESHs, leading to poor recoveries of some conjugated ESHs (Gomes *et al*., 2009a). Therefore, the GC-MS method was used in this study to analyse the conjugated ESHs.

The difficulty of analysing conjugated ESHs in complex matrices has contributed to the limited number of studies investigating their fate within animal wastes and treatment systems. This is despite the evidence suggesting conjugated ESHs represent a significant proportion (up to 49 %) of the total ESH load in DSE and DSE treatment systems (Hutchins *et al*., 2007; Zhang *et al*., 2014). Ignoring the significance and fate of conjugated ESHs within DSE and dairy effluent treatment systems (ETSs) can result in underestimating the performance of the treatment

system in removing ESHs and the potential impact of this agricultural waste stream on the environment upon recycling to pasture.

KURA Biotec BGS™ is a new and noval enzyme with a dual recombinant β-glucuronidase and arylsulfatase enzyme reagent with overlapping optimum incubation pHs (6.8 - 7.0) and temperatures (50°C - 55°C) allowing simultaneous deconjugation of glucuronides and sulphate conjugates in urine samples. The BGS™ glucuronidase and sulfatase activities are ≥ 200,000 U/mL and ≥ 250,000 U/mL respectively. The BGS™ β-glucuronidase and arylsulfatase enzyme's was selected to be used in the research due to its proclaimed ability to simultaneously deconjugate glucuronide and sulphate conjugates together with the glucuronidase and sulfatase activities provide a significant advance compared to the commonly used Sigma-Aldrich brand *Helix pomatia* (*H. pomatia*) β-glucuronidase enzyme that requires two deconjugation steps (chemical solvolysis and enzymatic hydrolysis) and has lower glucuronidase and sulphatase enzymatic activity (≥ 100,000 U/mL β-glucuronidase and ≤7,500 U/mL sulfatase). However, it is unclear how the BGS™ enzyme will perform compared to the *H. pomatia* enzyme using DSE and DSE sludge and effluent samples as this enzyme was designed for urine sample for medical purposes.

This chapter describes how these knowledge gaps were addressed by:

- assessing and validating the performance of a new commercial enzyme reagent (BGS™) to deconjugate sulphate and glucuronide ESH conjugates in samples from DSE treatment system, for analysis by GC-MS.
- applying the optimised deconjugation procedure to quantify total conjugated ESHs in the dissolved and solid phases of influent, sludge and effluent within a CAP DSE treatment system.
- determining the contribution of conjugated ESHs to the total load of ESHs in the CAP DSE treatment system.
- determining the distribution of conjugated ESHs between dissolved and solid phases of DSE and how this influences their fate within a CAP DSE treatment system.

- estimating the contribution of conjugated ESHs present as a potential source of free biologically active ESHs following treatment of DSE with a CAP treatment system.

3.2 Materials and Methods

3.2.1 The study farm

A description of the dairy farm and CAP used to treat DSE, and from which samples of influent, sludge and effluent were collected can be found in Chapter 2.

3.2.2 Chemicals and materials

All solvents (HPLC grade) and Hyflo Supercell C22 filter aid (VWR Chemicals) were supplied by Thermo Fisher Scientific, NZ. Deionized water was produced from a Milli-Q Millipore Integral 5 system. ^{13}C6-E1 and ^{13}C6-E2 with an isotopic (purity>99 %), were supplied by Cambridge Isotope Laboratories, and 17β-E2-d4 and E1-d4 (purity>98 %) were supplied by CDN Isotopes. 17α-E2, 17β-E2, E1 (purity>99 %), βE2-3,17-diS, βE2-3-G, βE2-17-G, E1-3-S (purity~95 %), triethylamine (purity>99 %), ammonium iodide (purity 99+%) and 2-mercaptoethanol (purity>98 %), trifluoroacetic acid (TFA) (purity 99%) and *H. pomatia* β-glucuronidase Type HP-2 (≥ 100,000 U/mL β-glucuronidase and ≤7,500 U/mL sulfatase) were supplied by Sigma Aldrich NZ. KURA Biotec BGSTM recombinant β-glucuronidase/sulphatase mix (50 and 10 % glycerol, *v/v*) (≥200,000 U/mL β-glucuronidase and ≥250,000-350,000 U/mL sulfatase), KURA Biotec Instant buffer II, and *N*-Methyl-*N* (trimethylsilyl) trifluoroacetamide (MSTFA) (UCT SMSTFA-0, Selectra-Sil) was supplied by PM Separations Australia. Strata™-X 33µm (200 mg and 500 mg) solid-phase extraction (SPE), Strata® Florosil (1 g) and Strata® NH2 (500 mg) cartridges were obtained from Phenomenex NZ. Granular anhydrous sodium sulphate, sodium acetate and sodium carbonate anhydrous (purity 99.5 %) were obtained from Merck NZ. Acetic acid (J.T Baker, 99.9 %) was obtained from ECP Ltd, NZ.

3.2.3 Collection, preparation and extraction of samples

The method of sample collection, preservation and storage of influent, sludge and effluent samples from the CAP, collected from March to November 2018 has been

previously described in Chapter 2. Briefly, the samples were centrifuged to separate the supernatant which was filtered (dissolved samples) and the centrifuged solids were lyophilised (solids samples). Total ESHs were extracted from the dissolved phase by SPE (Oasis HLB cartridges 500 mg) and following rinsing, the conjugated ESHs were eluted with a solution of methanol/ammonium hydroxide/Milli-Q water (Reddy et al., 2005) (March and April Samples) or methanol/Milli-Q-Water containing triethylamine (Labadie and Budzinski, 2005b) (July, August, October and November samples) in accordance with the different extraction and clean-up methods described in Chapter 2. Total ESH residues were extracted from the solid phase of each sample by accelerated solvent extraction (ASE), followed by SPE using Oasis HLB cartridges (1 g), and the conjugated ESHs were eluted with a solution of methanol/Milli-Q-Water containing triethylamine (Labadie and Budzinski, 2005b). The dissolved and solids phase fractions containing conjugated ESH eluents were stored at 4 °C before deconjugation.

3.2.4 Evaluation and optimisation of deconjugation procedure

The key aims and differences of the different trials included under the evaluation and optimisation of the deconjugation procedure are summarised in Table 3-1. Initially, a new enzymatic deconjugation reagent, Kura BioTec BGS™ recombinant β-glucuronidase/sulphatase enzyme mix, was used in the evaluation and optimisation of the deconjugation trials of conjugated ESHs. The purpose of the deconjugation trials was to evaluate the ability of the BGS™ recombinant enzyme mix to deconjugate four different conjugated ESHs (βE2-3,17-diS, βE2-3-G, βE2-17-G and E1-3-S) and once optimised, compare this with a previously validated method using a combination of *H. pomatia* β-glucuronidase enzyme and chemical solvolysis. The enzyme exhibiting best overall performance to deconjugate the EHSs would then be applied to analyse the conjugated ESHs in samples from the CAP ETS.

Table 3-1: Trials undertaken for the evaluation and optimisation of the deconjugation procedure organised by sequential order

Trial no.	Description[a]	Enzyme	Enzyme Incubation time[A]	Enzyme Incubation temperature[B]	Volume of Milli-Q-Water/Buffer /enzyme[C]
1	Enzymatic Hydrolysis	BGS™ (50% glycerol)	30	45	800/100/100
2	Enzymatic Hydrolysis	BGS™ (50% glycerol)	45	45	240/50/50
3	Enzymatic Hydrolysis	BGS™ (50% glycerol)	45	45	240/100/100
4	Enzymatic Hydrolysis	BGS™ (50% glycerol)	45	45	240/150/150
5	Enzymatic Hydrolysis	BGS™ (10% glycerol)	45	53	240/100/100
6	Solvolysis (using 8 mL vials)	N/A[D]	N/A	N/A	N/A
7	Solvolysis (using 1 mL vials)	N/A	N/A	N/A	N/A
8	Solvolysis followed by Enzymatic Hydrolysis	BGS™ (10% glycerol)	45	53	240/100/100
9	Solvolysis followed by Enzymatic Hydrolysis	BGS™ (10% glycerol)	180	53	240/100/100
10	Solvolysis followed by Enzymatic Hydrolysis	BGS™ (10% glycerol)	1440	53	240/100/100
11	Enzymatic Hydrolysis followed solvolysis	BGS™ (10% glycerol)	45	53	240/100/100
12	Solvolysis followed by Enzymatic Hydrolysis	*H. pomatia* (Type HP-2)	180	55	400/5000/30

A time in minutes. **B** expressed as °C. **C** expressed as µL. **D** not applicable. The solvolysis and *H. pomatia* enzymatic hydrolysis were completed based on a previous study performed by Labadie and Budzinski (2005a). The BGS™ enzymatic hydrolysis was performed based on J. L. Callejas (2019).

At the start of each trial (1-12), sets of duplicate or triplicate empty glass tubes were sequentially spiked with a surrogate standard mixture of ^{13}C6-E1 and ^{13}C6-E2 (100 ng mass of each) and a single conjugated ESH standard (βE2-3,17-diS or βE2-3-G or βE2-17-G or E1-3-S) (500 ng mass), following by evaporation to dryness under a stream of oxygen-free nitrogen gas (30 °C). To evaluate the recoveries of the spiked conjugated ESHs samples, the measured recoveries were compared against equivalent free ESHs spiked concentration. This concentration was calculated by

dividing the measured parent ESHs molecular weight by the associated conjugated group molecular weight and multiplying it by the spiked conjugated ESHs mass (500 ng).

3.2.4.1 Enzymatic hydrolysis (BGS™) of conjugated ESHs (Trial numbers 1-5)

The purpose of these trials was to assess the efficacy of the BGS™ recombinant enzyme reagent to deconjugate glucuronide and sulphate conjugates of ESHs. The procedural steps applied in these trials were based on the recommended method provided by KURA Biotec when using the BGS™ recombinant enzyme to deconjugate components in human urine (appendices, Figure A-1). The key parameters assessed in these trials included:

- The proportions of glycerol in which the BGS™ recombinant enzyme reagent was prepared (50 and 10 % glycerol) and incubation temperature (45 and 53 °C) of the enzymatic reagent. These factors were assessed because of changes to the proportion of glycerol in the supplied BGS™ recombinant enzyme reagent and associated changes to the recommended incubation conditions recommended by the enzyme manufacturer.
- Different volumes of Milli-Q-Water (800 and 240 µL) to Instant Buffer II and BGS™ recombinant enzyme reagent volumes (100, 200 and 300 µL), to assess the optimum enzyme to solution ratio. In these assessments, the ratio of the volume of Instant Buffer II and BGS™ recombinant enzyme was maintained as 1:1.
- Incubation times (30 and 45 min). Change of incubation time from 30 minutes (Trial 3) to 45 minutes (Trials 2, 3, 4 and 5) was made following consultation with Kura to enhance the efficiency of the BGS™ recombinant enzyme to deconjugate glucuronide and sulphate conjugates of ESHs.
- Type of SPE eluting solvent (methanol and DCM/methanol (95:5 *v/v*)). In trial 5, methanol was replaced with a stronger elution solution (DCM/methanol) to elute the ESHs from the Strata-X cartridges to improve recoveries and reduced solution evaporation time.

The dried sequentially spiked samples were re-dissolved in Milli-Q-Water and Instant buffer II (900 µL, 80:10 *v/v*) (Trial 1) or (290 µL, 24:5 *v/v*) (Trial 2) or (340 µL, 24:10 *v/v*) (Trial 3) or (390 µL, 24:15 *v/v*) (Trial 4). Subsequently, the aqueous buffered solutions were vortexed and the BGS™ enzyme reagent was added at the same volume as the added buffer (50 or 100 or 150 µL). The final solutions were mixed gently by vortex and incubated at 45 °C for 30 (Trial 1) or 45 (Trials 2-5) minutes. After returning to room temperature, an aliquot of Milli-Q-Water (4 mL, pH = 2) was added to each solution. Free ESHs were extracted from the Milli-Q water solutions by SPE using previously rinsed and conditioned Strata-X (200 mg, 6 mL) SPE cartridges at a flowrate of one drop per second, followed by a rinse/wash with Milli-Q-Water / methanol (4 mL, 9:1 *v/v*). The Strata-X SPE cartridges were dried under vacuum to remove the bulk of residual water, and the ESHs eluted with methanol (12 mL) (in Trial 5 methanol was replaced with DCM/methanol (12 mL, 95:5 *v/v*) as the elution solvent). The methanol or DCM/methanol eluent was evaporated to dryness under nitrogen gas (30 °C), re-dissolve in acetone (2 mL), and stored under refrigeration at 4 °C prior to derivatisation and GC-MS analysis.

3.2.4.2 Solvolysis of sulphate conjugated ESHs (Trials 6 and 7)

Sulphate conjugated ESHs are more persistent than their glucuronide analogues and typically require more stringent reaction conditions than those provided by enzymatic hydrolysis to be deconjugated to free ESHs, and chemical acid solvolysis is typically required for effective deconjugation. In trials 6 and 7, the solvolysis procedure, based on previously published methods by Labadie and Budzinski (2005a) and Combalbert *et al*. (2010) was implemented to assess its efficacy to deconjugate sulphate conjugated ESHs. The key parameter assessed in these trials was the volume of the vial in which the reaction was completed, and from which the final reaction mixture was recovered.

A solution of MeOH / tetrahydrofuran (1 mL, 20:80 *v/v*) followed by trifluoroacetic acid (10 µL) was added to the glass tubes (8 mL) or vials (1 mL) containing the dried conjugated ESH and carbon-13 labelled free ESH surrogate standards. The glass tubes or vials were vortexed to solubilise the conjugated and free ESHs, incubated at 45 °C for 30 min. After returning to room temperature, the reaction

mixture was neutralised with Na_2CO_3 (100 µL, 0.8 mol/L in Milli-Q-Water), evaporated to ~100 µL under a stream of oxygen-free nitrogen gas (30 °C), and Milli-Q-Water (4 mL, pH = 2) was added to the neutralised solution. The deconjugated free ESHs were recovered from the Milli-Q water solutions by SPE using previously rinsed and conditioned Strata-X (200 mg, 6 mL) SPE cartridges at a flowrate of one drop per a second, followed by a rinse/wash with Milli-Q-Water / methanol (4 mL, 9:1 *v/v*). The Strata-X SPE cartridges were dried under vacuum to remove the bulk of residual water, and the ESHs eluted with DCM/methanol (12 mL, 95:5 *v/v*). The collected eluent was dried under nitrogen gas (30 °C), re-dissolved in acetone (2 mL), and stored at 4 °C in a refrigerator prior to derivatisation and GC-MS analysis.

3.2.4.3 Chemical solvolysis followed by enzymatic hydrolysis (BGS™) of conjugated ESHs (Trials 8-10)

Trials 8-10 were completed to assess if the combination of chemical solvolysis and enzymatic hydrolysis using BGS™ recombinant enzyme improved the de-conjugation of ESH sulphate conjugates beyond that achieved by the BGS™ recombinant enzyme alone. The solvolysis procedure described in previously published methods (Meng and Sjövall, 1997; Labadie and Budzinski, 2005b; Combalbert et al., 2010) was adopted and used in combination with the enzymatic hydrolysis procedure from trial 5. This trial aimed to determine if the introduction of the chemical solvolysis step and increasing incubation time during enzymatic hydrolysis (45, 180 and 1440 minutes) improved the extent of deconjugation of the conjugated ESHs.

The same solvolysis and SPE procedures described previously were applied in this trial. Following the outcomes of Trials 6 and 7, 1 mL glass reacti-vials were subsequently used for the chemical solvolysis procedure. Following solvolysis and neutralisation, the solution was evaporated to ~100 µL under a stream of oxygen-free nitrogen gas (30 °C) and adjusted to ~240 µL with Milli-Q-Water (pH = 6.8). Instant buffer II (100 µL) was added, the solutions mixed by vortex and the BGS™ recombinant enzyme added (100 µL, 10 % glycerol, *v/v*). The BGS™ buffered solution was mixed gently by vortex, incubated at 53 °C for 45, 180, or 1440 mins,

cooled to room temperature, and Milli-Q-Water (4 mL, pH = 2) was added to each solution. Free ESHs were extracted from the Milli-Q water solutions by SPE using Strata-X (200 mg, 6 mL) cartridges as previously described (Trials 1-4) with the exception of using DCM/methanol (12 mL, 95:5 *v/v*) to elute the ESHs.

3.2.4.4 Enzymatic hydrolysis (BGS™) followed by Solvolysis (Trial 11)

The purpose of this trial was to confirm if reversing the sequence of the solvolysis and BGS™ enzymatic hydrolysis procedures improved the recovery of glucuronide ESHs as free ESHs. The residual acidity carried over by the solvolysis procedure to the BGS™ enzymatic hydrolysis procedure, could not be balanced by the enzyme buffer and the specific pH (pH = 6.8) required for optimal performance of the BGS™ enzyme was extremely difficult to achieve (Callejas, 2019). This problem could be overcome by reversing the solvolysis and BGS™ enzymatic hydrolysis procedures.

The dried sequentially spiked samples contained in 1 mL vials were re-dissolved in Milli-Q-Water (240 µL, pH = 2) and Instant buffer II (100 µL). Subsequently, the aqueous buffered solutions were vortexed and the BGS™ enzyme reagent was added (100 µL). The buffered BGS™ solution was mixed gently by vortex, incubated at 53 °C for 45 min, evaporated by Büchi Rotavapor R-200 rotary evaporation and re-dissolved in MeOH / tetrahydrofuran (1 mL, 20:80 *v/v*). Subsequently, trifluoroacetic acid (10 µL) was added and the acidified solution was vortexed, incubated at 45 °C for 30 min (Labadie and Budzinski, 2005b), neutralised with Na_2CO_3 (240 µL, 0.3 mol/L in Milli-Q-Water), evaporated to ~240 µL under a stream of oxygen-free nitrogen gas (30 °C) and Milli-Q-Water (4 mL, pH = 2) was added to the neutralised solution. Free ESHs were extracted from the Milli-Q water solutions by eluting them through previously conditioned Strata-X (200 mg, 6 mL) cartridges at a flowrate of one drop per a second followed by a rinse/wash with Milli-Q-Water / methanol (4 mL, 9:1 *v/v*). The Strata-X SPE cartridges were dried under vacuum to remove the bulk of residual water, and the ESHs eluted with DCM/methanol (12 mL, 95:5 *v/v*). The collected eluent was dried under nitrogen gas (30 °C), re-dissolved in acetone (2 mL), and stored at 4 °C in a refrigerator prior to derivatisation and GC-MS analysis.

3.2.4.5 Solvolysis followed by enzymatic hydrolysis (Helix pomatia) (Trial 12)

The purpose of this trial was to compare the performance of the optimised BGS^{TM} enzymatic hydrolysis and sequential chemical solvolysis ESH deconjugation procedure with a previously published procedure employing sequential chemical solvolysis and enzymatic hydrolysis using *H. pomatia* enzyme (Labadie and Budzinski, 2005b). The dried sequentially spiked samples were re-dissolved in MeOH / tetrahydrofuran (1 mL, 20:80 *v/v*) and trifluoroacetic acid (10 µL), vortexed and incubated at 45 °C for 30 min. Subsequently, the reaction mixture was neutralised with Na_2CO_3 (400 µL, 0.2 mol/L in Milli-Q-Water) and evaporated to ~400 µL under a stream of oxygen-free nitrogen gas (30 °C). Sodium acetate buffer (5 mL, pH=5) was added to the neutralised solution, following by mixing by vortex and the addition of the *H. pomatia* β-glucuronidase enzyme (30 µL). The buffered enzyme solution was mixed gently by vortex, incubated at 55 °C for 180 min and adjusted to pH = 2 using diluted sulphuric acid. Free ESHs were extracted from the pH adjusted solutions by SPE using Strata-X (200 mg, 6 mL) SPE cartridges as previously described.

3.2.5 Deconjugation of the CAP samples

The unavailability of suitable LC-MS-MS instrumentation precluded its use in this study. Therefore GC-MS was used in combination with enzymatic and chemical deconjugation to analyse conjugated ESHs in DSE and a DSE treatment system. The final procedure used to deconjugate, extract and analyse conjugated ESHs in the dissolved and solids phases of the extracted CAP samples is summarised in Figure 3-2.

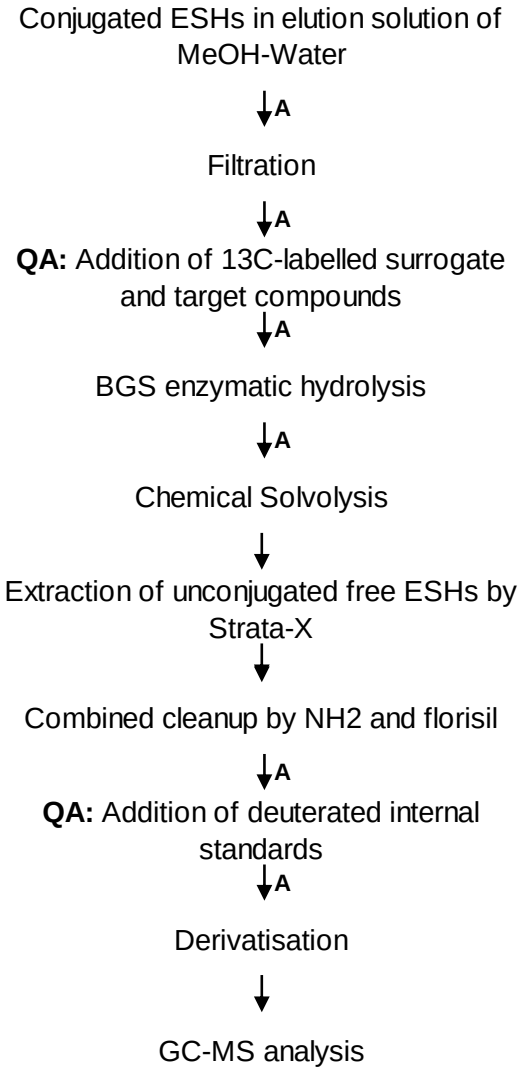

Figure 3-2: Schematic diagram of the chemical analysis procedure for conjugated ESHs. A=evaporation and re-dissolving step, QA=Quality assurance step)

The solutions containing conjugated ESHs from the solids and dissolved phase CAP ETS samples were dried by rotary evaporation (Büchi Rotavapor R-200), re-dissolved with methanol (2 mL), filtered through a mini-column of Hyflo Supercell C22 filter aid and collected in glass tubes (8 mL). The filtered sample extracts were evaporated to ~0.25 mL under a stream of oxygen-free nitrogen gas (30°C) and transferred to a reacti-vials (1 mL) with triplicate rinses of methanol (3 x 0.25 mL). The solids and dissolved sample extracts were evaporated to dryness under a stream of oxygen-free nitrogen gas (30°C) and re-dissolved in Milli-Q-Water (240 µL, pH = 6.8), Instant buffer II (100 µL) and BGS™ recombinant enzyme (100 µL). The buffered BGS™ solution was gently vortexed to mix and incubated (53°C, 45 min).

After incubation, the solutions were dried by centrifugal evaporation (Labconco ,1450 rpm, -4 °C, cold trap -105°C). The dried extracts were re-dissolved in methanol/tetrahydrofuran (1 mL, 2:8 *v/v*), transferred to a reacti-vials (1 mL), and trifluoroacetic acid (10 µL) was added. The solvolyis reaction was completed by incubating the reaction mixtures at 45°C for 30 minutes (Labadie and Budzinski, 2005b). At the conclusion of the reaction the solutions were returned to room temperature, neutralised with Na_2CO_3 (240 µL, 0.3 mol/L) and evaporated to ~240 µL under a stream of oxygen-free nitrogen gas (30°C). Milli-Q-Water (4 mL, pH = 2) was added to the neutralised solution and the free ESHs were extracted by eluting through Strata-X (500 mg, 6 mL) SPE cartridges at a flow rate of 5 mL/min. The Strata-X cartridges were dried under vacuum to remove the bulk of residual water and connected in series to a Florosil (1 g, 6 mL) SPE cartridge topped with ~3 cm layer of anhydrous granular sodium sulphate (dried overnight at 450°C) which was connected in series to a NH_2 (500 mg, 6mL) SPE cartridge (Labadie and Budzinski, 2005b). The connected cartridges were mounted in a SPE vacuum extraction manifold and the ESHs simultaneously eluted and purified by passing dichloromethane (DCM)/methanol (30 mL, 95:5 *v/v*) through the combined SPE cartridges and collecting the eluent in glass vials. The purified extracts were dried under nitrogen gas (30°C), re-dissolved in acetone (2 mL), and stored at 4°C prior to derivatisation.

3.2.6 Instrumental analysis of ESHs

All standards and CAP ETS samples were derivatised and analysed using GC-MS as previously reported (Chapter 2).

3.2.7 Quality assurance

QA samples, which were incorporated within each batch (n = 5-8) (dissolved or solids phase) of DSE samples included a Mill-Q-Water blank, a Milli-Q-Water spiked and a spiked matrix recovery sample. The recovery spiked matrix sample was obtained by evenly splitting a selected sample (the dissolved or solids phase of influent, sludge or effluent samples) into two, leaving one half unaltered while the other half was spiked with a mixture of conjugated ESHs containing 500 ng each. All samples, except the QA Milli-Q-Water blank, were spiked with a surrogate standard mixture of ^{13}C6-E1 and ^{13}C6-E2 (100 ng each). The QA Milli-Q-Water

spike and spiked matrix recovery samples were spiked with a mixture of conjugated ESHs containing βE2-17-G and E1-3-S (500 ng each).

The recovery of conjugated ESHs from the QA spiked matrix samples was determined by deducting the final measured concentration of free ESHs in the un-spiked half of the QA matrix sample from the half that was spiked with the mixture of conjugated ESHs. For determining overall recovery by the extraction method, a corresponding aliquot of the surrogate standard (^{13}C6-E1 and ^{13}C6-E2) and target parent compound (17α-E2, 17β-E2, E1) spike mixes added to each set of extracted and QA samples were transferred into a reacti-vial for use as a comparative standard for the calculation of their recovery. The preparation of the calibration solution was completed as previously described (Chapter 2).

3.2.8 Total estrogenicity

The total estrogenicity, expressed as the estrogen equivalents (EEQs) was calculated after assuming the conjugated ESHs would ultimately be deconjugated and converted into their free biologically active form. EEQs were calculated for individual free ESHs by multiplying their measured concentration by their respective potency factors determined from the ERCalux bioassay (Kolkman et al., 2013).

3.3 Results and discussions

3.3.1 Evaluation and optimisation of deconjugation procedure

3.3.1.1 Deconjugation trial outcomes

The mean % recovery of free ESHs produced from the deconjugation trials of glucuronide and sulphate conjugated ESHs are summarised in Figure 3-3 and reported in detail in the appendices (Table A-5 and Table A-6)

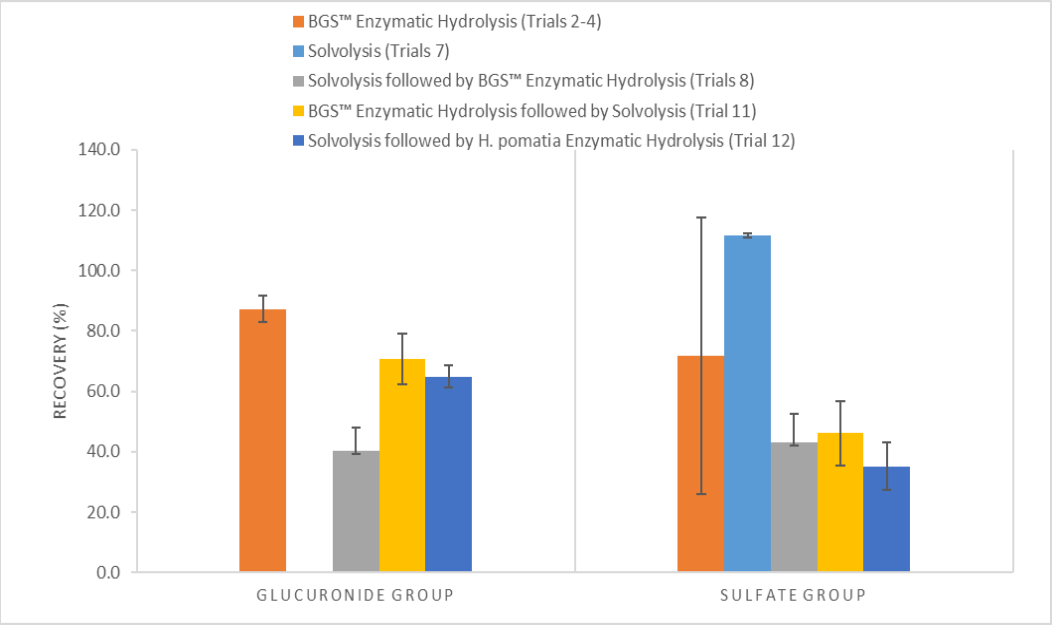

Figure 3-3 Deconjugation trial recovery of glucuronide or sulphate conjugated (mean (%) ± standard deviation of the mean).

Trials 1,5,6,9 and 10 results were not suitable due to poor reproducibility (Trial 5), or poor recovery of βE2-3,17-diS (Trials 1,5,6 and 10), E1-3-S (Trial 6), ^{13}C6-E2 (Trials 9 and 10) and βE2-3-G and βE2-17-G (Trials 9 and 10). Therefore, these were excluded from the assessment of the performance of the BGS™ to deconjugate sulphate and glucuronide ESH conjugates.

The BGS™ recombinant enzyme mix hydrolysis deconjugation trials (Trials 2-4) demonstrated a mean recovery of 87.2 % (98.4 % for 13C) and 71.9% (98.3 % for 13C) for the glucuronide and sulphate ESHs respectively, exhibiting the most efficient recovery (Sdev = 4.40%) of the glucuronide group but a diverse recovery range (Sdev = 45.8%) of the sulphate group. The variable recovery of the sulphate conjugated ESHs after deconjugation by the BGS™ indicated the need to introduce a chemical solvolysis step to improve the deconjugation efficiency of the sulphate conjugated ESHs. The solvolysis procedure (Labadie and Budzinski, 2005a) showed an improved mean recovery of 112% (90.4 % for 13C) of the sulphate conjugated group when the acidification was completed in 1 mL tubes (Trial 7). Incorporating the solvolysis procedure prior to the BGS™ enzymatic hydrolysis (Trial 8) (sequence previously performed by Labadie and Budzinski (2005a) and Combalbert *et al.* (2010) using the *H. pomatia* enzyme), demonstrated a mean

recovery of 40.3 % (45.5 % for 13C) and 43.0 % (87.5 % for 13C) for the glucuronide and sulphate conjugated ESHs respectively. These recoveries were related to the enzyme incubation time, whereby the highest mean recovery of the glucuronide and sulphate groups were obtained during the enzymatic incubation time of 45 minutes. At an enzymatic incubation time of 45 minutes, the solvolysis following the BGS™ enzymatic hydrolysis procedure provided slightly lower, but more repeatable recovery of the sulphate group than Trials 2-4 in which only the BGS™ enzymatic hydrolysis was used, however, this trial obtained reduced mean recovery of the glucuronide group in comparison with trials 2-4. The reduced recovery of the glucuronide and sulphate groups during the solvolysis following the BGS™ enzymatic hydrolysis procedure (Trial 8) was likely to be caused by the acidity carried over from the solvolysis procedure which could not be balanced by the enzyme buffer and the requisite small solution volumes to meet the BGS™ enzyme optimum pH level of 6.8 (J. L. Callejas, 2019). Changing the sequence of the procedure used in Trial 8 to BGS™ enzymatic hydrolysis followed by solvolysis (Trial 11), improved, in comparison with Trial 8, the BGS™ enzyme deconjugation performance of the glucuronide and sulphate with mean recoveries of 70.6 % (78.4 % for 13C) and 46.1 (97.2 % for 13C) respectively. However, sulphate Trial 11 resulted in reduced mean recoveries compared to the BGS™ hydrolysis and solvolysis when performed separately (Trials 2-4 and 7 respectively). For further comparison, the deconjugation procedure used by Labadie and Budzinski (2005a) using the *H. pomatia* enzyme (Trial 12), gave slightly reduced mean recoveries compared with the BGS™ hydrolysis following by the solvolysis procedure (Trial 11) with recoveries of 64.9 % (80.9 % for 13C) and 35.2 % (85.4 % for 13C) for the glucuronide and sulphate groups respectively.

In conclusion, when using the BGS™ enzyme to deconjugate ESHs it was necessary to reverse the commonly used sequence of solvolysis followed by enzymatic hydrolysis deconjugation. The BGS™ hydrolysis followed by the solvolysis procedure obtained the most stable and reproducible recovery of both the glucuronide and sulphate groups which were slightly better than the recoveries obtained by the deconjugation method using the *H. pomatia* enzyme and proved the

superiority of the new product, which was therefore selected to be used in this research for analysing the CAP samples.

3.3.2 Occurrence of conjugated ESHs in the influent, sludge and effluent of CAP treatment system

3.3.2.1 QA within field samples

The analysis of QA blanks from the extracted dissolved and solid-phase samples confirmed that there were no background traces of any of the conjugated ESHs or surrogate standards. Recoveries of the parent E2 and E1 from QA samples spiked with βE2-17-G and E1-3-S and surrogate standards ^{13}C6-E1 and ^{13}C6-E2 are summarised in Table 3-2.

Table 3-2: Recoveries after deconjugation process and extraction of the parent 17β-E2 and E1 spiked in the solids and dissolved phase and Milli-Q-water samples as βE2-17-G and E1-3-S, and surrogate standards ^{13}C6-E2 and ^{13}C6-E1.

Description	Parent 17β-E2	Parent E1	^{13}C6-E2	^{13}C6-E1
Spiked matrix-dissolved phase	87.6 (24.9, n=2)[A]	51.0 (22.7, n=2)	91.5 (6.3, n=2)	79.1 (18.6, n=2)
Spiked matrix-solids phase	70.8 (5.10, n=4)	46.8 (12.7, n=4)	77.4 (12.7, n=4)	80.6 (11.5, n=4)
Spiked Milli-Q-Water	75.8 (25.5, n=6)	39.2 (6.40, n=6)	67.4 (9.71, n=6)	74.4 (16.2, n=6)
Dissolved Phase Samples			83.2 (15.3, n = 21)	66.0 (35.7, n = 21)
Solids Phase Samples			78.4 (18.0, n = 18)	75.2 (18.5, n = 18)

[A] Values are expressed as mean %, (Sdev, n).

The mean recovery of the surrogate standards ^{13}C6-E2 and ^{13}C6-E1 from the spiked (βE2-17-G and E1-3-S) matrix dissolved and solids phase samples (77.4-91.5 %) was similar to that from the spiked Milli-Q-Water (67.4-74.4 %) and the analysed dissolved and solid phase field samples (66.0-83.2 %) and comparable to those obtained from the previous analysis of free ESHs from the same samples (Chapter 2, 68.7-117 %) and the recovery of deuterated E1 and E2 from previous studies of free ESHs in DSE and DSE treatment system, that is 91 % and 92 % respectively for E2-d4 and E1-d4 and 105 % for E2-d4 reported respectively by Gadd *et al.* (2010) and Sarmah et al. (2006). The mean recoveries of βE2-17-G and E1-3-S from the spiked dissolved and solid phases matrix samples and Milli-Q-Water samples were comparable to the recovery of dissolved phase conjugated ESHs in DSE (91-129 %) reported by Gadd *et al*. (2010), the recovery of E1-3-S (56 % and 72 %), 17β-E2-3-S (82 % and 95 %), E1-3-G (98 % and 64 %) and 17β-E2-3-G

(102 % and 73 %) from the faeces and urine respectively of cow, swine and chicken (Zhang et al., 2014) and spiked water (E1-3-S = 96 %, 17β-E2-17-G = 23 %) and swine lagoon effluent (E1-3-S = 110 %, 17β-E2-17-G = 150 %) (Hutchins *et al.*, 2007) using direct analysis by LC-MS-MS, and from river water (92 % for E2-G and 84 % for E2-G) in which chemical solvolysis and enzymatic hydrolysis were employed (Labadie and Budzinski, 2005b).

3.3.2.2 Concentration of conjugated ESHs in the dissolved and solid phases

Conjugated ESHs were detected in all analysed samples from the CAP ETS. The mean concentration of the conjugated glucuronide and sulphate conjugated forms sum (Σ Conjugated) of E1, 17b-E2, 17a-E2, and their corresponding total ESHs measured in the dissolved, solids and combined (total) phases are presented in Figure 3-4, Figure 3-5 and Figure 3-6 respectively and reported in details in the appendices (Table A-7 and Table A-8).

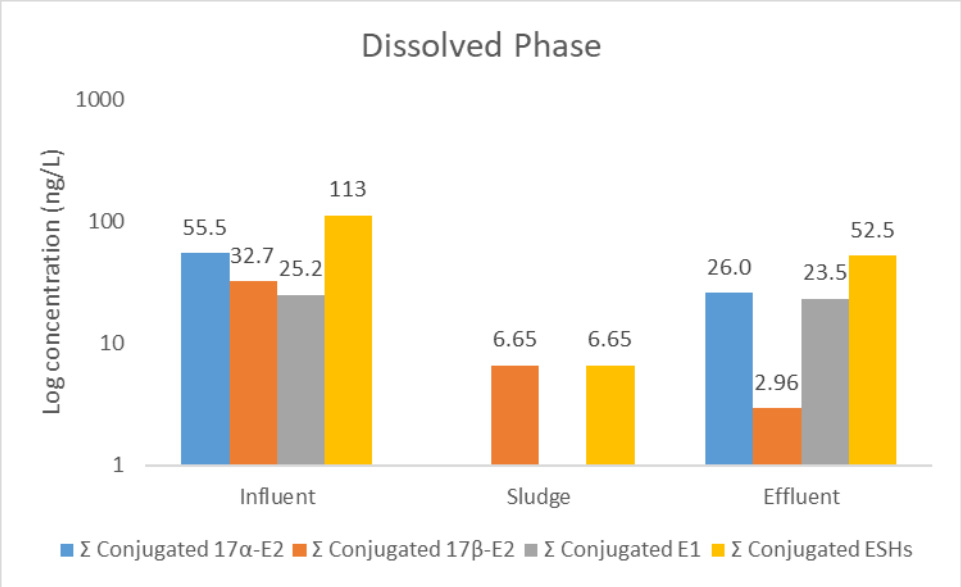

Figure 3-4: Mean concentration (Log scale) and sum of all conjugated ESHs for each of 17α-E2, 17β-E2, E1 and ESHs in the dissolved phase.

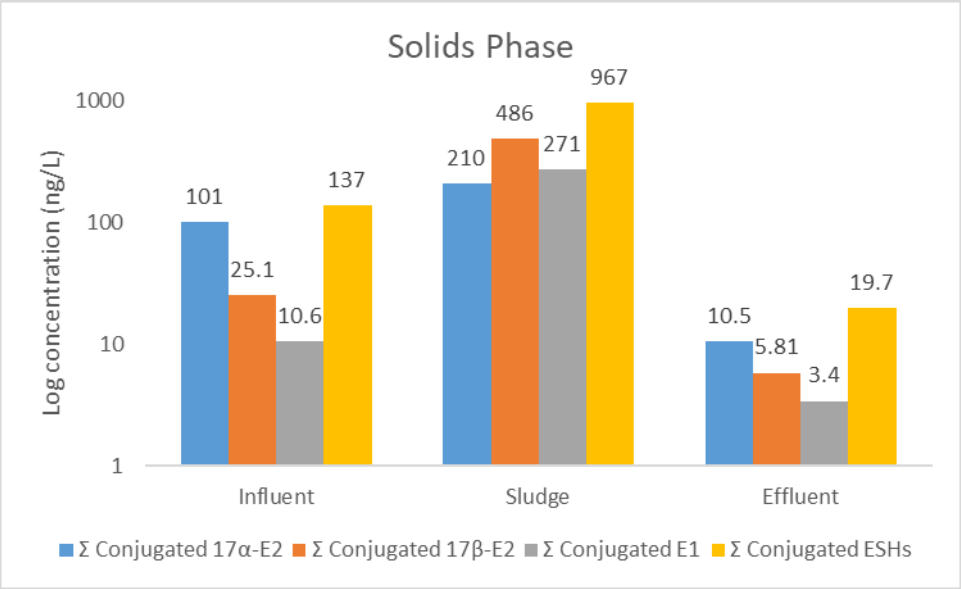

Figure 3-5: Mean concentration (Log scale) and sum of all conjugated ESHs for each of 17α-E2, 17β-E2, E1 and ESHs in the solids phase.

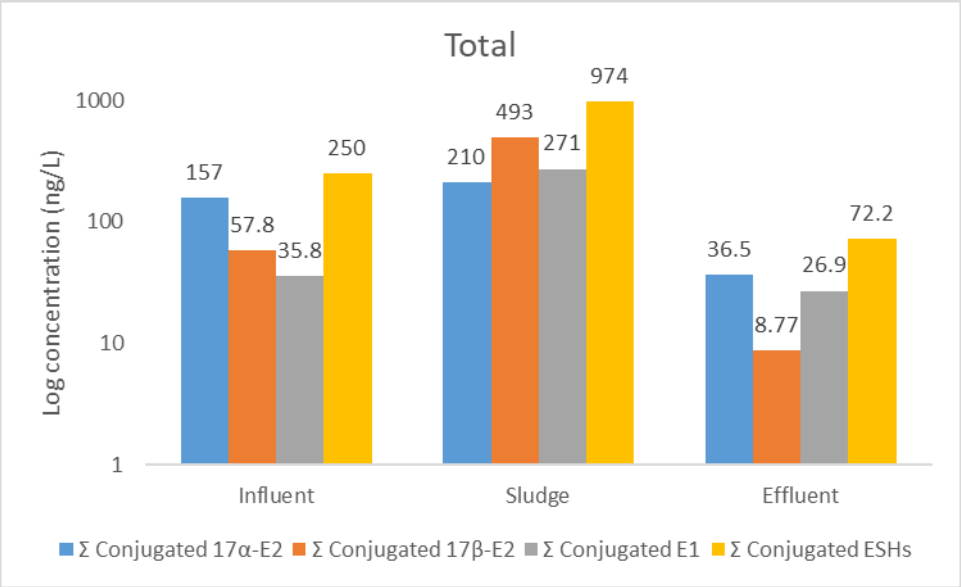

Figure 3-6: Mean concentration (Log scale) and sum of all conjugated ESHs for each of 17α-E2, 17β-E2, E1 and ESHs in the combined phase (total).

3.3.2.3 Concentration of conjugated ESHs (ng/L) in the dissolved phase of CAP influent, sludge and effluent

Unsurprisingly, the highest concentrations of conjugated ESHs measured in the dissolved phase were in the influent samples of the CAP ETS (Figure 3-4), in which 17α-E2 was measured in all the samples from March to November at concentrations

between 22.6 ng/L to 89.1 ng/L (mean = 55.5 ng/L), however the concentration of the 17α-E2 conjugates was the highest on only two of the six sampling occasions. In comparison, 17β-E2 and E1 detection frequencies were 83.3 % and 50.0 % respectively in which the corresponding concentrations were the highest for respectively three out of six and one out of six of the sampling occasions. Conjugated E1 provided the highest concentration overall (137 ng/L and mean of 25.2 ng/L) while conjugated 17β-E2 provided the lowest concentration overall with a maximum concentration of 67.4 ng/L (mean = 32.7 ng/L). The highest concentration of total conjugated ESHs of the dissolved influent samples was measured in the April sample (552 ng/L) and the lowest during October (69.8 ng/L) and November (97.1 ng/L) samples. This seasonal pattern in the concentration of Σ Conjugated ESHs exhibits a similar seasonal pattern to that which was previously observed for free ESHs (Chapter 2) and corresponds to calving being typically July to October.

In contrast to the influent samples, the only conjugated forms of conjugated ESHs measured in the dissolved phase of the CAP sludge were those of 17β-E2 (N.D-17.6 ng/L). Conjugated 17β-E2 was detected for three out of six sampling times corresponding to the August to November sampling times. The concentration of Σ Conjugated ESHs in the dissolved phase of the CAP sludge was between two- to eight-fold less than that in the corresponding samples of influent indicating that deconjugation have occurred within the CAP.

Conjugated ESHs were detected in the dissolved phase of all effluent samples, four out of six, two out of six and one out of six samples respectively for 17α-E2 (N.D-48.8 ng/L), 17β-E2 (N.D-9.00 ng/L) and E1 (N.D-141ng/L) and17α-E2 was predominant with mean concentrations of 26.0 ng/L. As observed for the CAP sludge dissolved samples, the conjugated ESHs in the dissolved phase of the effluent were not detected in the March and April samples. The mean concentration of the Σ Conjugated ESHs (52.5 ng/L) in the dissolved phase of the effluent was approximately half that of the dissolved influent sample Σ Conjugated ESHs concentration, but almost eight-fold higher than that in the corresponding samples of sludge.

The total conjugated ESHs measured in the dissolved phase of the influent is comparable with the conjugated ESH concentration range of 12-320 ng/L measured for DSE from 18 dairy farms in NZ (Gadd *et al*., 2010). Similarly, the sum of conjugated 17α-E2 and 17β-E2 measured concentration in the dissolved phase of the influent samples in this study are comparable with 17α-E2-3-S and 17β-E2-di-S detected in DSE of four farms in NZ at concentration ranges from N.D-230 ng/L and 17-230 ng/L respectively (Gadd *et al*., 2010). In comparison, the total conjugated ESHs measured in the dissolved phase of the influent is comparable to the conjugated ESH concentration measured in the dissolved phase of urine samples from replacement cow (132-173 ng/L (Zhang *et al*., 2014)) and farrowing sow manure (177 ng/L (Combalbert *et al*., 2010)), however, significantly less than the dissolved phase of samples from sow urine (42,534 ng/L (Zhang *et al*., 2014)) and higher than the dissolved phase of municipal waste (19.5-38 ng/L (Reddy *et al*., 2005; Ben *et al*., 2017)). The effluent Σ Conjugated ESHs concentration in the dissolved phase measured in this study is lower than the Σ Conjugated ESHs concentration of 299 ng/L (sum of E1-3-S, 17α-E2-3-S and 17β-E2-S) in dairy lagoon effluent (Hutchins *et al*., 2007), however, corresponds with slurry samples of anaerobic swine waste lagoon which had similar levels of E1-3-S (Yost *et al*., 2013).

3.3.2.4 Concentration of conjugated ESHs in the solids phase of CAP influent, sludge and effluent

The concentrations (ng/g) of conjugated ESHs measured in the solids phase of the samples from the CAP treatment system are presented in Table 3-3.

Table 3-3: Concentration of conjugated ESHs (ng/g) measured in the solid phase of raw influent, sludge and effluent samples of the CAP system

DSE/CAP INFLUENT										
Σconj	**Mar**	**Apr**	**Jul**	**Aug**	**Oct**	**Nov**	**Mean**	**Range[A]**	**Median**	**Sdev [B]**
17α-E2	2.93[C]	37.0	34.5	11.4	N.D[D]	1.76	14.6	N.D-37.0	7.16	16.9
17β-E2	N.D	9.00	8.19	4.46	N.D	N.D	3.61	N.D-9.00	2.23	4.24
E1	N.D	N.D	9.17	N.D	N.D	N.D	1.53	N.D-9.17	N.D	2.74
ΣESHs	2.93	46.0	51.8	15.9	N.D	1.76	19.7	N.D-51.8	9.39	23.4
CAP SLUDGE										
17α-E2	N.D	N.D	N.D	15.1	N.D	N.D	2.56	N.D-15.1	N.D	6.16
17β-E2	15.7	2.53	10.5	1.60	2.72	2.53	5.92	1.60-15.7	2.63	5.79
E1	N.D	N.D	19.8	N.D	N.D	N.D	3.30	N.D-19.8	N.D	8.09
ΣESHs	15.7	2.53	30.5	16.7	2.72	2.53	11.8	2.53-30.5	9.19	11.4
CAP EFFLUENT										
17α-E2	N.A[E]	N.A	10.2	8.00	N.D	N.D	4.56	N.D-10.2	4.00	5.34
17β-E2	N.A	N.A	5.19	4.91	N.D	N.D	2.52	N.D-5.19	2.46	2.92
E1	N.A	N.A	N.D	5.92	N.D	N.D	1.48	N.D-5.92	N.D	2.96
ΣESHs	N.A	N.A	15.4	18.8	N.D	N.D	8.56	N.D-15.4	7.71	10.0

[A] minimum to maximum. [B] standard deviation. [C] The measured concentration of conjugated ESHs in the solids phase of each sample (in ng/g). [D] not detected. [E] not available.

Although conjugated ESHs exhibit high water solubilities and demonstrate low log K_{oc} (Chen and Hu, 2010), conjugated ESHs were measured within the solid phase of the CAP ETS samples (Table 3-3). The adsorption characteristics of the conjugated ESH onto the solid phase due to the hydrophobic properties of the steroid moiety allowing hydrophobic bonding and increased affinity to the particulate phase. Other mechanisms can include hydrogen bonding and/or reduced polarity and electrostatic attributes when the glucuronide or the sulphate group is cleaved (Chen and Hu, 2010).

The mean measured concentration (in ng/g) of Σ Conjugated ESHs in the solids phase (Table 3-3) of the influent samples (19.7 ng/g) were slightly higher than the mean values of the sludge (11.8 ng/g) and the effluent (8.56 ng/g) samples. However, showed a similar profile to the dissolved influent sample (Figure 3-3) with 17α-E2 being the dominant species detected in five out of six samples (14.6 ng/g and maximum concentration of 37.0 ng/g), followed by 17β-E2 (3.61 ng/g detected in three out of six samples with a maximum concentration of 9.00 ng/g) and E1 (1.53 ng/g detected in only one sample at concentration of 9.17 ng/g). In

comparison, the concentrations and detection occurrence of the individual conjugated ESH in the solid phase of the sludge and effluent were 17α-E2 (respectively at 2.56 ng/g detected in one out of six samples with a maximum concentration of 15.1 ng/g and 4.56 ng/g detected in two out of six samples with a maximum concentration of 10.2 ng/g), 17β-E2 (respectively at 5.92 ng/g detected in six out of six samples with a maximum concentration of 15.7 and 2.52 ng/g detected in two out of six samples with a maximum concentration of 5.19 ng/g) and E1 (respectively at 3.30 ng/g detected in one sample at concentration of 19.8 ng/g and 1.48 ng/g detected in one sample at concentration of 5.92 ng/g).

To the best of our knowledge, our data is the first to report concentrations of conjugated ESHs in the solids phase of sludges (Solid Retention Time~30 days) from an anaerobic digestion treatment system, therefore making a useful contribution to the research on this topic. For comparison, lower concentrations of glucuronide and sulphate conjugated ESHs (0.4-1.3 ng/g and 0.3-0.8 ng/g respectively) were measured in treated municipal activated sludge (Ben *et al*., 2017).

3.3.2.5 Total concentration of conjugated ESHs (ng/L) in the CAP influent, sludge and effluent

The mean total combined Σ Conjugated ESHs concentration in the dissolved and solid phases (Figure 3-6) of the influent samples was 250 ng/L. The mean concentration of total Σ Conjugated ESHs measured in the dissolved and solid phase in the sludge samples was 974 ng/L. The greater proportion (967 ng/L) of Σ Conjugated ESHs were associated with the solid phase. The concentration of total Σ Conjugated ESHs concentration in the sludge was approximately four and 13.5 times higher than that in the influent and effluent samples respectively. However, in contrast to the influent and effluent samples, the predominant species in both solid and dissolved phases of sludge was Σ Conjugated 17β-E2 (486 ng/L) with a mean concentration of 492 ng/L detected in six out of six samples followed by E1 (271 ng/L) and 17α-E2 (210 ng/L) detected in one and two out of six samples respectively suggesting that the conjugated 17β-E2 species is less susceptible to deconjugated than E1 and 17α-E2.

As for the influent, the dominant species in the combined total effluent samples was Σ Conjugated 17α-E2 s with a mean concentration of 36.5 ng/L detected in four out of six samples followed, unlike the influent, by E1 (26.9 ng/L) and then 17β-E2 (8.76 ng/L) detected in one and three out of six samples respectively. The low measured conjugated 17β-E2 concentration in the effluent and high concentration in the sludge, suggesting that the conjugated 17β-E2 species are more amenable to staying in the sludge. The Σ Conjugated ESHs concentration in the combined total dissolved and solid phase of the effluent (Figure 3-6) of 72.1 ng/L is approximately 30% the conjugated ΣESHs concentration entering this system (influent) indicating the persistency of the conjugated ESHs through an anaerobic digestion system (Zhang *et al*., 2014) possibly in the form of conjugated sulphate ESHs (Gadd et al., 2010) and reduced removal capabilities compared with aerobic treatment (Zheng *et al*., 2013). The dominant parent conjugated ESHs measured in the dissolved and solid phase of the influent correlate well with other DSE free ESH studies that found the 17α-E2 is present in the highest concentration (Chapter 2) (Gadd *et al*., 2010; Noguera-Oviedo and Aga, 2016).

3.3.3 Transformation and fate of conjugated ESHs in CAP treatment system

The greatest proportion of the Σ Conjugated ESHs were associated with the solid phase of the sludge samples (Figure 3-6). The total mean concentrations of Σ Conjugated 17α-E2, 17β-E2 and E1 in the sludge samples increased (by 133 %, 848 % and 752 % respectively) compared with the measured total conjugated ESHs in the influent. The high increase of Σ Conjugated 17β-E2 and E1 in the sludge compared with the Σ Conjugated 17β-E2 and E1 in the influent indicates an increase of estrogenic potential of the sludge (Chapter 2) (Kolkman *et al*., 2013). In comparison, when observing the Σ Conjugated ESHs in the effluent samples, the total mean concentrations of the Σ Conjugated 17α-E2 and 17β-E2 were reduced by 75 % and 88 % respectively and E1 was slightly increased (by 110 %) compared with the measured total conjugated ESHs in the influent. The CAP treatment system demonstrated a total Σ Conjugated ESHs reduction of 67 %. The incomplete removal of the conjugated ESHs is possibly due to the persistence of sulphate conjugated 17α-E2, 17β-E2 and E1 in the DSE as such persistence has been shown

in animal waste (Zheng *et al*., 2013), sludge (Chen and Hu, 2010) and wastewater (Ben *et al*., 2017) treatment systems and soils (Bai *et al*., 2013). This could not be demonstrated in this study since the sulphate and glucuronide conjugated ESHs were assayed together due to the methodology employed. Future work might separately assay the glucuronide and subtract form the total to give sulphate contribution.

3.3.4 Contribution of conjugated ESHs (%) to the total load of ESHs in the CAP treatment system

The relative proportion that conjugated ESHs contribute to the total concentration of ESHs (free + conjugated) in the CAP ETS samples are presented in Figure 3-7 and reported in details in the appendices (Table A-9 to Table A-14).

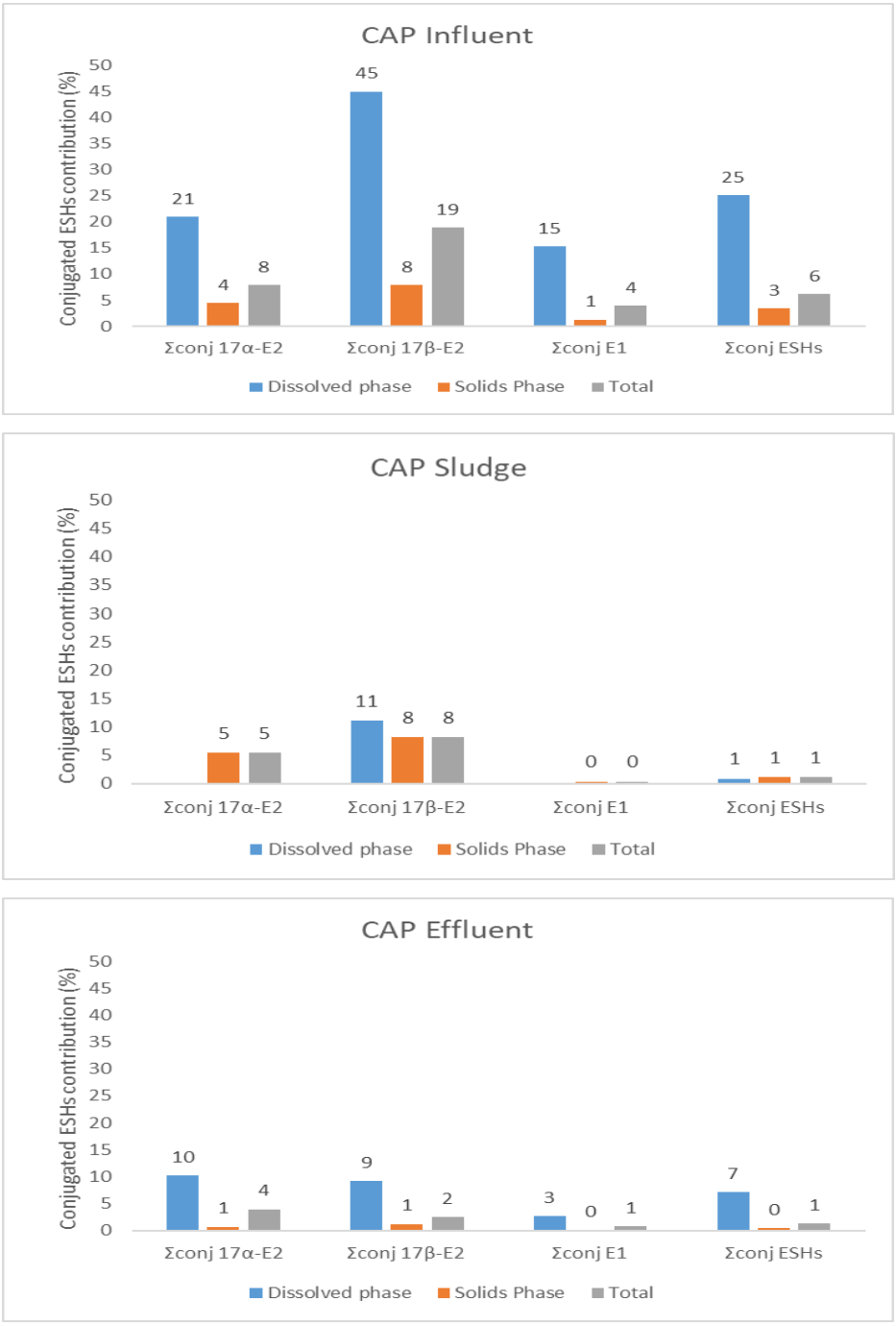

Figure 3-7: Phase related percentage contribution of conjugated ESHs (%) to the dissolved and solid phase and total ESH load within a CAP influent, sludge and effluent (∑ Conj=∑ Conjugated)

As expected, the contribution of conjugated species to total ESH load was greatest in the influent and substantially reduced in the sludge and effluent. This indicates that deconjugation is occurring in the system. In contrast to the profiles of free steroids shown in Chapter 2, where free E1 dominated sludge and effluent samples, conjugated 17β-E2 and 17α-E2 were the highest contributors in the sludge and effluent samples.

The Σ Conjugated ESHs distribution in the solids phase of the influent, sludge and effluent was lower (3 %, 1 % and 0 % respectively) than the contribution to the liquid phases. Overall, for combined solids and liquid phases, the conjugated ESHs comprise 6 % of the total ESHs in the influent and 1% of the sludge and effluent. Gadd *et al*. (2010), who considered only the liquid phase, found up to 22% of the total ESHs in dairy cow excreta were conjugated ESHs but conjugated ESHs in DSE contributed only 8 % of the total ESHs; these results parallel the findings here for the liquid phases. Zhang *et al*. (2014) reported 14.6-48.8 % contribution of conjugated ESHs to faeces and 10.6 % to urine of dairy cows; these results are in direct contrast to the finding in the current study of 25 % in the dissolved phase and 3 % in the solid phase of the influent to the CAP system. It is possible that the large volumes of water used to flush the effluent into the CAP system may change the distribution of the more water-soluble conjugated species. The same authors also found very large contributions of conjugated species in swine faeces and urine indicating a potentially far greater risk associated with ignoring conjugated ESHs in that species. However, stored (under anaerobic conditions) swine manure conjugated ESHs represented <10 % of the total hormones (Combalbert *et al*., 2012).

3.3.5 Conjugated ESHs Implications

A statistical summary of the calculated EEQs of the conjugated ESHs measured in the dissolved and solid phases of samples from the CAP are presented in Table 3-4 (full data set is provided in the appendices, Table A-15).

Table 3-4: Mean Estrogenic equivalents of conjugated ESHs measured in the dissolved and solid phases of 1 litre of raw influent, sludge and effluent of the CAP ETS.

	17α-E2	17β-E2	E1	ΣESHs
		Influent (n=6)		
Dissolved	0.56 (0.23-0.90)[A]	39.2 (N.D[C]-67.4)	0.14 (N.D-0.14)	39.9 (0.87-67.7)
Solids	1.22 (0.12-2.57)[B]	50.17 (N.D-62.6)	1.27 (N.D-1.27)	52.7 (N.D-65.2)
Total	1.57 (0.35-3.46)	89.4 (N.D-130)	1.41 (N.D-1.27)	92.6 (0.87-133)
		Sludge (n=6)		
Dissolved	N.D	13.3 (6.27-17.6)	N.D	13.3 (N.D-17.6)
Solids	6.30 (0.20-12.4)	486 (131-1284)	32.5 (32.5-32.5)	525 (143-1284)
Total	6.30 (0.20-12.4)	499 (137-1302)	32.5 (32.5-32.5)	538 (143-1302)
		Effluent (n=6)		
Dissolved	0.39 (N.D-0.49)	8.88 (N.D-9.00)	2.82 (N.D-2.82)	12.1 (N.D-9.37)
Solids	0.31 (N.D-0.35)	17.4 (N.D-17.9)	0.41 (N.D-0.41)	18.1 (N.D-18.3)
Total	0.70 (N.D-0.84)	26.3 (N.D-26.9)	3.23 (N.D-3.23)	30.2 (N.D-27.6)

[A] EEQ in 1 litre of sample (mean (range min to max)). [B] EEQ in 1 litre volume of sample calculated using the corresponding measured TS concentrations for influent, sludge and effluent samples. [C] Not detected.

The calculated estrogenicity of conjugated ESHs samples from the CAP ETS demonstrates the estrogenic potency of the samples is dominated as expected by the contribution of 17β-E2, with mean contributions of 96.5 %, 92.8 % and 87.1 % of total estrogenicity respectively for influent, CAP sludge, and CAP effluent. These results are similar to the 17β-E2 dominance contribution to the estrogenic potency of the free ESHs (Chapter 2). Although the contribution to total estrogenic activity of the conjugated species is small, the increased water solubility of these species can increase the movement of the ESHs in the environment and water ways when the sludge and effluent are applied to pasture (Casey *et al*., 2020) and subsequent deconjugation can increase the spread of activity over a wider area. The contribution of the overall estrogenic equivalents of the free and conjugated ESHs is discussed further in Chapter 6.

3.4 Conclusions

- Optimal performance of a new commercial enzyme for deconjugation was achieved using a BGS™ recombinant enzyme volume of 100 µL, incubating at 53°C for 45 minutes. Recoveries were similar to the *H. Pomatia* glucuronidase enzyme commonly used to analyse conjugated ESHs in animal waste. However, it was necessary to reverse the commonly used sequence of solvolysis followed by enzymatic hydrolysis because of the influence of residual acidity from solvolysis upon the former enzyme.
- The influent contains significant concentrations (251 ng/L) of conjugated estrogenic steroid hormones and therefore conjugated species need to be considered in future studies to get a more accurate estimate of estrogenic load.
- It is important to determine the existence of conjugated ESHs as they can persist through treatment systems and are more likely to reach surface water being a potential source, after deconjugation, of active and potent ESHs.
- Conjugated steroid hormones were found in the solid phase of the influent, sludge, and effluent samples.
- The influent and sludge of the CAP contained the highest concentrations of conjugated ESHs, while the effluent conjugated ESH levels were the lowest, indicating that some of the conjugated ESHs were deconjugated into free ESHs by anaerobic bacteria and/or degraded or adsorbed onto solids during anaerobic digestion.
- Analyses that include the conjugated fraction of ESHs provide a comprehensive assessment of the concentration and distribution of the different forms of ESHs within the CAP. Using this data, a model describing the fate of ESHs in the CAP can be developed, and the operational conditions that optimise removal/degradation can be identified (Basis of Chapter 6).
- Limitation: Using the deconjugation method, it was not possible to know which type of parent conjugated ESHs these ESHs originated from. the method used is also a very time-consuming and costly method. It is recommended that LC-MS-MS is used in preference.

Chapter 4:
Sorption of Estrogenic Steroid Hormones on New Zealand Grown *Pinus radiata* Powdered Biochar

The main objective of this study is to confirm the performance of powdered biochar to remove 17α-estradiol (17α-E2), 17β-estradiol (17β-E2) and estrone (E1) in clean water and to investigate the possible basis for removing/reducing estrogenic steroid hormones (ESHs) in dairy shed effluent (DSE) thereby improving the overall performance of the covered anaerobic pond (CAP) DSE treatment system.

4.1 Introduction

In recent years, there has been increasing environmental and health concerns over the discharge of micropollutants into the environment. Among these pollutants, endocrine-disrupting chemicals such as ESHs are of significant interest due to their high potency (Gomes *et al*., 2004) and ability to percolate through soils into the groundwater (Arnon et al., 2008; Steiner *et al*., 2010) and/or runoff into surface water (Labadie and Budzinski, 2005; Tremblay *et al*., 2018; Havens *et al*., 2020), ultimately reaching the drinking water supply (Du *et al*., 2020; Sodré and Sampaio, 2020). There is a growing global recognition that ESHs, even in concentrations as low as parts per trillion, have an impact on human, animal, and aquatic life in terms of reproductive health (Rempel, 2007; Li *et al*., 2019), sex ratio imbalances (Barber *et al*., 2011), hormone-related cancers (Ociepa-Zawal *et al*., 2010; Gonzalez *et al*., 2019) and metabolic disorders (Bhardwaj *et al*., 2019). Therefore there are clear benefits for human and wildlife health from ensuring that ESHs are not released into the environment.

Dairy cows are estimated to contribute around 79% of total estrogenic steroid hormones released by farmed animals in the European Union and 90% in the United States (US) (Lange *et al*., 2002; Kolodziej *et al*., 2004). New Zealand (NZ) has a strong dairy industry

with 6.4 million dairy cows in 2018 (StatsNZ, 2019). On average, DSE (combined waste of dairy cow urine, faeces, wash/recycled water and milk residue) contains approximately 44,000 ng/L of total (free and conjugated ESHs in the urine and faecal matter (Chapters 2 and 3). Previous studies show that 17β-E2, 17α-E2 and E1 are the most common free ESHs released to the environment by dairy cows (Sarmah *et al*., 2006; Zhang *et al*., 2014). These ESHs can be adsorbed to sludge (Chapter 2) and soils (Sarmah *et al*., 2008), and/or transformed and degraded by a combination of biotic and abiotic processes (Combalbert and Hernandez-Raquet, 2010; Liu *et al*., 2015; Ben *et al*., 2017; Ma and Yates, 2017). Nevertheless, a significant fraction of ESHs is still discharged on land and therefore into waterways in NZ (Tremblay *et al*., 2018), and other countries (Matthiessen *et al*., 2006; Arnon *et al*., 2008; Alvarez *et al*., 2013). This paper explores the use of biochar to intercept ESHs before they enter the waterways.

The organic carbon partition coefficient (log K_{oc}) for 17β-E2, 17α-E2 and E1 varies from 2.70 to 3.80 (Lai *et al*., 2000; Sarmah *et al*., 2008) (Chapter 2) making physical removal of ESHs by adsorption to carbonaceous compounds a promising method (Snyder *et al*., 2007; Liu *et al*., 2009; Delgado *et al*., 2012; Katsigiannis *et al*., 2015). The sorption mechanisms of ESHs include hydrophobic partitioning to organic carbon (Grathwohl, 1990; Lai *et al*., 2000) π–π electron donor-acceptor interactions and hydrogen bonding (Ahmed *et al*., 2018; Peiris *et al*., 2020). Surface area, pore size distribution and the concentration of oxygen-containing functional groups are the main factors that influence adsorbent adsorption capacity (Li *et al*., 2002; Matsui *et al*., 2012) and adsorption tends to occur in pores with similar dimensions to the target compound (Quinlivan *et al*., 2005; Bonvin *et al*., 2016).

Granular activated carbon (GAC) and powdered activated carbon (PAC) are the most commonly used and researched adsorbents for removing ESHs due to their high surface area, pore structure, and acid/base characteristics (Grover *et al*., 2011; Esmaeeli *et al*., 2017). Removal of organic compounds from wastewater usually involves filtering the water through gravity or pressure GAC filters (typical particle diameter > 0.1 mm), while PAC (typical particle diameter < 74.0 μm) is normally added to activated sludge or used in solid contact processes (Metcalf and Eddy, 2014). There are a number of studies that have compared the performance of PAC to GAC (Meinel *et al*., 2014; Esmaeeli *et al*.,

2017). PAC took longer for breakthrough to occur than GAC and had a higher removal rate when both were used as a filter media in a pilot-scale system to treat organic micropollutants (Meinel *et al*., 2014). Similarly, the ability of GAC to remove estradiol valerate, a medication, and progesterone in pharmaceutical wastewater was lower than PAC due to PAC having more accessible surface active sites for adsorption (Esmaeeli *et al*., 2017).

Biochar made by pyrolysis of, for example, agricultural waste such as corn stover or forestry waste, is a low cost carbonaceous material that can be effectively substituted for activated carbon to remove organic contaminants such as ESHs (Zheng *et al*., 2010; Ahmad *et al*., 2014; Gwenzi *et al*., 2017; Oliveira *et al*., 2017) as well as providing carbon sequestion when applied to land (Mohan *et al*., 2018; Maroušek *et al*., 2019). The surface properties of the biochar, the yield and the pore size distribution depend upon the raw material and the pyrolysis conditions used including temperature, retention time, heat transfer rate and air exposure (Ahmad *et al*., 2014; Metcalf and Eddy, 2014). Pyrolysis of biomass normally includes fast or slow configurations (Kambo and Dutta, 2015). Slow pyrolysis is performed at residence times of a few minutes to hours or days, and temperatures range between 100°C to 1000°C with biochar yields of up to 35 % of the raw material (Ahmad *et al*., 2014), while fast pyrolysis is performed at very short residence times of less than two seconds, and temperatures between 300°C to 1000°C with yields of up to 12 % (Ahmad *et al*., 2014; Inyang and Dickenson, 2015). The production of biochar as an adsorbent typically employs slow pyrolysis because of the high biochar yield and low operating costs compared with fast pyrolysis (Ahmed *et al*., 2016).

Biochar produced from wood is versatile, can act as electron receiver and/or acceptor (Enders *et al*., 2012; Ahmed *et al*., 2018; Peiris *et al*., 2020), and has a higher surface area than biochar from crop residue (Sarmah et al., 2010; Zhao *et al*., 2013) and animal manure (Sarfaraz *et al*., 2020) due to the cellular structure of wood which is retained when pyrolysed. Furthermore, biomass from lignin rich wood such as pine provides a high fixed carbon content (Enders *et al*., 2012), which is advantageous for adsorption as well as providing a highly stable structure.

Chapter 4: Sorption of estrogenic steroid hormones on New Zealand grown *Pinus radiata* powdered biochar

Forestry is a significant industry in NZ with forest products being NZ's third largest export earner. Plantation production forests cover approximately 7 % (~1.66 million hectares) of NZ's land which mostly consists of Radiata pine (90 %) and Douglas fir (6 %) (Ministry for Primary Industries, 2020). Typically, sawmill and crop wood residue are either dumped, burnt onsite as a source of energy or left to rot on land. The latter option, which has resulted in significant damage to coastlines and infrastructure during heavy rain events, seems likely to be banned by legislation fairly soon. Although there are some issues relating to cost of transport to the pyrolysis location, this wood residue could be readily pyrolysed to produce biochar that could be potentially be used by the dairy industry and/or individual farmers to reduce discharge of estrogenic compounds.

In this study, powdered biochar produced from *Pinus radiata* (with equivalent particle diameter as a commercial PAC) was investigated as an adsorbent for removing ESHs from water. The objectives of this study included:

- assessing the characteristics of *P. radiata* powdered biochar
- confirming the removal efficiency of 17α-E2, 17β-E2 and E1 by powdered biochar
- determining the percentage adsorption and kinetic and isotherm adsorption parameters of 17α-E2, 17β-E2 and E1 to powdered biochar
- establishing the framework for the subsequent experiment focusing on the sorption of ESHs from dairy shed effluent by biochar

4.2 Materials and Methods

4.2.1 Origin and production of biochar

Radiata pine woodchip was obtained from a local sawmill and pyrolysed by Massey University. Approximately 50 kg of woodchip (Moisture content = 10.2 %) was dried (60°C for 48 hours), pyrolysed in a portable batch vertical drum (height = 1,000 mm, radius = 750 mm) pyrolyser designed by Massey University (Bridges, 2013; Caco, 2017) (Figure 4-1) at 700°C for 6 hours and cooled producing approximately 14 kg of biochar (Cortez Pires de Campos, 2019).

The biochar was powdered using an IKA mill grinder and sieved using a 30 μm sieve (Quinlivan *et al*., 2005; Matsui *et al*., 2012; Bonvin *et al*., 2016), to achieve a product similar to a typical commercial PAC (15 – 30 μm) (Bonvin *et al*., 2016; Activated Carbon Technologies, 2022). The powdered biochar (Figure 4-2) was stored in a sealed container at room temperature before use.

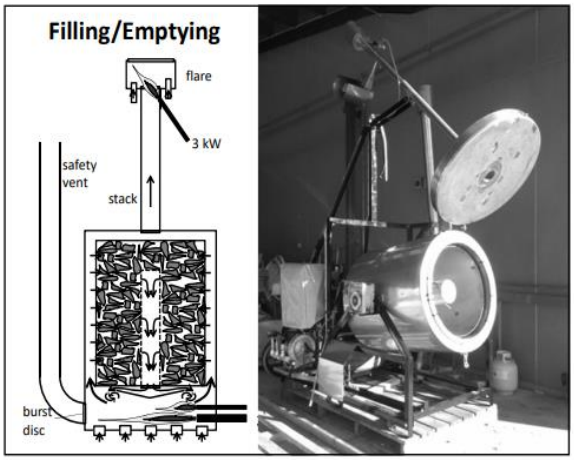

Figure 4-1: Illustration of Massey University 50 kg Pyrolyser used to prepare the studied biochar.

Figure 4-2: Powdered biochar used in this study.

4.2.2 Characterisation of Biochar

The powdered and sieved biochar was analysed for pH (ISO 10390:2005), size distribution using a Malvern Mastersizer 3000 analyser, specific surface area and pore size distribution using the Brunaur Emmertt Teller (BET) nitrogen adsorption isotherm method (NOVA-2000E), chemical structure and surface functional groups by Raman Spectroscopy (Ramanstation 400R, PerkinElmer) (McDonald-Wharry *et al*. (2013) and surface topography by Scanning Electron Microscopy (SEM) coupled with Electron Dispersive Spectroscopy (EDS). Elemental analysis (C, H, N, S, and O and ash contents) and inorganic compounds by Inductively Coupled Plasma-Mass Spectrometry (ICP-MS) were analysed by a certified laboratory.

4.3 Chemicals and materials

All solvents (HPLC grade), glass microfiber filters (GE Healthcare GF/F, 25 and 47mm diameter), Hyflo Supercell C22 filter aid (VWR Chemicals) and Hydromatrix (Dionex) were supplied by ThermoFisher Scientific, NZ. Deionized water was supplied by a Milli-

Q Millipore Integral 5 system. DL-Estrone-13,14,15,16,17,18-13C6 (^{13}C6-E1) and DL-Estradiol-13,14,15,16,17,18-13C6 (^{13}C6-E2) with an isotopic (purity > 99 %), were supplied by Cambridge Isotope Laboratories, 17β-estradiol-2,4,16,16-d4 (17β-E2-*d4)* and Estrone-2,4,16,16-d4 (E1-*d4)* (purity > 98 %) were supplied by CDN Isotopes, and 17α-E2, 17β-E2 and E1 (purity > 99 %) were supplied by Sigma Aldrich NZ. Calcium chloride dihydrate was obtained from Riedel-de Haen. Strata™-X 33µm (200 mg) solid-phase extraction (SPE) cartridges were obtained from Phenomenex NZ. Granular anhydrous sodium sulphate was obtained from Merck NZ. *N*-Methyl-*N* (trimethylsilyl) trifluoroacetamide (MSTFA) (UCT SMSTFA-0, Selectra-Sil) was supplied by PM Separations Australia. Triethylamine (purity > 99 %), ammonium iodide (purity > 99 %) and 2-mercaptoethanol (purity > 98 %) were obtained from Sigma Aldrich NZ.

4.4 ESH Adsorption

The distribution of ESHs between the solid phase (adsorbent) and aqueous phase is dependent on factors such as ESH concentration, biochar properties and environmental properties (Ahmad *et al*., 2014; Peiris *et al*., 2020). This study used ESH concentrations within the range found on dairy farm shed effluent, a solution pH of 7 and temperature of 20°C which are typical for dairy farm effluent (Chapter 6) and the environment within the NZ Waikato region. Biochar mass to solution volume ratio, and kinetic and isotherm adsorption trials were completed to determine biochar mass and adsorption behaviour of the ESHs to the powdered biochar (Figure 4-3). ESHs absorbed to the biochar were determined by measuring the change in concentration of ESH in solution, multiplying by the volume of solution, and dividing by the mass of biochar used (OECD 106 Guideline and ASTM D4646) (Sarmah *et al*., 2010; Tagliavini *et al*., 2017).

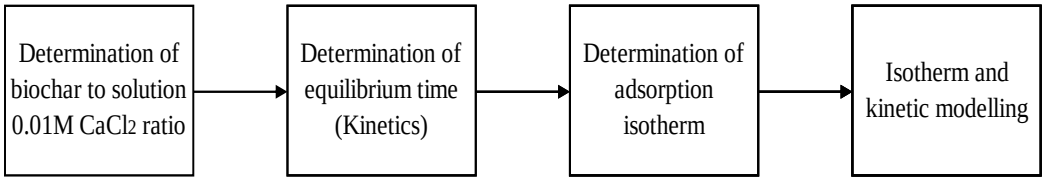

Figure 4-3: Outline of the ESHs adsorption trials

4.4.1 Determination of biochar to solution ratio

A stock of 0.01 M $CaCl_2$ pH 7 solution was prepared and split into three batches: the blank, one batch spiked with 17α-E2 and the other with E1 to make a final ESH concentration of 50 μg/L. 50 mL aliquots from each solution were added to 60 mL ASE glass bottles containing biochar added in the following quantities: 0, 0.5, 1, 2.5, 5, 10, 25, 50, 100, 250, 500 and 1000 mg (weighed using a Mettler Toledo XPE205 electronic balance). Each test for each type of ESH and mass of biochar was carried out in duplicate, a total of 44 tests, and two blanks. The sample bottles were sealed and positioned horizontally onto a shaking tray (IKA KS501), covered to prevent photodegradation and agitated at a temperature of 20°C and 150 RPM for 24 hours (Sarmah *et al*., 2010). The solution pH and temperature were measured before, during and after each experiment. The agitated biochar solution was filtered under vacuum using a GF/C filter (25 mm) and the filtrate (aqueous phase) was collected in a solvent clean 60 mL Accelerated Solvent Extraction (ASE) glass bottle, gravimetrically measured, preserved by adjusting the pH to 2.5 with concentrated sulphuric acid and stored in the dark at 4°C before extraction of the associated ESH (within 24 hours).

4.4.2 Determination of equilibrium time

The biochar mass determined in the biochar to solution ratio experiment was used to determine the equilibrium time of 17α-E2, 17β-E2 and E1 to the biochar. For each of 17α-E2, 17β-E2 and E1, three blank $CaCl_2$ solution (0.01 M, 50 mL) and nine different time intervals (0.5, 1, 2, 3, 6, 9, 12, 16, 24 hours) were used. Each time interval of the individual ESH contained triplicate samples at biochar mass of 1 mg and one corresponding control (no biochar) (four in total) in $CaCl_2$ solution (0.01 M, 50 mL, pH = 7) spiked with an ESH concentration of 2,500 ng/mL. Agitation, pH and temperature checks, filtration, gravimetric and preservation methods were the same as the biochar to solution ratio experiment.

4.4.3 Determination of adsorption isotherm

The biochar mass determined in the biochar to solution ratio experiment and used in the equilibrium time experiment of 17α-E2, 17β-E2 and E1 as well as the confirmed equilibrium time (24 hours) of 17α-E2, 17β-E2 and E1 confirmed in the equilibrium experiments was used to determine the 17α-E2, 17β-E2 and E1 adsorption isotherm to

the biochar. For each 17α-E2, 17β-E2 and E1, three blank $CaCl_2$ solutions (0.01 M, 50 mL) and seven different corresponding ESH concentrations (25, 50, 100, 250, 500, 750, 1000 µg/L) were used. Each individual ESH batch contained triplicate samples at biochar mass of 1 mg and one corresponding control (no biochar) in a $CaCl_2$ solution (0.01 M, 50 mL, pH = 7) spiked ESH (50 µg/L). Agitation, pH and temperature checks, filtration, gravimetric measurements and preservation methods were the same as Section 4.4.1.

4.4.4 Isotherm and kinetic modelling

The adsorption isotherm parameters were determined by fitting three commonly used isotherm models to experimental data:

4.4.4.1 Langmuir model (Equation 4-1):

$$q_e = \frac{q_m K_L C_e}{1 + K_L C_e} \quad (4\text{-}1)$$

Where q_e is the amount of ESH per unit weight of powdered biochar (ng/mg), C_e is the equilibrium concentration of ESH in the solution (ng/mL), q_m is the maximum adsorption capacity (ng/mg), and K_L is the constant related to the free energy of adsorption (mL/ng).

4.4.4.2 Freundlich model (Equation 4-2):

$$q_e = K_F C_e^{\frac{1}{n}} \quad (4\text{-}2)$$

Where K_F and 1/n are Freundlich constants. K_F indicates the adsorption capacity and 1/n is the heterogeneity factor.

4.4.4.3 Sips model (Equation 4-3)

$$q_e = \frac{K_L q_m C_e^{\frac{1}{n}}}{1 + K_L C_e^{\frac{1}{n}}} \quad (4\text{-}3)$$

The kinetic coefficients were determined using pseudo-first-order (Equation 4-4) and pseudo second-order kinetics (Equation 4-5) equations.

$$q_t = q_e(1 - \exp^{-k_1 t}) \quad (4\text{-}4)$$

Where q_t (ng/mg) is the ESH adsorbed at time t, q_e (ng/mg) is the adsorption capacity at equilibrium, k_1 (1/min) is the pseudo first order rate constant, and t is the contact time (min).

$$q_t = \frac{k_2 q_e^2 t}{(1 + q_e k_2 t)} \quad (4\text{-}5)$$

Where k_2 is the pseudo-second order rate constant (mg/ng min).

Pseudo-first-order assumes that the ESH adsorbed at time t (q_t) and the ESH equilibrium concentration (C_e) is the driving force for the adsorption of the ESH into the powdered biochar. In the pseudo–second-order kinetic model the assumption is that the rate-limiting step is chemical sorption or chemisorption and the ESH adsorption rate is dependent on adsorption capacity and not on concentration of the powdered biochar (Ahmed *et al*., 2018; Peiris *et al*., 2020).

Isotherm parameters were found by adjusting each parameter to reduce the sum of square errors (SSE) using Excel Solver™. The coefficient of determination (R^2) was used to determine the degree of fit of the isotherm and kinetic models results with the experimental data. The model that provided the best fit was selected to determine the sorption kinetics of 17α-E2, 17β-E2 and E1 onto powdered biochar using the pseudo first and second order kinetic models.

Removal efficiencies (in percentage) were calculated based on the concentrations of the target compounds using Equation 4-6.

$$R\ \% = \left[\frac{C_o - C_e}{C_o}\right] X\ 100 \quad (4\text{-}6)$$

Where C_o is the initial ESH concentration in the solution and C_e is the equilibrium ESH concentration in the solution (ng/mL).

4.5 Analytical method

4.5.1 Extraction of samples

The extraction of the samples was completed using a method based upon that previously described in Chapters 2 and 3. The filtered (dissolved) and pH adjusted samples (~50 mL, pH = 2.5) were spiked with a surrogate recovery standard of ^{13}C6-E1 and ^{13}C6-E2 at an equivalent concentration of 100 ng/mL and extracted by passing the samples through preconditioned Strata-X cartridges (200 mg) using a Teflon connector and mounted in a SPE vacuum extraction manifold. The SPE columns were rinsed with a solution of methanol/water (5 mL x 3, 10:90 *v/v*), dried under vacuum and connected in series to a premade (~5 cm) and acetone rinsed (30 mL) anhydrous granular sodium sulphate (dried overnight at 450°C) cartridge to remove any residual water. ESHs were eluted from the Strata-X and sodium sulphate cartridges with a mixture of dichloromethane (DCM)/methanol (12 mL, 95:5 *v/v*) at a flow rate of approximately 1 mL/min. The purified column eluent was collected in 15 mL centrifuge vials, evaporated to dryness under a stream of oxygen-free nitrogen gas (30°C), redissolved in acetone (1 mL) and stored at 4°C in a refrigerator prior to derivatisation and analysis.

4.5.2 Quality assurance

To eliminate the variability for the ESH spiked $CaCl_2$ solution concentration, a large volume (1 or 2 L) was freshly prepared at the start of each of the adsorption experiment in a Schott Bottle spiked with an individual ESH (in acetone) to a total final concentration of 50 µg/L (0.005 % acetone) per ESH. The ESH spiked $CaCl_2$ solution bottle was homogeneously mixed using a magnetic stirrer before aliquots (50 mL) were transferred to the ASE bottles. A non-spiked bulk (1 L) $CaCl_2$ solution was similarly prepared and used for the blank samples.

Quality assurance (QA) samples incorporated within each of the kinetic (n = 42) and isotherm (n = 38) experiment samples included:

- three comparison samples ($CaCl_2$ solution ESH spiked with no biochar samples that were promptly extracted without going through the adsorption method. These samples were used to confirm if there were any ESH losses during the adsorption method

- three $CaCl_2$ solution blanks and,
- control samples ($CaCl_2$ solution ESH spiked with no biochar) added to each set of the corresponding triplicate samples and used to determine if any of the ESH adsorbed onto the bottle

For determining overall recovery of the adsorption and analytical methods and the removal efficiency of the powdered biochar, a comparative standard was prepared by dispensing corresponding aliquots of the surrogate standard (^{13}C6-E1 and ^{13}C6-E2) and target compound (17α-E2, 17β-E2, E1) spike (in acetone) into a 1mL reacti-vial. Further information on the analytical method QA procedures and the preparation of calibration standards are described in Chapters 2 and 3.

4.5.3 Analysis of ESHs

The samples, QA extracts, comparative recovery standards, and calibration standards were dried to approximately 0.25 mL under nitrogen (30°C), internal standard solution added (equivalent to 250 ng each of 17β-E2-*d4* and E1-*d4*) and evaporated to dryness under nitrogen. ESHs were derivatised as their trimethylsilyl (TMS) ethers using an activated MSTFA/TMS mixture (Budzinski *et al*., 2006) and diluted with iso-octane (0.25 - 1 mL) and analysed using Gas Chromatography-Mass Spectrometry (GC-MS) as previously reported (Chapters 2 and 3).

4.6 Results and Discussion

4.6.1 Biochar characterisation

SEM images of the biochar (Figure 4-4) show it was highly friable, with particles ranging from 5 up to 200 μm, it retained the cellular structure of the original pine and there were no fibrous structures. This indicates that the wood was highly carbonised from pyrolysis, losing the hemicellulose, cellulose, pectin and other proteins that enabled the wood to maintain a flexible fibrous structure. Little surface deposition was observed indicating that coking, tar and salt deposition was low, an indication of low ash content and high sustained pyrolysis temperatures that prevented coking and encouraged cracking of the high molecular weight volatile compounds (Chen *et al*., 2008; Kazemi Shariat Panahi *et al*., 2020). This observation is supported by the measured low ash (Table 4-2) and

effective combustion and high pyrolysis temperature (Table 4-4) (Cortez Pires de Campos, 2019).

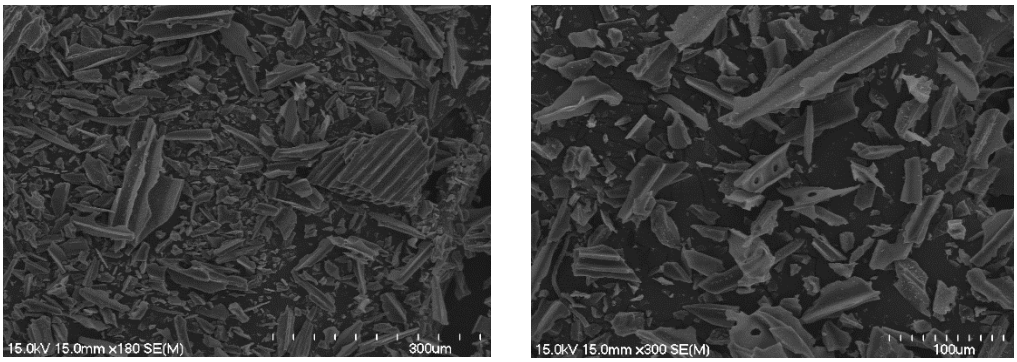

Figure 4-4: SEM pictures of the powdered biochar at 300 µm and 100 µm

The particle size distribution (Figure 4-5) of the powdered biochar was approximately gaussian with a mean particle size of 26.5 µm. This was supported by the SEM images which showed particles in a similar range indicating complete pyrolysis producing highly friable biochar i.e. a total loss of any fibrous structures enabling it to be readily ground and sieved resulting in a consistently sized biochar that could be safely used for lab-scale biochar adsorption experiments (If the pyrolysis had been incomplete, more fibrous structures would be present, and these would have been observed inside the IKA mill and sieve).

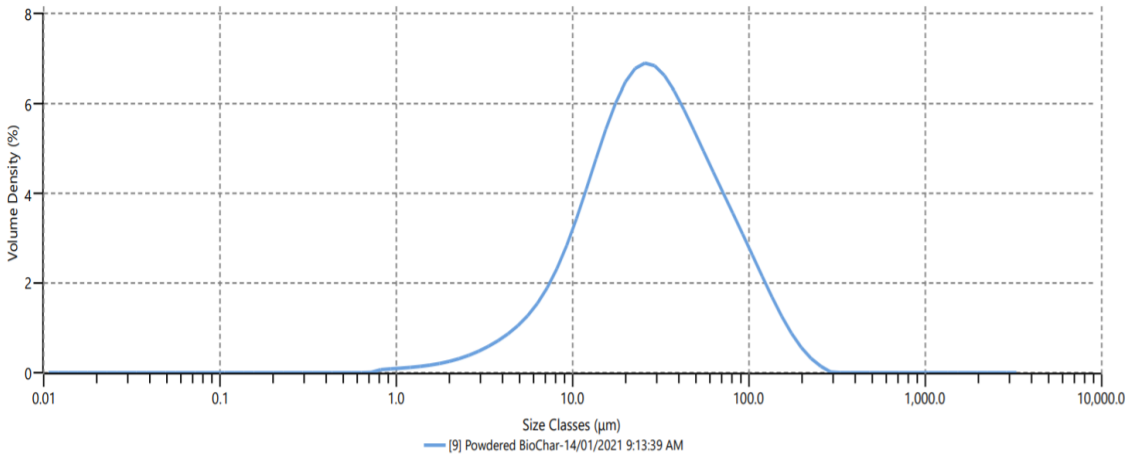

Figure 4-5: Particle size distribution of the Powdered Biochar

The surface area, pore volume and pore size were 82.5 m^2/g, 16.2 cm^3/g and 37.8 Å respectively (Table 4-1). The pore size of the biochar is similar to the polar surface area

(~40 Å) of 17β-E2 and E1 (Ahmed *et al*., 2018) which suggests adsorption will be high (Quinlivan *et al*., 2005; Bonvin *et al*., 2016; Tagliavini *et al*., 2017). The surface area of the powdered biochar was comparable to a biochar produced from rice husk, which was pyrolysed at 350 °C and 650 °C for 2 hours producing surface areas of 85 and 142 m^2/g respectively. However, the rice husk biochar had lower pore volumes of 0.057 and 0.187 cm^3/g (Jiang *et al*., 2017) compared to the biochar in this study (16.2 cm^3/g). The powdered biochar had a higher surface area than a *Eucalyptus globulus* based functionalised (activated) biochar pyrolyzed at 400°C for 2 hours which had a surface area of 1.18 m^2/g (Ahmed *et al*., 2018). In comparison, steam activated carbon produced from mill and forest residues using a rotary calciner at 815 °C had surface areas between 575.9 to 1283 m^2/g (Matsui *et al*., 2012) while commercial PAC and GAC have surface areas of 1070 to 1354 m^2/g respectively and pore volumes around 0.757 cm^3/g (Bonvin *et al*., 2016).

Table 4-1: Parameters of the powdered Massey biochar

Effective diameter (D_{10}) (µm)	Median diameter (D_{50}) (µm)	BET surface area (m^2/g)	Pore volume (cm^3/g)	Pore size (Å)
8.26	26.5	82.5	16.2	37.8

Elemental analysis of the powdered biochar (Table 4-2) showed that carbon was the main constituent (90.5%) and the biochar had O/C, H/C and (N+O)/C molar ratios of 0.39, 0.12. and 0.40 respectively, which places it as a Class 1 biochar (suitable as feedstock and for agricultural application) (European Biochar Foundation, 2012; International Biochar Initiative, 2015). The biochar had a volatile content of 4.2% and ash content of 1.4% by mass indicating that most of the volatile matter had been removed or fixed, which supports the SEM observations of very little surface tar and ash deposition resulting in a good biochar surface area (Enders *et al*., 2012). Furthermore, the high carbon content, low H/C ratio, and low volatile content show that the biochar was highly carbonised and the majority of the carbon was fixed (Enders *et al*., 2012; Crombie *et al*., 2013; Xiao *et al*., 2016), which explains the friability of the resulting char. The O/C and polarity index ((N+O)/C molar ratio values indicate a high pyrolytic temperature was used, resulting in low hydrophilic properties (Chun *et al*., 2004; Cornelissen *et al*., 2005) and low numbers of polar functional groups (Chen *et al*., 2008) suggesting that the surface chemistry of the biochar will have a strong affinity to ESH which is hydrophobic and non-polar (Li *et al*.,

2002; Wang *et al*., 2020). The carbon content is higher and ash content lower than that of biochar made from soft wood (450 °C for 2.5 hours) and hard wood (750 °C for a few minutes) which contained carbon (77 % and 74 %) and ash (17.30 % and 9.80 %) and which were used to reduce steroid hormone originating from poultry and swine manure applied to agricultural land (Alizadeh *et al*., 2018). Similarly, the carbon and ash contents are comparable to commercially available GACs, which have a carbon and ash content of 76.92 – 92.50 % and 1.84-3.37 % respectively and which are used to adsorb organic micropollutants (Quinlivan *et al*., 2005), and higher than PAC which has a carbon content of 59.3 % and which has been used to adsorb 17β-E2 and other emerging contaminants (Kim *et al*., 2016).

Table 4-2: Composition and pH of powdered biochar (sample mass = 25 g)

	Results	Unit
Moisture	3.7	%
Ash	1.4	%
Volatile matter	4.2	%
Gross calorific value	31.47	MJ/kg
Net calorific value	31.18	MJ/kg
Sulphur	0.01	%
Carbon	90.5	%
Hydrogen	0.93	%
Nitrogen	0.46	%
Oxygen	3.0	%
pH	8.9	

The ICP-MS analysis results showed that the powdered biochar contained metals, with concentrations as high as 2,480 mg/kg for potassium and 1,190 mg/kg for calcium (Table 4-3) potentially reducing the biochar capacity to adsorb the ESHs (Matsui *et al*., 2012). Furthermore, chromium and nickel concentrations were higher than expected at 252 and 136 mg/kg respectively, possibly due to these metals being leached from the pyrolysis vessel stainless steel drum into the biochar during the pyrolysis process. Overall, the concentrations of all the metals in the powdered biochar were lower than the International Biochar Initiative (IBI) maximum allowable test category B parameters thresholds (International Biochar Initiative, 2015) meeting the soil toxicity requirements for soil amendments, composts, and fertilisers.

Table 4-3: Inorganic analysis of the Powdered Massey Biochar

Metal	Concentration in biochar[A]	Metal	Concentration in biochar[A]	Metal	Concentration in biochar[A]
Aluminium	219	Copper	5.4	Selenium	<0.5
Antimony	<1	Iron	-	Silver	<0.5
Arsenic	0.85	Lanthanum	-	Sodium	145
Barium	3.2	Lead	0.2	Sulphur	87
Bismuth	<0.2	Lithium	<1	Strontium	5
Beryllium	<0.2	Magnesium	344	Thallium	<0.5
Boron	5	Manganese	63.6	Tin	<1
Cadmium	<0.1	Molybdenum	12.6	Uranium	<1
Caesium	-	Nickel	136	Vanadium	1.5
Calcium	1190	Phosphorus	156	Zinc	4
Chromium	252	Potassium	2480		
Cobalt	1.6	Rubidium	-		

[A] values are expressed as (mg/kg).

Raman analysis of the Massey biochar suggested the effective Heat Treatment Temperature (HTT) achieved was between 725 – 815 C° (Table 4-4). This high HTT is indicated by two prominent peaks in the Raman spectra at 1350 cm^{-1} (D band) and 1595 cm^{-1} (G band) and a minor peak at 1407 cm^{-1} (A band), which are absent or greatly diminished at low HTT (McDonald-Wharry *et al*., 2013). The high HTT and band position suggests that the nanostructure development of the biochar reached completion, i.e. the carbon/oxygen structures had been mostly carbonised (McDonald-Wharry *et al*., 2013). The Massey University 50 kg Pyrolyser operating conditions were set to pyrolyse the woodchips at 700°C, therefore, the Raman analysis results shows that this operating temperature was achieved and possibly exceeded.

Table 4-4: Raman analysis results

Description	Values
D band position (cm^{-1}).	1314
G band position (cm^{-1}).	1595
A band position (cm^{-1}).	1407
I(D)/I(G)	1.070
I(V)/I(G)	0.422
I(A)/I(G)	0.605
(I(A)-I(V))/(I(G)-I(V))	0.317
(I(D)-I(V))/(I(G)-I(V))	1.121
Photoluminescence slope/I(G)	0.546
Estimated Hydrogen Content	0.210
Effective HTT (Estimated using G band position)	724.6
Effective HTT (Estimated using I(V)/I(G))	814.9

Data evaluated based on a method developed by McDonald-Wharry et al (2013).

4.6.2 Quality assurance outcomes

The recovery of the targeted ESHs and surrogate standards ^{13}C6-E1 and ^{13}C6-E2 from the samples were high (median = 95.2 %) (Table 4-5) suggesting that the adsorption and analytical methods used are robust and consistent.

Table 4-5: Recovery of target QA ESHs (17α-E2, 17β-E2 and E1) and surrogate standards (^{13}C6-E1 and ^{13}C6-E2) obtained from the biochar to solution ratio and adsorption kinetic and isotherm experiments

	Biochar to solution	Adsorption kinetic	Adsorption isotherm	Mean
17α-E2 (Comparison) [A]	102 (0.64, n=4)[C]	99.1 (1.71, n=3)	N.A	101
17α-E2 (Control) [A]	99.6 (2.55, n=4)	96.8 (4.56, n=9)	102 (2.37, n=7)	99.5
17β-E2 (Comparison) [A]	N.A[D]	93.8 (2.32, n=3)	N.A	93.8
17β-E2 (Control) [A]	N.A	93.7 (1.88, n=9)	99.2 (2.62, n=7)	96.5
E1 (Comparison) [A]	93.9 (4.60, n=4)	102 (2.77, n=3)	N.A	98.0
E1 (Control) [A]	91.0 (3.37, n=4)	97.6 (2.44, n=9)	87.9 (3.32, n=7)	92.2
^{13}C6-E2 [B]	94.7 (3.32, n=44)	93.0 (8.10, n=117)	92.4 (3.64, n=55[E])	93.4
^{13}C6-E1 [B]	93.8 (4.96, n=44)	94.1 (10.6, n=117)	92.9 (3.23, n=55[E])	93.6

[A] spiked at 25 µg/L concentration. [B] spiked at 100 ng/L [C] values are expressed as (mean (%) (SDev (%), n)). [D] Not applicable. [E] Reduced number of surrogate standards was performed at the high concentration samples due to proven high recovery rate of the method and economic reasons.

The similarity between the recovery of the targeted ESHs comparison and control samples showing that ESHs losses to the sample bottles were negligible and no photodegradation or transformation of ESHs occurred during the adsorption trials.

4.6.3 Biochar to solution ratio

Typically, the adsorbent to solution ratio should ensure 50% of the contaminant is adsorbed, while ensuring that there is enough of the contaminant in the aqueous phase for it to be measured accurately (OECD-Guideline 106). Only powdered biochar masses of 0.5 and 1 mg showed detectable concentrations in the solution (120 – 1,469 ng/mL) (Table 4-6) and removals of 46.0 – 95.2 % were achieved for both 17α-E2 and E1 after 24 hours. Therefore, a biochar mass of 1 mg was used for the subsequent adsorption experiments.

Table 4-6: Adsorption (t=24 hours, pH = 7±0.2 and temperature = 20°C± 2°C) of target ESHs (17α-E2 and E1) spiked at ~50 µg/L (or ~2,500 ng/mL) into CaCl2 solution (50 mL) at different biochar masses

	17α-E2		E1	
Biochar mass[A]	**concentration in the aqueous phase[B]**	**Percentage adsorbed[C]**	**concentration in the aqueous phase[B]**	**Percentage adsorbed[C]**
0.5	1,469 (118, n=2)	46.0 (4.35, n=2)	1,089 (92.8, n=2)	56.2 (3.74, n=2)
1	389 (75.3, n=2)	92.7 (2.77, n=2)	120 (41.2, n=2)	95.2 (3.67, n=2)
2.5	14.1 (3.37, n=2)	99.5 (0.13, n=2)	N.D[D]	N.D
5	2.86 (2.77, n=2)	99.9 (0.05, n=2)	N.D	N.D
10 - 1000	N.D	N.D	N.D	N.D

[A] values are expressed as mg, [B] values are expressed as (mean (ng/mL) (SDev, n)), [C] values are expressed as (mean (%) (SDev, n)), [D] not detected in the dissolved phase indicating complete adsorption of ESH into the powdered biochar.

4.6.4 Adsorption kinetics

The removal of 17α-E2, 17β-E2 and E1 by the powdered biochar at different time intervals (n = 9) are presented in Figure 4-6 (full data is provided in the appendices, Table A-16, Table A-17 and Table A-18). 17α-E2, 17β-E2 and E1 were rapidly adsorbed onto the powdered biochar during the first 2 hours with 68 %, 70 % and 74 % respectively being absorbed within this time. Equilibrium was reached within 6-12 hours with 79–97% of the ESH being absorbed, and 93-94 % after 24 hours. This is in line with previous work where a commercial polymer-based spherical activated carbon achieved 96-99 % removal of E1 and E2 (Tagliavini *et al*., 2017). Concentrations of ESH on the biochar reached between 103-133 µg ESH/mg biochar, while solution detection concentrations dropped to as low as 120 ng/ml. Little difference in adsorption rates was observed between 17α-E2, 17β-E2; E1 adsorbed more rapidly and reached equilibrium after *circa* 6 hours, while 17α-E2, 17β-E2 took *circa* 12 hours to reach equilibrium.

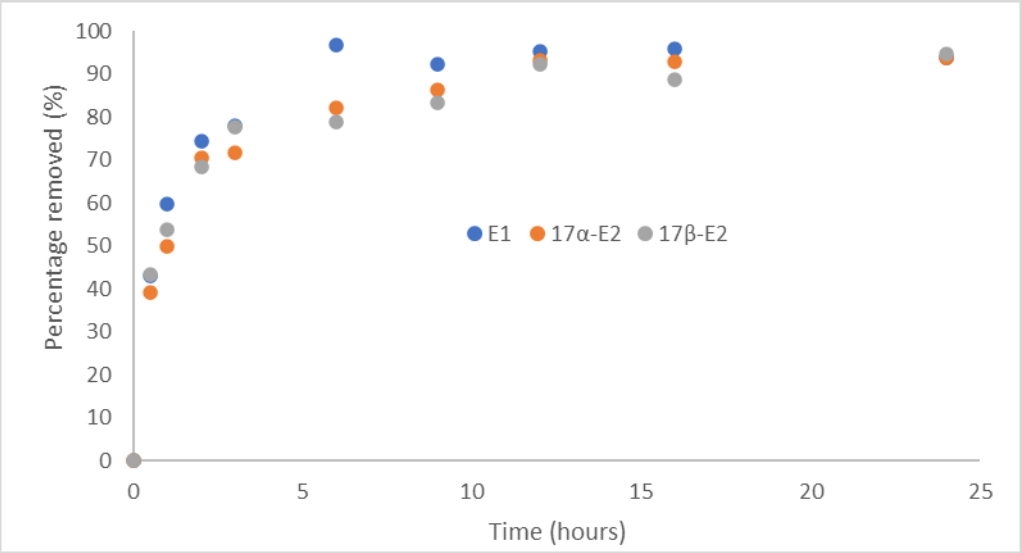

Figure 4-6: Percentage adsorbed of 17α-E2, 17β-E2 and E1 by the powdered biochar (1 ± 0.08 mg) at different time intervals (pH = 7 ±0.2, Temperature = 20°C± 2°C).

The rapid adsorption of E1 compared to 17α-E2 and 17β-E2 is comparable to the Ahmed et al. (2018) study and is because E1, which has only one OH group for H-bonding, has a lower aqueous solubility of 0.8 mg/L at 25 °C compared to 17α-E2, 17β-E2 which are 3.9 mg/L at 25 °C (Kennedy and Jin, 2006). The powdered biochar had better adsorption of E1 compared to other studies (~ 60 %) using a functionalised biochar dosed at 225 mg/L and E1 initial concentration of 465.9 µg/L (Ahmed *et al*., 2018), and had similar 17β-E2 removal compared to a commercial PAC (~50%) dosed at 25 mg/L and contact time of 1 hour (Kim *et al*., 2016).

4.6.5 Adsorption isotherm

The percentage removal and adsorption isotherm results for 17α-E2, 17β-E2 and E1 are presented in Figure 4-7 and Figure 4-8 respectively (full data is provided in the appendices, Table A-19, Table A-20 and Table A-21). At low starting concentrations (25 – 50 µg/L), the biochar showed similar removals of 17α-E2, 17β-E2 and E1 with 84 – 99 % of the ESHs being adsorbed. At higher ESH concentrations (> 400 µg/L), 17β-E2 had greater affinity to the biochar than 17α-E2 and E1, with 60 % of the 17β-E2 being removed and the biochar concentrations reaching 1,200 ng 17β-E2 /mg biochar, while 17α-E2 and E1 reached 400 ng / mg biochar. This could be due to the upward pointing orientation of the -OH group on the 17th carbon enabling greater access to binding sites on the biochar compared to 17α-E2 and E1. This means that the biochar is much better at

adsorbing 17β-E2 which has a much higher estrogenic potency than 17α-E2 and E1 (Chapters 2 and 3).

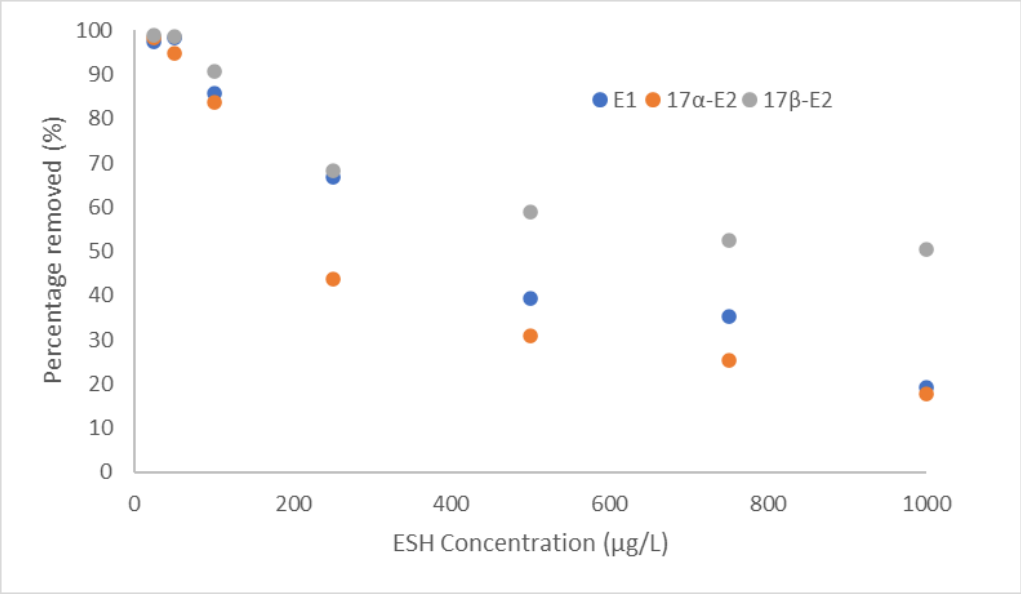

Figure 4-7: Percentage adsorbed of 17α-E2, 17β-E2 and E1 by the powdered biochar (1 ± 0.09 mg) at different concentrations (pH = 7 ±0.2, Temperature = 20°C± 2°C).

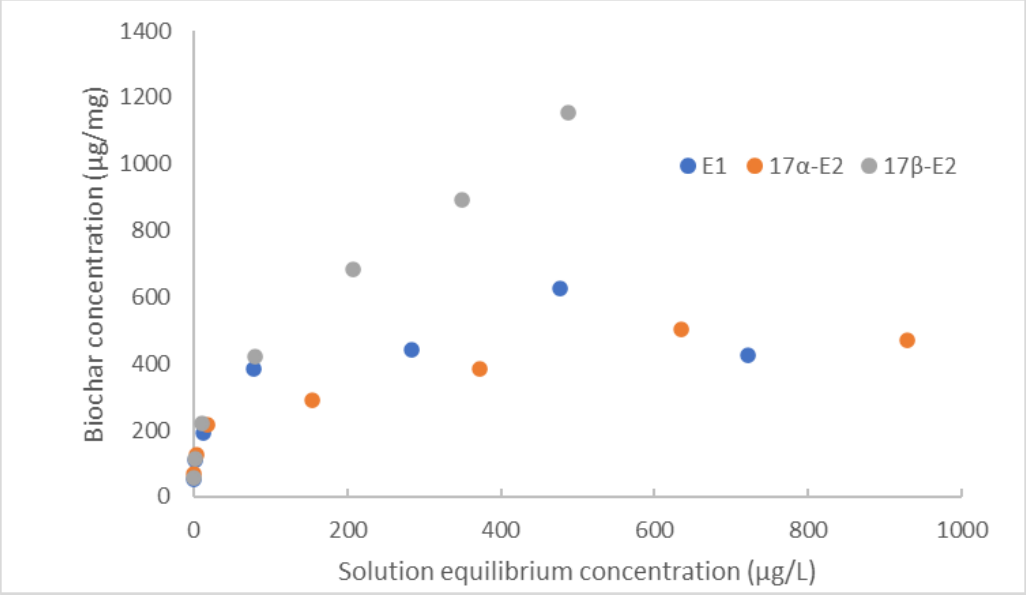

Figure 4-8: 17α-E2, 17β-E2 and E1 concentration in powdered biochar concentration (µg/mg) at different ESH solution equilibrium concentrations (pH = 7±0.2, Temperature = 20°C± 2°C).

4.6.6 Isotherm and kinetic modelling results

The most common isotherms used for modelling adsorption of ESHs onto biochar (Sarmah *et al*., 2010; Ahmed *et al*., 2018; Peiris *et al*., 2020) and activated carbon (AC) (Tagliavini *et al*., 2017) are the Freundlich and Langmuir isotherms. In this study, the Sips isotherm was also applied in addition to the Freundlich and Langmuir models Figure 4-9 (Full data is provided in the appendices, Table A-22, Table A-23 and Table A-24). All three isotherms fitted the 17α-E2, 17β-E2 and E1 adsorption data reasonably well (R^2>0.78) (Table 4-7) indicating that different adsorption mechanisms were potentially occurring (Peiris *et al*., 2020). However, the Sips model (a combined form of Langmuir and Freundlich models) obtained the best fit (R^2 = 0.93-0.99) and was therefore used to model the adsorption of 17α-E2, 17β-E2 and E1 to the powdered biochar.

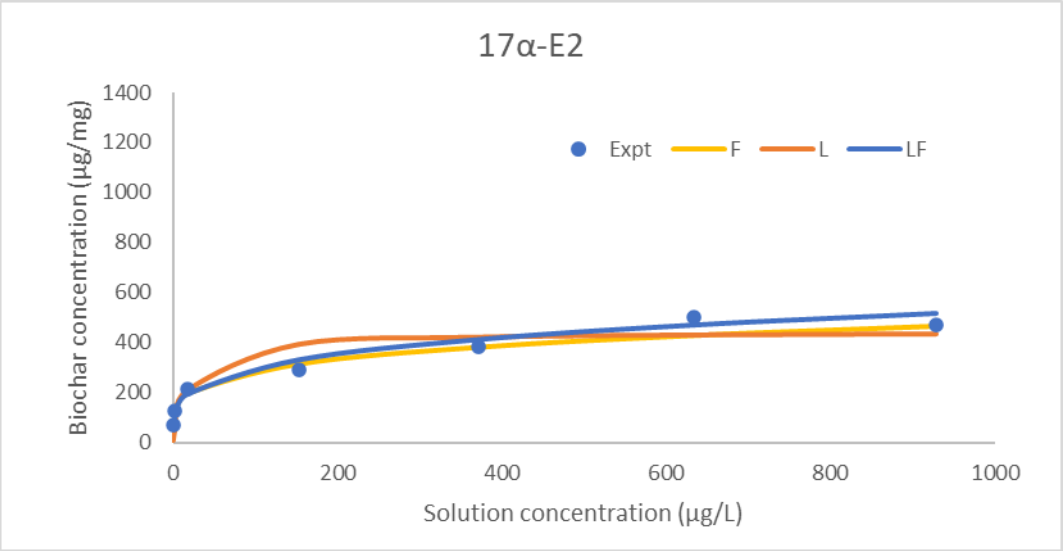

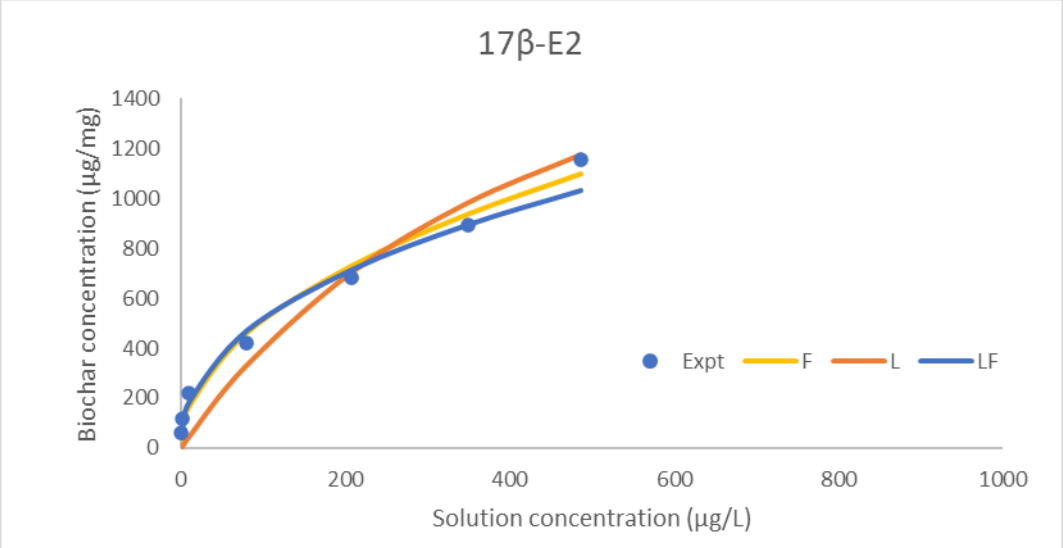

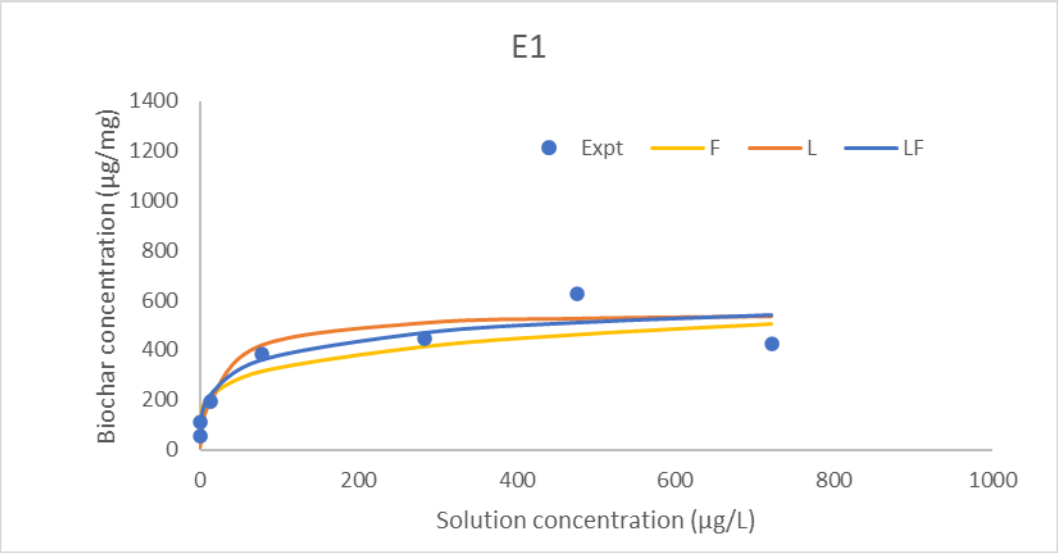

Figure 4-9: Freundlich (F), Langmuir (L) and Sips (LF) isotherm study of 17α-E2, 17β-E2 and E1 adsorption onto powdered biochar (biochar mass = 1 ± 0.09 mg, pH = 7 ±2, Temperature = 20°C± 2°C).

The suitability of the Sips model suggests that the surface of the powdered biochar is homogeneous (Chen *et al*., 2015) and the ESH adsorption is monolayer at the lower ESH concentration involving both chemical and physical sorption (Sun *et al*., 2011) while multi-layer adsorption occurs at higher concentrations. In particular, the powdered biochar was observed to have an extremely high adsorption capacity for 17β-E2, which is likely only achievable if adsorption was multi-layered (Ahmed *et al*., 2018).

The Sips model n^{-1} values were less than one for all the ESHs (Table 4-7) indicating the adsorption of ESH to the powdered biochar was favourable, as was also observed from Figure 4-9, which suggests that ESHs should be readily adsorbed at the low concentrations found in dairy shed effluent. The maximum ESH sorption capacities obtained from the Sips model were 500 µg/mg for 17α-E2 and E1, and 1,000 µg/mg for 17β-E2 (Figure 4-9).

Not many studies have examined adsorption of 17α-E2, which is the most abundant ESH in dairy shed effluent, and E1 (Ahmed *et al*., 2018) while most examined 17β-E2 (Ahmed *et al*., 2018). This is understandable since the most abundant ESH in municipal wastewater is 17β-E2 and it is the most estrogenically potent of the three ESHs. Kim *et al* (2016) and Liu *et al* (2019) found that the Freundlich model gave the best fit for ESH adsorption, suggesting heterogeneous adsorption on the biochar surface (Kim *et al*., 2016;

Liu *et al*., 2019). However, other studies have suggested that the Langmuir isotherm model gave the best fit (Ahmed *et al*., 2018; Dong *et al*., 2018) suggesting homogenous surface adsorption, while another, in agreement with this study, found that 17β-E2 adsorption is defined best by both Langmuir and Freundlich models (Tong *et al*., 2020).

Table 4-7: Isotherm model parameters

		17α-E2	
	Freundlich model	**Langmuir model**	**Sips model**
K	44036[A]	0.001016[B]	0.000040[B]
q_m[c]	N.A	442059	89403492
n^{-1}	0.22	N.A	0.25
R^2	0.96	0.78	0.98
		17β-E2	
	Freundlich model	**Langmuir model**	**Sips model**
K	8694[A]	0.00004[B]	0.00034[B]
q_m	N.A	2338913	35757262
n^{-1}	0.48	N.A	0.44
R^2	0.98	0.94	0.99
		E1	
	Freundlich model	**Langmuir model**	**Sips model**
K	54928[A]	0.000799[B]	0.022005[B]
q_m	N.A	552387	764120
n^{-1}	0.21	N.A	0.48
R^2	0.84	0.81	0.93

[A] values are expressed as ng/mg, [B] values are expressed as mL/ng, [C] values are expressed as ng/mg

Using the Sips equation for the adsorption isotherm and model parameters in Table 4-7, the kinetic coefficients were determined by fitting the pseudo-first and second order kinetic models to adsorption data. The pseudo second-order model best represented the adsorption kinetics of 17α-E2, 17β-E2 and E1 to the powdered biochar (Figure 4-10) (Full data is provided in the appendices, Table A-25, Table A-26 and Table A-27) with an R^2 of 0.95-0.98 (Table 4-8). This suggests that the adsorption process was governed by chemisorption involving valence forces through sharing or exchange of electrons between ESHs and the biochar (Liu *et al*., 2019; Peiris *et al*., 2020). Similarly, many biochar adsorption studies found the pseudo second-order model gave the best fit to adsorption data (Ahmed *et al*., 2018; Dong *et al*., 2018; Liu *et al*., 2019). Ahmed *et al*. (2018) found that the 17β-E2 and E1 adsorbed to the functionalised biochar mainly through external

mass transfer diffusion processes and adsorbed to the char by forming H-bonds as well as π-π electron-donor–acceptor interactions. Dong *et al*. (2018) observed that 17β-E2 became saturated on magnetic biochar nanoparticles over short contact times, likely due to rapid and easy access of 17β-E2 into the nanoscale porous structure of the biochar. Tagliavini *et al*. (2017) also found that at higher (>0.01 g/L) polymer-derived spherical activated carbon concentration, the adsorption results fitted the pseudo-first order model. This may be due to the activated carbon increased formation of polar linkages during sorption compared with the powdered biochar.

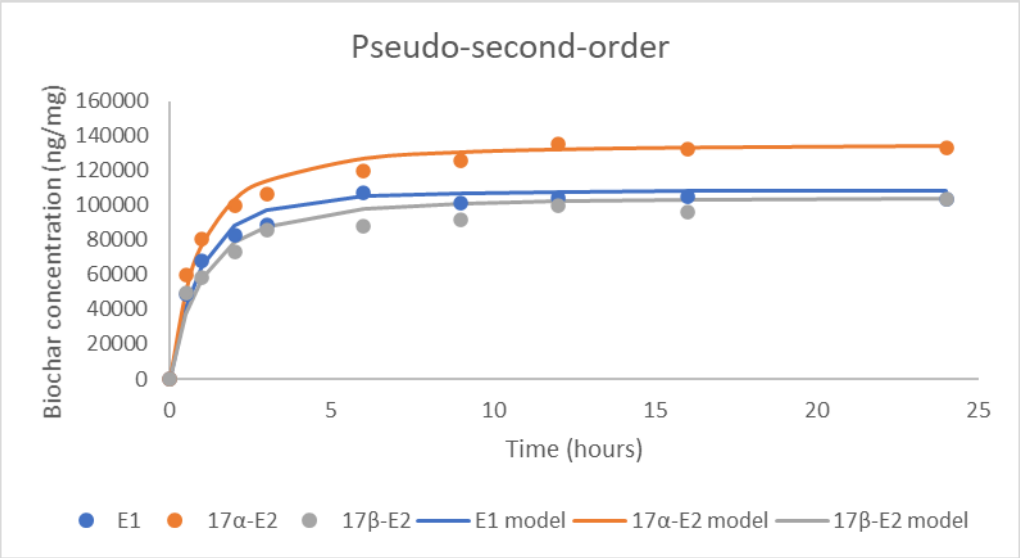

Figure 4-10:: Pseudo-second-order-rate kinetics model for 17α-E2, 17β-E2 and E1 adsorption onto the powdered biochar (1 mg ±0.06), ESH initial nominal concentration = 2,500 ng/mL, contact time = 24 hours, temperature = 20 ± 2 °C, pH=7.

Table 4-8: Kinetic model parameters

	17α-E2	
	Pseudo-first order model	**Pseudo-second order model**
k	0.33[A]	19.9[B]
R^2	0.92	0.95
	17β-E2	
	Pseudo-first order model	**Pseudo-second order model**
k	0.18	7.05
R^2	0.86	0.98
	E1	
	Pseudo-first order model	**Pseudo-second order model**
k	0.23	10.4
R^2	0.92	0.98

[A] values are expressed as min^{-1}, [B] values are expressed as $mg/ng.hour^{-1}$

4.7 Conclusions

- Dairy cows are the largest source of ESHs entering the New Zealand environment. There are clear benefits for human and wildlife health from ensuring that ESHs are not released into the environment. This study measured the performance of a low cost carbonaceous material (biochar), made from an abundant by product of the forestry and milling industry, to adsorb ESHs.
- Powdered biochar originated from *Pinus radiata* woodchip was prepared through an effective heat treatment range of 725 – 815°C, and retention time of 30 minutes, resulting in a surface area of 82.5 m2/g, a pore volume of 16.2 cm3/g, a size of 37.8 Å and carbon and ash contents of 90.5 % and 1.4 % respectively. At a concentration of 0.5 mg/L, the powdered biochar demonstrates the capability to efficiently remove 17α-E2, 17β-E2, and E1 from aqueous solutions containing ESH concentration of approximately 50 µg/mL with removal efficiencies ranging from 78.8% to 96.9%, and within a time frame of 6 hours. This time is kinetically favourable and compatible with the retention time (~24 hours) of most dairy shed effluent sumps for adequate removal of ESHs.
- The percentage adsorbed of 17α-E2, 17β-E2 and E1 at equilibrium (24 hours), biochar mass of 1 mg and low ESHs concentration range (25 – 50 µg/L) were in the order of 84 – 99 %. At higher ESHs concentration (> 250 µg/L), 17α-E2, 17β-E2 and E1 percentage adsorbed was reduced gradually below 70 % and proportional to the increased ESHs concentration. The lower ESHs concentration range corresponds well to the previously measured ESHs concentration in the dairy shed effluent, therefore barring competition from other contaminants, the powdered biochar presents promising ESHs removal capabilities.
- The Sips and Pseudo second order model provided the best fit to isotherm and kinetic data (R^2>0.93) indicating that the surface of the powdered biochar is homogeneous and the adsorption was monolayer at low ESH concentrations involving chemical and physical sorption while multi-layer adsorption occurred at the higher ESH concentrations.
- Further work is required to determine the ability of the powdered biochar to remove ESHs from dairy shed effluent.

Chapter 5:
Sorption of estrogenic steroid hormones by dairy shed effluent dosed with biochar

In Chapter 4 it was concluded that powdered biochar is capable of removing estrogenic steroid hormones 17α-estradiol (17α-E2), 17β-estradiol (17β-E2) and estrone (E1) at typical concentrations found in dairy shed effluent (Chapters 2 and 3) relatively efficiently (78.8 – 96.9%) and within a time (6 hours) compatible with the retention time (~24 hours) of most dairy farm effluent sumps. The main objective of this study was to confirm the performance of powdered biochar to remove 17α-E2, 17β-E2 and E1 in real dairy shed effluent samples.

5.1 Introduction

Popular dairy shed effluent (DSE) treatment systems in New Zealand (NZ) include separation systems such as a weeping wall or screw press arrangement coupled with a stirred pond/sump and/or storage pond and the traditional two pond arrangement (Chapter 6). There are only a small number of covered anaerobic pond (CAP) systems used in NZ to treat DSE. However, the CAP system is likely to increase in popularity due to its simplicity, sustainable performance, and ability to recover energy, reduce greenhouse emission by capturing and utilising/burning the methane produced therein and producing stable sludge and liquor rich in nutrients essential for crop irrigation/application (NIWA, 2008).

Anaerobic digestion systems such as the CAP system have achieved limited to no removal of estrogenic steroid hormones (ESHs) (Chapters 2-4) (Zhang *et al.*, 2014; Noguera-Oviedo and Aga, 2016). To enable the use of the anaerobic digestion system both to treat DSE and allow the removal of ESHs, an additional treatment stage needs to be included. Potential treatment stages that can be coupled with the CAP system to enhance the removal of ESH from DSE could include advanced treatment processes such as advanced chemical oxidation, enhanced aerobic biological processes, chlorination and ozonation

and membrane separation (Ahmed *et al*., 2017). However, these treatment methods are not practical for typical on-farm use and include high capital investment and operational costs. More simplified and cost effective ESH removal processes from wastewater that might suit the NZ dairy farm environment could include separation treatment methods such as coagulation, flocculation and precipitation, and adsorption (Schenck *et al*., 2012; Rovani *et al*., 2016; Tagliavini *et al*., 2017).

Adsorption is used in water and wastewater treatment to remove harmful contaminants by capturing these contaminants in a solid phase (Lai *et al*., 2000; Metcalf and Eddy, 2014). Adsorption is one of most environmentally friendly and promising methods for removing organic and inorganic micro pollutants (Torrellas *et al*., 2015; Tagliavini *et al*., 2017) as it can remove contaminants at very low concentrations, is suitable for continuous processes, can be integrated with other processes (Sophia A & Lima, 2018) and the adsorbent can be regenerated and reused (Delgado *et al*., 2012).

Adsorption with carbonaceous materials has shown effective removal of ESHs (Ahmad *et al*., 2014). Typical commercial adsorbent includes activated carbon (Li *et al*., 2002; Metcalf and Eddy, 2014), however biochar is a cost-effective alternative to activated carbon (Sun *et al*., 2011; Ahmad *et al*., 2014; Alizadeh *et al*., 2018). Biochar, a low-cost carbonaceous sorbent material, can provide promising removal performance of ESHs in water (Chapter 4) (Kim *et al*., 2016; Liu *et al*., 2019) and wastewater (Ahmed et al., 2018). To enhance the removal of ESHs, biochar can potentially be incorporated into the CAP system by mixing it into the CAP inlet arrangement (sump) (Chapter 2) and allowing sufficient contact time (>6 hours) for adsorption to occur (Chapter 4).

Dosing DSE with biochar has many benefits for anaerobic digestion, such as reducing ammonia inhibition (Mumme *et al*., 2014), increasing alkalinity (Shen *et al*., 2015), and providing a substrate for methanogenic bacteria (Cooney *et al*., 2016; Shen *et al*., 2015; Xu *et al*., 2015), as well as enhancing the phosphate, nitrogen and potassium adsorptive capabilities of the digestate (Salman *et al*., 2017; Shen *et al*., 2015; Yao *et al*., 2011) and reducing the hydraulic retention time required for digestion (Cooney *et al*., 2016; Fagbohungbe *et al*., 2017). When the effluent and sludge is discharged onto land, the biochar can improve soil properties such as water holding capacity, oxygen and carbon

content, pollutant immobilisation, and microbial abundance, as well as providing carbon sequestrating properties, increasing crop yields, and reducing greenhouse gas emissions (Gul *et al*., 2015; Agegnehu *et al*., 2017; Ding *et al., 2017)*.

Wastewater containing high solid content and organic matter can reduce removal efficiencies for ESHs (Matsui *et al*., 2012). Ahmed *et al*. (2018) found that 17β-estradiol (17β-E2) and estrone (E1) adsorbed more efficiently into biochar in deionised water than in membrane effluent and synthetic wastewater. The mechanisms by which adsorption capacity is reduced include blocking of the adsorbent pores and build-up of non-target adsorbates on the surface and/or competition for the active sites of the adsorbent (Newcombe *et al*., 1997, 2002b; Hepplewhite et al., 2004; Kilduff *et al*., 1998; Matsui *et al*., 2002). However, due to the low molecular size/weight of ESHs compared to the high molecular weights of other organic matter in DSE, most organic matter in DSE is unlikely to compete for the same adsorption sites on which the ESHs adsorb (Matsui *et al*., 2012; Haddad *et al*., 2019). Furthermore, previous studies have been completed to better understand the mechanism of competition and to mathematically model the competitive adsorption process to find ways to improve the activated carbon adsorbent performance in removing emerging contaminants through adsorption competition (Matsui *et al*., 2012; Jiang *et al*., 2017; Haddad *et al*., 2019). The studies have shown that high molecular weight organic matter favourably adsorbs on the exterior particle surface and does not completely penetrate the adsorbent (Matsui *et al*., 2012). Thus, adsorbate uptake rate for high molecular weight organic matter is largely through the increased external surface area of the adsorbent (Matsui *et al*., 2012) and additional absorbent (Ahmed *et al*., 2018). In contrast, absorbance of ESHs and other small persistent pollutant molecules will be governed by the internal pore surface of the adsorbate.

Chapter 5: Sorption of estrogenic steroid hormones by dairy shed effluent dosed with biochar

Chapter 4 showed that powdered biochar can effectively adsorb the ESHs 17α-E2 or 17β-E2 or E1 in pure water containing $CaCl_2$ solution. The purpose of this study was to answer the following research questions:

- can powdered biochar intercept the dairy ESHs from a real DSE sample by adsorption of the ESHs before the DSE enters the CAP system?
- what is the removal efficiency of 17α-E2, 17β-E2 and E1 from dairy shed effluent by powdered biochar?
- what are the magnitude and mechanisms of the competitive interactions between the ESHs and other organic and inorganic compounds within the DSE?
- what is the reduction in overall estrogenic potency of DSE treated by powdered biochar?

5.2 Materials and Methods

5.2.1 Sample collection and preparation

Grab samples of DSE (20 L) were collected (11th of May 2021) from a mechanically mixed sump (50 m^3) in a 200-hectare dairy farm supporting a herd of 550 dairy cows in the Waikato Region of NZ. The sump contained combined milking shed and feeding pad wash water and recycled green water. The DSE sample was collected immediately after morning milking and washing of the dairy shed and feed pad. A full description of the farm and sump, which were used in this study, is presented in Chapter 2.

The DSE within the sump was mixed by a mechanical stirrer for ten minutes before collecting a sample with a stainless-steel bucket. The sample was mixed, temperature and pH were analysed using a Eutech pH 150 meter and sub samples were transferred into solvent cleaned 4 x 4-L glass bottles and transported on ice to the laboratory. At the laboratory (~ 2 hours after the samples were collected), each 4 L glass bottle was mixed and a sub sample (4 x 375 mL) was transferred into 2-L Schott bottles, 9 x 1.5-L subsamples in total. The content of each 2-L Schott bottle was mixed and subsampled (500 mL) into individual containers and sent to an external certified laboratory for analysis of total solids (TS) and volatile solids (VS).

One sample (DSE comparison) was preserved immediately after subsampling by adjusting the pH to 2.5 with concentrated sulphuric acid and storing at 4 °C before further extraction and analysis of ESHs (within 20 hours). The rest of the samples were prepared for the adsorption trials.

5.2.2 Biochar

Powdered biochar made from *Pinus radiata* residues pyrolysed at ~700°C for 6 hours with mean particle diameter of 26.5 µm, surface area of 82.5 m^2/g and carbon content of 90.5% was used in this study to adsorb the DSE ESHs. The biochar was previously used successfully to remove ESHs from water ($CaCl_2$ solution) and its characteristics and performance were described in Chapter 4.

5.2.3 Chemicals and materials

A full description of the chemicals and materials used in this research is provided in Chapters 2, 3 and 4. However, for the purpose of this research, Waters Oasis HLB solid-phase extraction (SPE) cartridges, Biotage Isolute Florosil and bulk aminopropyl (NH_2) sorbent were replaced with Strata™-X 33µm (6 mL/500 mg) SPE, Florosil (15 mL/2 g) and NH_2 (6 mL/1 g) cartridges and were obtained from Phenomenex NZ. The enzyme, which was used for deconjugation, was *Helix pomatia (H. pomatia)* β-glucuronidase Type HP-2 (≥ 100,000 U/mL β-glucuronidase and ≤7,500 U/mL sulfatase) and was supplied by Sigma Aldrich NZ.

5.2.4 Batch adsorption trial

The batch adsorption trials were performed using a similar method to that described in Chapter 4. Seven different powdered biochar masses (5, 10, 20, 30, 50, 100 and 200 mg) were weighed (Mettler Toledo XPE205) into a clean 1-L Schott bottle, leaving one bottle as a control (DSE with no biochar) and another as blank (no biochar or DSE), nine bottles in total. The content of the remaining 2-L bottles (5.2.1) was mixed well and 0.5 L was poured into each of the control and biochar containing bottles. After pH and temperature were recorded, the bottles were positioned vertically onto a shaking tray (IKA KS501) together with the blank and control samples. The samples were covered with a towel to prevent photodegradation and agitated, to ensure that the biochar remined suspended, at 20°C and a speed of 150 rounds per minute for 24 hours (Chapter 4).

After 24 hours, the agitated samples were preserved by adjusting the pH to 2.5 with concentrated sulphuric acid and together with the DSE comparison sample, which had been stored at 4°C, were transferred into 250 mL polyethylene centrifuge tubes and centrifuged in a Sorvall RC 5C Plus centrifuge (10 °C, 30 min, 10,000 rpm) as described in Chapter 2. The supernatant was decanted and filtered through a glass microfiber filter (topped with a 5 mm layer of Hyflo Supercell C22 filter aid) and collected in a glass Schott bottle (0.5 L).

5.2.5 Isotherm modelling

The three isotherm models used in Chapter 4, Langmuir, Freundlich and Sips models, as well as, two additional models, Redlich-Peterson model (Redlich and Peterson, 1959) and coupled Freundlich Model (Modified Freundlich) were used to model the adsorption of ESHs in DSE.

The Redlich–Peterson isotherm (Equation 5-1) is an empirical isotherm incorporating three parameters and combines elements from both the Langmuir and Freundlich equations (Redlich and Peterson, 1959).

$$q_e = \frac{ACe}{1+BCe^{\beta}} \quad (5\text{-}1)$$

Where q_e is the amount of ESH per unit weight of powdered biochar (ng/mg), A and B are the Redlich-Peterson isotherm constants (L/mg and L/ng respectively), Ce is the equilibrium concentration of ESH in the solution (ng/L), and β is an exponent that lies between 0 and 1.

Modified Freundlich is an isotherm incorporating five parameters (Equation 5-2) and its mechanism involves two coupled Freundlich equations. The Modified Freundlich assumes that the dissolved ESHs are partitioned between being associated with the dissolved organic carbon in the DSE, some of which is adsorbed to the biochar or by direct adsorption of the ESHs to the powdered biochar.

$$q_e = K_{ESH/Biochar}(\alpha\, Ce)^{n1} + K_{DOC/Biochar}((1-\alpha)\, Ce)^{n2} \quad (5\text{-}2)$$

Where q_e is the amount of ESH per unit weight of powdered biochar (ng/mg), α represents the fraction of ESHs that are available for adsorption, Ce is the equilibrium concentration of ESH in the solution (ng/L), n_1 and n_2 are exponents and $K_{ESH/Biochar}$ and $K_{DOC/Biochar}$ are the partitioning coefficient of the available ESHs to biochar and DOC associated ESHs to biochar respectively.

As in Chapter 4, isotherm parameters were found by adjusting each parameter to reduce the sum of square errors (SSE) using Excel Solver(TM). The coefficient of determination (R^2) was used to determine the degree of fit of the isotherm model results with the experimental data.

5.2.6 Analytical method

5.2.6.1 Extraction and clean-up of samples

5.2.6.1.1 Dissolved phase – Free ESHs

The measures of quality assurance and extraction of ESHs from samples was performed using methods similar to those described in Chapters 2 and 3. The filtered and pH adjusted samples were spiked with a surrogate recovery standard of DL-Estrone-13,14,15,16,17,18-13C6 (^{13}C6-E1) and DL-Estradiol-13,14,15,16,17,18-13C6 (^{13}C6-E2) at an equivalent concentration of 100 ng/mL and extracted by passing the samples through preconditioned Strata-X cartridges fitted with a Teflon connector and mounted in a SPE vacuum extraction manifold. The SPE columns were dried under vacuum and rinsed with solutions of methanol/water containing triethylamine (TEA) (12.5 mL, 60:40 *v/v* methanol/milli-Q water with 0.005M TEA) (Labadie and Budzinski, 2005). The cartridges were dried under vacuum and were connected in series to a Florosil cartridge (2 g, 15 mL) and aminopropyl (0.5 g) (Burkhardt *et al*., 2005) cartridge topped with a ~3 cm layer of anhydrous granular sodium sulphate (dried overnight at 450 °C). The connected cartridges were mounted in a SPE vacuum extraction manifold and the ESHs simultaneously eluted and purified by passing through DCM/methanol (30 mL, 95:5 *v/v*). The collected eluent was dried under nitrogen gas (30 °C), redissolved in acetone (1 mL), and stored at 4 °C prior to derivatisation and analysis.

5.2.6.1.2 Solid phase – Free ESHs

A full description of the extraction of separated solids by ASE (Dionex ASE200) using a modified method of Burkhardt *et al*. (2005), and their purification by Florosil and aminopropyl adsorption chromatography is provided in Chapter 2.

5.2.6.1.3 Dissolved and Solid phase – Conjugated ESHs

The conjugated ESHs in methanol/water containing TEA were spiked (at an equivalent concentration of 100 ng/L) with surrogate standards ^{13}C6-E1 and ^{13}C6-E2 and dried by rotary evaporation (Büchi Rotavapor R-200), re-dissolved in MeOH / tetrahydrofuran (1 mL, 20:80 *v/v*) and trifluoroacetic acid (10 µL), vortexed and incubated at 45 °C for 30 min. Subsequently, the reaction mixture was neutralised with Na_2CO_3 (400 µL, 0.2 mol/L in Milli-Q-Water) and evaporated to ~400 µL under a stream of oxygen-free nitrogen gas (30 °C). Sodium acetate buffer (5 mL, pH=5) was added to the neutralised solution and mixed by vortex and *H. pomatia* β-glucuronidase enzyme (30 µL) was added. The buffered enzyme solution was mixed gently by vortex, incubated at 55 °C for 180 min and adjusted to pH 2 using dilute sulphuric acid. Free ESHs were extracted from the pH adjusted solutions by SPE using Strata-X SPE cartridges as previously described in Section 5.2.6.1.1.

5.2.6.2 Analysis of ESHs

The samples, QA extracts, comparative recovery standards, and calibration standards were dried to approximately 0.25 mL under nitrogen (30°C), internal standard solution added (equivalent to 250 ng each of 17β-E2-d4 and E1-d4) and evaporated to dryness under nitrogen. ESHs were derivatised to their trimethylsilyl esters (TMSI) using an activated *N*-Methyl-*N*-(trimethylsilyl)-trifluoroacetamide (MSTFA)/TMSI mixture (Budzinski *et al*., 2006), diluted with *iso*-octane and analysed using GC-MS as previously reported in Chapters 2 and 3.

5.3 Results

5.3.1 Physical and chemical analysis and quality assurance outcome

The physical and chemical properties of the DSE and the quality assurance results of the adsorption trial are presented in Table 5-1 to Table 5-5. (Further information regarding the DSE inorganic parameters is presented in appendices, Table A-28)

Table 5-1: Physical and organic chemical parameters of the split (prior to adding biochar) DSE adsorption samples

	pH	TS (mg/L)	VS (mg/L)
DSE Comparison	7.2	13703	9498
DSE Control	7.2	11949	8284
DSE 5	7.1	12139	8462
DSE10	7.1	12839	8992
DSE20	7.2	12735	8926
DSE 30	7.2	12753	8924
DSE 50	7.3	12121	8394
DSE 100	7.4	12535	8762
DSE 200	7.3	13257	9360

The standard deviations of the TS and VS of the DSE samples were very similar (4.5 % and 4.7 % respectively) indicating that the sub-sampling procedure was appropriate, and samples are representative. The mean recovery of the surrogate standards ^{13}C6-E1 and ^{13}C6-E2 from the free and conjugated ESH assays of the dissolved and solid phases of the adsorption samples were 82.2 % and 85.4 %, 59.8 % and 63.7 %, 81.8 % and 82.4 % and 87.9 % and 95.7 % respectively (Table 5-2 to Table 5-5).

Table 5-2: Recovery (expressed as %) of surrogate standards (^{13}C6-E1 and ^{13}C6-E2 spiked at 100 ng/L) obtained from the powdered biochar DSE adsorption experiment samples from the dissolved free ESHs samples

	^{13}C6-E2	^{13}C6-E1
DSE Comparison	98.9	89.9
DSE Control	71.4	84.7
DSE 5	74.6	93.0
DSE10	98.6	84.8
DSE 20	64.3	90.3
DSE 30	85.3	84.0
DSE 50	91.8	94.3
DSE 100	86.3	74.9
DSE 200	89.1	72.6

Table 5-3: Recovery (expressed as %) of surrogate standards (^{13}C6-E1 and ^{13}C6-E2 spiked at 100 ng/L) obtained from the powdered biochar DSE adsorption experiment samples from the dissolved conjugated ESHs samples

	^{13}C6-E2	^{13}C6-E1
DSE Comparison	82.9	71.8
DSE Control	65.5	103
DSE 5	102	89.3
DSE10	63.0	65.5
DSE 20	49.7	46.1
DSE 30	59.4	60.1
DSE 50	85.3	103
DSE 100	109	101
DSE 200	119	103

Table 5-4: Recovery (expressed as %) of surrogate standards (^{13}C6-E1 and ^{13}C6-E2 spiked at 100 ng/g) obtained from the powdered biochar DSE adsorption experiment samples from the solid phase free ESHs samples

	^{13}C6-E2	^{13}C6-E1
DSE Comparison	55.9	51.7
DSE Control	38.3	28.2
DSE 5	86.0	103
DSE10	43.7	38.4
DSE 20	58.0	53.8
DSE 30	76.5	82.5
DSE 50	35.4	25.9
DSE 100	88.5	99.0
DSE 200	60.9	81.3

Table 5-5: Recovery (expressed as %) of surrogate standards (^{13}C6-E1 and ^{13}C6-E2 spiked at 100 ng/g) obtained from the powdered biochar DSE adsorption experiment samples from the solid phase conjugated ESHs samples

	^{13}C6-E2	^{13}C6-E1
DSE Comparison	92.2	91.6
DSE Control	79.3	82.0
DSE 5	87.5	92.1
DSE10	89.7	97.4
DSE 20	85.8	96.0
DSE 30	N/A[A]	N/A
DSE 50	92.0	109
DSE 100	87.9	100
DSE 200	88.5	89.7

[A] Not available – loss of sample

The free and conjugated ESHs solids phase analysis in this study was completed to better understand the different removal mechanisms of the ESHs, equilibration of ESHs between dissolved and solid phases and the biochar, and to distinguish between the adsorption and biological degradation processes (Combalbert and Hernandez-Raquet, 2010; Liu *et al*., 2015). However, due to the low and inconsistent recovery of the ESHs in the solid phase, presented in the appendices (Table A-29), the results of the free and conjugated ESHs in the solid phase were excluded from this study. Therefore, in the absence of the solid phase analysis, the DSE ESHs adsorbed to the powdered biochar were determined indirectly using a similar method to that used in Chapter 4 by the analysis of the ESHs in the dissolved phase only. The amounts of ESHs adsorbed on the powdered biochar samples were calculated as the difference between the ESHs initially present in the dissolved phase of the DSE sample and the amount remaining in the dissolved phase at the end of the experiment (OECD 106 Guideline).

5.3.2 Adsorption trial experimental data

Removal of the individual ESH from the DSE is most likely to be directly connected to the adsorption of the individual ESH to the powdered biochar but may be a consequence of transformation between the different ESHs (Chapter 2) which can lead to a false conclusion regarding the removal of specific ESHs. Although previous studies found that transformation of DSE ESH occurs over a long residence time (20-30 days) in an anaerobic environment (Sarmah *et al*., 2006; Noguera-Oviedo and Aga, 2016) (Chapter 2), no research of which we are aware describes transformation of ESH at a shorter

residence time of 24 hours as utilised in this study. Therefore, it was assumed that no transformation between the ESH occurred during the current adsorption trial.

The percentage removal and adsorption results for free 17α-E2, 17β-E2 and E1 in the dissolved phase are presented in Figure 5-1 and Figure 5-2 (Full data is provided in the appendices, Table A-30 and Table A-31). At 17α-E2, 17β-E2 and E1 initial dissolved phase concentrations in DSE of 2,217, 329 and 147 ng/L respectively, and powdered biochar concentration ranges of 100 – 400 mg/L, the powdered biochar showed similar removal of 17α-E2 (78.0 - 90.2 %) to when 17α-E2 (94.7 – 98.4 %) was spiked into $CaCl_2$ solution at concentration of 25 – 50 µg/L with a biochar concentration of 0.02 mg/L (Chapter 4). However, in DSE, 17β-E2 and E1 removal (22.3 – 48.2 % and 14.9 – 61.6 % respectively) was much lower than the removal of 17β-E2 and E1 (98.9 and 97.5 % respectively) spiked into $CaCl_2$ solution at higher concentrations (400 – 500 µg/L).

Overall, the removal from DSE of ΣESHs by powdered biochar ranged between 68.9 – 81.8 % with biochar concentrations of 100 mg/L to 400 mg/L. However, when the concentration of the powdered biochar was increased above 100 mg/L to 200 mg/L and 400 mg/L there was no corresponding increase in ESH removal (Figure 5-1). This demonstrates that about 20 % of the ESHs were not available to absorb onto the solids (sludge and biochar) phase portion (Section 5.3.3). It is likely that the conjugated DSE portion could contribute to the reduced removal performance of the powdered biochar dosed in a real DSE sample due to the highly soluble nature of the conjugated ESHs and their low affinity to the biochar (Chapter 3). However, since the measured initial DSE total conjugated ESHs was low (30.6 ng/L) in comparison with the total free ESHs concentration of 2,693 ng/L, the conjugated ESHs portion is not likely to have had an impact on the adsorption performance of the DSE samples dosed with powdered biochar.

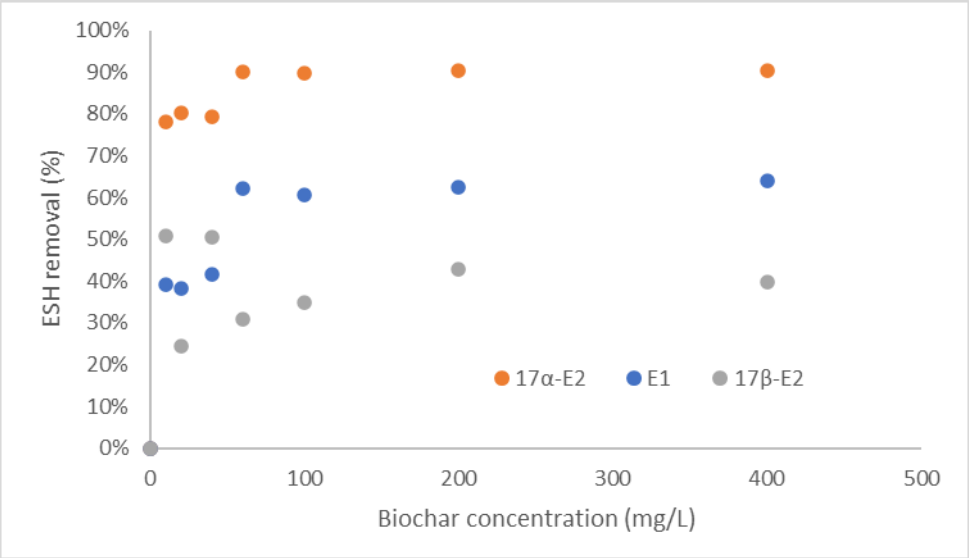

Figure 5-1: Percentage adsorbed of 17α-E2, 17β-E2, and E1 and by the powdered biochar concentration (pH = 7.2 ±0.1, Temperature = 20°C± 2°C).

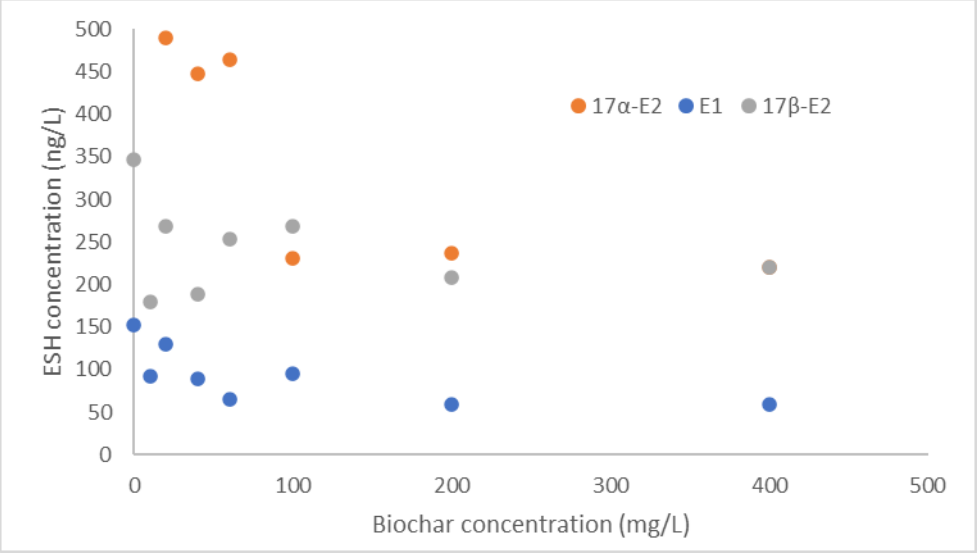

Figure 5-2: Concentration of non-absorbed 17α-E2, 17β-E2 and E1 concentration in the presence of different concentrations of biochar (pH = 7.2 ±0.1, Temperature = 20°C± 2°C).

5.3.3 Analysis of competitive adsorption by isotherm modelling

To distinguish between adsorption of ESHs and other organic material in the DSE on powdered biochar, adsorption modelling was completed. Only Freundlich, Redlich-Peterson and Modified Freundlich provided a good fit (R^2 = 0.53-0.68, 0.21-0.47 and 0.60-0.99 respectively) and therefore only these are discussed in this section.

Figure 5-3 (full data is provided in the appendices, Table A-32, Table A-33 and Table A-34) presents the experimental data and the Freundlich, Redlich-Peterson and Modified Freundlich model data associated with the partitioning of DSE 17α-E2, 17β-E2 and E1 to the powdered biochar at different powdered biochar ESH concentrations at equilibrium. The Freundlich, Redlich-Peterson and Modified Freundlich constants obtained are presented in Table 4-7.

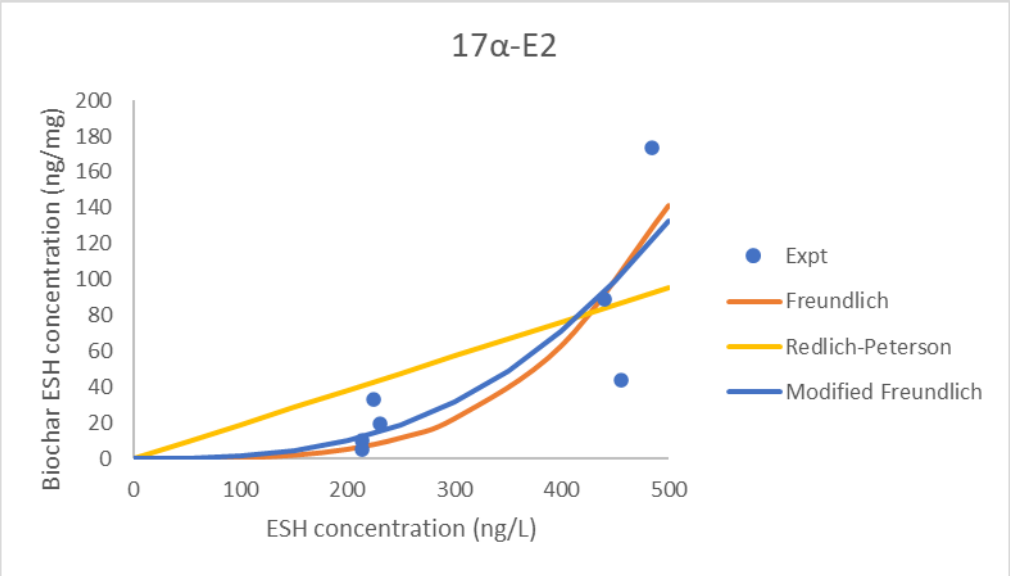

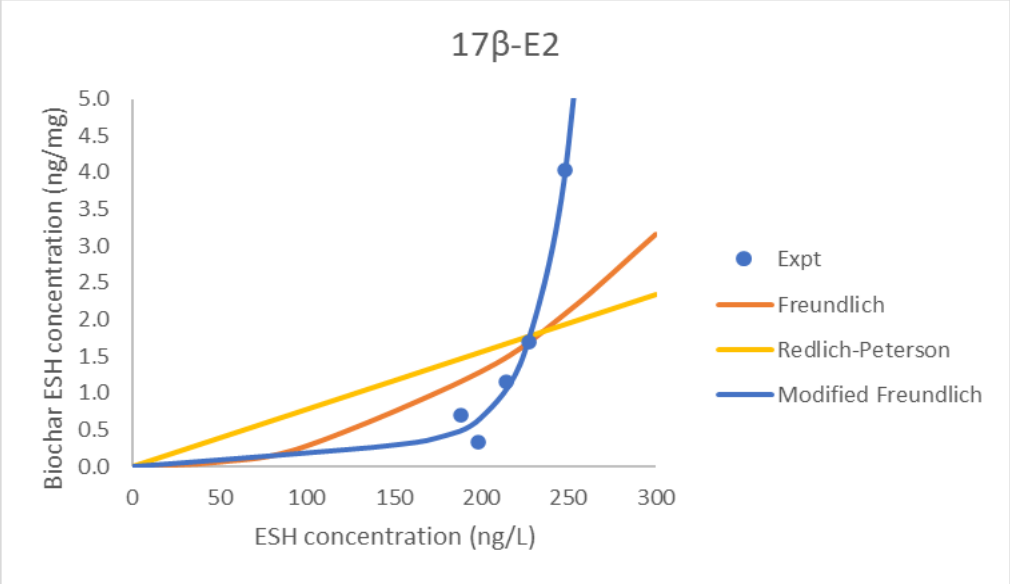

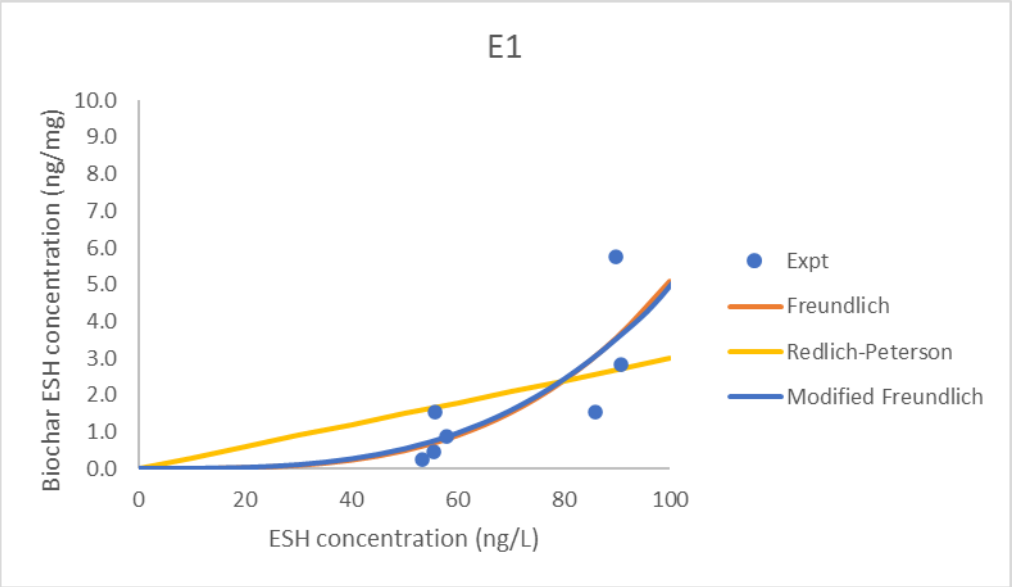

Figure 5-3: Experimental data vs Freundlich, Redlich-Peterson and Modified Freundlich model data associated with the partitioning of DSE 17α-E2, 17β-E2 and E1 to the powdered biochar at different powdered biochar ESH concentrations during equilibrium (24 hr). (The two outliers for 17β-E2 at ~162 ng/L are due to the higher than expected removals of 17β-E2 at 10 and 40 mg/L biochar, so these were neglected when fitting the isotherm curves.

Table 5-3: Freundlich and Modified Freundlich isotherm model parameters for DSE 17α-E2, 17β-E2 and E1

Freundlich			
	17α-E2	**17β-E2**	**E1**
K	2.52E-05	1.12E-05	8.19E-05
n	3.61	2.20	3.40
R^2	0.71	0.60	0.60
Number of data points	7	5	7
Redlich-Peterson			
A	1.97	5.94	3.37
n	0	0	0
B	0.57	0.13	0.05
R^2	0.47	0.34	0.21
Number of data points	7	5	7
Modified Freundlich			
	17α-E2	**17β-E2**	**E1**
$K_{ESH/biochar}$	1.215	0.621	1.386
$K_{DOC/biochar}$	0.0000	0.0016	0.0000
α	0.0106	0.0047	0.0149
n_1	2.81	11.69	3.21
n_2	1.00	1.03	1.00
R^2	0.70	0.99	0.60
Number of data points	7	5	7

Fitting the Modified Freundlich equation (equation 2) to the experimental data, the fit achieved (R^2 = 0.60 – 0.99) was better than the other models used (Figure 5-3), suggesting heterogeneous adsorption to the powdered biochar surfaces (Peiris *et al*., 2020; Tong *et al*., 2020), and this model was therefore selected to represent the competitive adsorption of ESHs in DSE to the powdered biochar. The Modified Freundlich pathway mechanisms of ESHs DSE adsorption onto the powdered biochar is illustrated in Figure 5-4.

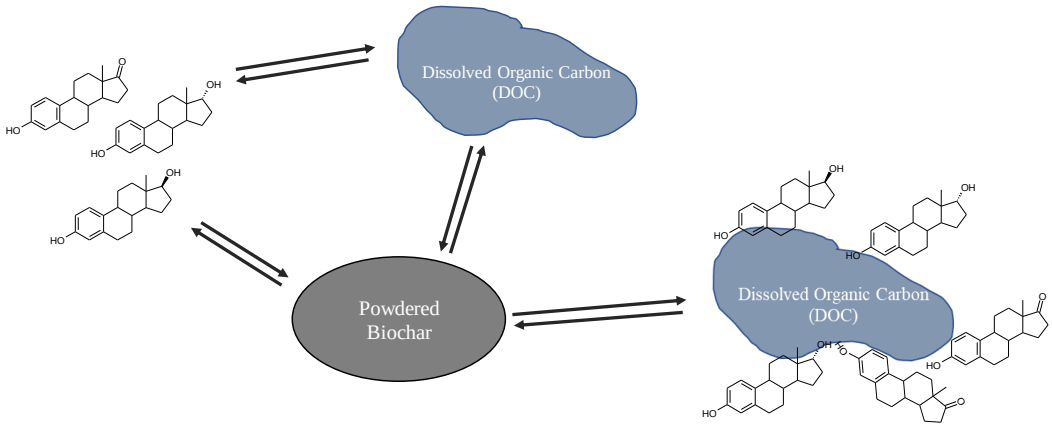

Figure 5-4: The Modified Freundlich pathway adsorption mechanism of DSE ESHs to powdered biochar

The Modified Freundlich α parameter which represents the fraction of ESH available for adsorption, was very low at 0.5 to 1.5%, suggesting a very strong interaction between the dissolved organic content and the ESHs ((1-α) = 98.5 - 99.5 %, Equation 5-2). This interaction between the ESHs and the DOC within the DSE is not surprising because of the high concentration of DOC (1.7 g/L) in the DSE compared to the concentration of the powdered biochar (0.01 – 0.4 g/L) and ESHs strong affinity for organic matter (log K_{oc} ranged from 3.06 to 3.80, Chapter 2). The adsorption of 17α-E2, 17β-E2 and E1 to the biochar was favoured over the DOC because the fitted $K_{ESH/Biochar}$ values were high (1.215, 0.621 and 1.386 respectively). Moreover, the adsorption of ESH associated with the organic matter into the biochar was negligible in the case of 17α-E2 and E1 because the fitted $K_{DOC/biochar}$ parameter was zero. However, some of the 17β-E2 associated with the organic matter was adsorbed onto the biochar ($K_{DOC/biochar}$ = 0.0016). Furthermore, the Modified Freundlich parameter n_2 for 17β-E2 was 1.03, suggesting a linear relationship at the lower DOC ESH concentrations and adsorption (Figure 5-6). It would have been useful to obtain some data points at the lower ESH equilibrium concentrations for 17β-

E2, e.g., around 100 ng/L to validate this, but the experiments were constrained by using real DSE samples containing typical DSE ESH concentrations. In contrast, the DSE ESHs parameters available for the powdered biochar were non-linear with n_1 values of 2.81 (17α-E2), 11.69 (17β-E2) and 3.21 (E1).

By plotting equilibrium ESH concentration in solution versus equilibrium ESH concentration on the biochar, it was found each ESH has a lower affinity for biochar in the presence of other contaminants compared to being in a clean $CaCl_2$ solution (Chapter 4). This shows that there are competitive interactions between the ESHs and the other matrix organic and inorganic components within the DSE (Solak *et al*., 2014; Peiris *et al*., 2020). At low ESH equilibrium concentration, little to no adsorption of the ESHs to the powdered biochar occurs (Figure 5-3). This is attributed to the affinity of the ESHs for the dissolved organic carbon portion (80%) within the DSE samples. However, at high ESH concentration, the organic portion within the DSE sample did not affect the adsorption to the powdered biochar as demonstrated in previous studies by Matsui *et al*. (2012) and Haddad *et al*. (2019).

To determine the amount of ESH adsorbed per unit weight of powdered biochar (q_e), the selected Modified Freundlich parameters (Figure 5-3) and different equilibrium concentrations for the ESHs (Ce) were used. After this, the starting ESH concentrations were calculated using Equation 5-3 and different powdered biochar masses up to 3000 mg/L.

$$C_{start} = \frac{q_e M_{powdered\ biochar} + CeV}{V} \quad (5\text{-}3)$$

The Modified Freundlich equation cannot be rearranged and solved for Ce once it was substituted into Equation 5-3, therefore a cubic spline was fitted to equilibrium ESH vs starting ESH plots and used to interpolate equilibrium ESH values given the starting ESH concentrations and different biochar masses used. Starting ESH concentration needed to be recalculated for each biochar mass and equilibrium ESH concentration.

Figure 5-5 presents the results calculated by the Modified Freundlich model and Equation 5-3 of DSE 17α-E2, 17β-E2, E1 and ΣESHs removal at different powdered biochar concentration (full data is provided in the appendices, Table A-35).

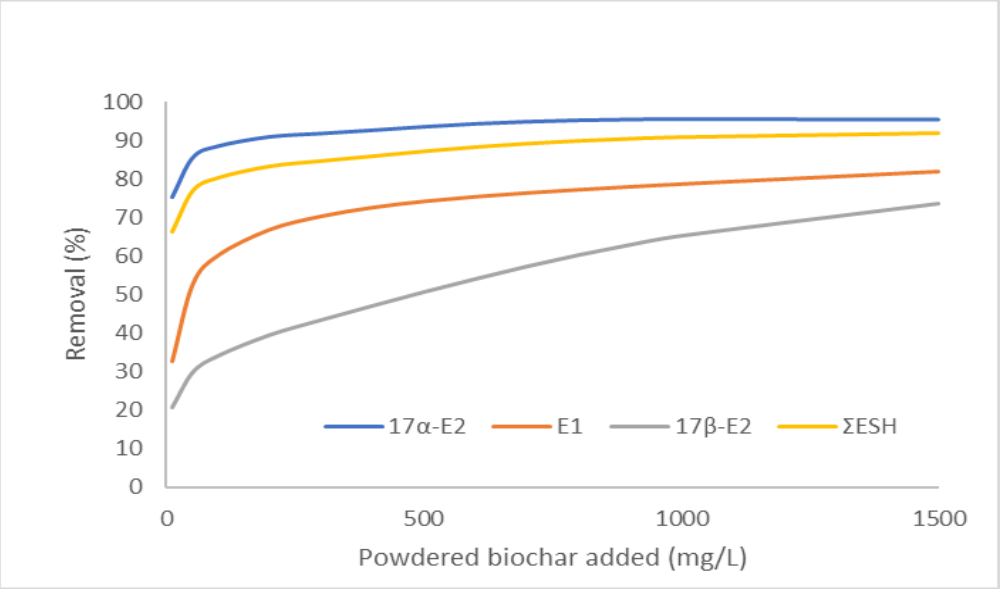

Figure 5-5: Modelled DSE 17α-E2, 17β-E2, E1 and ΣESHs removal at different powdered biochar concentration

Addition of powdered biochar mass to the DSE improves the removal of the ESHs from the DSE onto the powdered biochar (Ahmed *et al.*, 2018). Increasing the biochar concentration in the model from 100 mg/L to 1000 mg/L is estimated to increase the overall removal of the DSE ESHs from 80 % to 90 %. At a powdered biochar concentration of 1000 mg/L, approximately 96 % DSE 17α-E2, 65 % DSE 17β-E2, 78 % DSE E1 and 91 % of ΣESHs DSE are modelled to be removed by adsorption into the powdered biochar. Increasing the powdered biochar concentration in the model to higher than 1000 mg/L makes a negligible change in removal and therefore would not be a practical choice (Figure 5-5). With an average dairy herd size in NZ of 444 cows (Dairy NZ, 2021) and DSE per cow of 70 L/d (Heubeck. *et al.*, 2014), the daily DSE volume is approximately 31,000 L. To achieve overall removal of DSE ESHs in solution of 80-90 %, typically 3 – 30 kg powdered biochar per day would be required. This powdered biochar quantity range is realistic, however, the selection of biochar concentration and the type of biochar needed should be a factor of the DSE ESHs removal performance of the downstream dairy shed ETS units, such as the CAP and the storage pond as these systems can have additional ESHs removal capabilities (Chapter 6). Furthermore, at 91 % removal

of the ΣESHs concentration in the dissolved phase of the DSE some (~110 ng/L, 9 % of ΣESHs annual average concentration of 1230 ng/L (Chapter 2)) ESH would remain in the dissolved phase of the DSE and would require further treatment (Chapter 1). Moreover, the fate of the sludge and biochar adsorbed ESHs within the CAP system is unclear and would need additional investigation. However, it is speculated that the ESHs adsorbed into the solid phase containing sludge and powdered biochar would be retained and limited additional adsorption of the ESHs in the CAP system might occur because of absence of mixing and contact between the biochar and effluent (Chapter 2), but conversion of 17β-E2 bound the biochar to E1 could be expected.

Figure 5-6 (detailed information is provided in the appendices, Table A-36, Table A-37 and Table A-38) presents the modelled available ESHs concentration in the solution and the adsorbed ESHs to the powdered biochar (1000 mg/L) at different typical DSE 17α-E2, 17β-E2 and E1 concentration range (Chapter 2) at equilibrium. At typical 17α-E2, 17β-E2 and E1 DSE annual average dissolved phase concentrations of 1000, 100 and 150 ng/L respectively (Chapter 2) approximately 90, 64 and 80% respectively would be adsorbed into the powdered biochar dosed at concentration of 1000 mg/L, while the rest would remain in solution. At low starting ESH concentrations, there is very little adsorption onto the biochar, presumably due to competition from dissolved organic carbon, however after an ESH concentration of 1000 ng/L is surpassed equilibrium ESH concentration and ESH biochar concentration are proportional to starting ESH concentration.

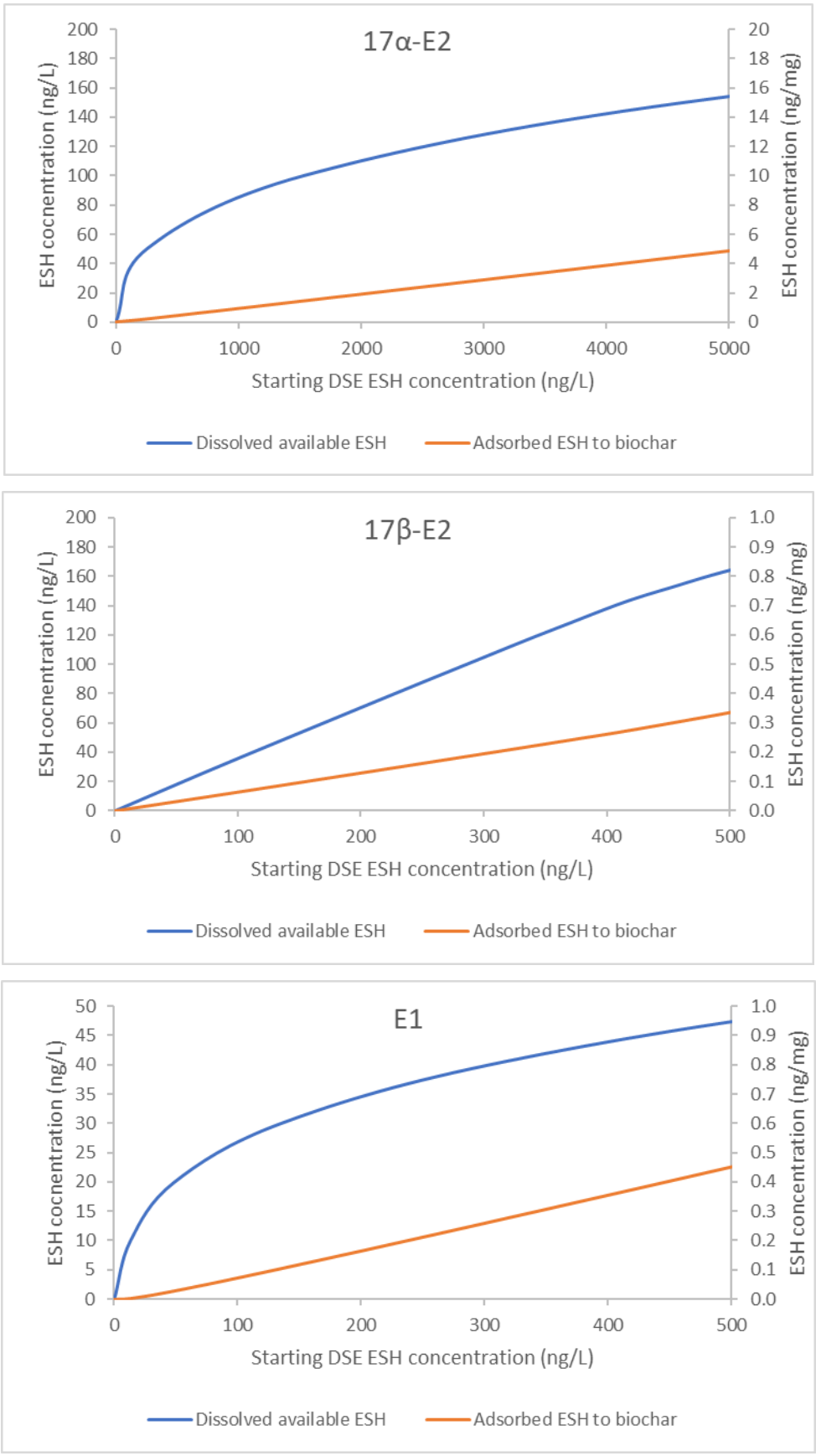

Figure 5-6: Modelled available ESHs concentration in the solution and the adsorbed ESHs to the powdered biochar (1000 mg/L) at different typical DSE 17α-E2, 17β-E2 and E1 concentration range at equilibrium.

There is not a lot of previous research reporting adsorption of organic contaminants, including ESHs, in raw municipal and/or agricultural wastewater using activated carbon or biochar. This is because absorption is typically used as a tertiary step after biological treatment, filtration, or sedimentation (Metcalf and Eddy, 2014; Ahmed *et al*., 2018) or as a treatment method for water (Meinel *et al*., 2014; Esmaeeli *et al*., 2017). The rationale behind this is to prevent rapid blockage of the adsorbent pores and build up on its surface (Newcombe *et al*., 2002b; Hepplewhite *et al*., 2004; Matsui *et al*., 2002) due to the high solid content within the influent and/or interaction between the organic matter with the biochar and ESHs (Peiris *et al*., 2020) which would lead to a poor removal performance and reduced cost effectiveness. The 17α-E2, 17β-E2, E1 and ΣESHs removals from the dissolved phase DSE found in this study were lower than those previously reported for E2 and E1 in synthetic wastewater and membrane bioreactor effluent (~100% for E1 and E2), however, the latter studies used a biochar concentration of 400 and 555 mg/L respectively at a solution pH of 3.0-3.25 (Ahmed *et al*., 2018), whereas this study used a native pH of ~7 and good removals were obtained. While adjusting DSE pH to 3 might improve ESH adsorption, practically it would be impractical to do so because of the large volumes of acid required to drop the pH of the DSE. Furthermore, dropping the pH to 3 to improve adsorption would reduce the performance of the CAP, where the methanogens favour a neutral pH, therefore one would need to provide a buffer tank for adsorption to take place and two inline mixing steps for pH reduction and neutralising the acid after adsorption.

5.3.4 Estrogenic potency

The estrogen equivalents (EEQs) and estrogenicity reduction of the resulting biochar treated DSE was determined by multiplying the concentration of each ESH by the relative potency factor obtained by the ER-CALUX bioassay (Chapter 2) (Kolkman et al., 2013). The EEQs for each compound measured in a biochar dosed DSE sample were summed to obtain the ΣEEQ for each sample. This was then divided by the starting estrogenicity of the DSE to determine a reduction in overall estrogenicity (Figure 5-7) (detailed information is provided in appendices, Table A-39).

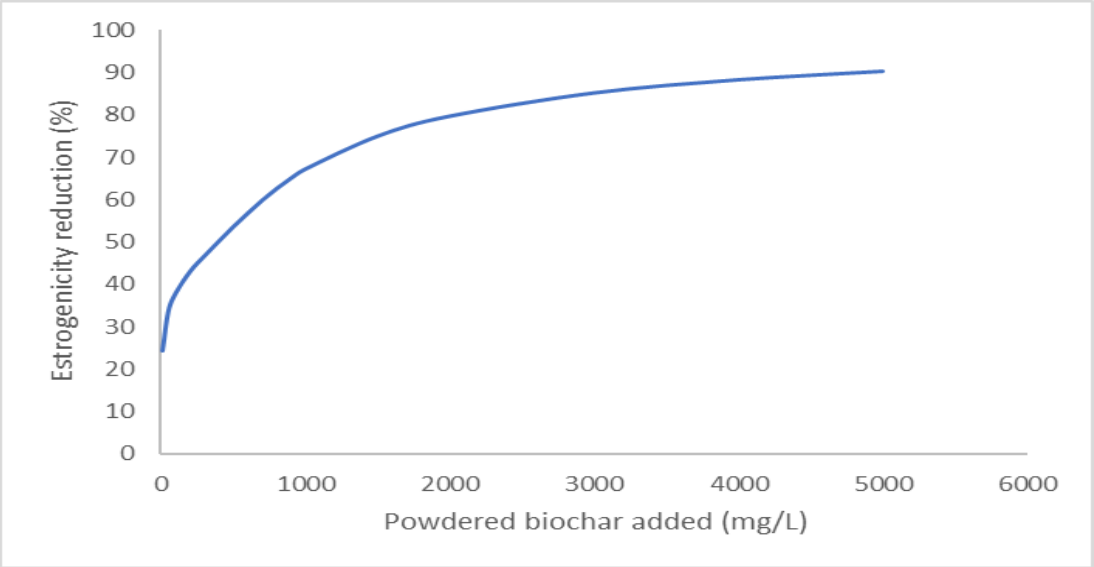

Figure 5-7: Modelled reduction in overall estrogenicity by addition of powdered biochar to DSE

Although the addition of powdered biochar provides effective removal of DSE 17α-E2 (95 %), 17α-E2 only has an estrogenicity of 0.01 of that of 17β-E2 (Kolkman *et al*., 2013), therefore overall reduction in estrogenicity will be driven by the removal of 17β-E2 (Chapter 2). Addition of powdered biochar to a concentration of 1000 mg/L resulted in a net reduction of ~91 % of the ΣESHs, however only 67.2 % reduction in overall estrogenicity (Figure 5-7). Nevertheless, increasing the biochar concentration higher than 1000 mg/L can reduce the overall estrogenicity further (Figure 5-7), however this would require a substantial additional amount of biochar. The estrogenicity reduction achieved by a powdered biochar concentration of 1000 mg/L is almost double the overall estrogenicity reduction of the CAP system, where ~35 % of the total (conjugated and free) ESHs were present in the dissolved phase of the CAP effluent compared to the total ESHs in the dissolved phase of the CAP influent (Chapter 2). Therefore, the addition of the recommended amount of biochar to the DSE prior to entering the CAP system can potentially enhance the performance of the CAP without the need to add more powdered biochar.

5.4 Conclusions

- Chapter 4 results showed that powdered biochar can provide promising removal performance of ESHs in clean water. This chapter presents the capabilities of a powdered biochar to intercept the dairy ESHs from a real dairy shed effluent sample. To enhance the removal of ESHs, powdered biochar is proposed to be dosed into the CAP inlet arrangement (sump) in which agitation and sufficient contact time occurs.
- Adsorption of organic contaminants and ESHs within raw municipal and/or agricultural wastewater is not a common treatment method. Absorption is typically used as a polishing step to ensure optimum adsorption and cost effectiveness. However, in the dairy agricultural environment, dosing dairy shed effluent with biochar can have many benefits, particularly before it enters the anaerobic digestion system. These benefits can include, improved anaerobic digestion's treatment performance and when the effluent and sludge containing biochar are applied to land, improved soil properties, increased crop yields and reduced greenhouse gas emissions. All these benefits, in addition to ESHs removal capabilities, make the use of biochar in the dairy farm ETS an attractive option.
- Based on the modelling, at a powdered biochar concentration of 100 mg/L and 1000 mg/L, approximately 87 % and 96 % 17α-E2, 34 % and 65 % 17β-E2, 78 % and 60 % E1 and 80 % and 91 % of ΣESHs were respectively removed by adsorption to the powdered biochar from the DSE. Increasing the powdered biochar concentration higher than 1000 mg/L made a negligible change to the adsorption performance.
- The Modified Freundlich Isotherm with two coupled Freundlich equations provided the best fit (R^2 = 0.60 – 0.99) to model the data for ESHs adsorption to powdered biochar suggesting that the dissolved ESHs are partitioned between being associated with the DSE dissolved organic carbon and the subsequent adsorption of the dissolved organic carbon to the biochar or by direct adsorption to the powdered biochar.
- The Modified Freundlich model results suggest a very strong interaction between the dissolved organic content and the ESHs due to the concentration of the former

compared with that of the powdered biochar and also the ESHs strong affinity for organic matter (log K_{oc} = 3.06 to 3.80). However, the adsorption of the ESHs to the powdered biochar was favoured over the dairy shed effluent dissolved organic matter. At a lower concentration only 17β-E2 associated with the organic matter tended to adsorb to the powdered biochar with a linear relationship, while 17α-E2 and E1 would be more likely to adsorb to the powdered biochar directly.

- With an average dairy herd size in NZ of 444 cows and dairy shed effluent generation per cow of 70 L/d, typically 3 – 30 kg powdered biochar per day would be required to achieve overall removal of 80-90% of dairy shed effluent ESHs in solution.
- The overall reduction in estrogenicity is driven by the removal of 17β-E2. A modelled powdered biochar dose of 1000 mg/L achieved 67.2 % reduction in overall estrogenicity. Increasing the biochar concentration higher than 1000 mg/L can reduce the overall estrogenicity further, however would require a substantial additional amount of biochar. However, as previously showed in Chapter 2, the CAP itself has some abilities to reduce the effluent estrogenicity by sequestering the ESHs in the dissolved phase to the sludge solids, therefore, the addition of the recommended amount of biochar to the dairy shed effluent prior to entering the CAP system can potentially enhance the performance of the CAP without the need to add more powdered biochar (Chapter 6).
- Further ESHs analysis work and robust modelling is required to assess the performance of the CAP dairy shed effluent treatment system dosed with powdered biochar and coupled with a storage pond, to remove ESHs.
- It is not clear how the ESHs adsorbed into the powdered biochar would behave upon entering the CAP system. Further research is required to assess the fate and adsorption capabilities of the powdered biochar adsorbed ESHs in an anaerobic condition with hydraulic retention time of up to 50 days.

Chapter 6:
Modelling the efficacy of a dairy farm based covered anaerobic pond treatment system dosed with powdered biochar to transform and remove estrogenic steroid hormones

---

As discussed in the previous chapters, the growing practise of recycling pond sludges and effluent from dairy shed effluent (DSE) treatment systems to land as a source of soil nutrients can impact aquatic ecosystems through the release of estrogenic steroid hormones (ESHs) to the environment due to their associated endocrine disrupting impacts. The covered anaerobic pond (CAP) is one of the available treatment methods for treating ESHs and a popular anaerobic digester configuration. Despite increasing adoption of on-farm CAPs to treat DSE and recover methane for on-site energy co-production, the fate of biologically active estrogenic steroid hormones (ESHs) within CAPs has not been addressed. In the previous chapters (Chapters 2 and 3), further work was identified as required to understand the load of ESHs released to the environment by modelling of the performance of the CAP system. Furthermore, Chapters 4 and 5 showed that powdered biochar can provide promising removal performance of ESHs in solution and DSE. This work includes the development of a typical dairy farm-based CAP treatment system model build to test the CAP efficacy to remove ESHs from DSE both with and without the addition of powdered biochar.

6.1 Introduction

Dairy farm effluent treatment systems in New Zealand (NZ) includes many different configurations such as a two-pond system, stirred pond and weeping wall (details regarding the different dairy farm effluent systems used in NZ are provided in the appendices, Section 7.2A.20). Farmers are able to select the effluent system according to their financial requirements, the farm's future intentions and operational and soil

conditions, as long as they adhere to regional council restrictions (Dairy NZ, 2014). These restrictions are specific to every regional authority and normally include maximum effluent application depth and rate, and maximum nutrient loading, along with other measures such as provision of sufficient effluent storage during wet conditions, properly sealed pond/s and no irrigation near water courses (Waikato Regional Council, n.d.). An average dairy farm in NZ contains 444 cows (Dairy NZ, 2021). A dairy cow typically spends about 10-20% of the day in a milking shed (IPENZ, 2017) during which it produces approximately 67 litres of dairy shed effluent (DSE) comprising faecal, urinary, and milk waste and wash water (Heubeck. *et al*., 2014) which equates to an average volume of effluent of 30 m^3 per day. The remaining 80-90 % of the time the faecal and urinary waste of dairy cows in NZ is deposited directly onto pasture. Deposition in the fields can cause many environmental issues such as the emission of greenhouse gases from nitrous oxide (urine patches), nitrogen leaching, and phosphorus washout (Toth *et al*., 2006; Luo *et al*., 2008; Liang *et al*., 2014; Eckard and Clark, 2019). These environmental issues and the related increased ecological concerns are driving farmers towards a more confined method of farming where the cow spends more time at the shed and therefore more effluent would be captured and require treatment.

Anaerobic digestion systems are used increasingly as a sustainable option for dealing with animal waste (Bidart *et al.*, 2014). The selection of the type of the anaerobic digestion system is driven by the farm effluent and manure handling system (U.S. Environmental Protection Agency, 2004) (principles of anaerobic digestion and examples for possible anaerobic digestion feeds in a dairy farm environment are provided in the appendices, Sections 7.2A.21 and 7.2A.22 respectively). The most popular anaerobic digester configurations for treating dairy biomass are the covered pond digester, complete mix digester, plug flow and fixed film digester (U.S. Environmental Protection Agency, 2004). The covered pond anaerobic digestion would normally be in the ground and have an impermeable gas collection cover. This system would typically have a long hydraulic retention time of 40 to 60 days, the solid feed content would be 0.5 – 3 % and the system would include no supplementary heat source. There are a number of covered anaerobic pond (CAP) systems operating in NZ that are designed to treat dairy shed and swine effluent (NIWA, 2008). The CAP system is likely to increase in popularity due to its

simplicity, sustainable performance, and ability to recover energy and reduce greenhouse gas emission by capturing and utilising/burning the methane. The stable sludge and liquor rich in nutrients thus produced can be utilised for crop nutrition (NIWA, 2008). Therefore, the CAP system was selected to be included in this research.

The key objective of an anaerobic digestion system such as the CAP system is the stabilisation of biosolids. This is accomplished through biological decomposition of the organic matter to methane and carbon dioxide and reduction of inorganic matter (mainly sulphate) in an oxygen free environment. Through the stabilisation process, recovery of energy, and reduction of odour, pathogen concentrations and mass are also achieved (Metcalf and Eddy, 2014). The fate of estrogenic steroid hormones (ESHs) during anaerobic digestion has been explored in different studies (Gonzalez-Gil *et al.*, 2016; Marti & Batista, 2014; Muller *et al.*, 2010; Noguera-Oviedo & Aga, 2016; Paterakis *et al.*, 2012; Samaras *et al.*, 2014; Zhang *et al.*, 2014a), but the results are not always conclusive, and most of them focus on 17β-estradiol (17β-E2) (the dominant form of estrogenic hormone in residential wastewater) and not on 17α-estradiol (17α-E2) (the dominant form of estrogenic hormone excreted by dairy cows) (Gadd *et al.*, 2010b; Noguera-Oviedo & Aga, 2016; Sarmah *et al.*, 2006). Some studies suggest that the anaerobic digestion operating temperature does not have a substantial influence on the removal of steroid hormones. In some studies, low removal rates (<25 %) of estrogens were observed (Gonzalez-Gil *et al.*, 2016; Malmborg & Magnér, 2015; Noguera-Oviedo & Aga, 2016; Zhang *et al.*, 2014a; Zheng *et al.*, 2012), however other studies suggest higher removal rates (40 – 70 %) (Carballa *et al.*, 2007; Muller *et al.*, 2010); these differences may be related to the difficulties related to analysis of ESH in the medium. Several studies suggest a change of estrogenic form during the anaerobic digestion process. During studies of sludge from wastewater plant anaerobic digestion, it was found that 17β-E2 was transformed to estrone (E1) (Czajka & Londry, 2006; Ruchiraset & Chinwetkitvanich, Furthermore, a study of dairy manure anaerobic digestion showed increased E1 concentrations and a decrease of 17α-E2 and17β-E2 (Noguera-Oviedo & Aga, 2016). It was found that the anaerobic digester sludge treatment system, in comparison to the secondary treatment processes (a popular method used to treat municipal waste) results in a lower removal of estrogens (Andersen *et al.*, 2003;

Ifelebuegu, 2011; Ruchiraset & Chinwetkitvanich, 2014) (More information regarding the fate and behaviour of ESHs in the environment and municipal wastewater treatment systems are provided in the appendices, Sections 7.2A.23 and 7.2A.24 respectively).

In addition to the lack of conclusive understanding regarding the fate of ESHs during anaerobic digestion, as far as we know, no research and/or modelling has been done to fully assess the performance of dairy farm effluent treatment systems (ETS) in NZ in general or the CAP coupled with a storage pond specifically (system that is currently in use and is foreseen to be used more commonly in the future), to remove estrogenic steroid hormones. The purpose of this study was to address this knowledge gap by,

a. assessing the load of ESHs (expressed as conjugated and free 17α-E2, 17β-E2, E1, and ΣESHs) entering a dairy farm-based CAP treatment system from a combined dairy cow milking shed and feeding pad.
b. developing and testing a model looking at the efficacy of a dairy farm-based CAP treatment system to transform, adsorb and remove ESHs.
c. providing an estimate of ESHs loads being released into the NZ environment from the recycling and discharge of CAP treated effluent and sludge.
d. using the data and the model outputs, to discuss the fate and potency of the different forms of estrogenic steroid hormone (Free and conjugated) in the effluent and sludge solids from the CAP that are applied to farm pasture, and the broader impact they may present within receiving environments.
e. Using the data and the model outputs, to assess and discuss the performance of a CAP dairy shed effluent treatment system dosed with powdered biochar to remove estrogenic steroid hormone.

6.2 Materials and Methods

6.2.1 The study farm and CAP effluent treatment system

The dairy farm and CAP system used to treat DSE, and from which samples of influent, sludge and effluent samples were collected has been previously described in Chapter 2. The 5,000 m^3 lined storage pond from whence the final effluent is drawn (by a pump) and

spray irrigated onto farm pasture is presented in Figure 6-1. The suction arrangement contains a float and pipe. The float moves with the water level as the water level changes to ensure only the supernatant is drawn from the storage pond. The solid portion would settle at the bottom of the pond. Removal of the solids from the storage pond at the study farm occurs every year, usually in May, using an agitator and a suction tanker. The solids removed from the storage pond are used for pasture application using the suction tanker inbuilt irrigation system.

Figure 6-1: Photographs of the storage pond (at approximately 30% full) and discharge pipe.

6.2.2 Work outline

The outline of the performance assessment of dairy farm effluent CAP DSE treatment system, coupled with a storage pond to remove ESHs from DSE, is summarised in Figure 6-2. The initial phase involved constructing a model using the study farm and CAP parameters as outlined in Section 6.2.1. Subsequently, the study farm CAP model was subjected to calibration using the annual average values obtained from the measurement of chemical and ESHs parameters detailed in Chapters 2 and 3. The calibration process allowed for the refinement of the model and the determination of associated calibrated parameters. The calibrated model, along with the derived parameters, was then employed to evaluate the performance of the study farm CAP treatment system throughout the milking season period, applying previously measured ESHs and flow data. Finally, by analysing the outcomes obtained from the performance model of the study farm CAP system, the implications of reusing effluent and sludge for land application, in

conjunction with a storage pond, were assessed, considering both the presence and absence of biochar.

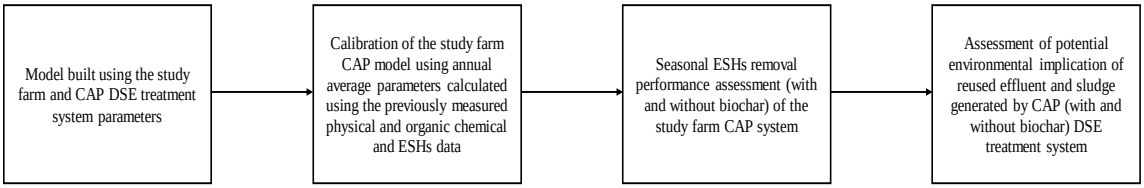

Figure 6-2: Outline of the work

6.2.3 Model description and operation

The CAP model was developed by separating the pond into a liquid and sludge layer, and then dividing those layers into six stages longitudinally modelled as individual mixed tanks operating in series creating altogether a plug flow arrangement (Levenspiel, 1999) (Figure 6-3). The number of stages and the model setup was selected to represent the shape and operation of the CAP system where DSE is pumped into the pond through a single pipe situated approximately 1.5 meter below the top water level at one end of the pond once to twice a day from the sump. A larger number of model stages would be better suited to characterise an ideal plug flow condition; however, these conditions would not reflect the CAP operation due to the intermediate mixing likely to be caused by the influent feed velocity through a narrow diameter pipe causing a jet effect in the pond. It is anticipated that there will be some mixing occurring in the liquid layer during the duration of the feeding process and dispersion of the effluent during times when the CAP is not fed by the pump which will lead to a slow movement of the effluent towards the outlet of the CAP system while the settleable solids within the effluent readily settle into the sludge. The sludge layer is mostly water, and mobile, therefore it is expected that the sludge would gradually migrate down the length of the pond as it is disturbed by the movement of the incoming water, therefore, the level of the sludge is approximately flat relative to the base of the pond (Fyfe *et al*., 2016). Periodically (once a year), to prevent sludge build up, the sludge is pumped out of the pond to maintain an average sludge level of approximately 0.7 m. As DSE is pumped into the CAP, the effluent within the pond is drained off via an internal weir into a manhole and subsequently into the storage pond and therefore the liquid level in the CAP is maintained.

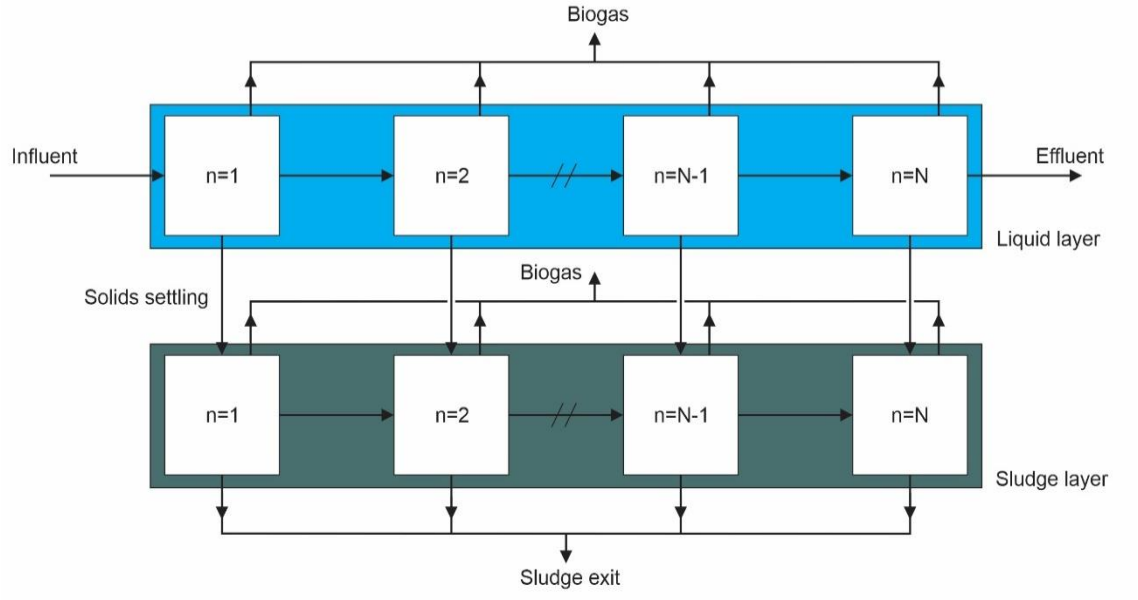

Figure 6-3: Model set up for the CAP system (n = number of stages; N = 6)

6.2.4 Model mass balance calculation

6.2.4.1 Calculation of the solids

In the liquid phase, the change in volatile solid and ash fractions are given by the mass flow of each in and out of each stage, the mass of each that settled, and the mass of volatile solids converted into gas (Equations 6-1 and 6-2; definitions for all equations can be found after Equation 6-7)

$$\frac{\Delta x_{VSL}|_{n,t}}{\Delta t} = \frac{(x_{VSL}|_{n-1,t-1} - x_{VSL}|_{n,t-1})\dot{m}_L}{m_{stage_L}|_{n,t-1}} - k_{set_{VS}}\, x_{VSL}|_{n-1,t-1} - k_{gas_{VS}}\, x_{VSL}|_{n-1,t-1} \quad (6\text{-}1)$$

$$\frac{\Delta x_{AshL}|_{n,t}}{\Delta t} = \frac{(x_{AshL}|_{n-1,t-1} - x_{AshL}|_{n,t-1})\dot{m}_L}{m_{stage_L}|_{n,t-1}} - k_{set_{Ash}}\, x_{AshL}|_{n-1,t-1} \quad (6\text{-}2)$$

In the sludge phase, the change in volatile solid and ash fractions are similarly given by the mass flow of each in and out of each stage, the mass of each that settled, and the mass of volatile solids converted into gas (Equations 6-3 and 6-4)

$$\frac{\Delta x_{VSS}|_{n,t}}{\Delta t} = \frac{x_{VSS}|_{n-1,t-1}\dot{m}_S|_{n-1,t-1} - x_{VSS}|_{n,t-1}(\dot{m}_S|_{n,t-1} + \dot{m}_{SD}|_{n,t-1})}{m_{stage_S}\Big|_{n,t-1}} +$$

$$k_{set_{VS}}\, x_{VSL}|_{n-1,t-1} \frac{m_{stage_L}\Big|_{n,t-1}}{m_{stage_S}\Big|_{n,t-1}} - k_{gas_{VS}}\, x_{VSS}|_{n-1,t-1} \quad (6\text{-}3)$$

$$\frac{\Delta x_{AshS}|_{n,t}}{\Delta t} = \frac{x_{AshS}|_{n-1,t-1}\dot{m}_S|_{n-1,t-1} - x_{AshS}|_{n,t-1}(\dot{m}_S|_{n,t-1} + \dot{m}_{SD}|_{n,t-1})}{m_{stage_S}\Big|_{n,t-1}} +$$

$$k_{set_{Ash}}\, x_{AshL}|_{n-1,t-1} \frac{m_{stage_L}\Big|_{n,t-1}}{m_{stage_S}\Big|_{n,t-1}} \quad (6\text{-}4)$$

The total change in mass in the sludge is calculated assuming a constant solids content in the sludge (Equation 6-5).

$$\Delta\, m_{stage_S}\Big|_{n,t} = \frac{(\Delta x_{VSS}|_{n,t} + \Delta x_{AshS}|_{n,t}) m_{stage_L}\Big|_{n,t-1}}{x_{SolidsS}} \quad (6\text{-}5)$$

Sludge mass flow is calculated based on the difference between sludge masses in each stage (Equation 6-6).

$$\dot{m}_S|_{n,t} = \left(m_{stage_S}\Big|_{n+1,t} - m_{stage_S}\Big|_{n,t}\right) J_S \quad (6\text{-}6)$$

Sludge mass discharge flow occurred every 365 days (or whenever desired) to reduce the total sludge mass for the stage back to a set sludge mass (for example to a sludge height of 0.7 m) (Equation 6-7).

$$\dot{m}_{SD}|_{n,t} = m_{stage_S}\Big|_{n,t} - m_{stage_{Sset}} \quad (6\text{-}7)$$

where: $m_{stage_S}\Big|_{n,t} > m_{stage_{Sset}}$

where x is mass fraction, $\dot{m}$ is mass flow (kg/day), m_{stage} is the mass in each stage (kg), k_{set} is the rate of settling (1/day), k_{gas} is the rate of conversion of volatile solids to biogas (1/day), L is liquid, S is sludge, VS is volatile solids, Ash is the ash, and VSL and VSS is

the volatile solids in the liquid and sludge layers respectively, $AshL$ and $AshS$ is the ash in the liquid and sludge layers respectively, n is stage, t is time (days), and J_S is rate of sludge migration between stages (1/day).

The CAP was modelled as a finite difference model in Microsoft Excel using the following boundary conditions:

At $n = 1,\ t = 1{:}T$

$$x_{VSL}|_{n-1,t} = x_{VS_{influent}}$$
$$x_{AshL}|_{n-1,t} = x_{Ash_{influent}}$$
$$x_{VSS}|_{n-1,t}\dot{m}_S|_{t,n-1} = 0$$
$$x_{AshS}|_{n-1,t}\dot{m}_S|_{t,n-1} = 0$$

At $n = N,\ t = 1{:}T$

$$x_{VSS}|_{n,t}\dot{m}_S|_{n,t} = 0$$
$$x_{AshS}|_{n,t}\dot{m}_S|_{n,t} = 0$$

At $t = 0$ and $n = 1{:}N$

$$x_{VSL}|_{n,t} = 0$$
$$x_{AshL}|_{n,t} = 0$$
$$x_{VSS}|_{n,t} = 0$$
$$x_{AshS}|_{n,t} = 0$$
$$m_{stage_S}\Big|_{n,t} = 0$$
$$m_{stage_L}\Big|_{n,t} = \frac{V_{CAP}\rho_L}{N}$$

with $\Delta t = 1$ day and total number of stages $N = 6$, V_{CAP} is the volume of the covered anaerobic pond (m^3), and ρ_L is the density of the liquid (~1000 kg/m^3).

6.2.4.2 Calculation of the ESHs mass balance (with and without biochar)

For modelling the ESH mass balances, it was assumed that the ESHs are partitioned to the organic and inorganic carbon and any ESH adsorbed to the settleable solids will settle out with the solids into the CAP sludge phase. Based on the chemical structure (aromatic ring) of the ESHs and its stability and complexity compared to the more chemically reactive DSE organic matter for example carbohydrates and proteins, it was assumed that the ESHs would degrade independently of the volatile solids in the CAP (Chapters 2 and 5), therefore the concentration of the ESHs were not linked to the concentration of the volatile or total solids, and the mass balance around ESHs could be calculated independently (Equation 6-8).

$$\frac{\Delta E|_{p,i,n,t}}{\Delta t} = E_{Trans}|_{p,i,n,t} + E_{Ads}|_{p,i,n,t} + E_{Con}|_{p,in,t} + E_{Set}|_{p,i,n,t} \quad (6\text{-}8)$$

Where E is ESH mass, p is the phase (dissolved liquid (p=1), solids in the liquid (p=2), sludge liquid (p=3) and sludge solid (p=4)), i is the type of ESH, *Trans* is the transport in the liquid or sludge, *Ads* is adsorption of the dissolved ESHs in the liquid phase into the solid phase, *Con* is the conversion of the ESHs from one type to another, and *Set* is the settling of ESHs attached to the settleable solids. For the purposes of modelling, it was assumed that all ESHs adsorption to the sludge and/or biochar that might occur would happen outside the CAP in the sump and within 24 hours (Chapters 4 and 5) and no desorption of the ESH would occur within the CAP. Therefore, ESHs adsorption and desorption inside the CAP is neglected. This enabled equations previously reported in Chapter 5 describing the adsorption of ESHs by powdered biochar, powdered biochar adsorption capabilities and estimated powdered biochar dosed CAP influent ESH concentrations to be used.

For ESHs in the dissolved and settleable solid phase (p=1,2) in the liquid E_{Trans} is given by Equation 6-9.

$$E_{Trans}|_{p,i,n,t} = \left(E|_{p,i,n-1,t-1} - E|_{p,i,n,t-1}\right)\frac{\dot{m}_L}{m_{stage_L}} \quad (6\text{-}9)$$

For ESHs in the liquid and solid phase in the sludge, p=3,4, E_{Trans} is given by Equation 6-10.

$$E_{Trans}|_{p,i,n,t} = \left(E|_{p,i,n-1,t-1} \frac{\dot{m}_S|_{p,n-1,t-1}}{m_{stage_S}|_{n-1,t-1}} - E|_{p,i,n,t-1} \frac{\dot{m}_S|_{p,n,t-1}}{m_{stage_S}|_{n,t-1}} \right) \quad (6\text{-}10)$$

Removal of ESHs attached to the settleable solids by settling from liquid phase (p=2) into the sludge phase (p=4) is given by Equation 6-11.

$$E_{Set}|_{p=2,i,n,t} = -k_{set_{VS}} E|_{p=2,i,n,t-1} \quad (6\text{-}11)$$

Addition of ESHs to the sludge phase (p=4) by settling from the liquid phase (p=2) is given by Equation 6-12.

$$E_{Set}|_{p=4,i,n,t} = k_{set_{VS}} E|_{p=2,i,n,t-1} \frac{m_{stage_L}|_{n,t-1}}{m_{stage_S}|_{n,t-1}} \quad (6\text{-}12)$$

For modelling changes in ESHs due to bacterial/enzymatic action, it was assumed the free and conjugated forms of 17α-E2 and 17β-E2 and the conjugated form of E1 are ultimately converted to the free form of E1 (Chapter 2), while the conjugated form of 17α-E2 will also be converted to the free form of 17α-E2 and the conjugated form of 17β-E2 will be converted to the free form of 17β-E2 (Chapter 3). This is assumed to happen in both the sludge phase and liquid phase (p=1-4) (Table 6-1). For simplicity, it was also assumed that each conversion would be first order, although if needed a pseudo second order equation could be used.

Table 6-1: Conversion parameters used for changes in ESHs due to bacterial/enzymatic action.

		Free ESH		
	ESH Species	**E1 (*f*, *i*=*1*)**	**17α-E2 (*f*, *i*=*2*)**	**17β-E2 (*f*, *i*=*3*)**
Free ESH	E1 (*f*, *i*=1)	0	0	0
	17α-E2 (*f*, *i*=2)	k_{f2f1}	0	0
	17β-E2 (*f*, *i*=3)	k_{f3f1}	0	0
Conjugated ESH	E1 (*c*, *i*=4)	k_{c4f1}	0	0
	17α-E2 (*c*, *i*=5)	k_{c5f1}	k_{c5f2}	0
	17β-E2 (*c*, *i*=6)	k_{c6f1}	0	k_{c6f3}

The free and conjugated ESH species conversion is given by Equations 6-13 to 6-18.

$$\frac{\Delta E|_{p,i=1,n,t}}{\Delta t} = -k_d E|_{p,i=1,n,t-1} + \sum_{i=1-3} k_{fif1}\, E|_{p,i,n,t-1} + \sum_{i=4-6} k_{cif1}\, E|_{p,i,n,t-1} \quad (6\text{-}13)$$

$$\frac{\Delta E|_{p,i=2,n,t}}{\Delta t} = -\left(k_d + k_{f2f1}\right)E|_{p,i=2,n,t-1} + k_{c5f2}E|_{p,i=5,n,t-1} \quad (6\text{-}14)$$

$$\frac{\Delta E|_{p,i=3,n,t}}{\Delta t} = -\left(k_d + k_{f3f1}\right)E|_{p,i=3,n,t-1} + k_{c6f2}E|_{p,i=6,n,t-1} \quad (6\text{-}15)$$

$$\frac{\Delta E|_{p,i=4,n,t}}{\Delta t} = -\left(k_d + k_{c4f1}\right)E|_{p,i=4,n,t-1} \quad (6\text{-}16)$$

$$\frac{\Delta E|_{p,i=5,n,t}}{\Delta t} = -\left(k_d + k_{c5f1} + k_{c5f2}\right)E|_{p,i=5,n,t-1} \quad (6\text{-}17)$$

$$\frac{\Delta E|_{p,i=6,n,t}}{\Delta t} = -\left(k_d + k_{c6f1} + k_{c6f3}\right)E|_{p,i=6,n,t-1} \quad (6\text{-}18)$$

Where k_d is the ESHs degradation rate coefficient and k_f and k_c are the ESHs free and conjugated conversion coefficients respectively.

The ESHs in the CAP was modelled as a finite difference model in Microsoft Excel(TM) using the following boundary conditions:

At $n = 1,\ t = 1{:}T$

$$E_{Trans}|_{p=1,2,i,n,t} = \left(E_{sump}\big|_{p,i,t} - E|_{p,i,n,t-1}\right)\frac{\dot{m}_L}{m_{stage_L}\big|_{n,t-1}}$$

$$E_{Trans}|_{p=3,4,i,n,t} = -E|_{p,i,n,t-1}\frac{\dot{m}_s|_{p,n,t-1}}{m_{stage_S}\big|_{n,t-1}}$$

At $n = N,\ t = 1{:}T$

$$E_{Trans}|_{p,i,n,t} = \left(E|_{p,i,n-1,t-1}\frac{\dot{m}_s|_{p,n-1,t-1}}{m_{stage_S}\big|_{n-1,t-1}}\right)$$

At $t = 0$ and $n = 1{:}N$

$$E|_{p,i,n,t} = 0$$

$$E_{Trans}|_{p,i,n,t} = 0$$

$$E_{Con}|_{p,in,t} = 0$$

$$E_{Set}|_{p,i,n,t} = 0$$

$$E_{Ads}|_{p,i,n,t} = 0$$

6.2.5 Model calibration

Generally, it is important to calibrate the model output using actual data to minimise uncertainties and errors when the model is used for simulation. Calibration allows an estimation of the model's reliability and provides a level of confidence in the model outputs. To calibrate the CAP model, real measured estrogen and solids concentrations of influent effluent and sludge were used and the CAP model parameters were found by adjusting each of the variable parameters (Table 6-2) to reduce the sum of square errors (SSE) using Excel Solver(TM). The coefficient of determination (R^2) was used to determine the degree of fit of the CAP model outputs (CAP sludge and effluent VS, ash and ESHs) data with the corresponding measured dataset.

The CAP model was enhanced by incorporating the mass effluent to mass sludge ratio value, which serves to account for the presence of sludge at the outlet of the CAP system and the occurrence of short-circuiting when the sludge layer becomes elevated and is not promptly removed from the system. This phenomenon of sludge carryover is supported by the observed increase in concentration and proportion of E1 (the predominant ESH found in the sludge) and 17α-E2 (the predominant ESH in the influent) in the CAP effluents, as discussed in Chapter 2.

Table 6-2: CAP model variables

Description	Parameter
Rate of volatile solid settling	$k_{set\ VS}$
Rate of ash settling	$k_{set\ ash}$
Rate of conversion of volatile solids to biogas	k_{gas}
Rate of sludge migration between stages	J_S
ESHs degradation coefficient	k_d
Mass effluent to sludge mixing ratio	k_{mix}

In order to ensure the completion of the calibration process, a thorough evaluation of the model, and representative characterisation of the operational capabilities of a typical dairy shed farm-based CAP system, it was crucial to select an appropriate dataset. Previous findings (Chapter 2) have indicated that the removal performance of ESHs in the CAP system is not consistent throughout the milking season. This variability in CAP performance can be attributed to several factors, including seasonal fluctuations in ESHs concentration (Chapters 2 and 3) and the DSE flow rate, as well as the influence of temperature and rainfall, the extended retention time within the CAP system, and the operational conditions of the CAP treatment system (Fyfe *et al*., 2016). Therefore, for effective calibration of the CAP model, it was imperative to identify a combination of measured data encompassing CAP influent, sludge, and effluent ESHs concentration, as well as corresponding flow measurements that are representative of a typical operational CAP system, taking into account these variations. This approach ensured that the calibrated CAP model can be employed in simulations with greater representativeness. Due to the CAP long retention time, the monthly ESHs measured in the effluent and sludge samples did not correspond with the influent sample, hance, the selected dataset used for the calibration of the CAP model was comprised of the annual average values of

CAP influent, effluent, and sludge ESHs concentration, as well as chemical parameters previously reported in Chapters 2 and 3, together with the corresponding annual average CAP influent flow monitoring data.

6.2.5.1 CAP dimensions and operating conditions used during the calibration process

The CAP data and operating conditions used in the CAP calibration process are based on the studied farm CAP properties and data and are presented in Table 6-3.

Table 6-3: Dimensions of the CAP system and operating conditions used in the calibration stage

Description	Value	Units
Inlet pipe diameter	150	mm
CAP upper width	20	m
CAP upper length	35	m
Water depth	3.75	m
Bands inclination	45	°
Number of cows	550	cows
Total CAP volume	1500	m^3
Sludge volume[A]	215	m^3
Desludging frequency	365	days
CAP Influent[B]	34311	L/d

[A] calculated based on an average sludge level of 0.7 m. [B] Average annual daily volume which entered the studied CAP system during 2018. The data was extracted from the farm HALO SYSTEM and consists of 17733 L/d of bore water, 3940 L/d of recycled water from the storage pond and 12638 L/d of rainfall.

Typically, when designing a CAP system, the CAP dimensions are determined according to feed loading rate (COD or VS), the hydraulic retention time (HRT) and the desludging frequency requirements which are all proportional to the operational temperature (Park and Craggs, 2007; Water New Zealand, 2017). Depending on the CAP operational temperature and feedstock composition, the CAP organic loading rates would range from 0.02 to 0.46 kg VS/m^3/day and HRT range from 25 to 60 days for most dairy farm systems in NZ (Park and Craggs, 2007). Based on the DSE annual VS concentration of 4175 mg/L (Table 6-5), flow rate of 34.3 m^3/d and the calculated VS loading of 145 kg/day, the recommended CAP volume should be between 1000 – 2500 m^3. Considering this, the CAP volume of the study farm (1500 m^3), falls within the lower range but is considered suitable for the intended DSE treatment and pasture irrigation purposes.

The annual daily CAP influent (DSE) volume of 34311 L/d and farm size of 550 cows, equated to approximately 62.4 L/cow/day. This volume per cow is slightly lower than the 70 L/cow/d previously observed in NZ (Gordon and Robert, 2007; Heubeck. *et al*., 2014) despite the fact that the study farm includes a feed pad and the majority of the previous study farms did not. Feed pads would normally be expected to increase the overall dairy farm water consumption and DSE volumes. However, this reduced DSE volume may be due to compliance the more recent strict regulations governing dairy farm water usage in NZ, which require dairy farmers to manage their water usage more carefully and comply with the resource consent requirements. The study farm obtains a sustainable water usage approach by making use of recycled and treated effluent water to wash the milking yard and feed pad. To conserve water, the study farm milking shed is manually washed using potable water sourced from bore water. The used wash water from the milking shed is directed to the flood wash tank designed to store recycled water and be used to clean the feed pad. The milking yard is typically cleaned twice a day using green water recycled from the storage pond supernatant. Similar to the recycled wash water from the milking shed, the recycled wash water from the milking yard would be directed to the flood wash tank. The recycled milking shed, and milking yard wash water stored in the flood wash tank are used to clean the feed pad daily.

6.2.5.2 Free and conjugated ESHs calibration data

Table 6-4 shows the free and conjugated ESHs annual average concentrations in the solid and dissolved phases of the CAP influent, sludge and effluent samples measured during 2018 and used to calibrate the CAP model (full data is presented in the appendices, Table A-40 to Table A-45).

Table 6-4: Annual average free and conjugated ESHs concentrations in the solid (ng/g) and dissolved (ng/L) phases of the influent, sludge and effluent samples from the CAP collected during 2018 that were used to calibrate the CAP model

	17α-E2	17β-E2	E1	ΣESHs
		CAP Influent (DSE)		
Free ESHs (dissolved)	973	103	153	1230
Conjugated ESH (dissolved)	55.5	39.2	50.3	113
Free ESHs (solid)	273	38.7	112	423
Conjugated ESHs (solid)	17.5	7.22	9.2	23.7
		CAP Sludge		
Free ESHs (dissolved)	30.1	46.3	710	786
Conjugated ESH (dissolved)	N.D[A]	13.3	N.D	13.3
Free ESHs (solid)	31.3	67.6	1033	1132
Conjugated ESHs (solid)	15.1	5.93	19.8	40.8
		CAP Effluent		
Free ESHs (dissolved)	267	72.1	610	949
Conjugated ESH (dissolved)	39.0	8.88	141	189
Free ESHs (solid)	181	71.0	733	985
Conjugated ESHs (solid)	9.10	5.05	5.92	20.1

[A] Not detected

6.2.5.3 Chemical parameters used to calibrate the CAP model

The annual average TS and VS concentration of the CAP influent, sludge and effluent were based on the data previously discussed in Chapters 2 and 5 their mean values are presented in Table 6-5.

Table 6-5: CAP influent, sludge and effluent chemical parameters used to calibrate the CAP model

	TS (mg/L)	VS (mg/L)	Solids fraction (wet basis)	VS fraction[A] (dry basis)	Ash fraction[B] (dry basis)
CAP Influent	6950	4175	0.007	0.60	0.40
CAP Sludge	82020	38380	0.082	0.47	0.53
CAP Effluent	3450	1270	0.004	0.37	0.63

[A] calculated by dividing VS with TS [B] calculated by 1 – VS fraction (dry basis)

The CAP influent, sludge and effluent TS and VS concentrations and VS and ash fractions used in this study are comparable to Fyfe *et al*. (2016) (influent TS and VS of 6048 mg/L and 3797 mg/L respectively, effluent TS and VS of 3000 mg/L and 1222 mg/L respectively and sludge TS and VS of 61216 mg/L and 33249 mg/L) and Hull-Cantillo *et al*. (2023) (effluent TS and VS of 3300 mg/L and 1850 mg/L respectively) who investigated a two-pond and weeping wall DSE treatment system respectively and

Heubeck et al. (2014) (Influent TS of 7803 mg/L) who surveyed nine different dairy farms across NZ. The TS and ash concentrations of the CAP effluent (3450 mg/L and 2180 mg/L respectively), suggest that the CAP total solids and ash removal performance are approximately 50% and 21% respectively. For comparison, Fyfe *et al*. (2016) indicated solids removal performance of 40-50% and ash removal of 18-20%.

Compiling the CAP influent flow (Table 6-3) and compositions of the samples (Table 6-5) enables the mass flows in and out of the CAP to be calculated (Table 6-6). In this calculation, it was assumed the volumetric flow of the CAP influent and effluent was the same, and the effect on overall mass flow from pumping out the sludge and the production of biogas was neglected.

Table 6-6: CAP influent and effluent mass flow calculation

Description	Influent	Effluent
Flow (L/cow/day)[A]	62.4	62.4
Mass solids (kg/day)	226	118
Mass VS (kg/day)	143	43.6
Mass ash (kg/day)	82.9	74.8
Mass solids (kg/cow/day)	0.41	0.21

[A] based on a flow of 34311 L/day and 550 cows (Table 6-3)

The influent mass solids of 0.41 kg/cow/day in this study was slightly lower than the 0.56 and 0.68 kg/cow/day reported by Fyfe *et al*. (2016) and Hull-Cantillo *et al*. (2023) respectively. According to Fyfe *et al.* (2016) literature survey, the influent mass of solids per cow per day varied between 0.05 and 2.05 kg, and this range was heavily influenced by the sampling method employed and the activities performed on the farm on the day of sampling. The value calculated for influent mass solids in this study is likely to be influenced by the inclusion of a feed pad and the higher overall water usage requirement compared with the farms without feed pads (Heubeck. *et al*., 2014) and the low intensity of the supplementary feed used in the current study farm.

The mass balance over the CAP influent and effluent allows the total sludge mass produced to be calculated (Table 6-7). As with the reduced influent mass solids, the produced daily sludge volumes of 1.31 m^3/d and 0.87 m^3/cow/d are lower than the daily sludge volumes of 1.57 m^3/d and 1.90 m^3/cow/d measured by Fyfe *et al*. (2016).

Table 6-7: CAP sludge mass flow calculation

Description	Sludge
Mass solids (kg/day)	108
Mass VS (kg/day)	100
Mass ash (kg/day)	8.06
Daily sludge volume (m^3/d)[A]	1.31
Annual sludge volume (m^3/d)	479
Sludge volume per cow (m^3/cow/day)	0.87

[A] based on solids fraction in the sludge of 0.082 (Table 6-5)

6.2.6 Performance assessment of the study farm CAP system to treat seasonal DSE ESHs loads

6.2.6.1 Free and conjugated ESHs CAP data

The variation in the total free and conjugated ESHs concentration for the individual ESH and ΣESHs over the nine-month (March to November) sampling was discussed in Chapters 2 and 3. Peak ΣESHs concentration were measured in DSE during April and July, which correlated with the late pregnancy and calving period on the study farm. Table 6-8 presents the measured concentrations of free and conjugated ESHs in both dissolved and solid phases of the CAP influent collected in 2018 (Chapters 2 and 3) used to assess the performance of the CAP treatment system.

Table 6-8: CAP Influent ESHs 2018 concentration data used to assess the seasonal ESHs removal performance and fate by CAP DSE treatment system

	Mar-18	Apr-18	Jul-18	Aug-18	Oct-18	Nov-18
CAP Influent free dissolved ESHs (ng/L)						
17α-E2	1610	2869	1065	243	28.6	21.7
17β-E2	233	242	108	14.7	7.04	15.1
E1	282	415	106	43.8	5.19	68.3
CAP Influent free solid ESHs (ng/g)						
17α-E2	309	413	689	174	28.1	23.9
17β-E2	61.0	50.1	63.4	16.7	16.6	24.4
E1	71.3	59.3	108	89.0	46.0	296
CAP Influent conjugated dissolved ESHs (ng/L)						
17α-E2	86.8	89.1	74.3	33.7	22.6	26.6
17β-E2	N.D[A]	6.56	30.5	67.4	40.1	51.6
E1	N.D	137	N.D	N.D	7.12	6.78
CAP Influent conjugated solid ESHs (ng/g)						
17α-E2	2.93	37.0	34.5	11.4	N.D	1.76
17β-E2	N.D	9.00	8.19	4.46	N.D	N.D
E1	N.D	N.D	9.17	N.D	N.D	N.D

[A] Not detected

6.2.6.2 CAP Influent volume and chemical parameters data

The DSE volumetric flow and TS and VS concentrations change over the year depending on the milking season, what is fed to the cows, rainfall, and wash water used by the farmer (Fyfe *et al*., 2016). Table 6-9 presents the measured CAP influent TS and VS concentration and the monitored (HALO system) CAP influent daily average monthly volumes that were used to assess the seasonal ESHs removal performance and fate by the study farm CAP DSE treatment system.

Table 6-9: CAP Influent daily volume, TS and VS 2018 data used to assess the seasonal ESHs removal performance and fate by CAP DSE treatment system

	CAP Influent					
	Mar	**Apr**	**July**	**Aug**	**Oct**	**Nov**
Daily volume (L/d)	26455	26040	30165	43926	44387	45987
TS (mg/L)	6950[A]	5200	6950[A]	8700	6200	7700
VS (mg/L)	4175[A]	3200	4175[A]	5200	3300	5000

[A] due to the absence of data during these months, annual average concentrations (Table 6-5) were used

Given the monthly average concentrations of the ESHs (Table 6-8), and corresponding volumetric flow of the CAP influent (Table 6-9), the mass flows of each ESH and their distribution between being free or conjugated in the liquid and solid phases was calculated and used to feed the CAP model.

6.2.6.3 Biochar used to enhance the ESHs removal performance of the CAP

As presented in Chapter 5, addition of powdered biochar concentration ranges between 100 - 1000 mg/L, achieved DSE removal performance of up to 96 %, 65 %, 60 % and 91 % of 17α-E2, 17β-E2, E1 and ΣESHs respectively. As discussed in Chapter 5, increasing the biochar concentration above 500 mg/L demonstrated negligible improvement to the ESHs removal performance of the powdered biochar. Therefore, for the seasonal CAP ESHs removal simulation, powdered biochar with specifications mentioned in Chapter 4 and concentration of 500 mg/L was used. At a powdered biochar concentration of 500 mg/L, 93.6 %, 50.6 %, 74.3 % and 87.3 % of 17α-E2, 17β-E2, E1 and ΣESHs were respectively removed from the dissolved phase of the DSE by adsorption to the powdered biochar (Chapter 5).

6.2.7 Assessment of potential environmental implication of free and conjugated ESHs in effluent and sludge re-used from a CAP used to treat DSE

As in Chapters 2, 3 and 5, the environmental implication of the effluent and sludge re-use was assessed by determining the potencies of the ESHs in each stream. The estrogen equivalents (EEQs) and estrogenicity reduction of the CAP (with and without biochar) was determined by multiplying the concentration of each ESH by the relative potency factor obtained by the ER-CALUX bioassay (Chapter 2) and (Kolkman et al., 2013). The EEQs for each compound modelled in the sludge and effluent streams were summed to obtain the ΣEEQ for each sample. This was then divided by the starting estrogenicity of the DSE to determine a reduction in overall estrogenicity.

6.3 Results and discussions

6.3.1 Model calibration

6.3.1.1 Solids fraction

Comparison of the CAP model solid fraction outputs with the actual measured data are presented in Table 6-10 and the associated CAP model variables in Table 6-11. The calibration results of the CAP model showed high accuracy (R^2 = 100%) score across all the datasets. This indicates that the model was able to perform well for the simulation of the solids and was ready for the simulation of the ESHs.

Table 6-10: CAP model solid output vs measured data

Description	CAP measured data	CAP modelled data	R^2 (%)
Effluent VS fraction	0.0013	0.0013	100
Effluent Ash fraction	0.0022	0.0022	100
Sludge VS fraction	0.0384	0.0384	100
Sludge Ash fraction	0.0436	0.0436	100
Biogas volume (m^3/d)	82.8	83.0	100

The measured and modelled effluent VS and Ash fraction of 0.0013 and 0.0022 respectively and respective reduction of 57.5 % and 18.1% is similar to Fyfe *et al*. (2016) who measured dairy shed two ponds treatment system effluent VS and Ash of 0.0012 and 0.0018 and respective reduction of 67.8 % and 20.5 %. The biogas volume model output of 82.8 m^3/d equates to 50 m^3/d of methane based on methane comprising 60 % of the biogas (Craggs *et al*. 2008) and methane yield of 0.34 m^3 CH_4 per kg VS ((VS = 145 kg VS/day (Section 6.2.5.1)). This methane yield is similar to the methane yield measured by the study farm electrician and comparable with numerous cow manure methane potential studies that determined methane yield factors between 0.20 and 0.28 m^3 CH_4/kgVS (Craggs *et al*. 2008, Heubeck *et al*. 2010, Pratt *et al*. 2012).

Table 6-11: CAP model solid variables

Description	Parameter	Value
Rate of volatile solid settling (kg/kg/day)	$k_{set\ VS}$	0.04645
Rate of ash settling (kg/kg/day)	$k_{set\ ash}$	0.00879
Rate of conversion of sludge volatile solids to biogas (kg/kg/day)	$k_{sludge\ gas}$	0.00686
Rate of conversion of liquid volatile solids to biogas (kg/kg/day)	$k_{effluent\ gas}$	0.00005
Rate of sludge migration between stages (kg/kg/day)	J_S	0.000002
Mass effluent to sludge mixing ratio	k_{mix}	2.095

Note: for simplicity, the resuspension of the sludge by the methane gas was neglected

Figure 6-4 and Figure 6-5 show the hypothetical volatile solids, ash and total solids profile in the liquid and sludge fractions of the CAP respectively. The VS settle at a rate approximately five times greater than the ash. As a result, the concentration of VS is higher at the initial stages of the CAP system closest to the influent, while the concentration of ash is higher at the end of the CAP system closest to the effluent exit. Similarly, initially the sludge has a much higher VS compared to the ash due to the VS settling at a much greater rate than the ash and the greater removal of VS by the CAP pond compared to the ash. However, over time the sludge VS is digested and converted to methane and CO_2 and the ash concentration in the sludge thus increases proportionately to the VS. The VS conversion to biogas in the CAP liquid is approximately 137 times slower than in the sludge (Table 6-11), indicating that the main driver for change in VS concentration in the liquid phase is likely to be due to settling and not biological degradation.

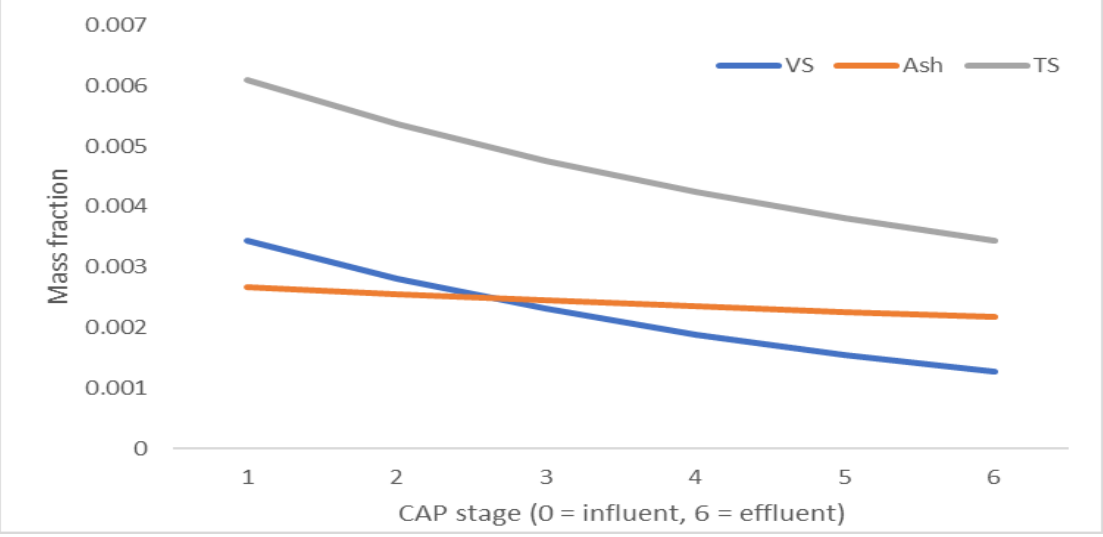

Figure 6-4: Modelled volatile solids, ash and total solids profile in the liquid part of the CAP.

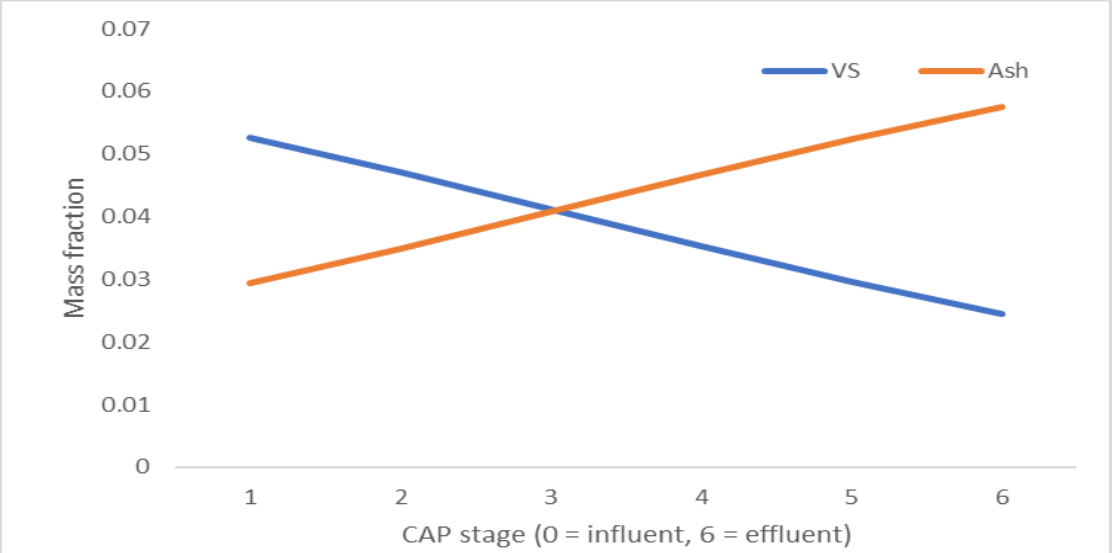

Figure 6-5: Modelled volatile solids and ash profile in the sludge of the CAP

A mass balance check was conducted on the CAP model, which involved comparing the total inputs and outputs of the model with the amount retained within the CAP. The analysis revealed that the overall percentage difference between these values was within 1.06% (Table 6-12).

Table 6-12: Balance check on the CAP model over a simulation time of 3720 days

	VS (kg)	Ash (kg)	Water (kg)	Gas (kg)	Total (kg)
Model Input					
	533012	354277	126780324		127667613
Motel Output					
Effluent	160276	275120	125272436		
Sludge	60018	74709	1507888		
Gas				308248	
Total	312718	4448	126780324		127658695
Sludge retained					
	10036	12367			22403
		Total percentage different			**-1.06%**

6.3.1.2 ESHs

Comparison of the CAP model ESHs outputs (concentration and load) with the actual data are presented in Table 6-13 and Table 6-14. The calibration results of the CAP model showed high accuracy for the effluent ESHs concentration and load (R^2 = 98.4 % and

R^2 = 98.6 % respectively) and sludge concentration and load (R^2 = 100 % and R^2 = 99.6 % respectively) score across all phases and ESHs species concentrations.

Table 6-13: Model output ESHs concentration vs actual measured ESHs concentration

	Free dissolved (ng/L)			Conjugated dissolved (ng/L)			Free solid (ng/g)			Conjugated solid (ng/g)		
	17α-E2	**17β-E2**	**E1**	**17α-E2**	**17β-E2**	**E1**	**17α-E2**	**17β-E2**	**E1**	**17α-E2**	**17β-E2**	**E1**
Effluent												
Model	271	76.9	614	43.3	10.6	38.6	109	59.2	727	2.67	1.02	2.96
Actual	267	72.1	610	39.0	8.88	1.41	181	71.0	733	9.10	5.05	5.92
Sludge												
Model	29.8	45.6	710	1.07	2.63	0.88	79.6	76.9	1036	1.82	0.65	2.63
Actual	30.1	46.3	710	N.D[A]	13.3	N.D	31.3	67.6	1033	15.1	5.93	19.8

[A] Not detected

Table 6-14: Model output ESHs load vs actual calculated ESHs load

	Free dissolved (mg/d)			Conjugated dissolved (mg/d)			Free solid (mg/d)			Conjugated solid (mg/d)		
	17α-E2	**17β-E2**	**E1**	**17α-E2**	**17β-E2**	**E1**	**17α-E2**	**17β-E2**	**E1**	**17α-E2**	**17β-E2**	**E1**
Effluent												
Model	9.12	2.59	20.7	1.46	0.36	1.30	12.8	6.92	85.1	0.31	0.12	0.35
Actual	8.99	2.43	20.5	1.31	0.03	4.75	21.2	8.31	85.8	1.07	0.59	0.69
Sludge												
Model	0.01	0.02	0.29	0.00	0.00	0.00	2.88	2.79	37.52	0.07	0.02	0.10
Actual	0.01	0.02	0.29	N.D[A]	0.01	N.D	1.13	2.45	40.99	0.55	0.21	0.72
Model output ESH Percentage Reduction (%)												
Effluent + sludge vs Influent	72.5	25.7	-302[B]	23.0	70.9	24.2	75.9	-5.19	-359	90.9	91.7	79.9
Effluent vs Influent	72.5	26.2	-296.3	23.0	71.0	24.2	80.4	25.0	-218	92.5	93.1	84.2
Actual data ESH Percentage Reduction (%)												
Effluent + sludge vs Influent	72.8	30.3	-299	30.6	75.3	-177	65.7	-16.5	-361.2	61.4	53.2	35.7
Effluent vs Influent	72.9	30.8	-294	30.6	75.8	-177	67.5	10.0	-221.1	74.5	65.7	68.4

[A] Not detected. [B] negative value indicating an increase

The modelled ΣESHs load in the CAP effluent and sludge and the CAP effluent alone were 199 mg/day and 156 mg/day respectively resulting in ΣESHs removal percentage of -18.5 and 9.53 % respectively. The ΣESHs daily loads and CAP removal performance produced by the model were comparable with the corresponding actual ΣESHs load of 185 mg/d and 141 mg/d and CAP actual removal performance of -27.5 % and -0.05 % respectively. Similarly, the modelled ΣESHs estogenicity reduction of the combined CAP effluent and sludge and the CAP effluent alone were 8.40 % and 29.1 % respectively. These ΣESHs estogenicity reduction rate are slightly different to the corresponding 1.17% and 18.7 % demonstrated by the actual data (Table 6-15).

The observed CAP ESHs removal performance, considering both the ESHs in the effluent and sludge compared to the influent, can be attributed to the characteristics of the sludge. The sludge contains a higher proportion of ESHs due to its elevated total solids (TS) content and the stronger affinity of ESHs for solid particles. As highlighted in Chapter 2, the sludge was found to consist of a substantial proportion (ranging from 98.6 % to 99.4%) of ESHs, predominantly associated with the solid phase. Consequently, the sludge acts as a reservoir rich in ESHs. However, during instances where the sludge level becomes excessively high, resulting in the mixing of sludge with the effluent, particularly during peak flow periods, imbalances occur, leading to suboptimal ESHs removal performance.

Table 6-15: Model output total ESHs load vs actual calculated ΣESHs estrogenicity

	Free dissolved	Conjugated dissolved	Free solid	Conjugated solid
	Model output ΣESH Estrogenicity Reduction (%)			
Effluent + sludge vs Influent	21.0	68.9	-18.3[A]	91.4
Effluent vs Influent	21.6	69.0	16.0	92.9
	Actual data ΣESH Estrogenicity Reduction (%)			
Effluent + sludge vs Influent	25.2	67.9	-29.1	53.0
Effluent vs Influent	25.8	68.4	1.71	65.9

[A] negative value indicating an increase

As discussed in the previous chapters (Chapters 2 and 3), the majority of free and conjugated forms of 17α-E2 and 17β-E2 will ultimately be converted to the free form of

E1 either directly or through the deconjugation process. This ESH transformation occurs in both the effluent and sludge. The fate of the individual ESH in the CAP dissolved and solid phases of the liquid and sludge are presented in Figure 6-6, Figure 6-7, Figure 6-8 and Figure 6-9. The dissolved free and conjugated 17α-E1 influent used for the calibration was initially 1029 ng/L. This concentration was reduced in the first stage of the CAP model to 843 ng/L down 315 ng/L by stage 6. This reduction corresponds with the conversion of 17α-E1 to E1 and the increase of E1 from 203 ng/L in the influent to 344 ng/L in the CAP stage 1, peaking at 652 ng/L in stage 6. The free and conjugated ESHs in the solid phase of the liquid followed a different trend and present a consistent reduction of 17α-E1, 17β-E2 and E1 throughout the CAP system, indicating that the solid phase associated ESH in the liquid would tend the settle rather than transfer. This settling is most likely linked to the enhanced VS settling rate compared with the ash (Table 6-11) and the greater affinity of the ESHs to the organic carbon (Chapter 2). In the sludge, the dominant dissolved ESH E1 presented similar characteristics to the solid phase in the liquid by steadily reducing throughout the CAP system from 991 ng/L in stage 1 to 445 ng/L in stage 6. In the solid phase of the sludge, E1 peaked around stage 3 at 1237 ng/g down 964 ng/g in stage 6, whereas 17α-E1 and 17β-E2 remained low (< 106 ng/g). Generally, the decrease in ESH was dominated by conversion to E1 (estrogenicity reduction) and settling (in term of ESHs removal from the dissolved phase).

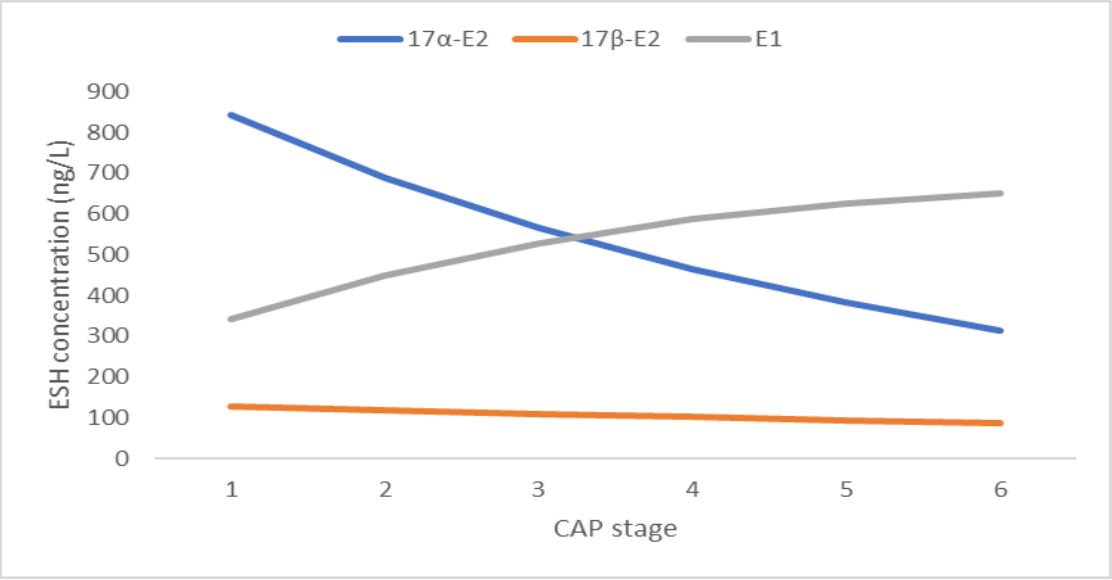

Figure 6-6: The fate of free and conjugated ESH in the CAP dissolved phase of the liquid over the simulation time and different CAP stages

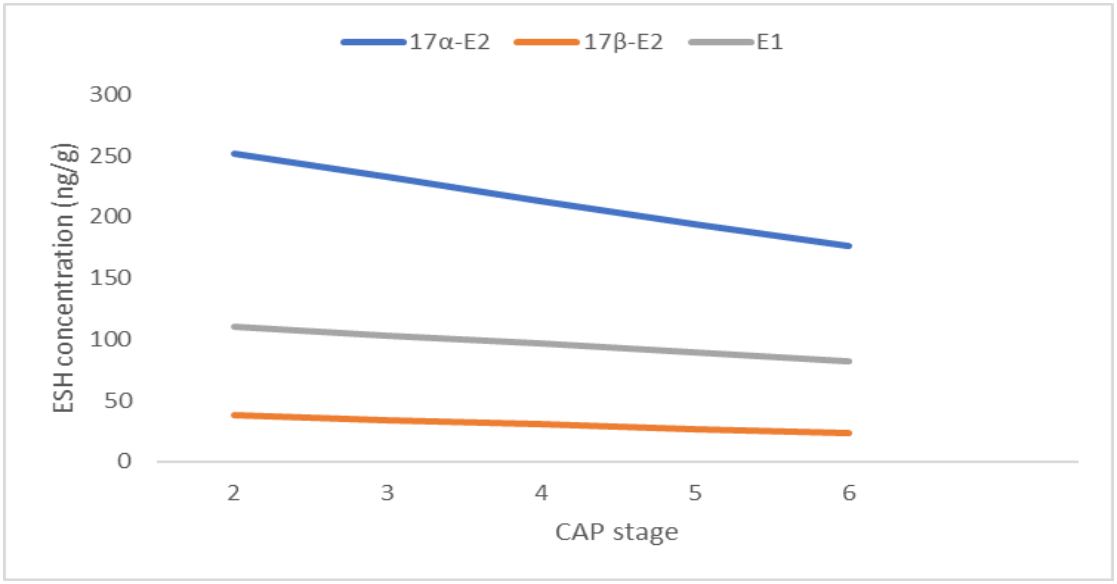

Figure 6-7: The fate of free and conjugated ESH in the CAP solid phase of the liquid over the simulation time and CAP stages

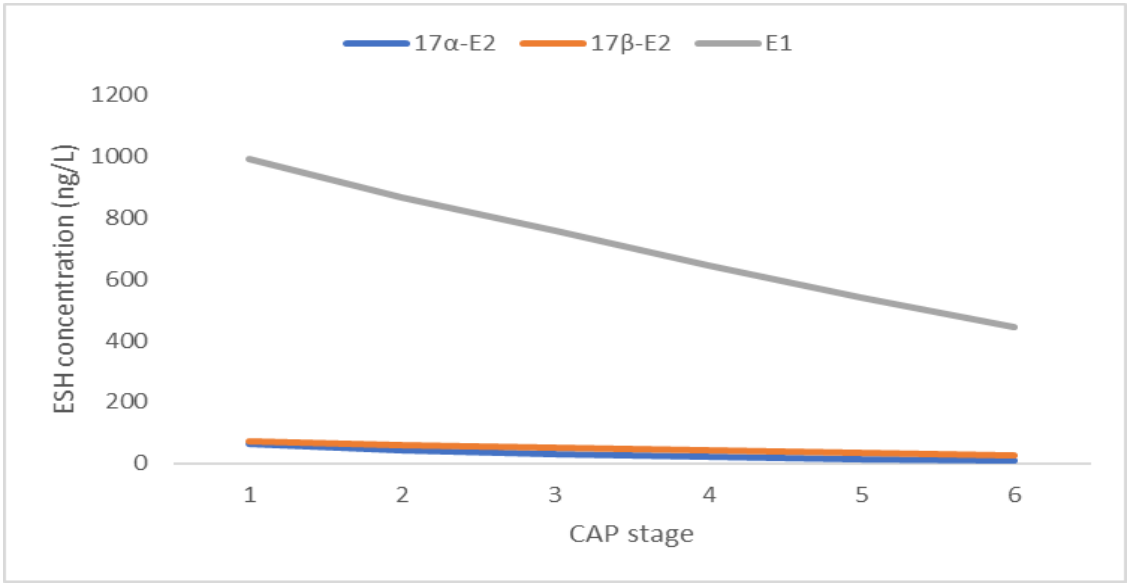

Figure 6-8: The fate of free and conjugated ESH in the CAP dissolved phase of the sludge over the simulation time and CAP stages

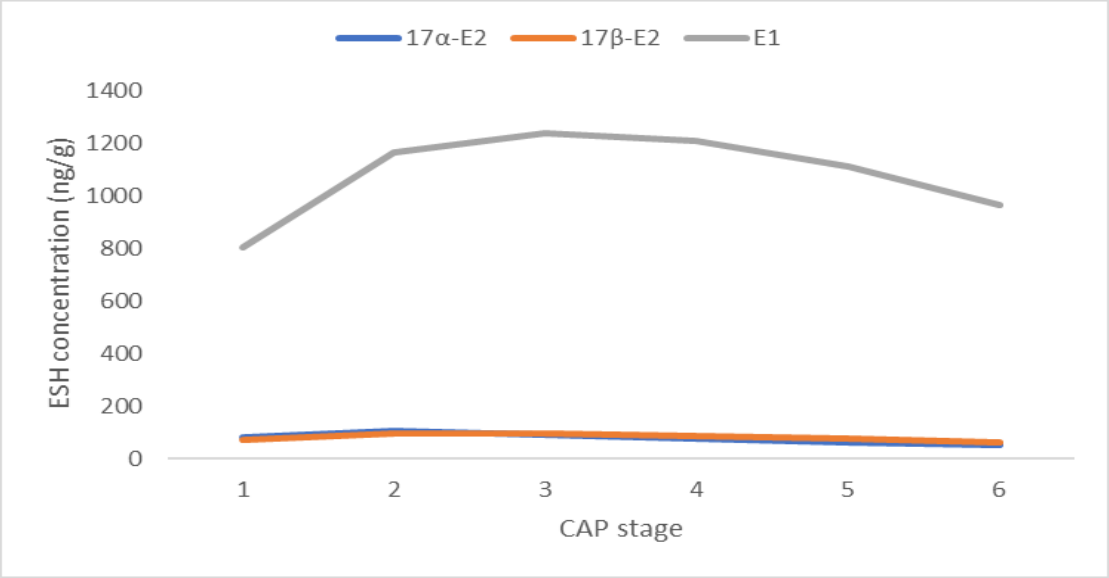

Figure 6-9: The fate of ESH in the CAP solid phase of the sludge over the simulation time and CAP stages

Table 6-16, Table 6-17, Table 6-18 and Table 6-19 present the CAP model ESH transformation variables using Equations 6-13 to 6-18.

Table 6-16: CAP model free and conjugated ESH species transformation variables (day^{-1}) – liquid dissolved phase

		Free ESH		
	ESH Species	**E1 (f, i=1)**	**17α-E2 (f, i=2)**	**17β-E2 (f, i=3)**
Free ESH	E1 (f, i=1)	0	0	0
	17α-E2 (f, i=2)	0.04071	0	0
	17β-E2 (f, i=3)	0.00535	0	0
Conjugated ESH	E1 (c, i=4)	0	0	0
	17α-E2 (c, i=5)	0.00085	0.000379355	0
	17β-E2 (c, i=6)	0.01749	0	0.02083
ESHs degradation coefficient	Kd	0.00954	0	0

[A] Based on the assumption that any solids within the effluent would settle into the sludge.

Table 6-17: CAP model free and conjugated ESH species transformation variables (day^{-1}) – liquid solid phase

		Free ESH		
	ESH Species	**E1 (f, i=1)**	**17α-E2 (f, i=2)**	**17β-E2 (f, i=3)**
Free ESH	E1 (f, i=1)	0	0	0
	17α-E2 (f, i=2)	0	0	0
	17β-E2 (f, i=3)	0.00617	0	0
Conjugated ESH	E1 (c, i=4)	0.01936	0	0
	17α-E2 (c, i=5)	0.01884	0.205	0
	17β-E2 (c, i=6)	0.01948	0	0.012
ESHs degradation coefficient	Kd	0	0	0

Table 6-18: CAP model free and conjugated ESH species transformation variables (day^{-1}) – sludge solid phase

		Free ESH		
	ESH Species	**E1 (f, i=1)**	**17α-E2 (f, i=2)**	**17β-E2 (f, i=3)**
Free ESH	E1 (f, i=1)	0	0	0
	17α-E2 (f, i=2)	0.01972	0	0
	17β-E2 (f, i=3)	0.00082	0	0
Conjugated ESH	E1 (c, i=4)	0.01513	0	0
	17α-E2 (c, i=5)	0.01830	0.01784	0
	17β-E2 (c, i=6)	0.01947	0	0.02178
ESHs degradation coefficient	Kd	0.00081	0	0

Table 6-19: CAP model free and conjugated ESH species transformation (day^{-1}) variables – sludge liquid phase

		Free ESH		
	ESH Species	**E1 (f, i=1)**	**17α-E2 (f, i=2)**	**17β-E2 (f, i=3)**
Free ESH	E1 (f, i=1)	0	0	0
	17α-E2 (f, i=2)	0.08299	0	0
	17β-E2 (f, i=3)	0.00260	0	0
Conjugated ESH	E1 (c, i=4)	0.23615	0	0
	17α-E2 (c, i=5)	0.01829	0.20298	0
	17β-E2 (c, i=6)	0.02659	0	0.00416
ESHs degradation coefficient	Kd	0.00055	0	0

Conversion of all free and conjugated ESHs to free E1 was predominant in all phases with the most rapid conversion rates in the sludge liquid phase (mean of 0.061 days^{-1}) and sludge solid phase (mean of 0.012 days^{-1}). ESH conversion rates in the liquid and solid

phases in the sludge were mostly similar except for the conversion of 17α-E2 to E1 which was faster in the solids phase compared to the liquid phase in the sludge. Free 17α-E2 to free E1 conversion rate in the liquid dissolved phase was dominant at 0.041 $days^{-1}$, compared to 0.083 and 0.020 $days^{-1}$ in the sludge liquid and solid phases. Conjugated ESH conversion to free ESH also occurred. The conjugated ESH conversion to free E1 was the dominant and rapid in the sludge liquid phase, following by a similar conversion rate in the liquid and sludge solid phases. Conversions of conjugated ESH to 17α-E2 and 17β-E2 were also observed in all phases at similar conversion rate which ranged from 0.0004 – 0.20 $days^{-1}$ (mean = 0.039 $days^{-1}$). Conjugated ESH conversion to free E1 can occur through direct deconjugation of conjugated E1 to free E1 at a rate of up to 0.236 $days^{-1}$ in the sludge liquid phase or through the conversion of free 17α-E2 and 17β-E2 (Chapters 2 and 3). As with the ESH conversion rate, the most rapid biological degradation rate occurred in the sludge liquid phase at 0.0055 $days^{-1}$ followed by in the liquid dissolved phase at 0.0095 $days^{-1}$. This suggests that the ESH conversion and biological degradation most commonly occurs in the sludge liquid phase.

6.3.2 Total seasonal DSE ESHs loads

The DSE volumetric flow and characteristics change over the year depending on the milking season, what is fed to the cows, rainfall, and wash water used by the farmer, and the biological activity will depend on the pond temperature which typically in CAP systems will depend on atmospheric, ground and incoming effluent temperatures. As shown in the previous section and in Chapters 2 and 3, these changes have a direct effect on the fate and removal performance of the ESHs in the CAP system. The daily DSE seasonal volume and ESHs loads are presented in Figure 6-10 and the monthly breakdown of the different free and conjugated ESH in the dissolved and solid phases are presented in Table 6-20.

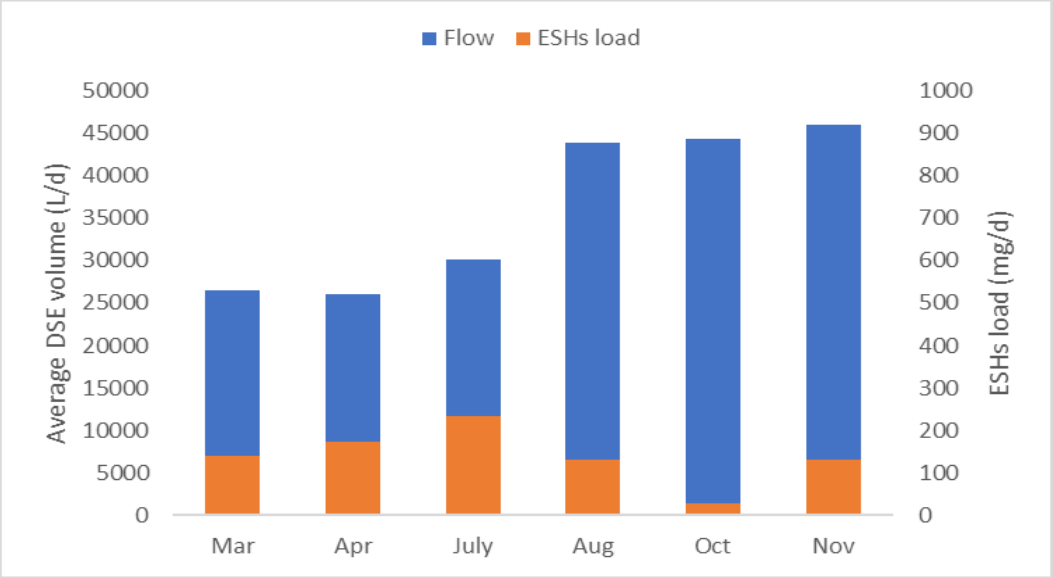

Figure 6-10: Actual seasonal DSE daily volume and total ESHs load

The highest total free and conjugated ESHs load in the DSE occurred during April and July (174 and 233 mg/d respectively) while the lowest loads during August, October and November (131, 28 and 131 mg/d respectively). The ESHs load variation correlates well to the DSE volumetric change occurring during the peak milking months (August – November), during which a large volume of water is used and dilution of the ESH may occur, and the late pregnancy of the milking cows and calving period (April – July) during which peak concentrations of ESHs in the faeces and urine of cows are excreted (Hoffmann *et al.*, 1997).

Table 6-20: Seasonal DSE ESHs load – model simulation input

	Mar	Apr	Jul	Aug	Oct	Nov
CAP Influent free dissolved ESHs (mg/day)						
17α-E2	42.3	74.3	31.9	10.6	1.26	0.99
17β-E2	6.12	6.27	3.24	0.64	0.31	0.69
E1	7.41	10.8	3.18	1.91	0.23	3.12
ΣESH	55.8	91.4	38.3	13.1	1.80	4.80
CAP Influent free solid ESHs (mg/day)						
17α-E2	56.8	55.9	145	66.5	7.74	8.47
17β-E2	11.2	6.79	13.3	6.38	4.57	8.64
E1	13.1	8.03	22.7	34.0	12.7	105
ΣESH	81.1	70.8	180	107	25.0	122
CAP Influent conjugated dissolved ESHs (mg/day)						
17α-E2	2.28	2.31	2.23	1.47	1.00	1.21
17β-E2	N.D	0.17	0.91	2.94	0.18	2.36
E1	N.D	3.55	N.D	N.D	0.31	0.31
ΣESH	2.28	6.03	3.14	4.40	1.49	3.88
CAP Influent conjugated solid ESHs (mg/day)						
17α-E2	0.54	5.01	7.23	4.36	N.D	0.62
17β-E2	N.D	1.22	1.72	1.70	N.D	N.D
E1	N.D	N.D	1.92	N.D	N.D	N.D
ΣESH	0.54	6.23	10.9	6.06	N.D	0.62

[A] Not detected

The contribution of the conjugated and free ESHs to the total ESHs load entering the CAP system is presented in Figure 6-11. On average, the total ΣESHs average load in the CAP influent was 140 mg/d, with 17α-E2 being the most dominant ESH with an average daily load of 88.3 mg/d following by E1 with a load of 38.1 mg/d. The conjugated ESHs constitute 5.45% of the total ESHs load entering the CAP system which equates to a load of 7.60 mg/d. This conjugated ESHs load cannot be disregarded as, if the conjugated ESHs are not converted to free ESHs and/or treated by the CAP, these highly water-soluble and mobile conjugated ESHs can readily reach surface and ground water where they can be potentially be transformed into the potent biologically active free form (Chapter 3).

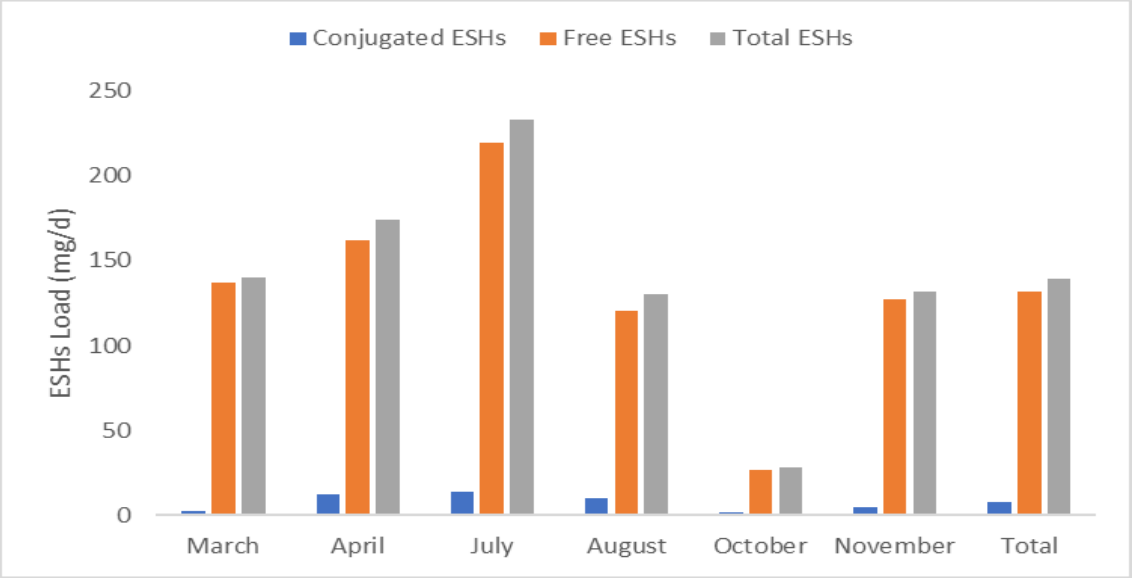

Figure 6-11:Modelled DSE conjugated and free ESHs loads

6.3.3 Performance assessment of the study farm CAP system to treat seasonal DSE ESHs with and without biochar – model output

The simulation of the farm CAP system was completed using the data presented in Section 6.2.6 and the model coefficients established during the calibration section.

6.3.3.1 CAP effluent

Presented in Table 6-21 and Table 22 are the CAP model simulation effluent results (concentration and load respectively) and the ESHs removal performance of the CAP system, both with and without biochar, throughout the milking season.

Table 6-21: Seasonal variation CAP modelled free and conjugated ESHs concentration in the dissolved and solid phase of the effluent and the ESHs removal performance of the CAP system, both with and without biochar, throughout the milking season.

		Free dissolved (ng/L)			Conjugated dissolved (ng/L)			Free solid (ng/g)			Conjugated solid (ng/g)		
		17α-E2	**17β-E2**	**E1**	**17α-E2**	**17β-E2**	**E1**	**17α-E2**	**17β-E2**	**E1**	**17α-E2**	**17β-E2**	**E1**
March	Effluent Model (no biochar)	316	137	1054	62.7	N.D[A]	N.D	104	75.4	618	0.34	N.D	N.D
	Effluent Model (with biochar)	26.1	71.0	116	63.0	N.D	N.D	163	87.8	901	0.31	N.D	N.D
April	Effluent Model (no biochar)	527	141	1796	63.5	1.29	95.5	131	62.8	794	3.77	0.84	N.D
	Effluent Model (with biochar)	30.3	73.5	140	63.7	1.31	95.9	260	79.1	1458	3.41	0.76	N.D
July	Effluent Model (no biochar)	252	75.1	635	55.9	7.65	N.D	256	89.2	1369	4.61	1.00	2.68
	Effluent Model (with biochar)	26.8	42.9	95.6	56.1	7.76	N.D	284	91.2	1451	4.29	0.93	2.51
Aug	Effluent Model (no biochar)	91.5	25.4	160	28.0	26.5	N.D	82.6	30.1	513	2.35	0.85	N.D
	Effluent Model (with biochar)	23.3	20.1	60.7	28.0	26.7	N.D	87.4	29.6	517	2.23	0.81	N.D
Oct	Effluent Model (no biochar)	10.5	6.02	19.0	18.6	1.56	5.79	11.4	24.0	147	N.D	N.D	N.D
	Effluent Model (with biochar)	7.43	3.45	14.6	18.7	1.57	5.81	11.1	22.9	136	N.D	N.D	N.D
Nov	Effluent Model (no biochar)	8.46	22.3	78.2	22.2	20.7	5.59	11.5	39.4	708	0.37	N.D	N.D
	Effluent Model (with biochar)	6.53	17.0	41.7	22.2	20.9	5.60	11.0	38.1	665	0.35	N.D	N.D
Average	Effluent Model (no biochar)	201	67.7	624	41.8	9.6	17.8	99.4	53.5	692	1.91	0.45	0.45
	Effluent Model (with biochar)	20.1	38.0	78.1	41.9	9.72	17.9	136	58.1	854	1.77	0.42	0.42

The modelled effluent concentrations of free ESHs, in the absence of biochar, were determined to be 892 ng/L. However, with the addition of biochar, this concentration decreased to 136 ng/L, indicating a significant reduction of 88.8 %. The concentrations of conjugated dissolved ESHs were found to be 69.2 ng/L without biochar and 69.5 ng/L with biochar, suggesting that the presence of biochar did not have a substantial impact on the conjugated ESHs in the dissolved phase. Similarly, the model predicted the concentrations of total conjugated ESH in the solids phase to be 2.80 ng/g without biochar and 2.60 ng/g with biochar, indicating a minimal effect of biochar on the conjugated ESHs in the solid phase. In contrast, the modelled concentrations of free ESHs in the solid phase were determined to be 854 ng/g without biochar and 1049 ng/g with biochar, revealing an increase of 18.6 % in the ESHs present in the solid phase when biochar was used. This observation implies that the presence of biochar facilitates the transfer of ESHs from the dissolved phase into the solid phase, which in turn enhances their removal by allowing for easier settling of the ESHs within the CAP system and/or subsequent treatment processes, such as the storage pond.

Table 6-22: Seasonal variation CAP modelled free and conjugated ESHs load (mg/d) in the dissolved and solid phase of the effluent and CAP ESHs removal performance with and without biochar

	Mar	Apr	July	Aug	Oct	Nov
	Dissolved Phase (Free and Conjugated ΣESHs)					
Effluent (no biochar)	40.7	67.4	30.3	14.2	2.69	7.11
Effluent (with biochar)	7.15	10.4	6.77	6.82	2.25	5.14
% Reduction (no biochar)	30.0	30.8	26.8	18.8	18.4	18.1
% Reduction (with biochar)	87.7	89.4	83.7	61.1	31.7	40.8
	Solid Phase (Free and Conjugated ΣESHs)					
Effluent (no biochar)	61.2	53.4	164	138	29.6	150
Effluent (with biochar)	100	114	197	152	30.8	155
% Reduction (no biochar)	25.0	30.6	14.3	-21.7[A]	-18.5	-22.2
% Reduction (with biochar)	-22.4	-48.5	-2.71	-34.1	-23.4	-26.8
	Combined Dissolved and Solid Phases (Free and Conjugated ΣESHs)					
Effluent (no biochar)	102	121	194	152	32.3	157
Effluent (with biochar)	107	125	203	158	33.1	161
% Reduction (no biochar)	27.1	30.7	16.5	-16.2	-14.2	-19.6
% Reduction (with biochar)	23.4	28.5	12.7	-21.3	-17.0	-22.3

Note: 500 mg/L of biochar was added to each month equated to biochar mass of 13.2 kg/d (March). 22.2 kg/d (Oct), 22.0 kg/d (Aug), 15.1 kg/d (July), 13.0 kg/d (April). [A] negative value indicating an increase.

The modelled seasonal average ESHs load in the CAP effluent differed between scenarios with and without biochar, measuring 126 mg/d (without biochar) and 131 mg/d (with biochar), respectively. The percentage reduction varied significantly throughout the season, ranging from -19.6 % to 30.7 % (without biochar) and -22.3 % to 28.5 % (with biochar). The daily loads of free and conjugated ESHs in the dissolved phase of the

effluent exhibited distinct patterns throughout the milking season, with and without biochar addition. In the absence of biochar, the highest daily free and conjugated ESHs loads in the dissolved phase of the effluent loads were observed during March, April, and July, ranging from 30.3 to 67.4 mg/d. Conversely, lower loads were recorded during August, October, and November, ranging from 2.69 to 14.2 mg/d, accompanied by ESHs reduction rates ranging from 18.1 % to 30.8 %. In comparison, when biochar was incorporated, the daily loads of free and conjugated ESHs in the dissolved phase were notably lower during March, April, and July and remained relatively consistent throughout the season, ranging from 2.25 to 10.4 mg/d. During these months, the use of biochar resulted in higher ESHs reduction rates, ranging from 83.7 % to 89.4 %. However, during August, October, and November, the removal performance was comparatively lower, ranging from 31.7 % to 61.1 % when biochar was employed.

The enhanced removal performance of free and conjugated ESHs in the dissolved phase of the effluent, observed when biochar was introduced into the CAP system, can be attributed to the improved adsorption of ESHs onto the biochar-enriched solid phase of the effluent (Chapter 5) and subsequent settling into the sludge. This conclusion is supported by the increased loads of free and conjugated ESHs, as well as the reduced removal performance, observed in the solid phase of the effluent when biochar was added to the influent, compared to the non-biochar dosed influent. The decrease in removal performance during the months of August, October, and November can be attributed to the higher influent flow rates (Figure 6-10) and the accumulation of sludge that typically occurs during this period. The study farm typically carried out sludge removal during the months of February to April each year, removing approximately 450 m^3 of the sludge and effluent mixture. The study farm's CAP system is characterised by a relatively shallow depth of 3.75 m. Due to the rapid accumulation of sludge calculated as 479 m^3/yr (Table 6-7), and the infrequent removal of sludge, which occurs approximately once a year, the sludge level within the CAP system is expected to increase over time, particularly during the months further away from the desludging event. The increased height of the sludge layer during the months further away from the desludging event contributed to the occurrence of short-circuiting, whereby the influent preferentially flowed across the upper surface of the CAP towards the outlet. This flow of fresh influent along the upper surface of the CAP resulted in disturbance and mixing with the upper layer of settling and

unconsolidated pond sludge. Consequently, the effluent discharged from the CAP outlet after April represented a mixture of fresh influent and the upper layer of accumulated pond sludge. This conclusion is supported by the observed increase in the concentration and proportion of E1 in the solids phase of the CAP effluent compared to the influent samples, specifically after April (Table 6-21 and Chapter 2).

6.3.3.2 CAP sludge

Table 6-23 provides the modelled output data of the loads of free and conjugated ESHs in both the dissolved and solid phases of the sludge, with and without biochar, after it is simulated to be removed annually from the CAP system and subsequently applied to land.

Table 6-23: CAP modelled free and conjugated ESHs mass (mg) in the dissolved and solid phase of the sludge with (500 mg/L) and without biochar

	17α-E2	**17β-E2**	**E1**	**ΣESH**
		Dissolved Phase Free ESH		
Sludge (no biochar)	2.87	5.00	73.7	81.6
Sludge (with biochar)	0.44	3.17	15.7	19.3
		Dissolved Phase Conjugated ESH		
Sludge (no biochar)	0.14	0.44	0.03	0.61
Sludge (with biochar)	0.16	0.47	0.04	0.67
		Solid Phase Free ESH		
Sludge (no biochar)	900	872	12698	14471
Sludge (with biochar)	1343	1044	16716	19103
		Solid Phase Conjugated ESH		
Sludge (no biochar)	16.3	3.79	5.07	25.17
Sludge (with biochar)	17.5	4.04	5.42	27.0
		Total (Dissolved and Solid Phases) Free and Conjugated ESH		
Sludge (no biochar)	919	882	12777	14578
Sludge (with biochar)	1361	1052	16737	19150

As anticipated, the predominant ESH found in the sludge is E1. A significant portion (approximately 99 %) of the ESHs are present in the solid phase, primarily as free ESHs. The introduction of biochar into the system led to a substantial reduction (76 %) in the concentration of free ESHs in the dissolved phase, while the levels of dissolved phase conjugated ESHs remained consistent. The reduction in free ESHs in the dissolved phase resulted in a corresponding increase in the concentration of free ESHs in the solid phase of the sludge.

In terms of total ESHs content, the sludge without biochar contained a mass of 14,578 mg of free and conjugated ESHs in the dissolved and solid phases, whereas the sludge with biochar had a total mass of 19,150 mg. Considering the annual volume of sludge removal, which amounted to 479 m^3 (Table 6-7), the concentrations of total ESHs in the sludge

were calculated to be 30.4 mg/m^3 and 40.0 mg/m^3 for the scenarios without biochar and with biochar, respectively.

As previously discussed, the inclusion of biochar in the system has a positive impact on ESHs removal from the liquid phase of the CAP, facilitating faster settling of ESHs into the sludge, as evidenced by the model results. Once the ESHs are retained within the sludge, they are more likely to undergo degradation or remain within the sludge until it is eventually removed from the CAP system. Consequently, the addition of biochar will allow the CAP effluent to contain less ESHs load when applied to the pasture. However, the fate of the ESHs-rich sludge and biochar mixture when applied to land remains uncertain. It is possible that the ESHs adsorbed onto the sludge and biochar mixture could undergo biological degradation (Mansell *et al*., 2004; Ying & Kookana, 2005) or be retained through adsorption processes (Casey *et al*., 2003; Mansell *et al*., 2004; Sarmah *et al*., 2008; Ying & Kookana, 2005). Nevertheless, these hypotheses require further investigation to provide conclusive evidence. It may be possible that the ESHs-rich sludge and biochar mixture be required to undergo further treatment before applying it to pasture. Cost benefit analysis would be required to find the most suitable sludge ESHs treatment to suit the farm environment (information regarding the use of anaerobic digestion in conjunction with a pyrolysis system is presented in the appendices, Section 7.2A.26)

6.3.3.3 Estrogenicity

Table 6-24 provides a summary of the estimated estrogenic activity, calculated based on the daily average load, for the free ΣESHs in the dissolved and solid phases of the CAP influent, effluent, and sludge, both with and without biochar.

Table 6-24: Modelled seasonal and mean estogenicity (expressed as estrogenic equivalents) of free ΣESHs in dissolved and solid phases

	Mar	Apr	July	Aug	Oct	Nov	Mean
Dissolved and Solid Phases							
Influent	18.7	14.7	18.8	8.51	5.23	11.6	12.9
Effluent (no biochar)	11.0	8.97	14.0	10.3	4.67	11.7	10.1
Effluent (with biochar)	11.2	9.00	14.5	10.6	4.83	12.0	10.4
Sludge (no biochar)	3.85	2.34	5.46	2.79	1.25	3.09	3.13
Sludge (with biochar)	5.22	3.87	6.03	2.97	1.33	3.24	3.78
Effluent vs Influent							
% Reduction (no biochar)	41.4	39.1	25.5	-20.5[A]	10.7	-0.82	15.9
% Reduction (with biochar)	40.1	38.9	22.8	-24.8	7.57	-3.70	13.5
Effluent + Sludge vs Influent							
% Reduction (no biochar)	20.9	23.3	-3.48	-53.3	-13.3	-27.5	-8.90
% Reduction (with biochar)	12.3	12.6	-10.7	-59.8	-17.9	-31.6	-15.9

[A] negative value indicating an increase

The calculated estrogenic activity displays an average estrogenicity reduction of 15.9 % in the CAP effluent compared to the influent when biochar was not used, and a slightly lower reduction of 13.5 % when biochar was present. However, when considering the combined estrogenicity of the effluent and sludge, the average reduction was -8.90 % without biochar and -15.9 % with biochar. The results demonstrate that the CAP system, regardless of the presence of biochar, plays a significant role in reducing estrogenic activity in the effluent of dairy wastewater, indicating its potential as an effective treatment method for mitigating the presence of estrogenic substances. However, when considering the estrogenic activity of the sludge, the overall reduction in estrogenicity by the CAP system is compromised due to the higher load of ESHs in the sludge, particularly E1, which exhibits greater estrogenic potency compared to 17α-E2 (Noguera-Oviedo and Aga, 2016). These findings highlight the need for further investigation to address the challenges associated with ESHs in the sludge.

6.3.4 Improved CAP system and operation – model output

In order to optimise the ESHs removal performance of the CAP system, it is crucial to ensure an adequate retention time that can accommodate the hydraulic load during peak milking months, specifically from August to November. This extended retention time allows sufficient opportunity for the absorbed ESHs to settle into the sludge where biological degradation is enhanced. The introduction of biochar into the CAP system offers the potential to enhance ESHs capture and settle-out rates, thereby reducing transfer time and potentially decreasing the required pond size and overall cost. Additionally, periodic removal of the sludge is essential to prevent short circuiting and the carry-over of sludge towards the outlet of the CAP. Monitoring the TS concentration in the effluent

can serve as an indicator for determining the appropriate timing for sludge removal. If the TS concentration shows a continuous increase, it suggests that sludge removal from the CAP system is necessary to maintain optimal performance.

Table 6-25 showcases the performance evaluation of an enhanced CAP system designed to facilitate improved ESHs removal. This enhanced system incorporates an increased CAP volume and depth of 2000 m^3 and 5 m respectively, which enables a higher retention time without the likelihood of sludge carry-over towards the CAP outlet. The table presents key performance indicators, such as ESHs removal efficiency and concentrations in the effluent and sludge, with and without the addition of biochar, for comparison between the improved CAP system and the study farm CAP system.

Table 6-25: Improved CAP system (volume = 2000 m^3 and depth of 5 m) effluent and sludge ESHs loads and performance data

	Effluent Total ESHs (mg/d)	Sludge Total ESHs (mg/d)	Removal Effluent vs Influent (%)	Removal Effluent+ Sludge vs Influent (%)	Estrogenicity reduction Effluent vs Influent (%)	Estrogenicity reduction Effluent+sludge vs Influent (%)
Modified CAP size and depth (no biochar)	44.7	57.0	67.9	26.2	70.4	33.1
Modified CAP size and depth (with biochar)	36.6	74.0	73.0	20.9	73.5	29.9

The implementation of the improved CAP system resulted in significant reductions in the total ESHs load of the study farm modelled effluent. Compared to the CAP of the study farm, the improved CAP system demonstrated decreased ESHs loads of 44.7 mg/d (no biochar) and 36.6 mg/d (with biochar), corresponding to ESHs concentrations of 1.31 ng/L and 1.06 ng/L based on an annual average daily volume of 34,311 L/d (Table 6-3). These concentrations align with the predicted no effect concentrations (PNECs) for steroid hormones which specify 17β- E2 short-term fish reproduction impacts of 2 ng/L, and for E1 of 6 ng/L (Caldwell *et al*., 2012) and short-term exposure of combined risk of E1, 17β-E2, 17α-ethinyl estradiol (17α-EE) and E3 expressed as 17β-E2 equivalents, in the order of 5 ng/L, while the long-term exposure rate was 2 ng/L (Anderson *et al*., 2012).

As expected, the modelled sludge in the improved CAP system exhibited higher ESHs concentrations, with an annual mass of 20,805 mg and a concentration of 43.4 mg/m3 (considering an annual volume of sludge removal of 479 m^3), while the sludge with biochar had a total mass of 27,010 mg and a concentration of 56.4 mg/m^3. These ESHs masses and concentrations are higher than the corresponding values of 14,578 mg and 30.4 mg/m^3 (no biochar) and 19,150 mg and 40.0 mg/m^3 (with biochar) observed in the modelled output of the study farm CAP system. This indicates improved settling of ESHs to the sludge. Furthermore, the improved CAP system demonstrated enhanced removal performance, with effluent vs influent removal percentages increasing from 4.05 % (no biochar) and 0.67 % (with biochar) in the study farm CAP system to 67.9 % and 73.0 % respectively in the improved CAP system. Similarly, the estrogenicity reduction also improved, increasing from 15.9 % (no biochar) and 13.5 % (with biochar) to 70.4% and 73.5 % respectively.

6.3.5 Limitations

The calibration data used in this study assumes a constant volumetric flow into the CAP pond, influent concentration, microbial activity, and plug flow throughout the year. In reality, these parameters can vary depending on factors such as the milking season, feed composition, rainfall, and wash water usage by the farmer. Additionally, the methanogenic activity in the pond is influenced by the temperature, which in turn depends on atmospheric, ground, and incoming effluent temperatures. These variations were not accounted for in the model. The effects of these parameters could be explored in the laboratory, but the size of equipment would be driven by the volume of liquid sample (1-2 L) required each time to be able to detect the ESHs, potentially requiring a 60 L reactor (assuming a residence time of 30-60 days) needing daily feeding using a substrate with controlled ESH concentrations (assuming the ESH concentrations are kept in a similar range to that observed in Chapter 2).

Another limitation is that the model does not consider the stratification of the sludge into different layers, such as a denser ash-rich layer and a less dense VS rich phase. Previous research by Fyfe et al. (2016) has shown that methanogenic activity is highest in the VS-rich phase. This aspect was not incorporated into the model, potentially impacting the accuracy of the results. The ESHs might be present in higher concentrations in the VS

rich phase compared to the ash-rich phase. This could be explored further in a laboratory set up that allowed selective sampling of the different layers of sludge.

Furthermore, Fyfe et al. (2016) observed that the flow in the pond tended to circulate around the outer perimeter, leading to slightly higher sludge height in that region. This phenomenon could be attributed to the location and orientation of the inlet pipes. However, flow hydraulics were not considered in the model due to the pond being covered, making it difficult to determine. Using a tracer method could provide information on hydraulics through mean residence time and tracer profile, however the long residence time of the liquid (up to 60 days) made it impractical to measure using this approach. The flow hydraulics could also impact on the distribution of solids and ESHs in the sludge, with the ESHs predominantly being present around the outer perimeter of the pond where the solids have settled first. Similarly, the impact of jetting, mixing, and sediment movement within the CAP on ESH concentrations across its spatial dimensions, encompassing length, breadth, and depth is unkown. This impact could not be established as the collection of samples is hindered by the restricted availability of suitable locations for sampling within the CAP. This limitation poses a challenge to the comprehensive assessment of ESHs distribution patterns in relation to the specified hydrodynamic processes.

Additionally, limitation associate in elucidating the anaerobic biochemical pathway responsible for the degradation of ESHs and experimentally quantifying the rates of degradation. This work is rendered challenging due to the necessity of collecting substantial sample sizes and the time-intensive nature of sample analysis.

An additional limitation of the study is the assumption that the ESHs adsorbed onto the powdered biochar in the sump would remain adsorbed throughout their retention in the CAP system. To validate this assumption, a desorption trial should be conducted under anaerobic conditions, simulating the actual conditions within the CAP system, for a duration of up to 60 days. This trial would provide valuable insights into the stability of ESHs adsorption onto biochar and assess the potential for desorption and re-release of these substances over time. By investigating the long-term behaviour of ESHs adsorption onto biochar, the reliability and effectiveness of using biochar as an adsorbent in the CAP

system could be better understood. This would also enable a better understanding of the the rates of conversion of the ESHs to E1 in the biochar compared to in the sludge.

6.3.6 Conclusions

- The calibration results of the CAP model demonstrated a high level of accuracy, with R^2 values ranging from 98.4% to 100% for the solids and ESHs datasets. These findings indicate that the CAP model is capable of effectively simulating the fate and removal performance of ESHs in a CAP DSE treatment system.
- The total free and conjugated ESHs load in the DSE showed variations throughout the year, with the highest loads observed in April and July (174 and 233 mg/d), and the lowest loads in August, October, and November (131, 28, and 131 mg/d). These variations align with changes in DSE volume, influenced by milking activity and cow pregnancy. Furthermore, the conjugated ESHs accounted for 5.45 % of the total DSE ESHs load, equivalent to 7.60 mg/d.
- The addition of biochar to the modelled study farm CAP system significantly reduced the concentration of free ESHs in the dissolved phase of the effluent by 88.8 %, from 892 ng/L to 136 ng/L. However, the presence of biochar had a minimal impact on the concentrations of conjugated ESHs in the dissolved and solid phases. In contrast, the concentrations of free ESHs in the solid phase of the effluent increased by 18.6 % when biochar was used, with values of 854 ng/g without biochar and 1049 ng/g with biochar.
- The sludge without biochar contained 14,578 mg of total ESHs, while the sludge with biochar had 19,150 mg. With an annual sludge removal volume of 479 m^3, the corresponding concentrations of total ESHs were 30.4 mg/m^3 (without biochar) and 40.0 mg/m^3 (with biochar).
- Biochar promotes ESHs removal from the dissolved phase to the solid phase, enabling the ESHs to settle within the CAP system, and potentially be removed in subsequent treatment processes.
- The decreased CAP ESHs removal performance is influenced by higher influent flow rates and sludge accumulation. The infrequent removal of sludge and shallow depth of the CAP system contribute to sludge level increase leading to short-circuiting and mixing of fresh influent with the upper layer of pond sludge.

Chapter 6: The efficacy of a dairy farm based covered anaerobic pond (CAP) treatment system dosed with powdered biochar to transform and remove estrogenic steroid hormones.

- Increasing the CAP volume and depth allowed for higher retention time and reduced sludge carry-over and resulted in a 19 % reduction in the total ESHs load of the effluent, with concentrations of 1.31 ng/L (no biochar) and 1.06 ng/L (with biochar). The improved CAP system demonstrated enhanced removal performance, with effluent vs influent removal percentages increasing to 67.9 % and 73.0 %, and estrogenicity reduction improving to 70.4 % and 73.5 % respectively.
- Further investigation is needed to determine the hydraulic conditions within the CAP system as well if the ESHs adsorbed onto the sludge and biochar mixture undergo biological degradation or conversion, and remain adsorbed within the CAP system and/or in sludge when applied to land.

Chapter 7:
Conclusions and Recommendations

This chapter presents the overall conclusions with respect to the objectives of the research as well as presenting recommendations for future research.

7.1 Conclusions

- This study provides new insights and perspectives on the treatment performance and fate of estrogenic steroid hormones (ESHs) in a covered anaerobic pond (CAP) dairy farm effluent treatment system by measuring the concentration of free and conjugated ESHs in the influent, sludge and effluent in both dissolved and solid phases over nine months. It also provides the results of a novel research and design tool for treating dairy shed effluent (DSE) ESHs by using powdered biochar and establishing a CAP treatment system model. The use of biochar and the developed model offer promising approaches to address the environmental challenges associated with the ESHs.
- Previous studies investigating the fate and concentration of ESHs in DSE treatment systems have focussed mainly on the dissolved phase and ignored the sludge and the solid phase. By doing so these studies have ignored a substantive source of, and sink for, ESHs within DSE treatment systems. This study confirmed the hypothesis that excluding the contribution of ESHs in the solid phase of DSE treatment systems overestimates the system's efficacy in removing ESHs. The exclusion of sludge and the solid phase significantly underestimates the concentration of ESHs in DSE treatment systems, and therefore, the mass of these endocrine disrupting chemicals being discharged to land via sludge and effluent re-use.

- This study assessed and validated the performance of a new commercial enzyme reagent (BGS™) to deconjugate sulphate and glucuronide ESH conjugates in samples from a DSE treatment system, for analysis by GC-MS. Optimal performance of a new commercial enzyme for deconjugation was achieved using a BGS™ recombinant enzyme volume of 100 µL, incubating at 53°C for 45 minutes. Recoveries were similar to the *H. pomatia* glucuronidase enzyme

commonly used to analyse conjugated ESHs in animal waste. However, it was necessary to reverse the commonly used sequence of solvolysis followed by enzymatic hydrolysis because of the influence of residual acidity from solvolysis upon the BGS™ enzyme.

- The total free and conjugated ESHs concentration and load in the DSE showed variations throughout the year, with the highest concentration and daily loads observed in April and July (7707 and 7718 ng/L and 174 and 233 mg/d respectively), and the lowest concentration and loads in August, October, and November (2460, 741 and 2595 ng/L and 131, 28, and 131 mg/d respectively). These variations align with changes in DSE volume, influenced by milking activity and cow pregnancy. The annual mean free and conjugated ESHs concentration and daily load were 4420 ng/L and 116 mg/d, while the conjugated ESHs accounted for 5.45 % of the total DSE load, equivalent to 7.60 mg/d and concentration of 251 ng/L.
- Conjugated ESHs were found in both dissolved and solid phases of the CAP effluent and sludge, indicating their persistence and potential to reach surface and groundwater when agricultural waste and effluent is applied to land due to their preferential partitioning into aqueous solutions. Ignoring the significance and fate of conjugated ESHs within DSE and dairy effluent treatment systems can result in underestimating the performance of the treatment system in removing ESHs and the potential impact of this agricultural waste stream on the environment upon recycling to pasture as these compounds are significantly more mobile than their corresponding free forms and can contaminate surface and groundwater when agricultural waste and effluent is applied to land.
- CAP treatment reduces the contribution of certain ESHs to overall estrogenicity while increasing others. 17α-E2 is transformed to the more persistent E1 in the CAP decreasing the estrogenicity of the CAP sludge and effluent. However, regardless of the conversion of 17α-E2 to E1, the overall estrogenicity calculated for the effluent of sludge samples is dominated by the presence of 17β-E2.
- Powdered biochar derived from radiata pine woodchip (pyrolysed at a temperature of approximately 750 °C) added at a mass of 1 mg per litre, demonstrates high (84 - 99 %) removal of the targeted 17α-E2, 17β-E2, and E1 from aqueous solutions within 6 hours.

- Powdered biochar with a mass range of 100 to 1000 mg was added to a litre of DSE resulting in the removal of up to 96 % of 17α-E2, 65 % of 17β-E2, 78 % of E1, and 91 % of total ESHs, through adsorption. The Modified Freundlich Isotherm, using two coupled Freundlich equations, provided the best fit (R^2 = 0.60 - 0.99 %) for modelling the adsorption of ESHs to powdered biochar. This suggested that a significant interaction between the dissolved organic content and the ESHs is occurring, primarily due to the higher concentration of dissolved organic matter compared to the powdered biochar and the strong affinity of ESHs for organic matter. Despite this strong interaction, the adsorption of ESHs to the powdered biochar was favoured over the adsorption to the dissolved organic matter present in the dairy shed effluent. Specifically, at lower concentrations, only 17β-E2 showed a tendency initially to associate with organic matter and subsequently adsorb to the powdered biochar. In contrast, 17α-E2 and E1 were more likely to adsorb directly to the powdered biochar rather than associating with the organic matter in the dairy shed effluent.
- A model was built to simulate the performance of the CAP in removing ESHs and better understand the fate of the ESHs in the covered anaerobic system. The calibration results of the CAP model demonstrated a high level of accuracy, with R^2 values ranging from 98.4 % to 100 % for the solids and ESHs datasets. These findings indicate that a CAP model can accurately simulate the fate and removal of ESHs.
- Model simulations show the addition of biochar to the system effectively facilitated the removal of the ESHs from the dissolved phase to the solid phase, causing them to settle into the sludge. This resulted in a significant decrease of 76 % in the concentration of free ESHs in the dissolved phase, while the levels of dissolved phase conjugated ESHs remained unchanged. Consequently, the reduction of free ESHs in the dissolved phase led to a proportional increase in the concentration of free ESHs in the solid phase of the sludge. Comparatively, the sludge without biochar contained a total of 14,578 mg of ESHs, whereas the sludge with biochar contained 19,150 mg. Considering an annual sludge removal volume of 479 m^3, the corresponding concentrations of total ESHs were measured at 30.4 mg/m^3 without biochar and 40.0 mg/m^3 with biochar.
- Model simulations also showed operational factors, such as flow rates and sludge accumulation, affected the ESH removal performance of the CAP system and

therefore the estrogenicity of the effluent and sludge. Increasing the volume and depth of the CAP improved removal efficiency and estrogenicity reduction. Increasing the CAP volume and depth allowed for higher retention time and reduced sludge carry-over and resulted in a 19 % reduction in the total ESHs load of the effluent, with concentrations of 1.31 ng/L (no biochar) and 1.06 ng/L (with biochar). The improved CAP system modelled enhanced removal performance, with effluent versus influent removal percentages increasing to 67.9 % and 73.0 %, and estrogenicity reduction improving to 70.4 % and 73.5 % without and with the use of the biochar respectively.

- This study highlights the need for careful design and operation of DSE treatment systems to address ESH contamination and potency.

7.2 Recommendations for future research

- The difficulty of analysing free and conjugated ESHs in complex matrices such as DSE has contributed to the limited number of studies investigating their fate within animal wastes and treatment systems. The use of GC-MS for analysing free and conjugated ESHs is limited due to challenges associated with the costly, complex and laborious multi-step cleaning, extraction and deconjugation process. In terms of conjugated ESHs, LC-MS-MS offers the advantage of directly analysing the different forms of conjugated ESHs, eliminating the need for deconjugation and derivatisation procedures, and allowing simultaneous analysis of free and conjugated ESHs and therefore it is the preferred method for future analysis of ESHs.
- Adsorption of organic contaminants and ESHs within raw municipal and/or agricultural wastewater is not a common treatment method. Adsorption is typically used as a polishing step to ensure maximum adsorption and cost effectiveness. However, in the dairy agricultural environment, dosing DSE with biochar can have many benefits, particularly before it enters the anaerobic digestion system. These benefits might include, improved anaerobic digestion treatment performance, including biogas production and, when the effluent and sludge containing biochar are applied to land, improved soil properties, increased crop yields and reduced greenhouse gas emissions. All these benefits, in addition to ESHs removal capabilities, make the use of biochar in the dairy farm effluent treatment system an attractive option. Further research is required to determine

the impact of adding biochar to a dairy farm effluent anaerobic digestion system on methane generation.

- Assumption of constant values for volumetric flow, influent concentration, microbial activity, and plug flow throughout the year were used in the calibration process of the CAP model. In reality, these parameters can vary due to factors like milking season, feed composition, rainfall, and wash water usage. Furthermore, the methanogenic activity in the pond is influenced by temperature, which depends on atmospheric, ground, and incoming effluent temperatures. These variations were not considered in the model. While the effects of these parameters could be explored in the laboratory, it would require large-scale equipment due to the volume of liquid sample (1-2 L) needed to detect the ESHs. This could potentially necessitate a 60 L reactor with daily feeding using a substrate containing controlled ESH concentrations, assuming they are within a similar range as observed in Chapter 2.
- The CAP model used in this study did not account for flow hydraulics, as the pond was covered, making it challenging to determine. While a tracer method could potentially provide information on hydraulics through mean residence time and tracer profile, the long residence time of the liquid (up to 60 days) made it impractical to measure using this approach. The flow hydraulics could also have an impact on the distribution of solids and ESHs in the sludge, with the ESHs primarily found where the solids have settled.
- This study assumed that the ESHs adsorbed onto the powdered biochar in the sump would remain adsorbed throughout their retention in the CAP system. To confirm the validity of this assumption, it is recommended to conduct a desorption trial under anaerobic conditions, mimicking the actual conditions within the CAP system, for a duration of up to 60 days. This trial would yield valuable insights into the stability of ESHs adsorption onto biochar and assess the potential for desorption and subsequent release of these substances over time. By investigating the long-term behaviour of ESHs adsorption onto biochar, a better understanding of the reliability and effectiveness of using biochar as an adsorbent in the CAP system can be gained. Additionally, it would provide insights into the conversion of ESHs to E1 while sorbed to the biochar compared to the sludge, further enhancing the comprehension of the overall process.

- This study focussed primarily on the adsorption capacity of the sludge and biochar and its potential use as an ESH sink in the anaerobic treatment system. However, the fate and behaviour of ESHs adsorbed onto the sludge and biochar mixture in terms of biological degradation, remain unexplored. To address this limitation, further research should be conducted to determine the extent of biological degradation and adsorption processes for ESHs adsorbed onto the sludge and biochar mixture under anaerobic conditions. This can be achieved through controlled laboratory experiments or pilot-scale studies that simulate the anaerobic conditions of the treatment system. By investigating the biological degradation of ESHs in the sludge-biochar mixture, a comprehensive understanding of the overall fate and removal mechanisms can be obtained.

References

Activated Carbon Technologies, 2022. Powdered Activated Carbon. http://www.activatedcarbon.co.nz/pac.htm.

Adeel, M., Song, X., Wang, Y., Francis, D., Yang, Y., 2017. Environmental impact of estrogens on human, animal and plant life: A critical review. Environment International 99, 107-119.

Agegnehu, G., Srivastava, A.K., Bird, M.I., 2017. The role of biochar and biochar-compost in improving soil quality and crop performance: A review. Applied Soil Ecology 119, 156-170.

Ahmad, M., Rajapaksha, A.U., Lim, J.E., Zhang, M., Bolan, N., Mohan, D., Vithanage, M., Lee, S.S., Ok, Y.S., 2014. Biochar as a sorbent for contaminant management in soil and water: A review. Chemosphere 99, 19-23.

Ahmed, M.B., Zhou, J.L., Huu Hao, N., Wenshan, G., 2016. Insight into biochar properties and its cost analysis. Biomass and Bioenergy 84, 76-86.

Ahmed, M.B., Zhou, J.L., Ngo, H.H., Guo, W., Thomaidis, N.S., Xu, J., 2017. Progress in the biological and chemical treatment technologies for emerging contaminant removal from wastewater: A critical review. J Hazard Mater 323(Pt A), 274-298.

Ahmed, M.B., Zhou, J.L., Ngo, H.H., Johir, M.A.H., Sornalingam, K., 2018. Sorptive removal of phenolic endocrine disruptors by functionalized biochar: Competitive interaction mechanism, removal efficacy and application in wastewater. Chemical engineering journal (Lausanne, Switzerland : 1996) 335, 801-811.

Alizadeh, S., Prasher, S.O., ElSayed, E., Qi, Z., Patel, R.M., 2018. Effect of biochar on fate and transport of manure-borne estrogens in sandy soil. Journal of Environmental Sciences (China) 73, 162-176.

Allen, E., Francis, B.F., Robertson, L.L., Colgate, C.E., Johnston, C.G., Doisy, E.A., Kountz, W.B., Gibson, H.V., 1924. The hormone of the ovarian follicle; its localization and action in test animals, and additional points bearing upon the internal secretion of the ovary. Developmental Dynamics 34(1), 133-181.

Alvarez, D.A., Shappell, N.W., Billey, L.O., Bermudez, D.S., Wilson, V.S., Kolpin, D.W., Perkins, S.D., Evans, N., Foreman, W.T., Gray, J.L., Shipitalo, M.J., Meyer, M.T., 2013. Bioassay of estrogenicity and chemical analyses of estrogens in streams across the United States associated with livestock operations. Water Research 47(10), 3347-3363.

Andaluri, G., Suri, R.P.S., Kumar, K., 2012. Occurrence of estrogen hormones in biosolids, animal manure and mushroom compost. Environmental Monitoring and Assessment 184(2), 1197-1205.

Anderson, P.D., Johnson, A.C., Pfeiffer, D., Caldwell, D.J., Hannah, R., Mastrocco, F., Sumpter, J.P., Williams, R.J., 2012. Endocrine disruption due to estrogens derived from humans predicted to be low in the majority of U.S. surface waters. Environmental Toxicology and Chemistry 31(6), 1407-1415.

Arnon, S., Dahan, O., Elhanany, S., Cohen, K., Pankratov, I., Gross, A., Ronen, Z., Baram, S., Shore, L.S., 2008. Transport of testosterone and estrogen from dairy-farm waste lagoons to groundwater. Environmental Science and Technology 42(15), 5521-5526.

Bai, X., Casey, F.X.M., Hakk, H., DeSutter, T.M., Oduor, P.G., Khan, E., 2013. Dissipation and transformation of 17β-estradiol-17-sulfate in soil–water systems. Journal of Hazardous Materials 260, 733-739.

Ballingall, J., Pambudi, D., 2017. Dairy Trade's Economic Contribution to New Zealand. NZIER report to DCANZ. New Zealand Institute of Economic Research, Wellington, New Zealand.

Barber, L.B., Brown, G.K., Nettesheim, T.G., Murphy, E.W., Bartell, S.E., Schoenfuss, H.L., 2011. Effects of biologically-active chemical mixtures on fish in a wastewater-impacted urban stream. Science of the Total Environment 409(22), 4720-4728.

Benoff, S., Auborn, K., Marmar, J.L., Hurley, I.R., 2008. Link between low-dose environmentally relevant cadmium exposures and asthenozoospermia in a rat model. Fertility and Sterility 89(2, Supplement), e73-e79.

Ben, W., Zhu, B., Yuan, X., Zhang, Y., Yang, M., Qiang, Z., 2017. Transformation and fate of natural estrogens and their conjugates in wastewater treatment plants: Influence of operational parameters and removal pathways. Water Research 124, 244-250.

Bergman, A., Heindel, J. J., Jobling, S., Kidd, K. A., & Zoeller, R. T. (Eds.) 2013. State of the Science of Endocrine Disrupting Chemicals - 2012. World Health Organization.

Bhardwaj, P., Au, C.C., Benito-Martin, A., Ladumor, H., Oshchepkova, S., Moges, R., Brown, K.A., 2019. Estrogens and breast cancer: Mechanisms involved in obesity-related development, growth and progression. The Journal of Steroid Biochemistry and Molecular Biology 189, 161-170.

Birkett, J.W., 2003a. Scope of the Problem. Birkett, J.W., Lester, J.N. (Eds.), Endocrine Disrupters in Wasrewater and Sludge Treatment Processes. IWA, Boca Raton, FL, pp. 1-34.

Birkett, J.W., 2003b. Sources of Endocrine Disrupters. Birkett, J.W., Lester, J.N. (Eds.), Endocrine Disrupters in Wastewater and Sludge Treatment Processes. IWA, Boca Raton, FL, pp. 35-57.

Bolan, N.S., Laurenson, S., Luo, J., Sukias, J., 2009. Integrated treatment of farm effluents in New Zealand's dairy operations. Bioresource Technology 100(22), 5490-5497.

Bonin, J.L., Simpson, M.J., 2007. Sorption of steroid estrogens to soil and soil constituents in single- and multi-sorbate systems. Environmental Toxicology and Chemistry 26(12), 2604-2610.

Bonvin, F., Jost, L., Randin, L., Bonvin, E., Kohn, T., 2016. Super-fine powdered activated carbon (SPAC) for efficient removal of micropollutants from wastewater treatment plant effluent. Water research (Oxford) 90, 90-99.

Borch, J., Ladefoged, O., Hass, U., Vinggaard, A.M., 2004. Steroidogenesis in fetal male rats is reduced by DEHP and DINP, but endocrine effects of DEHP are not modulated by DEHA in fetal, prepubertal and adult male rats. Reproductive Toxicology 18(1), 53-61.

Bridges, R., 2013. Design and characterisation of an 'open source' pyrolyser for biochar production : a thesis presented in partial fulfilment of the requirements for the degree of Master of Engineering in Chemical and Bioprocess Engineering at Massey University, Palmerston North, New Zealand. Masters thesis. Massey University. http://hdl.handle.net/10179/5864.

Budzinski, H., Devier, M.H., Labadie, P., Togola, A., 2006. Analysis of hormonal steroids in fish plasma and bile by coupling solid-phase extraction to GC/MS. Analytical and Bioanalytical Chemistry 386(5), 1429-1439.

Burkhardt, M.R., ReVello, R.C., Smith, S.G., Zaugg, S.D., 2005. Pressurized liquid extraction using water/isopropanol coupled with solid-phase extraction cleanup

for industrial and anthropogenic waste-indicator compounds in sediment. Analytica Chimica Acta 534(1), 89-100.

Burkholder, J., Libra, B., Weyer, P., Heathcote, S., Kolpin, D., Thorne, P.S., Wichman, M., 2007. Impacts of Waste from Concentrated Animal Feeding Operations on Water Quality. Environmental Health Perspectives 115(2), 308-312.

Caco, N.S.A., 2017. Pilot scale pyrolyser : compliance and mechanistic modeling : a thesis presented in partial fulfillment of the requirement for the degree of Master of Engineering in Chemical and Process Engineering at Massey University, Palmerston North, New Zealand. Masters thesis. Massey University. http://hdl.handle.net/10179/12201.

Caldwell, D.J., Mastrocco, F., Anderson, P.D., Lange, R., Sumpter, J.P., 2012. Predicted-no-effect concentrations for the steroid estrogens estrone, 17-estradiol, estriol, and 17-ethinylestradiol. Environmental Toxicology and Chemistry 31(6), 1396-1406.

Casey, F.X.M., Hakk, H., DeSutter, T.M., 2020. Free and conjugated estrogens detections in drainage tiles and wells beneath fields receiving swine manure slurry. Environmental Pollution 256, 113384.

Casey, F.X.M., Larsen, G.L., Hakk, H., imunek, J., 2003. Fate and transport of 17-estradiol in soil-water systems. Environmental Science and Technology 37(11), 2400-2409.

Casey, F.X.M., Selbie, D., Hakk, H., Richards, K.G., 2019. Leaching of Free and Conjugate Natural Estrogens in Soil Monoliths. Water, Air, and Soil Pollution 230(2).

Chen, B., Zhou, D., Zhu, L., 2008. Transitional Adsorption and Partition of Nonpolar and Polar Aromatic Contaminants by Biochars of Pine Needles with Different Pyrolytic Temperatures. Environmental science & technology 42(14), 5137-5143.

Chen, C., Zhou, W., Lin, D., 2015. Sorption characteristics of N-nitrosodimethylamine onto biochar from aqueous solution. Bioresource technology 179, 359-366.

Chen, Q., Shi, J., Wu, W., Liu, X., Zhang, H., 2012. A new pretreatment and improved method for determination of selected estrogens in high matrix solid sewage samples by liquid chromatography mass spectrometry. Microchemical Journal 104, 49-55.

Chen, T.-S., Chen, T.-C., Yeh, K.-J.C., Chao, H.-R., Liaw, E.-T., Hsieh, C.-Y., Chen, K.-C., Hsieh, L.-T., Yeh, Y.-L., 2010. High estrogen concentrations in receiving river discharge from a concentrated livestock feedlot. Science of The Total Environment 408(16), 3223-3230.

Chen, X., Hu, J., 2010. Adsorption of natural estrogens and their conjugates by activated sludge. Water, Air, and Soil Pollution 206(1-4), 251-261.

Chun, Y., Sheng, G., Chiou, C.T., Xing, B., 2004. Compositions and Sorptive Properties of Crop Residue-Derived Chars. Environmental science & technology 38(17), 4649-4655.

Combalbert, S., Hernandez-Raquet, G., 2010. Occurrence, fate, and biodegradation of estrogens in sewage and manure. Applied Microbiology and Biotechnology 86(6), 1671-1692.

Combalbert, S., Bellet, V., Dabert, P., Bernet, N., Balaguer, P., Hernandez-Raquet, G., 2012. Fate of steroid hormones and endocrine activities in swine manure disposal and treatment facilities. Water Research 46(3), 895-906.

Combalbert, S., Pype, M.-L., Bernet, N., Hernandez-Raquet, G., 2010. Enhanced methods for conditioning, storage, and extraction of liquid and solid samples of manure for determination of steroid hormones by solid-phase extraction and gas chromatography-mass spectrometry. Analytical and Bioanalytical Chemistry 398(2), 973-984.

Cooke, P.S., Nanjappa, M.K., Ko, C., Prins, G.S., Hess, R.A., 2017. Estrogens in Male Physiology. Physiol. Rev. 97(3), 995-1043.

Cooney, M.J., Lewis, K., Harris, K., Zhang, Q., Yan, T., 2016. Start up performance of biochar packed bed anaerobic digesters. Journal of Water Process Engineering 9, e7-e13.

Cornelissen, G., Gustafsson, Ö., Bucheli, T.D., Jonker, M.T.O., Koelmans, A.A., van Noort, P.C.M., 2005. Extensive Sorption of Organic Compounds to Black Carbon, Coal, and Kerogen in Sediments and Soils: Mechanisms and Consequences for Distribution, Bioaccumulation, and Biodegradation. Environmental science & technology 39(18), 6881-6895.

Cortez Pires de Campos, A., 2019. Guidelines for small scale biochar production system to optimise carbon sequestration outcome : a thesis presented in partial fulfilment of the requirements for the degree of Master of Engineering in Bioprocessing Engineering at Massey University, Palmerston North, New Zealand. Masters thesis. Massey University. http://hdl.handle.net/10179/15335.

Craggs, R.J., Tanner, C.C., Sukias, J.P.S., Davies-Colley, R.J., 2003. Dairy farm wastewater treatment by an advanced pond system. Water Science and Technology 48, 291-297.

Crombie, K., Masek, O., Sohi, S.P., Brownsort, P., Cross, A., 2013. The effect of pyrolysis conditions on biochar stability as determined by three methods. GCB Bioenergy 5(2), 122-131.

Dairy NZ, 2014a. Facial eczema, management for New Zealand dairy herds, Hanilton.

Dairy NZ, 2014b. Farm Dairy Effluent (FDE) Systems, planning the right system for your farm, Hamilton, New Zealand.

Dairy NZ, 2014c. QuickStats about Dairying. https://www.dairynz.co.nz/media/1357994/quickstats-new-zealand.pdf.

Dairy NZ, 2021. New Zealand Dairy Statistics 2020-21. https://online.flippingbook.com/view/800797035/2/.

Delgado, L.F., Charles, P., Glucina, K., Morlay, C., 2012. The removal of endocrine disrupting compounds, pharmaceutically activated compounds and cyanobacterial toxins during drinking water preparation using activated carbon--a review. Sci Total Environ 435-436, 509-525.

Ding, Y., Liu, Y., Liu, S., Huang, X., Li, Z., Tan, X., Zeng, G., Zhou, L., 2017. Potential Benefits of Biochar in Agricultural Soils: A Review. Pedosphere 27(4), 645-661.

Dodds, E.C., Goldberg, L., Lawson, W., Robinson, R., 1938. Oestrogenic activity of certain synthetic compounds. Nature 141(3562), 247-248.

Dong, X., He, L., Hu, H., Liu, N., Gao, S., Piao, Y., 2018. Removal of 17β-estradiol by using highly adsorptive magnetic biochar nanoparticles from aqueous solution. Chemical engineering journal (Lausanne, Switzerland : 1996) 352, 371-379.

Du, B., Fan, G., Yu, W., Yang, S., Zhou, J., Luo, J., 2020. Occurrence and risk assessment of steroid estrogens in environmental water samples: A five-year worldwide perspective. Environmental Pollution 267, 115405.

Eckard, R.J., Clark, H., 2019. Potential solutions to the major greenhouse-gas issues facing Australasian dairy farming. Animal production science 60(1), 10-16.

Enders, A., Hanley, K., Whitman, T., Joseph, S., Lehmann, J., 2012. Characterization of biochars to evaluate recalcitrance and agronomic performance. Bioresource technology 114, 644-653.

Esmaeeli, F., Gorbanian, S.A., Moazezi, N., 2017. Removal of Estradiol Valerate and Progesterone using Powdered and Granular Activated Carbon from Aqueous Solutions. International Journal of Environmental Research 11(5-6), 695-705.

European Biochar Foundation, 2012. European Biochar Certificate - Guidelines for a Sustainable Production of Biochar, Arbaz, Switzerland. https://www.european-biochar.org/en.

European Commission, 2016. Endocrine Disruptors. http://ec.europa.eu/environment/chemicals/endocrine/. (Accessed Retrieved January, 2018.

Fagbohungbe, M.O., Herbert, B.M.J., Hurst, L., Ibeto, C.N., Hong, L., Usmani, S.Q., Semple, K.T., 2017. The challenges of anaerobic digestion and the role of biochar in optimizing anaerobic digestion. Waste Management 61, 236-249.

Fan, J., Xiao, J., Liu, D., Ye, G., Luo, J., Houlbrooke, D., Laurenson, S., Yan, J., Chen, L., Tian, J., Ding, W., 2017. Effect of application of dairy manure, effluent and inorganic fertilizer on nitrogen leaching in clayey fluvo-aquic soil: A lysimeter study. Science of The Total Environment 592(Supplement C), 206-214.

Frąc, M., Jezierska-Tys, S., Oszust, K., Gryta, A., Pastor, M., 2017. Assessment of microbiological and biochemical properties of dairy sewage sludge. International Journal of Environmental Science and Technology 14(4), 679-688.

Fyfe, J., Hagare, D., Sivakumar, M., 2016. Dairy shed effluent treatment and recycling: Effluent characteristics and performance. Journal of Environmental Management 180, 133-146.

Gadd, J.B., Northcott, G.L., Tremblay, L.A., 2010a. Passive secondary biological treatment systems reduce estrogens in dairy shed effluent. Environmental Science and Technology 44(19), 7601-7606.

Gadd, J.B., Tremblay, L.A., Northcott, G.L., 2010b. Steroid estrogens, conjugated estrogens and estrogenic activity in farm dairy shed effluents. Environmental Pollution 158(3), 730-736.

Goeppert, N., Dror, I., Berkowitz, B., 2015. Fate and transport of free and conjugated estrogens during soil passage. Environmental Pollution 206, 80-87.

Gomes, R.L., Deacon, H.E., Lai, K.M., Birkett, J.W., Scrimshaw, M.D., Lester, J.N., 2004. An assessment of the bioaccumulation of estrone in Daphnia magna. Environmental toxicology and chemistry 23(1), 105-108.

Gomes, R.L., Lester, J.N., 2003. Endocrine Disrupters in Receiving Waters. Birkett, J.W., Lester, J.N. (Eds.), Endocrine Disrupters in Wastewater and Sludge Treatment Processes. IWA, Boca Raton, FL, pp. 177-217.

Gomes, R.L., Meredith, W., Snape, C.E., Sephton, M.A., 2009a. Analysis of conjugated steroid androgens: Deconjugation, derivatisation and associated issues. Journal of Pharmaceutical and Biomedical Analysis 49(5), 1133-1140.

Gomes, R.L., Scrimshaw, M.D., Lester, J.N., 2009b. Fate of conjugated natural and synthetic steroid estrogens in crude sewage and activated sludge batch studies. Environmental Science and Technology 43(10), 3612-3618.

Gonzalez, T.L., Rae, J.M., Colacino, J.A., 2019. Implication of environmental estrogens on breast cancer treatment and progression. Toxicology 421, 41-48.

Gordon, S., Robert, R., 2007. Reasonable Stock Water Requirements Guidelines for Resource Consent Applications Horizons Regional Council,. https://www.boprc.govt.nz/media/470831/reasonable-stock-water-requirements-guidelines-horizons.pdf.

Grathwohl, P., 1990. Influence of organic matter from soils and sediments from various origins on the sorption of some chlorinated aliphatic hydrocarbons: Implications on K(oc) correlations. Environmental Science and Technology 24(11), 1687-1693.

Grover, D.P., Zhou, J.L., Frickers, P.E., Readman, J.W., 2011. Improved removal of estrogenic and pharmaceutical compounds in sewage effluent by full scale

granular activated carbon: Impact on receiving river water. Journal of Hazardous Materials 185(2), 1005-1011.

Gul, S., Whalen, J.K., Thomas, B.W., Sachdeva, V., Deng, H., 2015. Physico-chemical properties and microbial responses in biochar-amended soils: Mechanisms and future directions. Agriculture, Ecosystems & Environment 206, 46-59.

Gwenzi, W., Chaukura, N., Noubactep, C., Mukome, F.N.D., 2017. Biochar-based water treatment systems as a potential low-cost and sustainable technology for clean water provision. J Environ Manage 197, 732-749.

Haddad, M., Oie, C., Vo Duy, S., Sauvé, S., Barbeau, B., 2019. Adsorption of micropollutants present in surface waters onto polymeric resins: Impact of resin type and water matrix on performance. The Science of the total environment 660, 1449-1458.

Hanselman, T.A., Graetz, D.A., Wilkie, A.C., 2003. Manure-Borne Estrogens as Potential Environmental Contaminants: A Review. Environmental Science and Technology 37(24), 5471-5478.

Hanselman, T.A., Graetz, D.A., Wilkie, A.C., Szabo, N.J., Diaz, C.S., 2006. Determination of steroidal estrogens in flushed dairy manure wastewater by gas chromatography-mass spectrometry. Journal of Environmental Quality 35(3), 695-700.

Havens, S.M., Hedman, C.J., Hemming, J.D.C., Mieritz, M.G., Shafer, M.M., Schauer, J.J., 2020. Occurrence of estrogens, androgens and progestogens and estrogenic activity in surface water runoff from beef and dairy manure amended crop fields. Science of The Total Environment 710, 136247.

Heubeck., S., Nagels., J., Craags, R., 2014. Variability of effluent quality and quantity on dairy farms in New Zealand. National Institute of Water and Atmospheric Research Ltd (NIWA).

Hoffmann, B., Goes de Pinho, T., Schuler, G., 1997. Determination of free and conjugated oestrogens in peripheral blood plasma, feces and urine of cattle throughout pregnancy. Experimental and Clinical Endocrinology & Diabetes 105(5), 296-303.

Hormones Endocrine System. University of Kentucky. Animal Sciences, Power Point presentation.http://www.uky.edu/Ag/AnimalSciences/instruction/asc564/Hormones_Lecture.pdf

Höjer, A., Adler, S., Purup, S., Hansen-Møller, J., Martinsson, K., Steinshamn, H., Gustavsson, A.M., 2012. Effects of feeding dairy cows different legume-grass silages on milk phytoestrogen concentration. Journal of Dairy Science 95(8), 4526-4540.

Hull-Cantillo, M., Lay, M., Kovalsky, P., 2023. Anaerobic Digestion of Dairy Effluent in New Zealand, Time to Revisit the Idea? Energies (Basel) 16(6), 2859.

Hutchins, S.R., White, M.V., Hudson, F.M., Fine, D.D., 2007. Analysis of Lagoon Samples from Different Concentrated Animal Feeding Operations for Estrogens and Estrogen Conjugates. Environmental Science & Technology 41(3), 738-744.

Ifelebuegu, A.O., 2011. The fate and behavior of selected endocrine disrupting chemicals in full scale wastewater and sludge treatment unit processes. International Journal of Environmental Science and Technology 8(2), 245-254.

International Biochar Initiative, 2015. Standardized Product Definition and Product Testing Guidelines for Biochar That Is Used in Soil. https://www.biochar-international.org/wp
content/uploads/2018/05/IBI_Biochar_Standards_V2.1_Final.pdf.

Inyang, M., Dickenson, E., 2015. The potential role of biochar in the removal of organic and microbial contaminants from potable and reuse water: A review. Chemosphere 134, 232-240.

IPENZ, 2017. Practice note 21 - Farm dairy effluent ponds. Engineering New Zealand. https://www.dairynz.co.nz/media/5788063/ipenz-practice-note-21-farm-dairy-effluent-ponds.pdf.

Ishitobi, H., Watanabe, C., 2005. Effects of low-dose perinatal cadmium exposure on tissue zinc and copper concentrations in neonatal mice and on the reproductive development of female offspring. Toxicology Letters 159(1), 38-46.

James, M.O., 2011. Steroid catabolism in marine and freshwater fish. The Journal of Steroid Biochemistry and Molecular Biology 127(3), 167-175.

Jiang, L., Liu, Y., Liu, S., Zeng, G., Hu, X., Hu, X., Guo, Z., Tan, X., Wang, L., Wu, Z., 2017. Adsorption of Estrogen Contaminants by Graphene Nanomaterials under Natural Organic Matter Preloading: Comparison to Carbon Nanotube, Biochar, and Activated Carbon. Environmental science & technology 51(11), 6352-6359.

Jimenez, E.I., Garcia, V.P., 1992. Relationships between organic carbon and total organic matter in municipal solid wastes and city refuse composts. Bioresource Technology 41(3), 265-272.

J. L. Callejas, M.V., M. Rozas., 2019. Developmet and charactrerization of an enzyme formulation for sulfatase and glucuronidase in a single step. Presented at ASMS.

John Ballingall, Daniel Pambudi, 2017. Dairy Trade's Economic Contribution to New Zealand Institute of Ecomonic Research, Wellington, New Zealand. https://nzier.org.nz/static/media/filer_public/29/33/29336237-3350-40ce-9933-a5a59d25bd31/dairy_economic_contribution_update_final_21_february_2017.pdf.

Johnson, I., Harvey, P., 2002. Study on the Scientific Evaluation of 12 Substances in the Context of Endocrine Disrupter Priority List of Actions. Ref: UC 6052. WRc-NSF for European Commission, Marlow, U.K.

Kabir, E.R., Rahman, M.S., Rahman, I., 2015. A review on endocrine disruptors and their possible impacts on human health. Environmental Toxicology and Pharmacology 40(1), 241-258.

Kambo, H.S., Dutta, A., 2015. A comparative review of biochar and hydrochar in terms of production, physico-chemical properties and applications. Renew. Sust. Energ. Rev. 45, 359-378.

Karen, A.K., Paul, J.B., Kenneth, H.M., Vince, P.P., Robert, E.E., James, M.L., Robert, W.F., 2007. Collapse of a fish population after exposure to a synthetic estrogen. Proceedings of the National Academy of Sciences 104(21), 8897.

Katsigiannis, A., Noutsopoulos, C., Mantziaras, J., Gioldasi, M., 2015. Removal of emerging pollutants through Granular Activated Carbon. Chemical Engineering Journal 280, 49-57.

Kazemi Shariat Panahi, H., Dehhaghi, M., Ok, Y.S., Nizami, A.-S., Khoshnevisan, B., Mussatto, S.I., Aghbashlo, M., Tabatabaei, M., Lam, S.S., 2020. A comprehensive review of engineered biochar: Production, characteristics, and environmental applications. J. Cleaner Prod. 270, 122462.

Kennedy, J.F., Jin, M., 2006. Carbohydrate Polymers 63(2), 290.

Khetan, S.K., 2014. Endocrine disruptors in the environment. Wiley, Hoboken, New Jersey.

Kim, E., Jung, C., Han, J., Her, N., Park, C.M., Jang, M., Son, A., Yoon, Y., 2016. Sorptive removal of selected emerging contaminants using biochar in aqueous solution. Journal of industrial and engineering chemistry (Seoul, Korea) 36, 364-371.

Kjaer, J., Olsen, P., Bach, K., Barlebo, H.C., Ingerslev, F., Hansen, M., Sorensen, B.H., 2007. Leaching of estrogenic hormones from manure-treated structured soils. Environmental Science and Technology 41(11), 3911-3917.

Kolkman, A., Schriks, M., Brand, W., Bäuerlein, P.S., van der Kooi, M.M.E., van Doorn, R.H., Emke, E., Reus, A.A., van der Linden, S.C., de Voogt, P., Heringa, M.B., 2013. Sample preparation for combined chemical analysis and in vitro bioassay application in water quality assessment. Environmental Toxicology and Pharmacology 36(3), 1291-1303.

Kolodziej, E.P., Harter, T., Sedlak, D.L., 2004. Dairy wastewater, aquaculture, and spawning fish as sources of steroid hormones in the aquatic environment. Environmental Science and Technology 38(23), 6377-6384.

Kumar, V., Johnson, A.C., Nakada, N., Yamashita, N., Tanaka, H., 2012. De-conjugation behavior of conjugated estrogens in the raw sewage, activated sludge and river water. Journal of Hazardous Materials 227-228, 49-54.

Kumar, V., Nakada, N., Yamashita, N., Johnson, A.C., Tanaka, H., 2015. Influence of Hydraulic Retention Time, Sludge Retention Time, and Ozonation on the Removal of Free and Conjugated Estrogens in Japanese Activated Sludge Treatment Plants. CLEAN – Soil, Air, Water 43(9), 1289-1294.

Labadie, P., Budzinski, H., 2005a. Determination of steroidal hormone profiles along the Jalle d'Eysines River (near Bordeaux, France). Environmental Science and Technology 39(14), 5113-5120.

Labadie, P., Budzinski, H., 2005b. Development of an analytical procedure for determination of selected estrogens and progestagens in water samples. Anal. Bioanal. Chem. 381(6), 1199-1205.

Lai, K.M., Johnson, K.L., Scrimshaw, M.D., Lester, J.N., 2000. Binding of waterborne steroid estrogens to solid phases in river and estuarine systems. Environmental Science and Technology 34(18), 3890-3894.

Lange, I.G., Daxenberger, A., Schiffer, B., Witters, H., Ibarreta, D., Meyer, H.H.D., 2002. Sex hormones originating from different livestock production systems: fate and potential disrupting activity in the environment. Analytica Chimica Acta 473(1), 27-37.

Langford, K., Lester, J.N., 2003. Fate and Behavior of Endocrine Disrupters in Wastewater Treatment Processes. Birkett, J.W., Lester, J.N. (Eds.), Endocrine Disrupters in Wastewater and Sludge Treatment Processes. IWA, Boca Raton, FL, pp. 103-144.

Lee, L.S., Strock, T.J., Sarmah, A.K., Rao, P.S.C., 2003. Sorption and dissipation of testosterone, estrogens, and their primary transformation products in soils and sediment. Environmental Science and Technology 37(18), 4098-4105.

Levenspiel, O., 1999. Chemical reaction engineering, 3rd ed. Wiley, New York.

Li, L., Quinlivan, P.A., Knappe, D.R.U., 2002. Effects of activated carbon surface chemistry and pore structure on the adsorption of organic contaminants from aqueous solution. Carbon 40(12), 2085-2100.

Li, M., Sun, L., Wang, D., 2019. Roles of estrogens in fish sexual plasticity and sex differentiation. General and Comparative Endocrinology 277, 9-16.

Liang, Y., Cao, X., Zhao, L., Xu, X., Harris, W., 2014. Phosphorus Release from Dairy Manure, the Manure-Derived Biochar, and Their Amended Soil: Effects of Phosphorus Nature and Soil Property. Journal of environmental quality 43(4), 1504-1509.

Liu, S., Liu, Y., Jiang, L., Zeng, G., Li, Y., Zeng, Z., Wang, X., Ning, Q., 2019. Removal of 17β-Estradiol from water by adsorption onto montmorillonite-carbon hybrids derived from pyrolysis carbonization of carboxymethyl cellulose. Journal of environmental management 236, 25-33.

Liu, S., Ying, G.-G., Zhang, R.-Q., Zhou, L.-J., Lai, H.-J., Chen, Z.-F., 2012. Fate and occurrence of steroids in swine and dairy cattle farms with different farming scales and wastes disposal systems. Environmental Pollution 170, 190-201.

Liu, Z.H., Kanjo, Y., Mizutani, S., 2009. Removal mechanisms for endocrine disrupting compounds (EDCs) in wastewater treatment - physical means, biodegradation, and chemical advanced oxidation: a review. Science of The Total Environment 407(2), 731-748.

Liu, Z.-H., Lu, G.-N., Yin, H., Dang, Z., Rittmann, B., 2015. Removal of natural estrogens and their conjugates in municipal wastewater treatment plants: A critical review. Environmental Science and Technology 49(9), 5288-5300.

Longhurst, R.D., Roberts, A.H.C., O'Conner, M.B., 2000. Farm dairy effluent: A review of published data on chemical and physical characteristics in New Zealand. New Zealand Journal of Agricultural Research 43(1), 7-14.

Lopez-Alonso, M., Rey-Crespo, F., Herrero-Latorre, C., Miranda, M., 2017. Identifying sources of metal exposure in organic and conventional dairy farming. Chemosphere 185, 1048-1055.

Lopez-Mosquera, M.E., Moiron, C., Carral, E., 2000. Use of dairy-industry sludge as fertiliser for grasslands in northwest Spain: Heavy metal levels in the soil and plants. Resources, Conservation and Recycling 30(2), 95-109.

Luo, J., Saggar, S., Bhandral, R., Bolan, N., Ledgard, S., Lindsey, S., Sun, W., 2008. Effects of irrigating dairy-grazed grassland with farm dairy effluent on nitrous oxide emissions. Plant and soil 309(1-2), 119-130.

Ma, L., Yates, S.R., Ashworth, D., 2016. Parent and conjugated estrogens and progestagens in surface water of the Santa Ana River: Determination, occurrence, and risk assessment. Environmental Toxicology and Chemistry 35(11), 2657-2664.

Ma, L., Yates, S.R., 2017. Degradation and metabolite formation of estrogen conjugates in an agricultural soil. Journal of Pharmaceutical and Biomedical Analysis 145(Supplement C), 634-640.

Manono, B.O., Moller, H., Morgan, R., 2016. Effects of irrigation, dairy effluent dispersal and stocking on soil properties of the Waimate District, New Zealand. Geoderma Regional 7(1), 59-66.

Mansell, D.S., Bryson, R.J., Harter, T., Webster, J.P., Kolodziej, E.P., Sedlak, D.L., 2011. Fate of endogenous steroid hormones in steer feedlots under simulated rainfall-induced runoff. Environmental Science and Technology 45(20), 8811-8818.

Mansell, J., Drewes, J.E., Rauch, T., 2004. Removal mechanisms of endocrine disrupting compounds (steroids) during soil aquifer treatment. Water Science and Technology 50(2), 229-237.

Maroušek, J., Strunecký, O., Stehel, V., 2019. Biochar farming: defining economically perspective applications. Clean technologies and environmental policy 21(7), 1389-1395.

Matsui, Y., Yoshida, T., Nakao, S., Knappe, D.R.U., Matsushita, T., 2012. Characteristics of competitive adsorption between 2-methylisoborneol and natural organic matter on superfine and conventionally sized powdered activated carbons. Water research (Oxford) 46(15), 4741-4749.

Matthiessen, M.K., Larney, F.J., Brent Selinger, L., Olson, A.F., 2005. Influence of Loss-on-Ignition Temperature and Heating Time on Ash Content of Compost and Manure. Communications in Soil Science and Plant Analysis 36(17-18), 2561-2573.

Matthiessen, P., Arnold, D., Johnson, A.C., Pepper, T.J., Pottinger, T.G., Pulman, K.G.T., 2006. Contamination of headwater streams in the United Kingdom by oestrogenic

hormones from livestock farms. Science of the Total Environment 367(2-3), 616-630.

McDonald-Wharry, J., Manley-Harris, M., Pickering, K., 2013. Carbonisation of biomass-derived chars and the thermal reduction of a graphene oxide sample studied using Raman spectroscopy. Carbon 59, 383-405.

Meinel, F., Ruhl, A.S., Sperlich, A., Zietzschmann, F., Jekel, M., 2014. Pilot-Scale Investigation of Micropollutant Removal with Granular and Powdered Activated Carbon. Water, air, and soil pollution 226(1), 1-10.

Meng, L.-J., Sjövall, J., 1997. Method for combined analysis of profiles of conjugated progesterone metabolites and bile acids in serum and urine of pregnant women. Journal of Chromatography B: Biomedical Sciences and Applications 688(1), 11-26.

Metcalf, Eddy, 2014. Wastewater Engineering: Treatment and Resource Recovery, Fifth Edition. McGraw-Hill Education, New York.

Mills, L.J., Chichester, C., 2005. Review of evidence: are endocrine-disrupting chemicals in the aquatic environment impacting fish populations? Science of The Total Environment 343(1-3), 1-34.

Mina, O., Gall, H.E., Saporito, L.S., Elliott, H.A., Kleinman, P.J.A., 2017. Relative role of transport and source-limited controls for estrogen, TDP, and DOC export for two manure application methods. Agriculture, Ecosystems & Environment 247, 308-318.

Ministry for Primary Industries, 2020. New Zealand's Forests Statistics https://www.mpi.govt.nz/forestry/new-zealand-forests-forest-industry/forestry/new-zealands-forests-statistics/.

Ministry of the Environment, Japan,, 2010. Further Actions to Endocrine Disrupting Effects of Chemical Substances. EXTEND 2010. MOE, Tokyo, Japan.

Mohan, D., Abhishek, K., Sarswat, A., Patel, M., Singh, P., Pittman, C.U., 2018. Biochar production and applications in soil fertility and carbon sequestration-a sustainable solution to crop-residue burning in India. RSC Adv. 8(1), 508-520.

Moore, S.C., Matthews, C.E., Ou Shu, X., Yu, K., Gail, M.H., Xu, X., Ji, B.-T., Chow, W.-H., Cai, Q., Li, H., Yang, G., Ruggieri, D., Boyd-Morin, J., Rothman, N., Hoover, R.N., Gao, Y.-T., Zheng, W., Ziegler, R.G., 2016. Endogenous Estrogens, Estrogen Metabolites, and Breast Cancer Risk in Postmenopausal Chinese Women. JNCI: Journal of the National Cancer Institute 108(10), djw103-djw103.

Mumme, J., Srocke, F., Heeg, K., Werner, M., 2014. Use of biochars in anaerobic digestion. Bioresour Technol 164, 189-197.

Natural Resources Conservation Service, n.d. Animal Feeding Operations. https://www.nrcs.usda.gov/wps/portal/nrcs/main/national/plantsanimals/livestock/afo/. (Accessed January, 2018).

Nelson, D.W., Sommers, L.E., 1996. Total Carbon, Organic Carbon amd Organic Matter. Methods of Soil Analysis: Part 3 Chemical Methods. Soil Science Society of America, Inc., American Society of Agronomy, Inc., Madison, Wisconsin, USA, pp. 961-1010.

Njåstad, K.M., Adler, S.A., Hansen-Møller, J., Thuen, E., Gustavsson, A.M., Steinshamn, H., 2014. Gastrointestinal metabolism of phytoestrogens in lactating dairy cows fed silages with different botanical composition. Journal of Dairy Science 97(12), 7735-7750.

Noguera-Oviedo, K., Aga, D.S., 2016. Chemical and biological assessment of endocrine disrupting chemicals in a full scale dairy manure anaerobic digester with thermal pretreatment. Science of The Total Environment 550, 827-834.

Norris, D.O., Carr, J.A., 2005. Endocrine Disruption: Biological Bases for Health Effects in Wildlife and Humans. Oxford University Press, Cary.

Norvill, Z.N., Shilton, A., Guieysse, B., 2016. Emerging contaminant degradation and removal in algal wastewater treatment ponds: Identifying the research gaps. Journal of Hazardous Materials 313, 291-309.

Ociepa-Zawal, M., Rubis, B., Wawrzynczak, D., Wachowiak, R., Trzeciak, W.H., 2010. Accumulation of environmental estrogens in adipose tissue of breast cancer patients. Journal of Environmental Science and Health - Part A Toxic/Hazardous Substances and Environmental Engineering 45(3), 305-312.

Ogunlaja, O.O., Parker, W.J., 2015. Assessment of the removal of estrogenicity in biological nutrient removal wastewater treatment processes. Sci Total Environ 514, 202-210.

Oliveira, F.R., Patel, A.K., Jaisi, D.P., Adhikari, S., Lu, H., Khanal, S.K., 2017. Environmental application of biochar: Current status and perspectives. Bioresour Technol 10.1016/j.biortech.2017.08.122.

Page, L.H., Ni, J.-Q., Heber, A.J., Mosier, N.S., Liu, X., Joo, H.-S., Ndegwa, P.M., Harrison, J.H., 2014. Characteristics of volatile fatty acids in stored dairy manure before and after anaerobic digestion. Biosystems Engineering 118, 16-28.

Pan, L., Xia, X., Feng, Y., Jiang, C., Cui, Y., Huang, Y., 2008. Exposure of Juvenile Rats to the Phytoestrogen Daidzein Impairs Erectile Function in a Dose‐Related Manner in Adulthood. Journal of Andrology 29(1), 55-62.

Park, J.B.K., Craggs, R.J., 2007. Biogas production from anaerobic waste stabilisation ponds treating dairy and piggery wastewater in New Zealand. Water Science and Technology 55(11), 257-264.

Peiris, C., Nawalage, S., Wewalwela, J.J., Gunatilake, S.R., Vithanage, M., 2020. Biochar based sorptive remediation of steroidal estrogen contaminated aqueous systems: A critical review. Environmental Research 191.

Quinlivan, P.A., Li, L., Knappe, D.R.U., 2005. Effects of activated carbon characteristics on the simultaneous adsorption of aqueous organic micropollutants and natural organic matter. Water research (Oxford) 39(8), 1663-1673.

Raman, D.R., Layton, A.C., Moody, L.B., Easter, J.P., Sayler, G.S., Burns, R.T., Mullen, M.D., 2001. Degradation of estrogens in dairy waste solids: Effects of acidification and temperature. Transactions of the American Society of Agricultural Engineers 44(6), 1881-1888.

Raman, D.R., Williams, E.L., Layton, A.C., Burns, R.T., Easter, J.P., Daugherty, A.S., Mullen, M.D., Sayler, G.S., 2004. Estrogen content of dairy and swine wastes. Environmental Science and Technology 38(13), 3567-3573.

Rattan, S., Sharma, R., 2017. Hormones in Ageing and Longevity, 1st ed. 2017. ed. Springer International Publishing, Cham.

Reddy, S., Iden, C.R., Brownawell, B.J., 2005. Analysis of steroid conjugates in sewage influent and effluent by liquid chromatography-tandem mass spectrometry. Analytical Chemistry 77(21), 7032-7038.

Redlich, O., Peterson, D.L., 1959. A Useful Adsorption Isotherm. The Journal of Physical Chemistry 63(6), 1024-1024.

Rempel, M.A., 2007. Impacts of environmental estrogen exposure on DNA damage and reproduction in marine organisms. ProQuest LLC.

Rovani, S., Rodrigues, A.G., Medeiros, L.F., Cataluña, R., Lima, É.C., Fernandes, A.N., 2016. Synthesis and characterisation of activated carbon from agroindustrial waste—Preliminary study of 17β-estradiol removal from aqueous solution. Journal of Environmental Chemical Engineering 4(2), 2128-2137.

Sarfaraz, Q., Silva, L., Drescher, G., Zafar, M., Severo, F., Kokkonen, A., Molin, G., Shafi, M., Shafique, Q., Solaiman, Z., 2020. Characterization and carbon mineralization of biochars produced from different animal manures and plant residues. Scientific reports 10(1), 955.

Sarmah, A.K., Northcott, G.L., Leusch, F.D., Tremblay, L.A., 2006. A survey of endocrine disrupting chemicals (EDCs) in municipal sewage and animal waste effluents in the Waikato region of New Zealand. Science of The Total Environment 355(1-3), 135-144.

Sarmah, A.K., Northcott, G.L., Scherr, F.F., 2008. Retention of estrogenic steroid hormones by selected New Zealand soils. Environmental International 34(6), 749-755.

Sarmah, A.K., Srinivasan, P., Smernik, R.J., Manley-Harris, M., Antal Jr, M.J., Downie, A., Van Zwieten, L., 2010. Retention capacity of biochar-amended New Zealand dairy farm soil for an estrogenic steroid hormone and its primary metabolite. CSIRO, pp. 648-658.

Scherr, F.F., Sarmah, A.K., Di, H.J., Cameron, K.C., 2009. Degradation and metabolite formation of 17-estradiol-3-sulphate in New Zealand pasture soils. Environment International 35(2), 291-297.

Schenck, K., Rosenblum, L., Wiese, T.E., Wymer, L., Dugan, N., Williams, D., Mash, H., Merriman, B., Speth, T., 2012. Removal of estrogens and estrogenicity through drinking water treatment. J. Water Health 10(1), 43-55.

Scrimshaw, M.D., Lester, J.N., 2003. Fate and Behavior of Endocrine Disrupters in Sludge Treatment and Disposal. Birkett, J.W., Lester, J.N. (Eds.), Endocrine Disrupters in Wastewater and Sludge Treatment Processes. IWA, Boca Raton, FL, pp. 145-176.

Shrestha, S.L., Casey, F.X.M., Hakk, H., Smith, D.J., Padmanabhan, G., 2012. Fate and transformation of an estrogen conjugate and its metabolites in agricultural soils. Environmental Science and Technology 46(20), 11047-11053.

Sim, W.J., Lee, J.W., Shin, S.K., Song, K.B., Oh, J.E., 2011. Assessment of fates of estrogens in wastewater and sludge from various types of wastewater treatment plants. Chemosphere 82(10), 1448-1453.

Snyder, S.A., Adham, S., Redding, A.M., Cannon, F.S., DeCarolis, J., Oppenheimer, J., Wert, E.C., Yoon, Y., 2007. Role of membranes and activated carbon in the removal of endocrine disruptors and pharmaceuticals. Desalination 202(1-3), 156-181.

Sodré, F.F., Sampaio, T.R., 2020. Development and application of a SPE-LC-QTOF method for the quantification of micropollutants of emerging concern in drinking waters from the Brazilian capital. Emerging Contaminants 6, 72-81.

Solak, S., Vakondios, N., Tzatzimaki, I., Diamadopoulos, E., Arda, M., Kabay, N., Yüksel, M., 2014. A comparative study of removal of endocrine disrupting compounds (EDCs) from treated wastewater using highly crosslinked polymeric adsorbents and activated carbon. Journal of chemical technology and biotechnology (1986) 89(6), 819-824.

StatsNZ, 2019. Dairy cattle numbers dip again. https://www.stats.govt.nz/news/dairy-cattle-numbers-dip-again.

Steiner, L.D., Hong, K.C., Cameron, V.J., Bidwell, G.L., Northcott, G.L., 2010. Transport and modeling of estrogenic hormones in a dairy farm effluent through undisturbed soil lysimeters. Environmental Science and Technology 44(7), 2341-2347.

Stephan Heubeck, John Nagels, Craggs, R., 2014. Variability of Effluent Quality and Quantity nn Dairy Farms in New Zealand. National Institute of Water and Atmospheric Research Ltd (NIWA).

https://www.massey.ac.nz/~flrc/workshops/14/Manuscripts/Paper_Heubeck_2014.pdf.

Sumpter, J.P., 1995. Feminized responses in fish to environmental estrogens. Toxicology Letters 82-83, 737-742.

Sumpter, J.P., Jobling, S., 2013. The occurrence, causes, and consequences of estrogens in the aquatic environment. Environmental Toxicology and Chemistry 32(2), 249-251.

Sun, K., Ro, K., Guo, M., Novak, J., Mashayekhi, H., Xing, B., 2011. Sorption of bisphenol A, 17α-ethinyl estradiol and phenanthrene on thermally and hydrothermally produced biochars. Bioresource Technology 102(10), 5757-5763.

Tagliavini, M., Engel, F., Weidler, P.G., Scherer, T., Schafer, A.I., 2017. Adsorption of steroid micropollutants on polymer-based spherical activated carbon (PBSAC). J Hazard Mater 337, 126-137.

Tetreault, G.R., Bennett, C.J., Shires, K., Knight, B., Servos, M.R., McMaster, M.E., 2011. Intersex and reproductive impairment of wild fish exposed to multiple municipal wastewater discharges. Aquatic Toxicology 104(3), 278-290.

Tong, X., Jiang, L., Li, Y., Chen, X., Zhao, Y., Hu, B., Zhang, F., 2020. Function of agricultural waste montmorillonite-biochars for sorptive removal of 17β-estradiol. Bioresource technology 296, 122368-122368.

Torrellas, S.Á., García Lovera, R., Escalona, N., Sepúlveda, C., Sotelo, J.L., García, J., 2015. Chemical-activated carbons from peach stones for the adsorption of emerging contaminants in aqueous solutions. Chemical Engineering Journal 279, 788-798.

Toth, J.D., Dou, Z., Ferguson, J.D., Galligan, D.T., Ramberg Jr, C.F., 2006. Nitrogen- vs. phosphorus-based dairy manure applications to field crops: Nitrate and phosphorus leaching and soil phosphorus accumulation. Journal of environmental quality 35(6), 2302-2312.

Tremblay, L.A., Gadd, J.B., Northcott, G.L., 2018. Steroid estrogens and estrogenic activity are ubiquitous in dairy farm watersheds regardless of effluent management practices. Agriculture, Ecosystems & Environment 253, 48-54.

U.S. Environmental Protection Agency, 1997. Special report on environmental endocrine disruption: and effects assessment and analysis, , Washington, D.C.

U.S. Environmental Protection Agency, 2001. Managing Manure Nutrients at Concentrated Animal Feeding Operations, Washington, United States.

U.S. Environmental Protection Agency, 2013. Literature review of contaminants in livestock and poultry manure and implications for water quality.

U.S. Environmental Protection Agency, 2017a. Endocrine Disruptor Screening Program (EDSP) Overview. https://www.epa.gov/endocrine-disruption/endocrine-disruptor-screening-program-edsp-overview. (Accessed January 2018).

U.S. Environmental Protection Agency, 2017b. Endocrine Disruptor Screening Program Timeline. https://www.epa.gov/endocrine-disruption/endocrine-disruptor-screening-program-timeline. (Accessed January 2018).

Vethaak, A.D., Lahr, J., Schrap, S.M., Belfroid, A.C., Rijs, G.B.J., Gerritsen, A., de Boer, J., Bulder, A.S., Grinwis, G.C.M., Kuiper, R.V., Legler, J., Murk, T.A.J., Peijnenburg, W., Verhaar, H.J.M., de Voogt, P., 2005. An integrated assessment of estrogenic contamination and biological effects in the aquatic environment of The Netherlands. Chemosphere 59(4), 511-524.

Waikato Regional Council, n.d. Applying effluent to land. https://www.waikatoregion.govt.nz/Community/Your-community/For-Farmers/Effluent-management/Applying-effluent-to-land/.

Wang, H., Shan, L., Lv, Q., Cai, S., Quan, G., Yan, J., 2020. Production of hierarchically porous carbon from natural biomass waste for efficient organic contaminants adsorption. J. Cleaner Prod. 263, 121352.

Water New Zealand, 2017. Waste Stabilisation Ponds: Design and Operation. https://www.parklink.com.au/wp-content/uploads/2020/10/20171130-final-WEBSITE.pdf.

World Health Organization, 2012. State of the Science of Endocrine Disrupting Chemicals. http://www.who.int/ceh/publications/endocrine/en/.

Xiao, X., Chen, Z., Chen, B., 2016. H/C atomic ratio as a smart linkage between pyrolytic temperatures, aromatic clusters and sorption properties of biochars derived from diverse precursory materials. Scientific reports 6(1), 22644-22644.

Ying, G.-G., Kookana, R.S., Ru, Y.-J., 2002. Occurrence and fate of hormone steroids in the environment. Environment International 28(6), 545-551.

Yost, E., Meyer, M., Dietze, J., Meissner, B., Worley-Davis, L., Williams, C., Lee, B., Kullman, S., 2013. Comprehensive Assessment of Hormones, Phytoestrogens, and Estrogenic Activity in an Anaerobic Swine Waste Lagoon. Environmental Science & Technology 47(23), 13781.

Yost, E.E., Meyer, M.T., Dietze, J.E., Williams, C.M., Worley-Davis, L., Lee, B., Kullman, S.W., 2014. Transport of steroid hormones, phytoestrogens, and estrogenic activity across a swine lagoon/sprayfield system. Environmental Science and Technology 48(19), 11600-11609.

Yu, Z., Gunn, L., Wall, P., Fanning, S., 2017. Antimicrobial resistance and its association with tolerance to heavy metals in agriculture production. Food Microbiology 64, 23-32.

Zhang, H., Shi, J., Liu, X., Zhan, X., Chen, Q., 2014a. Occurrence and removal of free estrogens, conjugated estrogens, and bisphenol A in manure treatment facilities in East China. Water Research 58, 248-257.

Zhang, H., Shi, J., Liu, X., Zhan, X., Dang, J., Bo, T., 2014b. Occurrence of free estrogens, conjugated estrogens, and bisphenol A in fresh livestock excreta and their removal by composting in North China. Environmental Science and Pollution Research 21(16), 9939-9947.

Zhang, H., Shi, J., Liu, X., Zhan, X., Dang, J., Bo, T., 2014. Occurrence of free estrogens, conjugated estrogens, and bisphenol A in fresh livestock excreta and their removal by composting in North China. Environmental Science and Pollution Research 21(16), 9939-9947.

Zhao, L., Cao, X., Mašek, O., Zimmerman, A., 2013. Heterogeneity of biochar properties as a function of feedstock sources and production temperatures. Journal of Hazardous Materials 256-257, 1-9.

Zhao, Z., Knowlton, K.F., Love, N.G., Fang, Y., 2007. The removal of estrogens in different dairy manure treatments. American Society of Civil Engineers (ASCE), Tampa, FL, United states.

Zheng, W., Guo, M., Chow, T., Bennett, D.N., Rajagopalan, N., 2010. Sorption properties of greenwaste biochar for two triazine pesticides. Journal of Hazardous Materials 181(1-3), 121-126.

Zheng, W., Li, X., Yates, S.R., Bradford, S.A., 2012. Anaerobic transformation kinetics and mechanism of steroid estrogenic hormones in dairy lagoon water. Environmental Science and Technology 46(10), 5471-5478.

Zheng, W., Yates, S.R., Bradford, S.A., 2008. Analysis of steroid hormones in a typical dairy waste disposal system. Environmental Science and Technology 42(2), 530-535.

Zheng, W., Zou, Y., Li, X., Machesky, M.L., 2013. Fate of estrogen conjugate 17α-estradiol-3-sulfate in dairy wastewater: Comparison of aerobic and anaerobic degradation and metabolite formation. Journal of Hazardous Materials 258-259, 109-115.

Ziegler, R.G., Fuhrman, B.J., Moore, S.C., Matthews, C.E., 2015. Epidemiologic studies of estrogen metabolism and breast cancer. Steroids 99(Part A), 67-75.

Appendices

A.1 Physical, Inorganic and organic chemical parameters (supporting information Section 2.3.1)

Table A-1: Physical and organic properties of DSE samples

Parameter	Units	Mar	Apr	July	Aug	Oct	Nov
INFLUENT							
pH		7.22	8.24	7.18	7.36	N.A[A]	8.16
Temp	°C	19.1	18.0	13.0	11.6	N.A	18.0
TS	mg/L	N.A	5200	N.A	8700	6200	7700
VTS	mg/L	N.A	3200	N.A	5200	3300	5000
POM[B]	%	83.4	81.0	76.5	73.2	77.6	79.7
POC[C]	%	45.0	43.8	41.3	39.5	41.9	43.0
SLUDGE							
pH		6.88	6.90	6.88	6.98	N.A	7.03
Temp	°C	30.9	21.6	14.2	13.1	N.A	18.8
TS	mg/L	76039	N.A	N.A	N.A	N.A	88000
VTS	mg/L	38380	N.A	N.A	N.A	N.A	N.A
POM	%	58.2	48.2	59.8	60.1	61.2	65.5
POC	%	31.4	26.0	32.3	32.4	33.0	35.4
EFFLUENT							
pH		7.53	6.87	6.72	6.71	N.A	6.88
Temp	°C	20.2	18.7	11.9	12.4	N.A	18.0
TS	mg/L	N.A	4000	N.A	N.A	N.A	2900
VTS	mg/L	N.A	1360	N.A	N.A	N.A	1180
POM	%	N.A	34.0	60.6	63.7	60.9	40.7
POC	%	N.A	18.4	32.7	34.4	32.9	22.0

[A] N.A = Not available. [B] Particulate organic matter. [C] Particulate organic carbon.

A.2 Concentration of ESHs in the dissolved and solids phases (supporting information Section 2.3.4)

Table A-2: Mass of ESHs (ng) in the dissolved and solids phases of 1L of sample

	March			April			July		
DSE/CAP INFLUENT									
	Dissolved	Solid[A]	Total	Dissolved	Solid	Total	Dissolved	Solid	Total
17α-E2	1610	2147	3757	2869	2869	5738	1065	4789	5854
17β-E2	233	424	657	242	348	590	108	441	549
E1	282	496	778	415	412	827	106	753	859
ΣESHs	2125	3067	5192	3526	3629	7155	1279	5983	7262
CAP SLUDGE									
	Dissolved	Solid	Total	Dissolved	Solid	Total	Dissolved	Solid	Total
17α-E2	38.9	2074	2113	33.8	2028	2062	24.2	3109	3133
17β-E2	55.3	4182	4237	46.4	3805	3851	34.3	6193	6227
E1	881	61528	62409	835	84948	85783	581	71570	72151
ΣESHs	975	67784	68759	915	90781	91696	640	80872	81511
CAP EFFLUENT									
	Dissolved	Solid	Total	Dissolved	Solid	Total	Dissolved	Solid	Total
17α-E2	3.50	9.04	12.5	106	100	206	782	1907	2689
17β-E2	3.11	12.9	16.0	65.3	96.2	162	142	419	561
E1	68.7	90.7	160	1098	1476	2574	682	3258	3940
ΣESHs	75.3	113	189	1269	1672	2941	1606	5584	7190
	August			**October**			**November**		
DSE/CAP INFLUENT									
	Dissolved	Solid	Total	Dissolved	Solid	Total	Dissolved	Solid	Total
17α-E2	243	1212	1455	28.6	195	224	21.7	166	188
17β-E2	14.7	116	131	7.04	115	122	15.1	170	185
E1	43.8	619	663	5.19	320	325	68.3	2057	2125
ΣESHs	302	1947	2249	40.8	630	671	105	2393	2498
CAP SLUDGE									
	Dissolved	Solid	Total	Dissolved	Solid	Total	Dissolved	Solid	Total
17α-E2	27.0	2640	2667	35.3	2816	2851	21.4	2731	2752
17β-E2	33.5	5759	5792	64.9	6947	7012	43.1	6381	6424
E1	561	66711	67272	771	116124	116895	628	107348	107976
ΣESHs	622	75110	75731	871	125887	126758	693	116460	117152
CAP EFFLUENT									
	Dissolved	Solid	Total	Dissolved	Solid	Total	Dissolved	Solid	Total
17α-E2	416	1047	1463	208	433	641	84.5	239	324
17β-E2	142	503	645	69.0	334	403	11.3	106	117
E1	756	2379	3135	1011	4074	5085	43.7	3901	3945
ΣESHs	1314	3929	5243	1288	4841	6129	140	4246	4386

[A]ng of ESHs in solids of 1L of sample calculated by ng ESH /g solids x gm solid/L sample = ng ESH/L

A.3 Statistical summary of the mass of ESHs (ng) in the dissolved and solids phases of 1L of sample for the months of March to November (supporting information Section 2.3.4)

Table A-3: Statistical summary of the mass of ESHs (ng) in the dissolved and solids phases of 1L of sample for the months of March to November

INFLUENT															
	Dissolved					**Solids**					**Total**				
	mean	**SDev**	**Median**	**Min**	**Max**	**mean**	**SDev**	**Median**	**Min**	**Max**	**mean**	**SDev**	**Median**	**Min**	**Max**
17α-E2	973	1126	654	21.7	2869	1896	1774	1680	166	4789	2869	2612	2606	188	5854
17β-E2	103	110	62	7.04	242	269	153	259	115	441	372	251	367	122	657
E1	153	160	87	5.19	415	776	646	558	320	2057	930	617	803	325	2125
ΣESHs	1230	1387	791	40.8	3526	2942	1810	2730	630	5983	4171	2766	3845	671	7262
SLUDGE															
	Dissolved					**Solids**					**Total**				
	mean	**SDev**	**Median**	**Min**	**Max**	**mean**	**SDev**	**Median**	**Min**	**Max**	**mean**	**SDev**	**Median**	**Min**	**Max**
17α-E2	30.1	7	30.4	21.4	38.9	2566	429	2686	2028	3109	2596	425	2710	2062	3133
17β-E2	46.3	12	44.8	33.5	64.9	5545	1266	5976	3805	6947	5591	1266	6010	3851	7012
E1	710	137	700	561	881	84705	22510	78259	61528	116124	85414	22514	78967	62409	116895
ΣESHs	786	153	782	621	975	92816	23408	85827	67784	125887	93601	23411	86604	68759	126758
EFFLUENT															
	Dissolved					**Solids**					**Total**				
	mean	**SDev**	**Median**	**Min**	**Max**	**mean**	**SDev**	**Median**	**Min**	**Max**	**mean**	**SDev**	**Median**	**Min**	**Max**
17α-E2	267	290	157	3.50	782	623	730	336	9.04	1907	889	1018	483	12.5	2689
17β-E2	72.1	61	67.2	3.11	142	245	200	220	12.9	503	317	257	282	16.0	645
E1	610	456	719	43.7	1098	2530	1541	2819	90.7	4074	3140	1689	3538	160	5085
ΣESHs	949	663	1279	75.3	1606	3398	2080	4088	113	5584	4346	2503	4815	189	7190

A.4 Estrogenic equivalents of ESHs in the dissolved and solids phases (supporting information Section 2.3.9)

Table A-4: Estrogenic equivalents of ESHs in the dissolved and solids phases of 1L of sample

	March			April			July		
DSE/CAP INFLUENT									
	Dissolved	Solid[A]	Total	Dissolved	Solid	Total	Dissolved	Solid	Total
17α-E2	16.1	21.5	37.6	28.7	28.7	57.4	10.7	47.9	58.5
17β-E2	233	424	657	242	348	590	108	441	549
E1	5.64	9.92	15.6	8.3	8.24	16.5	2.12	15.1	17.2
ΣESHs	**255**	**455**	**710**	**279**	**385**	**664**	**121**	**504**	**625**
CAP SLUDGE									
	Dissolved	Solid	Total	Dissolved	Solid	Total	Dissolved	Solid	Total
17α-E2	0.39	20.7	21.1	0.34	20.3	20.6	0.24	31.1	31.3
17β-E2	55.3	4182	4237	46.4	3805	3851	34.3	6193	6227
E1	17.6	1231	1248	16.7	1699	1716	11.6	1431	1443
ΣESHs	**73.3**	**5434**	**5506**	**63.4**	**5524**	**5588**	**46.1**	**7655**	**7702**
CAP EFFLUENT									
	Dissolved	Solid	Total	Dissolved	Solid	Total	Dissolved	Solid	Total
17α-E2	0.04	0.09	0.13	1.06	1.00	2.06	7.82	19.1	26.9
17β-E2	3.11	12.9	16.0	65.3	96.2	162	142	419	561
E1	1.37	1.81	3.19	21.7	29.5	51.5	13.6	65.2	78.8
ΣESHs	**4.52**	**14.8**	**19.3**	**88.1**	**127**	**215**	**163**	**503**	**667**
	August			**October**			**November**		
DSE/CAP INFLUENT									
	Dissolved	Solid	Total	Dissolved	Solid	Total	Dissolved	Solid	Total
17α-E2	2.43	12.1	14.5	0.259	1.95	2.24	0.22	1.66	1.88
17β-E2	14.7	116	131	7.04	115	122	15.1	170	185
E1	0.88	12.4	13.3	0.10	6.40	6.50	1.37	41.1	42.5
ΣESHs	**18.0**	**141**	**159**	**7.43**	**123**	**131**	**16.7**	**213**	**229**
CAP SLUDGE									
	Dissolved	Solid	Total	Dissolved	Solid	Total	Dissolved	Solid	Total
17α-E2	0.27	26.4	26.7	0.35	28.2	29.0	0.21	27.3	28.0
17β-E2	33.5	5759	5793	64.9	6947	7012	43.1	6381	6424
E1	11.2	1334	1345	15.4	2323	2338	12.6	2147	2160
ΣESHs	**45.0**	**7119**	**7165**	**80.7**	**9298**	**9379**	**55.9**	**8555**	**8612**
CAP EFFLUENT									
	Dissolved	Solid	Total	Dissolved	Solid	Total	Dissolved	Solid	Total
17α-E2	4.16	10.47	14.6	2.08	4.33	6.41	0.85	2.39	3.24
17β-E2	142	503	645	69.0	334	403	11.3	106	117
E1	15.1	47.6	62.7	20.2	81.5	102	0.87	78.0	78.9
ΣESHs	**161**	**561**	**722**	**91.3**	**420**	**511**	**13.0**	**186**	**199**

[A]EEQs of ESHs in solids of 1L of sample calculated by ng ESH /g solids x gm solid/L sample = ng ESH

A.5 Kura Biotec BGS™ Hydrolysis Protocol (supporting information Section 3.2.4)

KURA® BIOTEC

BGS™ HYDROLYSIS STEPWISE PROTOCOL

1. Optional: urine specimen centrifugation, 5 minutes at 4°C at 20,000 x g.
2. Pipette 30 µL of urine.
3. Add buffer + ISDs + distilled water + enzyme according to Table 2.
4. Mix gently but thoroughly.
5. Incubate 30 minutes at 45°C.
6. Proceed with preferred quantification process.

TABLE 2. HYDROLYSIS MIX COMPOSITION

Compound	Volume (µL)
Urine	30
Instant Buffer II	30
Distilled water	180
Internal Standards (10% MeOH)	30
BGS™	30
TOTAL	300

NOTES

- The above protocol is based on an initial volume of 30 µl of urine, however, the mix could be adapted to any required urine volume by keeping the given proportions.
- The mix should not exceed 1% v/v final concentration of MeOH. Sulfatase activity decreases if a higher MeOH concentration is added to the mix.
- It's important to keep a consistent enzyme-to-urine ratio in order to achieve expected recoveries within 30 minutes, not only in spiked urine, but also in authentic specimens.
- It's important to keep a urine dilution of at least 10X, to preserve the activity of the arylsulfatase, which is strongly inhibited by phosphates present in the urine.

REFERENCES

1. Da Silva, K., Kwan, R. and Rabbia, V., et al (2016). Poster Streamlining Sample Preparation with Second Generation Enzymes. Presented at Society of Forensic Toxicologists Conference, Inc. View it here
2. ElSohly Laboratories, Inc., (2016). BGTurbo glucuronidase evaluation for the hydrolysis of morphine-3-Glucoronide and codeine-6-Glucuronide at different concentrations at 10 minutes and comparison with EBG and IMCZYME at different incubation times. Evaluation carried out for Kura Biotec. View it here
3. Shellinger, A. and Carr, P., (2004). Solubility of Buffers in Aqueous–Organic Effluents for Reversed-Phase Liquid Chromatography. View it here

PRECAUTIONS AND DISCLAIMER

This document is for R&D use only, not for use in diagnostic procedures. Please consult the Material Safety Data Sheet for information regarding hazards and safe handling practices.

CONTACT AND SUPPORT

To ask questions, solve problems, suggest protocol or product enhancements or report new applications, please contact us at www.kurabiotec.com or email us at Info@kurabiotec.com.

PATENTS & TRADEMARKS

Kura Biotec® and BGTurbo® are registered trademarks of Kura Biotec SpA in Chile.
HYDROLYZE-ANALYZE™, EBG™ and BAMf™ are trademarks of Kura Biotec SpA in Chile.

U.S. Patent Nos. 20180067116 and patents pending.

©2019 Kura Biotech Inc.
2373 E Pacifica Place
Rancho Dominguez, CA, 90220, US
+1 800 332 1448

Figure A-1: BGS enzyme protocol (including an indicative method used as a base for the development of the DSE conjugated ESHs method

A.6 Optimisation of the deconjugation procedure (supporting information Section 3.3.1.1)

Table A-5: Recovery of parent 17β-E2 from Milli-Q-Water spiked with the glucuronide ESH conjugates βE2-3-G and βE2-17-G (spiked at 500 ng each) and the free estrogenic steroid surrogate standard ^{13}C6-E2 (spiked at 100 ng)

Trial	Description	Enzyme	Enzyme Incubation time[A]	Enzyme Incubation temperature[B]	Milli-Q-Water/Buffer /enzyme volume[C]	βE2-3-G recovery		βE2-17-G recovery	
						Parent 17β-E2	^{13}C6-E2	Parent 17β-E2	^{13}C6-E2
1	Enzymatic Hydrolysis	BGS (50% glycerol)	30	45	800/100/100	74.8 (4.17, n=2)[D]	102 (3.25, n=2)	78.8 (0.78, n=2)	102 (1.41, n=2)
2	Enzymatic Hydrolysis	BGS (50% glycerol)	45	45	240/50/50	85.4 (1.20, n= 2)	101 (1.41, n=2)	87.9 (2.94, n=2)	97.4 (3.37, n=2)
3	Enzymatic Hydrolysis	BGS (50% glycerol)	45	45	240/100/100	81.1 (3.25, n=2)	92.6 (1.56, n=2)	91.5 (7.10, n=2)	97.7 (9.91, n=2)
4	Enzymatic Hydrolysis	BGS (50% glycerol)	45	45	240/150/150	87.0 (0.28, n=2)	99.4 (0.28, n=2)	90.3 (2.05, n=2)	102 (5.09, n=2)
5	Enzymatic Hydrolysis	BGS (10% glycerol)	45	53	240/100/100	57.0 (31.3, n=4)	67.9 (27.8, n=4)	60.6 (23.6, n=4)	73.2 (24.6, n=4)
6	Solvolysis (using 8 mL tube)[E]	N/A[F]	N/A	N/A	N/A	N/A	N/A	N/A	N/A
7	Solvolysis (using 1 mL vial)[E]	N/A	N/A	N/A	N/A	N/A	N/A	N/A	N/A
8	Solvolysis followed by Enzymatic Hydrolysis	BGS (10% glycerol)	45	53	240/100/100	36.3 (6.79, n=2)	54.0 (6.51, n=2)	44.4 (8.27, n=2)	36.9 (6.08, n=2)

9	Solvolysis followed by Enzymatic Hydrolysis	BGS (10% glycerol)	180	53	240/100/100	11.0 (9.64, n=2)	35.7 (5.09, n=2)	14.4 (0.66, n=2)	13.4 (2.23, n=2)
10	Solvolysis followed by Enzymatic Hydrolysis	BGS (10% glycerol)	1440	53	240/100/100	12.0 (2.33, n=2)	65.1 (38.9, n=2)	9.80 (2.84, n=2)	10.1 (0.90, n=2)
11	Enzymatic Hydrolysis followed solvolysis	BGS (10% glycerol)	45	53	240/100/100	76.1 (N/A, n=1)	82.7 (N/A, n=1)	67.9 (9.90, n=2)	74.1 (16.8, n=2)
12	Solvolysis followed by Enzymatic Hydrolysis	Helix P (Type HP-2)	180	55	400/5000/30	67.7 (1.22, n=3)	83.0 (1.65, n=3)	62.2 (2.72, n=3)	78.9 (3.00, n=3)

A expressed as minutes. **B** expressed as °C. **C** expressed as µL. **D** mean recovery value expressed as % (standard deviation, number of samples). **E** Chemical solvolysis of glucuronidated ESHs was not assessed. **F** not applicable. Note: The solvolysis and Helix P enzymatic hydrolysis were completed based on previous studies performed by Labadie and Budzinski (2005a). The BGS™ enzymatic hydrolysis was performed based on J. L. Callejas (2019).

Table A-6: Recovery of parent 17β-E2 and E1 from Milli-Q-Water spiked with the sulphate ESH conjugates βE2-3,17-diS and E1-3-S (spiked at 500 ng each), and the free estrogenic steroid surrogate standards ^{13}C6-E2 and ^{13}C6-E1(spiked at 100 ng each)

Trial	Description	Enzyme	Enzyme Incubation time[A]	Enzyme Incubation temperature[B]	Milli-Q-Water/Buffer /enzyme volume[C]	βE2-3,17-diS		E1-3-S	
						Parent 17β-E2	^{13}C6-E2	Parent E1	^{13}C6-E1
1	Enzymatic Hydrolysis	BGS (50% glycerol)	30	45	800/100/100	2.17 (1.25, n=2)[D]	104 (6.29, n=2)	45.0 (0.92, n=2)	104 (0.71, n=2)
2	Enzymatic Hydrolysis	BGS (50% glycerol)	45	45	240/50/50	121 (4.24, n= 2)	101 (2.19, n=2)	26.9 (1.63, n=2)	103 (3.00, n=2)
3	Enzymatic Hydrolysis	BGS (50% glycerol)	45	45	240/100/100	109 (10.34, n=2)	92.1 (3.05, n=2)	27.5 (2.75, n=2)	99.8 (0.10, n=2)
4	Enzymatic Hydrolysis	BGS (50% glycerol)	45	45	240/150/150	116 (9.90, n=2)	92.8 (0.64, n=2)	31.1 (0.37, n=2)	102 (4.00, n=2)
5	Enzymatic Hydrolysis	BGS (10% glycerol)	45	53	240/100/100	0.38 (0.37, n=4)	68.1 (17.5, n=4)	33.8 (12.4, n=4)	72.9 (17.4, n=4)
6	Solvolysis (using 8 mL tube)[E]	N/A[F]	N/A	N/A	N/A	42.4 (1.70, n=2)	107 (2.12, n=2)	44.3 (3.54, n=2)	104 (4.24, n=2)
7	Solvolysis (using 1 mL vial)[E]	N/A	N/A	N/A	N/A	112 (0.71, n=2)	90.4 (4.17, n=2)	N/A	N/A
8	Solvolysis followed by Enzymatic Hydrolysis	BGS (10% glycerol)	45	53	240/100/100	34.7 (3.04, n=2)	59.5 (0.92, n=2)	50.6 (1.20, n=2)	116 (2.12, n=2)
9	Solvolysis followed by Enzymatic Hydrolysis	BGS (10% glycerol)	180	53	240/100/100	39.4 (27.3, n=2)	53.5 (17.1, n=2)	39.5 (0.60, n=2)	69.6 (10.4, n=2)
10	Solvolysis followed by Enzymatic Hydrolysis	BGS (10% glycerol)	1440	53	240/100/100	9.17 (0.35, n=2)	34.8 (0.31, n=2)	N/A	N/A
11	Enzymatic Hydrolysis followed solvolysis	BGS (10% glycerol)	45	53	240/100/100	36.7 (N/A, n=1)	91.2 (N/A, n=1)	48.5 (10.7, n=4)	103 (30.1, n=4)
12	Solvolysis followed by Enzymatic Hydrolysis	Helix P (Type HP-2)	180	55	400/5000/30	29.8 (7.37, n=6)	86.4 (3.25, n=6)	40.6 (3.41, n=6)	84.3 (6.69, n=6)

[A] expressed as minutes. [B] expressed as °C. [C] expressed as µL. [D] mean recovery value expressed as % (standard deviation, number of samples). [E] Chemical solvolysis of glucuronidated ESHs was not assessed. [F] not applicable. Note: The solvolysis and Helix P enzymatic hydrolysis were completed based on previous studies performed by Labadie and Budzinski (2005a). The BGS™ enzymatic hydrolysis was performed based on J. L. Callejas (2019).

A.7 Concentration of conjugated ESHs in the dissolved and solid phases (supporting information Section 3.3.2.2)

Table A-7: Mass of conjugated ESHs (ng) in the dissolved and solid phases of 1L of sample

	March			April			July		
DSE/CAP INFLUENT									
Σconj	Dissolved[A]	Solid[B]	Total	Dissolved	Solid	Total	Dissolved	Solid	Total
17α-E2	86.8	20.4	107	89.1	257	346	74.3	240	314
17β-E2	N.D[C]	N.D	N.D	6.56	62.6	69.1	30.5	56.9	87.4
E1	N.D	N.D	N.D	137	N.D	137	N.D	63.7	63.7
ΣESHs	86.8	20.4	107	233	320	552	105	360	465
CAP SLUDGE									
Σconj	Dissolved	Solid	Total	Dissolved	Solid	Total	Dissolved	Solid	Total
17α-E2	N.D	N.D	N.D	N.D	N.D	N.D	N.D	19.7	19.7
17β-E2	N.D	1284	1284	N.D	208	208	N.D	860	860
E1	N.D	N.D	N.D	N.D	N.D	N.D	N.D	1626	1626
ΣESHs	N.D	1284	1284	N.D	208	208	N.D	2505	2505
CAP EFFLUENT									
Σconj	Dissolved	Solid	Total	Dissolved	Solid	Total	Dissolved	Solid	Total
17α-E2	N.D	N.D	N.D	N.D	N.D	N.D	40.2	35.3	75.5
17β-E2	N.D	N.D	N.D	N.D	N.D	N.D	N.D	17.9	17.9
E1	N.D	N.D	N.D	N.D	N.D	N.D	N.D	N.D	N.D
ΣESHs	N.D	N.D	N.D	N.D	N.D	N.D	40.2	53.2	93.4
	August			October			November		
DSE/CAP INFLUENT									
Σconj	Dissolved	Solid	Total	Dissolved	Solid	Total	Dissolved	Solid	Total
17α-E2	33.7	79.2	113	22.6	N.D	22.6	26.6	12.2	38.8
17β-E2	67.4	31.0	98.4	40.1	N.D	40.1	51.6	N.D	51.6
E1	N.D	N.D	N.D	7.12	N.D	7.12	6.78	N.D	6.78
ΣESHs	101	110	211	69.8	N.D	69.8	84.9	12.2	97.1
CAP SLUDGE									
Σconj	Dissolved	Solid	Total	Dissolved	Solid	Total	Dissolved	Solid	Total
17α-E2	N.D	1241	1241	N.D	N.D	N.D	N.D	N.D	N.D
17β-E2	16.0	131	147	17.6	223	241	6.27	208	214
E1	N.D	N.D	N.D	N.D	N.D	N.D	N.D	N.D	N.D
ΣESHs	16.0	1372	1388	17.6	223	241	6.27	208	214
CAP EFFLUENT									
Σconj	Dissolved	Solid	Total	Dissolved	Solid	Total	Dissolved	Solid	Total
17α-E2	30.1	27.6	57.7	48.8	N.D	48.8	37.0	N.D	37.0
17β-E2	N.D	16.9	16.9	8.75	N.D	8.75	9.00	N.D	9.00
E1	141	20.4	161	N.D	N.D	N.D	N.D	N.D	N.D
ΣESHs	170	65.0	236	57.6	N.D	57.6	46.0	N.D	46.0

[A] values are expressed as ng/L. [B]ng of conjugated ESHs in solids of 1L of sample calculated by ng conjugated ESH /g solids x gm solid/L sample = ng conjugated ESH/L. [C] not detected

Table A-8: Statistical summary of the mass of conjugated ESHs (ng) in the dissolved and solid phases of 1L of sample for the months of March to November

DSE/CAP INFLUENT															
	Dissolved					Solids					Total				
Σconj	**Mean[A]**	**Sdev[B]**	**Median**	**Min**	**Max**	**Mean**	**Sdev**	**Median**	**Min**	**Max**	**Mean**	**Sdev**	**Median**	**Min**	**Max**
17α-E2	55.5	31.2	54.0	22.6	89.1	101	117	49.8	N.D	257	157	139	110	22.6	346
17β-E2	32.7	26.0	35.3	N.D[C]	67.4	25.1	29.5	15.5	N.D	62.6	57.8	24.2	69.1	N.D	98.4
E1	25.2	54.9	3.39	N.D	137	10.6	26.0	N.D	N.D	63.7	35.8	61.7	35.4	N.D	137
ΣESHs	113	59.8	94.0	69.8	233	137	162	65.3	N.D	360	250	207	159	69.8	552
CAP SLUDGE															
	Dissolved					**Solids**					**Total**				
Σconj	**Mean**	**Sdev**	**Median**	**Min**	**Max**	**Mean**	**Sdev**	**Median**	**Min**	**Max**	**Mean**	**Sdev**	**Median**	**Min**	**Max**
17α-E2	N.D	N.D	N.D	N.D	N.D	210	505	N.D	N.D	1241	210	864	630	N.D	1241
17β-E2	6.65	8.25	3.14	N.D	17.6	486	475	215	131	1284	492	469.6	228	147	1284
E1	N.D	N.D	N.D	N.D	N.D	271	664	N.D	N.D	1626	271	N.D	1626	N.D	1626
ΣESHs	6.65	8.25	3.14	N.D	17.6	967	931	754	208	2505	973	929	763	208	2505
CAP EFFLUENT															
	Dissolved					**Solids**					**Total**				
Σconj	**Mean**	**Sdev**	**Median**	**Min**	**Max**	**Mean**	**Sdev**	**Median**	**Min**	**Max**	**Mean**	**Sdev**	**Median**	**Min**	**Max**
17α-E2	26.0	21.0	33.5	N.D	48.8	10.5	16.4	N.D	N.D	35.3	36.5	16	53.3	N.D	75.5
17β-E2	2.96	4.58	N.D	N.D	9.00	5.81	9.00	N.D	N.D	17.9	8.80	4.9	13.0	N.D	17.9
E1	23.5	57.5	N.D	N.D	141	3.40	8.34	N.D	N.D	20.4	27.0	N.D	161	N.D	161
ΣESHs	52.5	62.9	43.1	N.D	171	19.7	30.7	N.D	N.D	65.0	72.0	88	75.5	N.D	236

[A] values are expressed as ng/L. [B] standard deviation. [C] not detected

A.8 Contribution of conjugated ESHs to the dissolved and solid phases ESH load within a CAP influent, sludge and effluent (supporting information Section 3.3.4)

Table A-9: Concentration of conjugated and free ESHs measured in the dissolved and solid phases of raw influent, sludge and effluent of the CAP system (March and April)

	March						April					
DSE/CAP INFLUENT												
	Dissolved Phase ESHs		**Solids Phase ESHs**		**Total[A] ESHs**		**Dissolved Phase ESHs**		**Solids Phase ESHs**		**Total ESHs**	
	ΣConj[B]	**Free**	**ΣConj**	**Free**	**ΣConj**	**Free**	**ΣConj**	**Free**	**ΣConj**	**Free**	**ΣConj**	**Free**
17α-E2	86.8[C]	1610	20.4	2147	107	3757	89.1	2869	257	2869	346	5738
17β-E2	N.D[D]	233	N.D	424	N.D	657	6.56	242	62.6	348	69.1	590
E1	N.D	282	N.D	496	N.D	778	137	415	N.D	412	137	827
ΣESHs	86.8	2125	20.4	3067	107	5192	233	3526	320	3629	552	7155
CAP SLUDGE												
17α-E2	N.D	38.9	N.D	2074	N.D	2113	N.D	33.8	N.D	2028	N.D	2062
17β-E2	N.D	55.3	1284	4182	1284	4237	N.D	46.4	208	3805	208	3851
E1	N.D	881	N.D	61528	N.D	62409	N.D	835	N.D	84948	N.D	85783
ΣESHs	N.D	975	1284	67784	1284	68759	N.D	915	208	90781	208	91696
CAP EFFLUENT												
17α-E2	N.D	3.50	N.D	9.04	N.D	12.5	N.D	106	N.D	100	N.D	206
17β-E2	N.D	3.11	N.D	12.9	N.D	16.0	N.D	65.3	N.D	96.2	N.D	162
E1	N.D	68.7	N.D	90.7	N.D	160	N.D	1098	N.D	1476	N.D	2574
ΣESHs	N.D	75.3	N.D	113	N.D	189	N.D	1269	N.D	1672	N.D	2941

[A] combined dissolved and solid phase. [B] ΣConj = ΣConjugated. [C] The measured concentration of conjugated ESHs in the corresponding phase of each sample (in ng/L). [D] not detected.

Table A-10: Concentration of conjugated and free ESHs measured in the dissolved and solid phases of raw influent, sludge and effluent of the CAP system (July and August)

	July						August					
DSE/CAP INFLUENT												
	Dissolved Phase ESHs		**Solids Phase ESHs**		**Total[A] ESHs**		**Dissolved Phase ESHs**		**Solids Phase ESHs**		**Total ESHs**	
	ΣConj[B]	**Free**	**ΣConj**	**Free**	**ΣConj**	**Free**	**ΣConj**	**Free**	**ΣConj**	**Free**	**ΣConj**	**Free**
17α-E2	74.3[C]	1065	240	4789	314	5854	33.7	243	79.2	1212	113	1455
17β-E2	30.5	108	56.9	441	87.4	549	67.4	14.7	31.0	116	98.4	131
E1	N.D[D]	106	63.9	753	63.7	859	N.D	43.8	N.D	619	N.D	663
ESHs	105	1279	360	5983	465	7262	101	302	110	1947	211	2249
CAP SLUDGE												
17α-E2	N.D	24.2	19.7	3109	19.7	3133	N.D	27.0	1241	2640	1241	2667
17β-E2	N.D	34.3	860	6193	860	6227	16.0	33.5	131	5759	147	5792
E1	N.D	581	1626	71570	1626	72151	N.D	561	N.D	66711	N.D	67272
ESHs	N.D	640	2505	80872	2505	81511	16.0	622	1372	75110	1388	75731
CAP EFFLUENT												
17α-E2	40.2	782	35.3	1907	75.5	2689	30.1	416	27.3	1047	57.7	1463
17β-E2	N.D	142	17.9	419	17.9	561	N.D	142	16.9	503	16.9	645
E1	N.D	682	N.D	3258	N.D	3940	141	756	20.4	2379	161	3135
ESHs	40.2	1606	53.2	5584	93.4	7190	170	1314	65.0	3929	236	5243

[A] combined dissolved and solid phase. [B] ΣConj = ΣConjugated. [C] The measured concentration of conjugated ESHs in the corresponding phase of each sample (in ng/L). [D] not detected.

Table A-11: Concentration of conjugated and free ESHs measured in the dissolved and solid phases of raw influent, sludge and effluent of the CAP system (October and November)

	October						November					
DSE/CAP INFLUENT												
	Dissolved Phase ESHs		**Solids Phase ESHs**		**Total[A] ESHs**		**Dissolved Phase ESHs**		**Solids Phase ESHs**		**Total ESHs**	
	ΣConj[B]	**Free**	**ΣConj**	**Free**	**ΣConj**	**Free**	**ΣConj**	**Free**	**ΣConj**	**Free**	**ΣConj**	**Free**
17α-E2	22.6[C]	28.6	N.D[D]	195	22.6	224	26.6	21.7	12.2	166	38.8	188
17β-E2	40.1	7.04	N.D	115	40.1	122	51.6	15.1	N.D	170	51.6	185
E1	7.12	5.19	N.D	320	7.12	325	6.78	68.3	N.D	2057	6.78	2125
ESHs	69.8	40.8	N.D	630	69.8	671	84.9	105	12.2	2393	97.1	2498
CAP SLUDGE												
17α-E2	N.D	35.3	N.D	2816	N.D	2851	N.D	21.4	N.D	2731	N.D	2752
17β-E2	17.6	64.9	223	6947	241	7012	6.27	43.1	208	6381	214	6424
E1	N.D	771	N.D	116124	N.D	116895	N.D	628	N.D	107348	N.D	107976
ESHs	17.6	871	223	125887	241	126758	6.27	693	208	116460	214	117152
CAP EFFLUENT												
17α-E2	48.8	208	N.D	433	48.8	641	37.0	84.5	N.D	239	37.0	324
17β-E2	8.75	69.0	N.D	334	8.75	403	9.00	11.3	N.D	106	9.00	117
E1	N.D	1011	N.D	4074	N.D	5085	N.D	43.7	N.D	3901	N.D	3945
ESHs	57.6	1288	N.D	4841	57.6	6129	46.0	140	N.D	4246	46.0	4386

[A] combined dissolved and solid phase. [B] ΣConj = ΣConjugated. [C] The measured concentration of conjugated ESHs in the corresponding phase of each sample (in ng/L). [D] not detected.

Table A-12: Phase related contribution of conjugated ESHs to the dissolved and solid phases and total ESH load within a CAP influent, sludge and effluent (March-July)

	March			April			July		
DSE/CAP INFLUENT									
	ΣConj[A] ESHs Dissolved Phase	**ΣConj ESHs Solids Phase**	**ΣConj ESHs Total[B]**	**ΣConj ESHs Dissolved Phase**	**ΣConj ESHs Solids Phase**	**ΣConj ESHs Total**	**ΣConj ESHs Dissolved Phase**	**ΣConj ESHs Solids Phase**	**ΣConj ESHs Total**
17α-E2	5.12[C]	0.94	2.77	3.01	8.22	5.69	6.52	4.77	5.09
17β-E2	N.D[D]	N.D	N.D	2.64	15.3	10.5	22.0	11.4	13.7
E1	N.D	N.D	N.D	24.8	N.D	14.2	N.D	7.82	6.90
ESHs	3.92	0.66	2.02	6.20	8.10	7.16	7.59	5.68	6.02
CAP SLUDGE									
	ΣConj ESHs Dissolved Phase	**ΣConj ESHs Solids Phase**	**ΣConj ESHs Total**	**ΣConj ESHs Dissolved Phase**	**ΣConj ESHs Solids Phase**	**ΣConj ESHs Total**	**ΣConj ESHs Dissolved Phase**	**ΣConj ESHs Solids Phase**	**ΣConj ESHs Total**
17α-E2	N.D	N.D	N.D	N.D	N.D	N.D	N.D	0.63	0.62
17β-E2	N.D	23.5	23.3	N.D	5.18	5.12	N.D	12.2	12.1
E1	N.D	N.D	N.D	N.D	N.D	N.D	N.D	2.22	2.20
ESHs	N.D	1.86	1.83	N.D	0.23	0.23	N.D	3.00	2.98
CAP EFFLUENT									
	ΣConj ESHs Dissolved Phase	**ΣConj ESHs Solids Phase**	**ΣConj ESHs Total**	**ΣConj ESHs Dissolved Phase**	**ΣConj ESHs Solids Phase**	**ΣConj ESHs Total**	**ΣConj ESHs Dissolved Phase**	**ΣConj ESHs Solids Phase**	**ΣConj ESHs Total**
17α-E2	N.D	N.D	N.D	N.D	N.D	N.D	4.89	1.82	2.73
17β-E2	N.D	N.D	N.D	N.D	N.D	N.D	N.D	4.10	3.09
E1	N.D	N.D	N.D	N.D	N.D	N.D	N.D	N.D	N.D
ESHs	N.D	N.D	N.D	N.D	N.D	N.D	2.44	0.94	1.28

[A] ΣConj = ΣConjugated. [B] combined dissolved and solid phases. [C] The phase related contribution of conjugated ESHs (in %). [D] not detected.

Table A-13: Phase related contribution of conjugated ESHs to the dissolved and solid phases and total ESH load within a CAP influent, sludge and effluent (August-November)

	August			October			November		
DSE/CAP INFLUENT									
	ΣConj[A] ESHs Dissolved Phase	**ΣConj ESHs Solids Phase**	**ΣConj ESHs Total[B]**	**ΣConj ESHs Dissolved Phase**	**ΣConj ESHs Solids Phase**	**ΣConj ESHs Total**	**ΣConj ESHs Dissolved Phase**	**ΣConj ESHs Solids Phase**	**ΣConj ESHs Total**
17α-E2	12.2[C]	6.13	7.21	44.1	N.D	9.16	55.1	6.85	17.1
17β-E2	82.1	21.1	42.9	85.1	N.D	24.7	77.4	N.A	21.8
E1	N.D[D]	N.D	N.D	57.8	N.D	2.14	9.03	N.A	0.32
ESHs	25.1	5.35	8.58	63.1	N.D	9.42	44.7	0.51	3.74
CAP SLUDGE									
	ΣConj ESHs Dissolved Phase	**ΣConj ESHs Solids Phase**	**ΣConj ESHs Total**	**ΣConj ESHs Dissolved Phase**	**ΣConj ESHs Solids Phase**	**ΣConj ESHs Total**	**ΣConj ESHs Dissolved Phase**	**ΣConj ESHs Solids Phase**	**ΣConj ESHs Total**
17α-E2	N.D	32.0	31.8	N.D	N.D	N.D	N.D	N.D	N.D
17β-E2	32.3	2.22	2.48	21.3	3.11	3.32	12.7	3.16	3.22
E1	N.D	N.D	N.D	N.D	N.D	N.D	N.D	N.D	N.D
ESHs	2.51	1.79	1.80	1.98	0.18	0.19	0.90	0.18	0.18
CAP EFFLUENT									
	ΣConj ESHs Dissolved Phase	**ΣConj ESHs Solids Phase**	**ΣConj ESHs Total**	**ΣConj ESHs Dissolved Phase**	**ΣConj ESHs Solids Phase**	**ΣConj ESHs Total**	**ΣConj ESHs Dissolved Phase**	**ΣConj ESHs Solids Phase**	**ΣConj ESHs Total**
17α-E2	6.75	2.54	3.79	19.0	N.D	7.07	30.5	N.D	10.3
17β-E2	N.A	3.25	2.55	11.3	N.D	2.13	44.3	N.D	7.14
E1	15.7	0.85	4.88	N.A	N.D	N.D	N.D	N.D	N.D
ESHs	11.5	1.63	4.31	4.28	N.D	0.93	24.7	N.D	1.04

[A] ΣConj = ΣConjugated. [B] combined dissolved and solid phases. [C] The phase related contribution of conjugated ESHs (in %). [D] not detected.

Table A-14: Statistical summary of phase related contribution of conjugated ESHs to the dissolved, solid and total phase ESH load within a CAP influent, sludge and effluent

DSE/CAP INFLUENT												
	Dissolved phase				Solids Phase				Total			
Σconj	**Mean**	**Range[A]**	**Median**	**Sdev [B]**	**Mean**	**Range[A]**	**Median**	**Sdev [B]**	**Mean**	**Range[A]**	**Median**	**Sdev [B]**
17α-E2	21.0	3.01-55.0	9.35	22.6	4.47	N.D-8.22	5.45	3.30	7.84	2.77-9.18	6.44	5.02
17β-E2	44.9	N.D-85.1	49.7	40.9	7.96	N.D-21.1	5.72	9.24	18.9	N.D-42.9	17.8	14.6
E1	15.28	N.D-57.8	4.52	23.0	1.30	N.D-7.83	N.D	3.20	3.93	N.D-14.2	1.23	5.69
ESHs	25.1	3.93-63.1	16.3	24.3	3.38	N.D-8.09	3.01	3.42	6.2	2.02-9.42	6.59	2.58
CAP SLUDGE												
17α-E2	N.D	N.D	N.D	N.D	5.43	N.D-32.0	N.D	13.0	5.40	N.D-31.9	N.D	12.9
17β-E2	11.1	N.D-32.4	6.35	13.6	8.22	2.23-23.5	4.16	8.32	8.25	2.48-13.3	4.22	8.16
E1	N.D	N.D	N.D	N.D	0.37	N.D-2.22	N.D	0.91	0.37	N.D-2.20	N.D	0.90
ESHs	0.90	N.D-2.52	0.45	1.11	1.21	0.18-3.00	1.01	1.19	1.20	0.18-2.98	1.01	1.18
CAP EFFLUENT												
17α-E2	10.2	N.D-30.5	5.82	12.1	0.73	N.D-2.56	N.D	1.16	3.97	N.D-10.3	3.26	4.05
17β-E2	9.26	N.D-44.3	N.D	17.8	1.23	N.D-3.25	N.D	1.92	2.49	N.D-7.14	2.34	2.63
E1	2.62	N.D-15.7	N.D	6.41	0.14	N.D-0.85	N.D	0.35	0.82	N.D-4.89	N.D	2.00
ESHs	7.17	N.D-24.8	3.36	9.62	0.43	N.D-1.62	N.D	0.70	1.26	N.D-4.31	0.98	1.59

[A] minimum to maximum. **[B]** standard deviation. **[C]** values are expressed as percentage (%). **[D]** not detected as no conjugated ESHs was measured.

A.9 Conjugated ESHs Implications (supporting information Section 3.3.5)

Table A-15: Estrogenic equivalents of conjugated ESHs in the dissolved and solids phases of 1L of sample

	March			April			July		
DSE/CAP INFLUENT									
	Dissolved	Solid[A]	Total	Dissolved	Solid	Total	Dissolved	Solid	Total
17α-E2	0.87	0.20	1.01	0.89	2.57	3.46	0.74	2.4	3.14
17β-E2	N.D[B]	N.D	N.D	6.56	62.6	69.1	30.5	56.9	87.4
E1	N.D	N.D	N.D	N.D	N.D	N.D	N.D	1.27	1.27
ΣESHs	0.87	0.20	1.01	7.45	65.2	72.6	31.24	60.6	91.8
CAP SLUDGE									
	Dissolved	Solid	Total	Dissolved	Solid	Total	Dissolved	Solid	Total
17α-E2	N.D	N.D	N.D	N.D	N.D	N.D	N.D	0.20	0.20
17β-E2	N.D	1284	1284	N.D	208	208	N.D	860	860
E1	N.D	N.D	N.D	N.D	N.D	N.D	N.D	32.5	32.5
ΣESHs	N.D	1284	1248	N.D	208	208	N.D	893	893
CAP EFFLUENT									
	Dissolved	Solid	Total	Dissolved	Solid	Total	Dissolved	Solid	Total
17α-E2	N.D	N.D	N.D	N.D	N.D	N.D	0.40	0.35	0.76
17β-E2	N.D	N.D	N.D	N.D	N.D	N.D	N.D	17.9	17.9
E1	N.D	N.D	N.D	N.D	N.D	N.D	N.D	N.D	N.D
ΣESHs	N.D	N.D	N.D	N.D	N.D	N.D	0.40	18.3	18.7
	August			October			November		
DSE/CAP INFLUENT									
	Dissolved	Solid	Total	Dissolved	Solid	Total	Dissolved	Solid	Total
17α-E2	0.34	0.79	1.13	0.23	N.D	0.23	0.27	0.12	0.39
17β-E2	67.4	31.0	98.4	40.1	N.D	40.1	51.6	N.D	51.6
E1	N.D	N.D	N.D	0.14	N.D	0.14	0.14	N.D	0.14
ΣESHs	67.7	31.8	99.5	40.5	N.D	40.5	52.0	0.12	52.1
CAP SLUDGE									
	Dissolved	Solid	Total	Dissolved	Solid	Total	Dissolved	Solid	Total
17α-E2	N.D	12.4	12.4	N.D	N.D	N.D	N.D	N.D	N.D
17β-E2	16.0	131	147	17.6	223	241	6.27	208	214
E1	N.D	N.D	N.D	N.D	N.D	N.D	N.D	N.D	N.D
ΣESHs	16.0	143	159	17.6	223	241	6.27	208	214
CAP EFFLUENT									
	Dissolved	Solid	Total	Dissolved	Solid	Total	Dissolved	Solid	Total
17α-E2	0.30	0.28	0.58	0.50	N.D	0.50	0.37	N.D	0.37
17β-E2	N.D	16.9	16.9	8.75	N.D	8.75	9.00	N.D	9.00
E1	2.82	0.41	3.23	N.D	N.D	N.D	N.D	N.D	N.D
ΣESHs	3.12	17.6	10.7	9.24	N.D	9.24	9.37	N.D	9.37

[A]EEQs of conjugated ESHs in solids of 1L of sample calculated by ng ESH /g solids x gm solid/L sample = ng conjugated ESH/L. [B] not detected

A.10 Adsorption kinetics (supporting information Section 4.6.4)

Table A-16: Adsorption kinetic of target 17α-E2, triplicate samples spiked at nominal concentration of ~2,500 ng/mL (50 mL CaCl2) into a fix biochar mass (1 mg ± 0.08 mg) at pH = 7 ±0.2 and temperature = 20°C± 2°C

	17α-E2		
Time [A]	**Solution concentration (C_t)**	**Percentage adsorbed**	**Powdered biochar ESH concentration**
0	2,931 (50.5)[B]	N.C[E]	N.C
0.5	1,732 (132)	39.2 (4.47)[C]	59,956 (4,383)[D]
1	1,300 (75.1)	49.9 (2.54)	80,461 (1,216)
2	857 (116)	70.4 (3.91)	99,697 (3,805)
3	772 (48.6)	71.6 (1.64)	106,193 (516)
6	517 (36.5)	82.0 (1.23)	119,900 (3,328)
9	397 (37.2)	86.4 (1.26)	125,890 (1,405)
12	203 (29.1)	93.2 (0.98)	135,499 (3,953)
16	218 (34.7)	92.8 (1.17)	132,570 (3,662)
24	184 (72.5)	93.6 (2.45)	133,366 (1,089)

[A] Actual values expressed as hours, [B] values are expressed as (mean (ng/mL) (SDev), [C] values are expressed as (mean (%) (SDev), [D] values are expressed as (mean (ng/mg) (SDev), [E] not applicable as no biochar was used.

Table A-17: Adsorption kinetic of target 17β-E2, triplicate samples spiked at nominal concentration of ~2,500 ng/mL (50 mL CaCl2) into a fix biochar mass (1 mg ± 0.08 mg) at pH = 7 ±0.2 and temperature = 20°C± 2°C

	17β-E2		
Time [A]	**Solution concentration (C_t)**	**Percentage adsorbed**	**Powdered biochar ESH concentration**
0	2,233 (55.3)[B]	N.C[E]	N.C
0.5	1,243 (22.7)	43.3 (0.95)[C]	49,322 (1,876)[D]
1	1,031 (44.2)	53.8 (1.86)	58,146 (3,388)
2	731 (41.9)	68.3 (1.76)	73,360 (4,459)
3	491 (27.4)	77.8 (1.15)	85,654 (2,731)
6	461 (38.4)	78.8 (1.61)	88,290 (3,175)
9	378 (21.7)	83.4 (0.91)	91,534 (2,774)
12	171 (23.3)	92.2 (0.98)	99,451 (3,787)
16	253 (54.1)	88.6 (2.27)	95,798 (3,009)
24	121 (24.9)	94.7 (1.05)	103,846 (1,705)

[A] Actual values expressed as hours, [B] values are expressed as (mean (ng/mL) (SDev), [C] values are expressed as (mean (%) (SDev), [D] values are expressed as (mean (ng/mg) (SDev), [E] not applicable as no biochar was used.

Table A-18: Adsorption kinetic of E1, triplicate samples spiked at nominal concentration of ~2,500 ng/mL (50 mL CaCl2) into a fix biochar mass (1 mg ± 0.08 mg) at pH = 7 ±0.2 and temperature = 20°C± 2°C

	E1		
Time [A]	**Solution concentration (C_t)**	**Percentage adsorbed**	**Powdered biochar ESH concentration**
0	2,270 (61.9)[B]	N.A[E]	N.A
0.5	1,259 (140)	43.0 (5.85)[C]	48,447 (6,000)[D]
1	888 (130)	59.8 (5.44)	68,181 (5,493)
2	569 (134)	74.3 (5.62)	82,570 (8,689)
3	465 (25.0)	78.1 (1.04)	88,727 (3,424)
6	65.2 (14.8)	96.9 (0.62)	107,353 (3,136)
9	164 (49.8)	92.4 (2.08)	101,555 (5,185)
12	110 (45.9)	95.2 (1.92)	104,498 (4,712)
16	92.7 (11.9)	95.7 (0.50)	104,994 (3,550)
24	137 (89.7)	93.7 (3.76)	103,507 (1,904)

[A] Actual values expressed as hours, [B] values are expressed as (mean (ng/mL) (SDev), [C] values are expressed as (mean (%) (SDev), [D] values are expressed as (mean (ng/mg) (SDev), [E] not applicable as no biochar was used.

A.11 Adsorption isotherm (supporting information Section 4.6.5)

Table A-19: Adsorption isotherm of target 17α-E2, triplicate samples spiked at different concentration into fixed biochar mass (1 mg ± 0.09 mg) and time interval (24 hours)

	17α-E2		
Concentration [A]	**Solution equilibrium concentration (C_e)**	**Percentage adsorbed**	**Powdered biochar ESH concentration**
1,434	23.0 (0.95)[B]	98.4 (0.07)[C]	68,942 (1,536)[D]
2,781	147 (37.1)	94.7 (1.33)	127,080 (1,098),
5,445	886 (283)	83.7 (5.19)	214,996 (2,243)
13,657	7,689 (289)	43.7 (2.12)	290,801 (17,248)
26,996	18,631 (386)	31.0 (1.43)	384,956 (19,716)
42,549	31,715 (438)	25.5 (1.03)	503,184 (15,071)
56,516	46,470 (954)	17.8 (1.69)	469,990 (45,854)

[A] Actual values expressed as ng/mL, [B] values are expressed as (mean (ng/mL) (SDev), [C] values are expressed as (mean (%) (SDev), [D] values are expressed as (mean (ng/mg) (SDev).

Table A-20: Adsorption isotherm of target 17β-E2, triplicate samples spiked at different concentration into fixed biochar mass (1 mg ± 0.09 mg) and time interval (24 hours)

	17β-E2		
Concentration [A]	**Solution equilibrium concentration (C_e)**	**Percentage adsorbed**	**Powdered biochar ESH concentration**
1,206	13.1 (3.31)[B]	98.9 (0.27)[C]	58,322 (1,151)[D]
2,421	35.0 (8.59)	98.6 (0.36)	115,107 (2,996)
5,181	482 (45.9)	90.7 (0.89)	222,143 (14,023)
12,594	3,985 (338)	68.4 (2.69)	419,332 (18,771)
25,228	10,376 (329)	58.9 (1.30)	683,430 (17,284)
36,642	17,428 (632)	52.4 (1.72)	892,308 (28,765)
49,020	24,339 (939)	50.3 (1.92)	1,155,865 (87,149)

[A] Actual values expressed as ng/mL, [B] values are expressed as (mean (ng/mL) (SDev), [C] values are expressed as (mean (%) (SDev), [D] values are expressed as (mean (ng/mg) (SDev).

Table A-21: Adsorption isotherm of target E1, triplicate samples spiked at different concentration into fixed biochar mass (1 mg ± 0.09 mg) and time interval (24 hours)

	E1		
Concentration [A]	**Solution equilibrium concentration (C_e)**	**Percentage adsorbed**	**Powdered biochar ESH concentration**
1,098	27.6 (1.34)[B]	97.5 (0.12)[C]	51,799 (816)[D]
2,264	40.4 (7.61)	98.2 (0.34)	110,109 (1,231)
4,577	654 (144)	85.7 (3.15)	192,901 (4,865)
11,849	3,933 (153)	66.8 (1.29)	383,061 (5,044)
23,362	14,181 (707)	39.3 (3.03)	443,205 (36,883)
36,783	23,850 (1,321)	35.2 (3.59)	625,176 (52,411)
44,716	36,070 (1,286)	19.3 (2.88)	424,860 (59,466)

[A] Actual values expressed as ng/mL, [B] values are expressed as (mean (ng/mL) (SDev), [C] values are expressed as (mean (%) (SDev), [D] values are expressed as (mean (ng/mg) (SDev).

A.12 Isotherm and kinetic modelling results (supporting information Section 4.6.6)

Table A-22: Freundlich, Langmuir and Slips isotherm model results in comparison to the experimental data of 17α-E2 (biochar mass = 1 ± 0.09 mg, pH = 7 ±0.2, Temperature = 20°C± 2°C).

	17α-E2			
Concentration [A]	**Experimental data[B]**	**Freundlich model[C]**	**Langmuir model[C]**	**Sips model[C]**
1,434	68,942	87,626	10,072	77,918
2,781	127,080	131,733	57,415	123,647
5,445	214,996	195,440	209,369	193,241
13,657	290,801	314,130	391,884	330,457
26,996	384,956	381,522	419,874	411,556
42,549	503,184	428,787	428,750	469,524
56,516	469,990	466,319	432,889	516,120

[A] Actual values expressed as ng/mL, [B] values are expressed as (mean (ng/mg), [C] values are expressed as ng/mg.

Table A-23: Freundlich, Langmuir and Slips isotherm model results in comparison to the experimental data of 17β-E2 (biochar mass = 1 ± 0.09 mg, pH = 7 ±0.2, Temperature = 20°C± 2°C).

	17β-E2			
Concentration [A]	**Experimental data[B]**	**Freundlich model[C]**	**Langmuir model[C]**	**Sips model[C]**
1,206	58,322	29,836	1,270	37,913
2,421	115,107	47,768	3,387	58,511
5,181	222,143	167,982	45,842	186,156
12,594	419,332	462,269	331,666	470,185
25,228	683,430	731,247	703,515	713,090
36,642	892,308	937,595	981,112	892,438
49,020	1,155,865	1,100,366	1,174,753	1,030,478

[A] Actual values expressed as ng/mL, [B] values are expressed as (mean (ng/mg), [C] values are expressed as ng/mg.

Table A-24: Freundlich, Langmuir and Slips isotherm model results in comparison to the experimental data of E1 (biochar mass = 1 ± 0.09 mg, pH = 7 ±0.2, Temperature = 20°C± 2°C).

	E1			
Concentration [A]	**Experimental data[B]**	**Freundlich model[C]**	**Langmuir model[C]**	**Sips model[C]**
1,098	51,799	110,716	11,902	67,690
2,264	110,109	120,013	17,257	789,99
4,577	192,901	216,219	189,597	218,897
11,849	383,061	315,899	419,030	361,231
23,362	443,205	414,253	507,584	469,372
36,783	625,176	462,367	524,842	510,260
44,716	424,860	504,613	533,861	540,639

[A] Actual values expressed as ng/mL, [B] values are expressed as (mean (ng/mg), [C] values are expressed as ng/mg.

Table A-25: Pseudo-first and second order kinetic models results in comparison to the experimental data of 17*α*-E2 (biochar mass = 1 ± 0.08 mg, pH = 7 ±0.2, Temperature = 20°C± 2°C).

	17*α*-E2		
Time [A]	**Experimental data[B]**	**Pseudo-first-order model[C]**	**Pseudo-second-order model[C]**
0	0	0	0
0.5	59,956	39,942	51,176
1	80,461	70,446	77,836
2	99,697	109,282	103,520
3	106,193	126,117	114,189
6	119,900	135,717	127,056
9	125,890	135,830	130,646
12	135,499	135,831	132,241
16	132,570	135,831	133,323
24	133,366	135,831	134,285

[A] Actual values expressed as hours, [B] values are expressed as (mean (ng/mg), [C] values are expressed as ng/mg.

Table A-26: Pseudo-first and second order kinetic models results in comparison to the experimental data of 17β-E2 (biochar mass = 1 ± 0.08 mg, pH = 7 ±0.2, Temperature = 20°C± 2°C).

	17β-E2		
Concentration [A]	**Experimental data[B]**	**Pseudo-first-order model[C]**	**Pseudo-second-order model[C]**
0	0	0	0
0.5	49,322	29,354	37,027
1	58,146	52,436	57,820
2	73,360	82,900	78,683
3	85,654	96,691	87,497
6	88,290	104,951	98,087
9	91,533	105,051	100,988
12	99,451	105,052	102,261
16	95,798	105,052	103,115
24	103,846	105,052	103,866

[A] Actual values expressed as hours, [B] values are expressed as (mean (ng/mg), [C] values are expressed as ng/mg.

Table A-27: Pseudo-first and second order kinetic models results in comparison to the experimental data of E1 (biochar mass = 1 ± 0.08 mg, pH = 7 ±0.2, Temperature = 20°C± 2°C).

	E1		
Concentration [A]	**Experimental data[B]**	**Pseudo-first-order model[C]**	**Pseudo-second-order model[C]**
0	0	0	0
0.5	48,447	41,395	41,395
1	68,181	65,191	65,191
2	82,570	88,244	88,244
3	88,727	96,927	96,927
6	107,353	105,290	105,290
9	101,555	106,994	106,994
12	104,498	107,650	107,650
16	104,994	108,059	108,059
24	103,507	108,400	108,400

[A] Actual values expressed as hours, [B] values are expressed as (mean (ng/mg), [C] values are expressed as ng/mg.

A.13 Inorganic analysis of the DSE (supporting information Section 5.3.1)

Table A-28: Inorganic analysis of the DSE

Metal	Concentration in DSE (mg/L)	Metal	Concentration in DSE (mg/L)
Aluminium	26.5	Magnesium	78.5
Antimony	<0.0042	Manganese	2.85
Arsenic	<0.021	Molybdenum	0.014
Barium	0.43	Nickel	0.017
Bismuth	0.0595	Potassium	525
Beryllium	<0.021	Rubidium	0.98
Boron	0.385	Selenium	<0.021
Cadmium	0.00195	Silver	<0.0022
Caesium	0.0069	Sodium	68
Calcium	131.5	Sulphur	34
Chromium	0.0195	Strontium	0.315
Cobalt	0.02325	Thallium	<0.0011
Copper	0.37	Tin	<0.011
Iron	28.5	Uranium	0.00245
Lanthanum	0.026	Vanadium	0.0445
Lead	0.0218	Zinc	1.255
Lithium	0.047		

Average values of two set of DSE analysis samples completed during August and October 2018 as part of Chapter 2 investigation. The analysis was completed by an external certified laboratory using an extended total metal analysis that includes nitric acid digestion, ICP-MS, screen level (APHA 3125 B 22nd edition 2012).

A.14 Free and conjugated ESHs solid phase results (excluded from this research due to low recovery and inconsistent results) (supporting information Section 5.3.2)

Table A-29: Concentration of the free and conjugated ESHs measured in the solid phase of the adsorption samples (ng/g)

	DSE comparison			DSE control			DSE 5		
	Free	Conjugated	Total	Free	Conjugated	Total	Free	Conjugated	Total
17α-E2	124	15.0	139	91.6	3.95	95.6	579	38.9	619
17β-E2	23.1	3.88	26.9	22.8	5.10	27.9	98.7	6.59	105
E1	46.4	28.8	75.2	32.9	2.61	35.5	128	9.57	138
ΣESHs	194	47.7	241	147	11.7	159	806	56.0	862
	DSE 10			**DSE 20**			**DSE 30**		
	Free	Conjugated	Total	Free	Conjugated	Total	Free	Conjugated	Total
17α-E2	171	6.21	177	461	5.61	467	1288	NA[A]	1288
17β-E2	34.7	6.10	40.8	97.6	ND[B]	97.6	160	NA	160
E1	46.9	8.49	55.4	80.4	2.03	82.4	148	NA	148
ΣESHs	253	20.8	274	639	7.64	647	1596	NA	1596
	DSE 50			**DSE 100**			**DSE 200**		
	Free	Conjugated	Total	Free	Conjugated	Total	Free	Conjugated	Total
17α-E2	62.8	3.67	66.4	1578	5.69	1584	652	5.45	658
17β-E2	18.5	ND	18.5	184	ND	184	112	ND	112
E1	23.5	1.59	25.1	176	11.54	188	135	1.59	127
ΣESHs	105	5.25	110	1938	17.2	1956	899	7.04	906

[A] Not available – loss of sample. [B] Not detected

A.15 Free and conjugated ESHs dissolved results (Supporting information Section 5.3.2)

Table A-30: Concentration of the free and conjugated ESHs measured in the dissolved phase of the adsorption samples (ng/L)

	DSE comparison			DSE control			DSE 5		
	Free	Conjugated	Total	Free	Conjugated	Total	Free	Conjugated	Total
17α-E2	2217	8.24	2226	2656	5.46	2662	485	4.76	490
17β-E2	329	17.3	346	378	19.3	398	162	17.3	179
E1	147	5.02	152	253	2.90	256	89.9	2.37	92.3
ΣESHs	2693	30.6	2724	3288	27.7	3316	737	24.5	762
	DSE 10			**DSE 20**			**DSE 30**		
	Free	Conjugated	Total	Free	Conjugated	Total	Free	Conjugated	Total
17α-E2	440	6.97	447	456	7.64	464	224	7.52	231
17β-E2	248	21.0	269	162	25.6	188	227	25.4	253
E1	90.9	38.9	130	86.0	3.06	89.1	55.9	9.77	65.6
ΣESHs	779	66.9	846	705	36.3	741	507	42.7	550
	DSE 50			**DSE 100**			**DSE 200**		
	Free	Conjugated	Total	Free	Conjugated	Total	Free	Conjugated	Total
17α-E2	230	6.38	237	214	6.33	220	213	3.87	217
17β-E2	214	53.6	268	188	19.3	208	198	21.6	220
E1	58.1	37.0	95.0	55.4	4.17	59.6	53.3	6.04	59.3
ΣESHs	503	97.0	600	457	29.8	487	465	31.5	496

Table A-31: Adsorption trial percentage adsorption (%) of dissolved phase free and conjugated ESHs, at different biochar concentration and fix time interval (24 hours) (pH = 7.2 ±0.1, Temperature = 20°C± 2°C).

Biochar concentration (mg/L)	17α-E2	17β-E2	E1	ΣESHs
0	0	0	0	0
10	78.0	48.2	39.5	72.0
20	79.9	22.3	14.9	68.9
40	79.2	45.7	41.5	72.8
60	89.6	27.0	56.9	79.8
100	89.4	22.6	37.6	78.0
200	90.1	40.0	60.9	82.1
400	90.2	36.5	61.1	81.8

A.16 Analysis of competitive adsorption by isotherm modelling (Supporting information Section 5.3.3)

Table A-32: Freundlich isotherm model results in comparison to the experimental data of DSE 17α-E2, 17β-E2 and E1 respectively

	17α-E2		17β-E2		E1	
Powdered biochar concentration (mg/L)	**Experimental data (ng/mg)**	**Model data (ng/mg)**	**Experimental data (ng/mg)**	**Model data (ng/mg)**	**Experimental data (ng/L)**	**Model data (ng/mg)**
10	173	127	N/A[A]	N/A	5.75	3.55
20	88.9	89.2	4.04	2.08	2.82	3.69
40	44.0	102	N/A	N/A	1.53	3.06
60	33.2	7.75	1.69	1.71	1.52	0.71
100	19.9	8.61	1.14	1.50	0.89	0.80
200	10.0	6.55	0.70	1.13	0.46	0.69
400	5.0	6.52	0.33	1.27	0.24	0.60

[A] excluded from the curve fitting due to higher than expected removal.

Table A-33: Redlich-Peterson isotherm model results in comparison to the experimental data of DSE 17α-E2, 17β-E2 and E1 respectively

	17α-E2		17β-E2		E1	
Powdered biochar concentration (mg/L)	**Experimental data (ng/mg)**	**Model data (ng/mg)**	**Experimental data (ng/mg)**	**Model data (ng/mg)**	**Experimental data (ng/L)**	**Model data (ng/mg)**
10	173	92.4	N/A[A]	N/A	5.75	2.69
20	88.9	83.9	4.04	1.95	2.82	2.72
40	44.0	86.9	N/A	N/A	1.53	2.57
60	33.2	42.6	1.69	1.78	1.52	1.67
100	19.9	43.9	1.14	1.68	0.89	1.74
200	10.0	40.7	0.70	1.47	0.46	1.66
400	5.0	40.6	0.33	1.55	0.24	1.59

[A] excluded from the curve fitting due to higher than expected removal.

Table A-34: Modified Freundlich isotherm model results in comparison to the experimental data of DSE 17α-E2, 17β-E2 and E1 respectively

	17α-E2		17β-E2		E1	
Powdered biochar concentration (mg/L)	**Experimental data (ng/mg)**	**Model data (ng/mg)**	**Experimental data (ng/mg)**	**Model data (ng/mg)**	**Experimental data (ng/L)**	**Model data (ng/mg)**
10	173	122	N/A[A]	N/A	5.75	3.52
20	88.9	92.8	4.04	4.03	2.82	3.64
40	44.0	103	N/A	N/A	1.53	3.05
60	33.2	13.9	1.69	1.71	1.52	0.77
100	19.9	15.0	1.14	1.05	0.89	0.87
200	10.0	12.2	0.70	0.50	0.46	0.75
400	5.0	12.1	0.33	0.63	0.24	0.66

[A] excluded from the curve fitting due to higher than expected removal.

A.17 Removal performance of DSE 17α-E2, 17β-E2, E1 and ΣESHs respectively by powdered biochar (Supporting information Section 5.3.3)

Table A-35: Removal performance of DSE 17α-E2, 17β-E2, E1 and ΣESHs respectively by powdered biochar

Biochar Concentration (mg/L)	**17α-E2 Removal (%)**	**17β-E2 Removal (%)**	**E1 Removal (%)**	**ΣESHs Removal (%)**
10	75.2	20.7	32.7	66.2
50	85.6	29.8	52.7	77.0
100	88.6	34.1	60.3	80.4
200	91.0	39.5	66.9	83.4
300	91.8	43.4	70.4	84.8
400	92.7	47.0	72.7	86.0
500	93.6	50.6	74.3	87.3
600	94.4	54.0	75.5	88.4
700	94.9	57.2	76.5	89.3
800	95.3	60.2	77.3	90.0
900	95.5	62.8	78.1	90.6
1000	95.6	65.2	78.8	91.0
1500	95.5	73.5	82.0	92.0

A.18 Modelled available ESHs for powdered biochar (Supporting information Section 5.3.3)

Table A-36: Modelled available DSE 17α-E2 for powdered biochar

DSE 17α-E2 Concentration (ng/L)	Available 17α-E2 in solution (ng/L)	Modelled 17α-E2 /Biochar concentration (ng/mg)	17α-E2 adsorption on powdered biochar (ng)[A]
0	0	0	0
255	50.0	0.21	205 (80.4[B])
1539	100	1.44	1439 (93.5)
4649	150	4.50	4499 (96.8)
10299	200	10.1	10099 (98.1)
19162	250	18.9	18912 (98.7)
31873	300	31.6	31573 (99.1)

[A] calculated based on powdered biochar concentration of 1000 mg/L. [B] Percentage (express in %) of ESHs removed by the powdered biochar

Table A-37: Modelled available DSE 17β-E2 for powdered biochar

DSE 17β-E2 Concentration (ng/L)	Available 17β-E2 in solution (ng/L)	Modelled 17β-E2 /Biochar concentration (ng/mg)	17β-E2 adsorption on powdered biochar (ng)[A]
0	0	0	0
69.3	25.0	0.04	44.3 (63.9[B])
141	50.0	0.09	90.7 (64.5)
213	75.0	0.14	138 (64.8)
286	100	0.19	186 (65.0)
360	125	0.24	235 (65.3)
442	150	0.29	292 (66.1)
567	175	0.39	392 (69.1)
868	200	0.67	668 (77.0)

[A] calculated based on powdered biochar concentration of 1000 mg/L. [B] Percentage (express in %) of ESHs removed by the powdered biochar

Table A-38: Modelled available DSE E1 for powdered biochar

DSE E1 Concentration (ng/L)	Available E1 in solution (ng/L)	Modelled E1/Biochar concentration (ng/mg)	E1 adsorption on powdered biochar (ng)[A]
0	0	0	0
13.1	10.0	0	0.00
48.4	20.0	0.03	28.4 (12.4[B])
134	30.0	0.10	104 (25.8)
302	40.0	0.26	262 (39.6)
586	50.0	0.54	536 (51.7)
1022	60.0	0.96	962 (61.6)

[A] calculated based on powdered biochar concentration of 1000 mg/L. [B] Percentage (express in %) of ESHs removed by the powdered biochar

A.19 Estrogenic potency (Supporting information Section 5.3.4)

Table A-39: Modelled factored estrogenic equivalents and reduction in estrogenicity of ESHs in the DSE sample dosed at different powdered biochar concentration

Powdered biochar concentration (mg/L)	17α-E2 Equivalent (ng/L)[A]	17β-E2 Equivalent (ng/L)[A]	E1 Equivalent (ng/L)[A]	ΣESHs Equivalent (ng/L)[A]	Reduction in estrogenicity (%)
0	22.3	346	3.05	371	0
10	5.50	261	1.98	268	24.2
50	3.20	231	1.39	235	33.5
100	2.53	217	1.17	220	37.7
200	2.00	199	0.97	202	42.9
300	1.08	186	0.87	189	46.6
400	1.62	174	0.80	177	50.1
500	1.42	162	0.76	165	53.5
600	1.25	151	0.72	153	56.7
700	1.12	141	0.69	142	59.8
800	1.04	131	0.67	133	62.5
900	1.00	122	0.65	124	65.0
1000	0.97	115	0.63	116	67.2
2000	1.08	70.4	0.46	71.9	79.7
3000	1.07	51.0	0.39	52.5	85.2
4000	0.96	40.1	0.39	41.5	88.3
5000	0.86	33.1	0.41	34.4	90.3

[A] calculated by multiplying the modelled concentration of 17α-E2, 17β-E2 and E1 by its relative potency factor (0.01,1 and 0.02 respectively) obtained by the ER-CALUX bioassay (Kolkman et al., 2013).

A.20 NZ dairy farming and examples of key dairy farm effluent system (supporting information for Section 6.1)

On NZ farms, cows are typically spending the majority of their time in paddocks (IPENZ, 2017). All farms will have a stand-off pad (milking yard) and milking shed, both of which have an impermeable concrete surface. Some farms include a feed pad, which is situated adjacent to the milking yard and may or may not include an impermeable surface, or it may have a permeable surface consisting of wood chips. The time a cow spends in the milking yard, in the milking shed or feed pad will depend on the farmer's operation, the number of cows, and the throughput through the milking shed, which will depend on whether or not the farm is using a herringbone or rotary milking system, and what system the farm is, i.e. whether or not the cows are primarily grass-fed, or there is some supplemental feeding with e.g. maize or palm expeller kernel. There are many types of

recommended dairy farm effluent (DFE) and applicator systems (Dairy NZ, 2014), this section covers the predominant effluent systems in NZ.

A.20.1Two-pond system

Traditional effluent treatment in NZ includes a two-pond system arrangement (**Figure A-2**).

Figure A-2: Traditional two-pond system for the treatment of dairy effluent

The pond systems normally include anaerobic and facultative pond designs for the removal of organic matter and solids, before subsequent discharge of the effluent. These treatment systems do not incorporate active/mechanical oxidation, relying instead upon passive oxidation from the atmosphere. As such, these systems provide uncontrolled treatment performance that relies of the surrounding environmental conditions to treat the concentrated dairy shed waste stream and therefore were found not to be effective in reducing nutrients such as nitrogen and phosphate (Bolan *et al.*, 2009; Craggs *et al.*, 2003). Although the two-pond system are not very common these days and are not sitting under the classification of DFE system in the local authorities, they are still around. Farmers tend to pump the top layer (supernatant) from either the first or the second pond and utilise it for land irrigation, while leaving the settled solids at the bottom of the ponds. The hydraulic retention time of this system is normally very high because originally, they were designed to act as anaerobic and facultative ponds. Anaerobic and facultative ponds normally have a hydraulic retention times of up to 50 days (Norvill et al., 2016).

A.20.2 Stirred sump or pond

A stirred sump or pond (**Figure A-3**) is normally used in conjunction with a travelling irrigator (high rate irrigation system) as the method of application and a stone trap as a pre-treatment (Dairy NZ, 2014).

Figure A-3: Stirred dairy effluent sump

In this system, the primary treated effluent is stirred on a regular basis or just before pumping to ensure minimum sedimentation occurs at the bottom of the tank. The stirred effluent from the sump is applied to pasture and/or directed to the storage pond during times that effluent cannot be directed to land. Another variation to this system includes a larger capacity pond equipped with pump and stirrer (normally portable system connected and driven by a tractor) that also act as a storage facility.

A.20.3 Passive or mechanical solids separation

Solids separation is required to minimise any operational issues such as pipe and pump blockages and to ensure the liquid effluent can be pumped more efficiently and over longer lengths. Passive and mechanical separation systems would normally be used in conjunction with a low rate sprinkler system (Dairy NZ, 2014).

The most popular separator system in NZ is the passive weeping wall arrangement (**Figure A-4**). The weeping wall includes a sludge storage area (either lined pond or a concrete structure) which has a narrow-slotted wall at the outlet. The liquid effluent drains through the wall into a drainage channel and to the storage pond or sump. The solids remain in

the storage area for a period of four to six months before they dug out and applied to land normally by a tanker spreading method.

Figure A-4: Passive separator – weeping wall system

A.21 Anaerobic digestion principals (supporting information for Section 6.1)

Conversion of the organic matter within the biosolids to methane involves several groups of bacteria that carry out specific chemical and biochemical reactions at several stages. These stages consist of hydrolysis, fermentation and methane formation process (Metcalf and Eddy, 2014). The hydrolysis stage is responsible for converting the complex and insoluble organic matter into material that can be assimilated by the bacteria. The hydrolysis step is normally considered the limiting stage as no stabilisation of the biosolids can occur without proper functioning of this step. It is important to mention that not all the biosolids organic matter can be broken down during the hydrolysis stage as some comprises a non-biodegradable organic portion and cannot be biologically degraded.

Following the hydrolysis stage, the hydrolysed organics will be fermented to long chain organic acids, sugars, and amino acids. Furthermore, acetic acid, hydrogen and carbon dioxide are also formed during the production of the organic acids. The acetic acid and hydrogen serve as the major substrates for the formation of methane and other biogas gases. During the conversion of the acetic acid into methane gas, waste stabilisation occurs and the methane leaves the system and can be utilised as an energy source. Carbon

dioxide is also produced is the anaerobic digestion process, this compound could escape as gas or be converted to bicarbonate alkalinity (Parkin & Owen, 1986).

An efficient operation of anaerobic digestion will ensure there is a balance between the acid and hydrogen forming bacteria and the methane producing bacteria. System imbalance will generate high volatile acid concentration and high hydrogen levels leading to low pH that will inhibit methanogenic activity (Fagbohungbe *et al.*, 2017). To ensure efficient anaerobic digestion, parameters such as retention time, contact between the bacteria and substrate, alkalinity, pH and constant temperature conditions and concentration of nutrients, non-toxic materials and feed need to be optimised. Optimisation of these conditions will permit the development and maintenance of a large and stable population of methane-forming bacteria leading to high production of methane gas. Among these parameters, solids retention time is a key factor to ensure bacterial growth as well as prevent wash out of the bacteria. Another key parameter is temperature. The operating temperature of anaerobic digestion determines the metabolic activities of the microbial population and affects the gas transfer rate and the settling characteristics of the sludge. Anaerobic digestion temperature can range between ambient temperatures to 57°C. Most anaerobic digestion will operate in the mesophilic range of 30°C - 38°C, while others operate at the thermophilic temperature range of 50°C to 57°C. Anaerobic digestion using a pond system will normally operate under ambient temperatures. Whatever type of anaerobic digestion is used, it is important to keep the temperature stable because the bacteria, especially the methane bacteria, are sensitive to temperature variation (Metcalf and Eddy, 2014).

Furthermore, the composition of the feedstock is very important during the anaerobic digestion process. To enhance the methane production of the anaerobic digestion system and reduce inhibition, a combination of two or more feeds to optimise the anaerobic digestion operating conditions are commonly used (Yangin-Gomec & Ozturk, 2013). Feed adjustment would normally be made to achieve appropriate carbon to nitrogen ratio and pH buffering capabilities (Troy *et al.*, 2013) and also allow for microbial adaption by reduction of the of the concentration of the inhibitor by increasing the ratio of the co-substrate (Fagbohungbe *et al.*, 2017). For example, bio-oil from the pyrolysis system (system that produces biochar, material that is used in this research to treat ESHs from the DSE) can also be used as a feed to the anaerobic digestion system to produce more energy (Hubner & Mumme, 2015; Torri & Fabbri, 2014). On contrast, the use of non-

suitable feed can lead to the inhibition of bacterial activity. For example, inhibition of bacterial activity can be caused by organic substrates that contain high amount of protein, lipids, metals, pesticides, antibiotics and other organic compounds (Alvarez *et al.*, 2010; Sousa *et al.*, 2013; Yangin-Gomec & Ozturk, 2013). Examples for possible anaerobic digestion feeds in a dairy farm environment (Dairy NZ, 2017) are presented below:

- Manure scraped from the feed pads. This feed can be diluted or thickened by air drying or by adding bedding materials and can contain a solid content of 15-25 %. Manure from the feed pad is often stored before being directed to the effluent system or directly spread on the farm. This "aged" feed would tend to have low energy value and normally not be suitable for biogas and energy production.
- Diary shed effluent generated at the milking shed. This feed includes manure, milk residue and washing water, making this feed dilute with a solid content of less than one percent.
- Dairy shed effluent separated solid portion sourced from the passive or mechanical separation system. This material can contain a solid content of 4 – 20 % depending on the solid separation system used. This material would normally either be stored in a bunker or a tank.

A.22 Complete mix digester, plug flow, fixed film digester and concentrated animal feeding operation (supporting information for Section 6.1)

The most popular anaerobic digester configurations for treating dairy biomass are presented below.

A.22.1 Continuous stirred tank reactor

A complete mix digester or continuous stirred tank reactor (CSTR), would normally be above ground, however, some below ground arrangements can also be found. The solid feed content would normally be 3 – 10 % with a hydraulic retention time of 15 days or higher. The complete mix digester content would be mixed by motor or pump, and the reactor/tank would normally be heated (U.S. Environmental Protection Agency, 2004)

A.22.2 Plug flow digester

The plug flow digester is a long narrow tank normally designed for feeds with a range of 11 – 13 % total solids and hydraulic retention time of 15 days or more (U.S.

Environmental Protection Agency, 2004). The digester content would move through the digester as new feed is added. This system would normally be heated and can include vertical mixing techniques. The plug flow digester is the most common anaerobic digestion system installed on farms in the USA (U.S. Environmental Protection Agency, 2017a).

A.22.3 Fixed film digester

Fixed film digesters include a medium, normally plastic or wood chips, that support a thin layer of anaerobic bacteria. This system is designed for feeds with a range of 1 – 5 % total solids and hydraulic retention time of five days or less. The feed would pass through the media and be digested as it comes into contact with the bacteria (biofilm) attached to the medium.

A.22.4 Concentrated animal feeding operation

In comparison to the New Zealand dairy operation, the United States (US) use a concentrated animal feeding operation (CAFO). The CAFO is normally used for a large herd (over 700 dairy cows) that is confined on site that operates for more than 45 days during the year. In these systems feed is normally brought to the cow rather than the cow grazing in the paddocks (Natural Resources Conservation Service, n.d.). The CAFO system is known to present a greater risk to the environment due to the increased volume of effluent and contaminants (Burkholder et al., 2007), therefore the effluent treatment systems of the CAFO need to be designed carefully. The CAFO system normally consists of a rain water diversion facility, a waste collection system, a waste storage pond, an animal waste treatment facility and an animal waste transfer system (U.S. Environmental Protection Agency, 2001).

The CAFO treatment facility normally includes physical, biological and chemical treatments. The physical treatment commonly involves a solid separation arrangement, while the treatment takes place in an anaerobic or aerobic lagoon or in an anaerobic digester. Composting of the animal waste is also used to improve the handling and reduce odour and nuisance problems associated with the animal waste (U.S. Environmental Protection Agency, 2001).

A.23 Application of animal effluent and sludge to land (supporting information for Section 6.1)

Many factors can influence the fate and behaviour of ESHs in the environment, including the type of effluent/solids, the application rate and the method of application (Mina *et al.*, 2017). The transport behaviour of steroid hormones can be assessed by knowing the concentration discharge, load discharge and various relationship coefficients. Two methods, surface broadcast and shallow disk injection, of dairy manure application were tested over a period of seven months to confirm the transport behaviour of steroid hormones resulting from each method. It was found that shallow disk injection significantly reduced steroid hormones transport through runoff (Mina *et al.*, 2017).

Soils containing preferential flow can cause leaching of steroid hormones to ground water (Steiner *et al.*, 2010). A study of animal manure-treated fields examined the leaching rate of 17β-estradiol and estrone under-regulated and acceptable manure irrigation rates and found that these hormones leach rapidly from the root zone during storm events. In this study estrone was found to leach more readily than 17β-estradiol (Kjaer *et al.*, 2007). Other studies showed that steroid hormones tend to adsorb onto soil and sediment, because of the presence of organic carbon in the soil (Casey *et al.*, 2003; Mansell *et al.*, 2004; Sarmah *et al.*, 2008; Ying & Kookana, 2005) or biologically degrade (Mansell *et al.*, 2004; Ying & Kookana, 2005). The difference in the results was assumed to be due to the lack of macropores within the laboratory-scale soil column caused due to the handling of the soil, leading to longer persistence time of the contaminants. Longer persistence time will provide better conditions for the hormones to be adsorbed or degrade (Kjaer *et al.*, 2007). Other reasoning for the long persistence of the contaminants in soils and therefore the advancement of the adsorption capacities in solid, is due to the existence of anaerobic conditions that enable minimum to no degradation of the steroid hormones' components (Ying & Kookana, 2005). Degradation of free estrogens in soil was found to occur rapidly (within seven days) in a soil column under aerobic conditions. However, under anaerobic conditions most of the estrogens will persist in the soil with little, to no, degradation. The exception is 17β-estradiol, where biological degradation was found to be much slower (Peterson *et al.*, 2005; Ying & Kookana, 2005). Furthermore, 17β-estradiol was found to be converted into estrone during both aerobic and anaerobic conditions (Sarmah *et al.*, 2008; Ying & Kookana, 2005).

A.24 Municipal wastewater treatment systems and ESHs (supporting information for Section 6.1)

Municipal wastewater treatment system in NZ normally includes some form of an activated sludge system where anoxic, aerobic and clarification (by clarifier) or separation (by membranes) stages with and without the use of chemicals (Metcalf and Eddy, 2014). Previous studies that looked at the fate of different ESHs in various wastewater treatment plant configurations suggest that the ESHs entering the wastewater treatment plant from municipal source are generally removed during the treatment process, leading to reduced concentration in the treated effluent (Ifelebuegu, 2011; Ogunlaja and Parker, 2015). The removal of the ESHs was found to mainly occur during the secondary biological treatment, with the rates of removal related to the nitrification rates, recirculation rate, temperature and the hydraulic retention time, dissolved oxygen and sludge age (Andersen *et al.*, 2003; Hamilton *et al.*, 2016; Ifelebuegu, 2011; Leusch *et al.*, 2006; Marti & Batista, 2014). More advanced treatment technologies, such as membrane bioreactors or anaerobic anoxic, aerobic arrangements, have been found to have superior performance than the lower technology plants, such as an oxidation ditch (Ifelebuegu, 2011). Tertiary treatments were also found to improve the removal of ESHs through solids removal. Furthermore, methods such as adsorption, ozonation, reverse osmosis and nanofiltration are reported to be effective in the removal of the ESHs, in comparison to the activated sludge and biofiltration methods (Ifelebuegu, 2011; Liu *et al.*, 2009b; Snyder *et al.*, 2007). While wastewater treatment plants showed between 75% to 100% removal, mainly through biodegradation and adsorption of estrogens, resulting in a low level of ESHs in the treated effluent (Andersen *et al.*, 2003; Ifelebuegu, 2011; Janex-Habibi *et al.*, 2009; Leusch *et al.*, 2006; Ruchiraset & Chinwetkitvanich, 2014), at the same time, high concentrations of ESHs were found in the digested sludge (Andersen *et al.*, 2003). During the investigation of an enhanced biological removal plant, it was found that a large portion (80 – 90 %) of the estrogens entering the plant were removed by adsorption into the solids (Ruchiraset & Chinwetkitvanich, 2014).

A.25 CAP influent, effluent and sludge 2018 measured ESHs data (supporting information for Section 6.2.5.2)

Table A-40: Free and conjugated ESHs concentrations dissolved (ng/L) phase of the influent samples of the CAP collected during 2018

	Mar-18	Mar-21	Apr-18	May-21	Jul-18	Aug-18	Oct-18	Nov-18
				Free				
17α-E2	1610	744	2869	2247	1065	243	28.6	21.7
17β-E2	233	343	242	341	108	14.7	7.04	15.1
E1	282	178	415	209	106	43.8	5.19	68.3
ΣESHs	2125	1265	3526	2497	1279	302	40.8	105
				Conjugated				
17α-E2	86.8	11.8	89.1	18.4	74.3	33.7	22.6	26.6
17β-E2	N.D	22.6	6.56	35.1	30.5	67.4	40.1	51.6
E1	N.D	2.90	137	11.11	N.D	N.D	7.12	6.78
ΣESHs	86.8	37.3	233	64.6	105	101	69.8	84.9
				Total				
17α-E2	1697	756	2958	2265	1139	277	51.2	48.3
17β-E2	233	366	249	376	139	82.1	47.1	66.7
E1	282	181	552	220	106	43.8	12.3	75.1
ΣESHs	2212	1302	3759	2562	1384	403	111	190

Table A-41: Free and conjugated ESHs concentrations solid (ng/g) phase of the influent samples of the CAP collected during 2018

	Mar-18	Mar-21	Apr-18	May-21	Jul-18	Aug-18	Oct-18	Nov-18
				Free				
17α-E2	309	30.3	413	662	689	174	28.1	23.9
17β-E2	61	21.6	50.1	143	63.4	16.7	16.6	24.4
E1	71.3	146	59.3	131	108	89	46	296
ΣESHs	441	198	522	936	861	280	90.7	344
				Conjugated				
17α-E2	2.93	5.28	37.0	14	34.5	11.4	N.D	1.76
17β-E2	N.D[A]	5.16	9.0	4.62	8.19	4.46	N.D	N.D
E1	N.D	2.5	N.D	27.7	9.17	N.D	N.D	N.D
ΣESHs	2.93	12.9	46.0	46.3	51.8	15.9	N.D	1.76
				Total				
17α-E2	312	35.6	450	676	724	185	28.1	25.7
17β-E2	61	26.8	59.1	148	71.6	21.2	16.6	24.4
E1	71.3	149	59.3	159	117	89.0	46.0	296
ΣESHs	444	211	568	982	913	296	90.7	346

[A] Not detected

Table A-42: Free and conjugated ESHs concentrations dissolved (ng/L) phase of the sludge samples of the CAP collected during 2018

	Mar-18	Mar-21	Apr-18	May-21	Jul-18	Aug-18	Oct-18	Nov-18
				Free				
17α-E2	38.9	N.A[A]	33.8	N.A	24.2	27.0	35.3	21.4
17β-E2	55.3	N.A	46.4	N.A	34.3	33.5	64.9	43.1
E1	881	N.A	835	N.A	581	561	771	628
ΣESHs	975	N.A	915	N.A	640	622	871	693
				Conjugated				
17α-E2	N.D[B]	N.A	N.D	N.A	N.D	N.D	N.D	N.D
17β-E2	N.D	N.A	N.D	N.A	N.D	16.0	17.6	6.27
E1	N.D	N.A	N.D	N.A	N.D	N.D	N.D	N.D
ΣESHs	N.D	N.A	N.D	N.A	N.D	16.00	17.6	6.27
				Total				
17α-E2	38.9	N.A	33.8	N.A	24.2	27.0	35.3	21.4
17β-E2	55.3	N.A	46.4	N.A	34.3	49.5	82.5	49.4
E1	881	N.A	835	N.A	581	561	771	628
ΣESHs	975	N.A	915	N.A	640	638	889	699

[A] Not available (not tested). [B] Not detected

Table A-43: Free and conjugated ESHs concentrations solid (ng/g) phase of the sludge samples of the CAP collected during 2018

	Mar-18	Mar-21	Apr-18	May-21	Jul-18	Aug-18	Oct-18	Nov-18
				Free				
17α-E2	25.3	N.A[A]	24.7	N.A	37.9	32.2	34.3	33.3
17β-E2	51	N.A	46.4	N.A	75.5	70.2	84.7	77.8
E1	750	N.A	1036	N.A	873	813	1416	1309
ΣESHs	826	N.A	1107	N.A	986	916	1535	1420
				Conjugated				
17α-E2	N.D[B]	N.A	N.D	N.A	N.D	15.1	N.D	N.D
17β-E2	15.7	N.A	2.53	N.A	10.5	1.60	2.72	2.53
E1	N.D	N.A	N.D	N.A	19.8	N.D	N.D	N.D
ΣESHs	15.7	N.A	2.53	N.A	30.5	16.7	2.72	2.53
				Total				
17α-E2	25.3	N.A	24.7	N.A	37.9	47.3	34.3	33.3
17β-E2	66.7	N.A	48.9	N.A	86.0	71.8	87.4	80.3
E1	750	N.A	1036	N.A	893	813	1416	1309
ΣESHs	842	N.A	1110	N.A	1017	933	1538	1423

[A] Not available (not tested). [B] Not detected

Table A-44: Free and conjugated ESHs concentrations dissolved (ng/L) phase of the effluent samples of the CAP collected during 2018

	Mar-18	Mar-21	Apr-18	May-21	Jul-18	Aug-18	Oct-18	Nov-18
				Free				
17α-E2	3.50	88.1	106.00	307	782	416	208	84.5
17β-E2	3.11	871	65.3	709	142	142	69.0	11.3
E1	68.7	75.9	1098	96.5	682	756	1011	43.7
ΣESHs	75.3	1035	1269	1112	1606	1314	1288	140
				Conjugated				
17α-E2	N.D[A]	N.D	N.D	N.D	40.2	30.1	48.8	37.0
17β-E2	N.D	3.96	N.D	8.50	N.D	N.D	8.75	9.00
E1	N.D	13.50	N.D	7.18	N.D	141	N.D	N.D
ΣESHs	N.D	17.5	N.D	15.7	40.2	170	57.6	46.0
				Total				
17α-E2	3.50	88.1	106	307	822	446	257	122
17β-E2	3.11	875	65.3	718	142	142	77.8	20.3
E1	68.7	89.4	1098	104	682	897	1011	43.7
ΣESHs	75.3	1053	1269	1128	1606	1484	1346	186

[A] Not detected

Table A-45: Free and conjugated ESHs concentrations solid (ng/g) phase of the effluent samples of the CAP collected during 2018

	Mar-18	Mar-21	Apr-18	May-21	Jul-18	Aug-18	Oct-18	Nov-18
				Free				
17α-E2	2.62	8.82	29.0	158	553	304	126	69.2
17β-E2	3.74	441	27.9	722	121	146	96.8	30.8
E1	26.3	20.0	428	58.9	944	690	1181	1131
ΣESHs	32.6	470	485	939	1618	1139	1403	1231
				Conjugated				
17α-E2	N.D[A]	0.87	N.D	0.89	10.2	8.00	N.D	N.D
17β-E2	N.D	1.74	N.D	2.01	5.19	4.91	N.D	N.D
E1	N.D	3.57	N.D	4.27	N.D	5.92	N.D	N.D
ΣESHs	N.D	6.18	N.D	7.17	15.4	18.8	N.D	N.D
				Total				
17α-E2	2.62	9.69	29.0	159	563	312	126	69.2
17β-E2	3.74	443	27.9	724	126	151	96.6	30.8
E1	26.3	23.57	428	63.2	944	696	1181	1131
ΣESHs	32.6	476	485	946	1633	1158	1403	1231

[A] Not detected

A.26 Anaerobic digestion and pyrolysis

Anaerobic digestion and pyrolysis are two technologies to degrade biomass, producing some added value and renewable bioenergy products (Feng & Lin, 2017). The integration of these two technologies has been researched in recent years with the majority of research focusing on bioenergy recovery (Feng & Lin, 2017; Salman *et al.*, 2017).

Through the combination of anaerobic digestion and pyrolysis, by-products such as bio-oil, biogas and biochar can be produced. The biogas and bio-oil have the potential to generate sufficient energy to make the system self-sufficient and overcome the energy requirement and operation deficiency of each individual process (Feng & Lin, 2017) or to feed the pre-treatment dewatering system (Monlau *et al.*, 2015) as well as replace traditional fossil fuels such as petroleum (Gercel, 2011). The integrated system was found to produce up to 42% more energy than if it was a stand-alone anaerobic digestion system (Monlau *et al.*, 2015; Salman *et al.*, 2017; Shen *et al.*, 2015). Cost of life analysis indicates that an integrated anaerobic/pyrolysis system can have a return rate of 16.5 % with a payback period of 6.1 years (Salman *et al.*, 2017).

Through the combination of anaerobic digester and pyrolysis system, digestate from the anaerobic digestor was found to improve the energy production of the pyrolysis system, as well as the quality of the bio-oil (Liang *et al.*, 2015), however, surface area of the char and its heating value was reduced (Xue-Ding *et al.*, 2017). Biochar from the pyrolysis system added to the anaerobic digestor overcame inhibition problems such as ammonia inhibition (Mumme *et al.*, 2014; Shen *et al.*, 2015), increased alkalinity (Shen *et al.*, 2015), supported well balanced biomethanation bacteria on the biochar (Cooney *et al.*, 2016; Shen *et al.*, 2015; Xu *et al.*, 2015) as well as enhancing phosphate, nitrogen and potassium adsorption capabilities of the digestate (Salman *et al.*, 2017; Shen *et al.*, 2015; Yao *et al.*, 2011).

Adding the pyrolysis oil to the anaerobic digestion system feed can be used for the purposes of production of fuel (Torri & Fabbri, 2014). However, the pyrolysis bio-oil can contain up to 400 complex organic compounds (Hubner & Mumme, 2015), making it toxic to the anaerobic microorganisms within the anaerobic digester and therefore is likely to require further treatment so it can be used (Cordella *et al.*, 2012).

Three main configurations of the combined anaerobic digestion and pyrolysis were studied. These include (1) anaerobic digestion-pyrolysis (2) pyrolysis-anaerobic digestion and (3) anaerobic digestion-pyrolysis-anaerobic digestion.

The anaerobic digestion followed by a pyrolysis system seems to be the most popular configuration for treating biomass (Feng & Lin, 2017). This system gave an increased net energy gain and sustainability, as well as reducing greenhouse emission as anaerobic digestate is not applied directly to land (Odlare *et al.*, 2012).

In the pyrolysis-anaerobic digestion system, by-product from the pyrolysis system are fed into the anaerobic digestion system. This arrangement allows support of biofilm and favours the establishment of bio methanation bacteria on the biochar within the anaerobic digestion system that can double production of methane (Shen *et al.*, 2015; Xu *et al.*, 2015) as well as digesting the pyrolysis bio-oil. Some research suggests that introduction of a high concentration of bio-oil to the anaerobic digestion system may create a toxic environment to anaerobic digestion system microorganisms (Cordella *et al.*, 2012; Feng & Lin, 2017). Further research suggests that bioconversion of the bio-oil requires a long lag time for the anaerobic microorganisms to acclimatised so bio-oil can be converted at an acceptable rate (Torri & Fabbri, 2014). Another way to overcome this problem is by applying pyrolysis pre-treatment or post-treatment to ensure the pyrolysis products are more digestible (Luque *et al.*, 2014).

The third configuration of anaerobic digestion-pyrolysis-anaerobic digestion is similar to the anaerobic digestion-pyrolysis-anaerobic configuration; however, it includes recycling of the pyrolysis products back into the anaerobic digestion system. This system allows flexibility and selection of the anaerobic digestion feedstock for optimum gas production, and utilisation of the pyrolysis bio-oil (Hubner & Mumme, 2015).